THE UNIVERSITY OF CHICAGO

EVOLUTION AND DEVELOPMENT OF THE VERTEBRATE MECHANOSENSORY LATERAL LINE

A DISSERTATION SUBMITTED TO

THE FACULTY OF THE DIVISION OF THE BIOLOGICAL SCIENCES

AND THE PRITZKER SCHOOL OF MEDICINE

IN CANDIDACY FOR THE DEGREE OF

DOCTOR OF PHILOSOPHY

GRADUATE PROGRAM IN INTEGRATIVE BIOLOGY

BY

VISHRUTH VENKATARAMAN

CHICAGO, ILLINOIS

DECEMBER 2025

For my teacher, Shyamala Krishnan,

And for James O'Shea, friend, mentor, philosopher and guide, who taught me the love of fossil fish.

ABSTRACT

The mechanosensory lateral line is a crucial sensory system ancestrally present in all vertebrate lineages. Identifiable in the earliest vertebrate fossils, lateral lines have been evolving for half a million years through major morphological transformations in vertebrate evolution. The lateral line is essential for behaviors like schooling, predation, and escape. Developing from a series of ectodermal placodes, it consists of a series of receptor cells called neuromasts distributed over the heads and trunks of aquatic organisms. The cranial component of the lateral line in jawed vertebrates consists of lines around the orbit, on the cheek and on the lower jaw. While the trunk lateral line has been studied in detail as a model for cell migration in zebrafish, very little is known about the cranial lateral line. This dissertation takes an integrative approach combining data from palaeontology, comparative anatomy and developmental biology to examine the evolution and development of the cranial lateral line system in vertebrates. Contrary to previous hypotheses of lateral line evolution as a direct, linear transformation from conditions in jawless to jawed vertebrates, we propose a scenario where lateral lines evolved independently in agnathans and gnathostomes, and were marked by a radical phase of remodelling preceding the advent of jaws, resulting in a shift from a postorbital to a preorbital location of complex lateral lines. This shift may have been essential for colonization of the water column by jawed vertebrates.

Focusing on the cranial lateral line system in zebrafish, I show that the neural crest, an important cell type, is closely physically associated with the lateral line and is required for normal lateral line development. Abrogation of the neural crest, through genetic or pharmacological manipulations results in stereotypical deficits to the lateral line system. I further describe the development of the lateral line system in postembryonic and larval stages of zebrafish and show that superficial neuromasts are added continuously through development via a variety of mechanisms including the migration of a new primordium, intercalation between

existing neuromasts or budding from an existing neuromast. I also describe a novel cross-placodal mechanism involved in the development of a subset of cranial neuromasts. Using experimental ablations, I demonstrate that zebrafish undergo a developmental switch in ontogeny after which innervation becomes indispensable for lateral line development. Taken together, my findings shed new light on the evolution of vertebrate lateral line morphologies, show how interactions with other tissues may influence lateral line development and uncover new developmental mechanisms underlying the growth of the lateral line system. These findings lay the foundation for future studies on this ancient, crucial and complex sensory system.

- TABLE OF CONTENTS

LIST OF FIGURES

TABLES

ACKNOWLEDGMENTS

नहि सुशिक्षितो ऽपि नटबटुः स्वस्कन्धमारोढुं पटुः

“No matter how well trained, the tumbler’s boy, he will never stand on his own shoulders.”

First and foremost, I am deeply indebted to my advisors, Mike Coates and Vicky Prince for their years of unsurpassed guidance. This work would not have been possible without their sincerity, support, insight and Himalayan patience through the good times and the bad. I owe Vicky for teaching me everything I know about zebrafish directly, down to the smallest detail of protocol, and for constantly reminding me how to be a good scientist and writer. I owe Mike for never failing to encourage my passion for evolutionary biology while always helping me become a more fully-formed evolutionary thinker and communicator. Mike and Vicky have taught me resilience, resourcefulness and humility, and have been bulwarks of support throughout every piece of the dissertation process. They have been unflinchingly supportive throughout my graduate career including when the going got tough with compassion and sagacity. I could not have asked for better mentors.

I am grateful to my thesis committee- Cliff Ragsdale, Neil Shubin, Willy Bemis and Lance Grande for never failing to keep me on track, and for encouraging my interests throughout these eight years. Their consistent support in reading draft chapters and papers, help with navigating the vagaries of graduate school and future opportunities and much needed injections of common sense have helped me become a more grounded, practical and sensible researcher. Thanks to Cliff in particular for proofreading my manuscripts and to Willy and Lance for their never-ending, boundless enthusiasm. I am grateful to Neil for supporting my more adventurous research

directions and generously allowing me to work in the intellectually sparkling environment of the Shubin lab, and to be able to interact with and learn from the amazing postdoctoral researchers there, including Shiri Kult-Perry, Neelima Sharma, Sam Nor Thanks to Andrew Gillis for his enthusiastic support and mentorship during my time at MBL, and for training me from the ground up to do embryology on skates.

Thanks to Marco Lopez, Theresa Christiansen and Noel McGrory for being the best mentees and collaborators anyone could have ever asked for, and for your exceptional diligence and tenaciousness throughout your time here. I am excited, and proud, to see what the future holds for you.

Thans to all my teachers over the years, including Phil Donoghue, Nipam Patel, Seth Finnegan, Brent Mishler and Shyamala Krishnan– I could not have gotten here without your mentorship.

This journey would not have been possible without the support and friendship of current and former members of the Coates and Prince labs. Thanks in particular to Abby Caron for being a phenomenally supportive, compassionate, encouraging lab mate, and for being a co-traveller in this journey with me from the very beginning. I am also deeply grateful to Elaine Kushkowski for being a fantastically wonderful friend, and for taking the time to help me with experimental directions and for always being around to commiserate in the less fortunate of times. Elaine and Abby, thank you for all these years. Thanks to Puddles Kushkowski for never failing to deliver smiles when it mattered most.

Thanks to Ben Otoo, Stephanie Sang, Tetsuto Miyashita, Kristen Tietjen, Ana Beiriger, Noor Singh, Manny Rocha, Lisa Schnetz, Kamil Ahsan, Michael Wen and all the members of the Prince and Coates labs for making graduate school a healthy, happy experience through the years. I could not have asked for a better group of colleagues and mentors. Manny, thank you for being a wonderful mentor during my first rotation in a developmental biology laboratory.

I am also immensely grateful to the current and former members of the Organismal Biology and Anatomy department, and the Committee on evolutionary biology including Reuben Ng, Melissa Wood, Abhimanyu Lele, Alec Wilken, Magdalen Mercado, Stephanie Baumgart, Gayani Senevirathne, Alexa Wemberly, Sam Gartner, Kelsy Stilson, Emily Hillan, Rossy Natale, Selena Martinez, Laura Hunter and so many others for being a phenomenal cohort, and for your enthusiasm and support throughout this process.

Thanks to faculty in the Darwinian Sciences cluster including David Jablonski, Graham Slater, Callum Ross, Urs Schmidt-Ott, Zeray Alemseged, Paul Sereno, Robert Ho, Sue Kidwell, Zhe-Xi Luo and Mark Westneat for their wisdom and enthusiastic support at every phase of my journey. Thanks to Callum and Georgina Voegele for allowing me the incredible experience of learning human anatomy.

A very special thanks to Audrey Aronowsky and Marcy Hochberg for their unfailing and incredible diligence in helping me navigate the intricacies of academia.

Thanks to Nidhaanjit Jain, Kaleb Sellers, Andrew Pocklington, Grace Garrity and the rest of the Jimmy's crew for many nights of insightful discussions and debates and for

being an essential support system. Thanks to Athindra, Vishnu, Bernadette, Nitin, Swati, Rukmini, Priya, Raj and Maya for wonderful food, frolic and conversation and ensuring Chicago always felt like home. And finally, thanks to my parents, Uma and Venkat, and my grandmother, Revathy, for unfailingly supporting all my interests and passions, including my science for three decades, your wisdom and guidance, and your ever-present affection.

For chapter 2, I would like to thank Willy Bemis, Lance Grande, Cliff Ragsdale and Neil Shubin for extended helpful discussions and comments on drafts of this manuscript. I am also grateful to Andrew Gillis, Philippe Janvier, Tetsuto Miyashita, Ben Otoo, Abby Caron, Joaquin Navajas Acedo and members of the Coates, Prince and Shubin groups for generously sharing their expertise and discussing all aspects of this work. I am indebted to Richard Dearden, and a second anonymous reviewer, for their thorough and thoughtful reviews, which improved the manuscript. I am grateful to Bill Simpson of the Field Museum of Natural History, Chicago, and Stig Walsh of the National Museum of Scotland, Edinburgh, for access to collections and support throughout the use thereof. Figs 8 and 9 from Stone (1928) reprinted with permission from the *Journal of Comparative Neurology* (Wiley).

For chapter 3, I would like to thank Tatjana Piotrowski for providing the *Tg(sox10:gal4;UAS:NTR-mCherry)* and *Tg(cldnB:GFP)* transgenic lines and for helpful discussions at the inception of the project. I thank Katie Kindt for providing the *Tg(Hgn39d:EGFP)* enhancer trap line, Lindsey Barske for providing the *Tg(-28.5Sox10:cre;ef1a:loxP-dsRed-loxP-egfp*) line, and Hugo Parker and Robb Krumlauf for providing the *Tg(dRA:GFP)* insertion line. I would like to thank Ryan Anderson for

invaluable advice on use of nitroreductase lines, and for sharing Nifurpirinol reagent with me. I am grateful to Karen Echeverri for generously making her space and equipment available to us during our visits to the Marine Biological Laboratory, and to Andrew Gillis and Cliff Ragsdale for providing helpful comments on the manuscript. I would also like to thank Adam Kuuspalu, Elaine Kushkowski, Michael Wen, Chris Bjornsson, Carsten Wolf, and Christine Labno for advice and assistance with imaging and image processing. Finally, I thank Adam Kuuspalu, Vanity Spruill, and Troy McInerney for expert zebrafish care.

For chapter 4, I would like to thank Tatjana Piotrowski and Joaquin Navajas Acedo for sharing the *Tg*(*CldnB:GFP*) line, and Katie Kindt for the *Tg(Hgn39d:GFP*) line. I am grateful to Sam Norris for advice on clearing methods, and to Christine Labno, Adam Kuuspalu, and Chris Wreden for imaging training and assistance. I thank Elaine Kushkowski for designing the larval zebrafish molds and assisting with 3D printing, and Isabella Cisneros for performing an initial comprehensive literature review of lateral line innervation. My thanks to members of the Prince Lab and Michael Coates for helpful feedback throughout the course of this study, and to Cliff Ragsdale and Andrew Gillis for their expert comments on the manuscript.

I am also indebted to my sources of funding, the Eunice Kennedy Shriver National Institute of Child Health & Human Development of the National Institutes of Health award T32HD055164, the Department of Education GAANN Training in Integrative and Comparative Neuromechanics award P200A220020.

CHAPTER ONE: INTRODUCTION

The lateral line: form and function

The lateral line system is a sensory modality ancestrally found in all vertebrate lineages. It consists of a mechanosensory and electrosensory component, used to detect stimuli in aquatic environments. The system is essential for key behaviors like schooling, predation and escape. The mechanosensory lateral line consists of a network of canals (embedded in the dermis) or superficial grooves on the head and trunk of the organism. Situated within these canals are receptor units called neuromasts, consisting of central hair cells surrounded by support cells, and connected to the medial octavolateral nucleus of the hindbrain by afferent nerves. These neuromasts serve to detect flow stimuli and currents as the water flows over them, owing to a deflection of their hair cells. These stimuli are then transmitted to the brain and utilized by the fish to interpret changes to water current, velocity and acceleration. Recent studies have revealed other important functional roles for the lateral line system. It has been noted that fish use the lateral line to differentiate between self-generated eddy currents and water flow from other fish near them. Further, it has also been suggested that the lateral line and auditory system, which also contains hair cells, may be part of a larger bioacoustic sensory modality (Webb et al., 2008). Sound also travels through the water in the form of compression waves. While the auditory system broadly perceives ‘far-field’ acoustic stimuli and the lateral line system detects ‘near-field’ changes to water current, the distinction between the two remains blurred, and it is possible that the lateral line system functions along with the auditory system and the Weberian apparatus to process both sound and current information (Webb et al*.,* 2008).

Figure 1-1 is a representative teleost, based on the mooneye *Hiodon* adapted from Hilton (2002) and its lateral line system. The lateral line network is differentiated into distinct head and trunk components, which, as discussed in the following section, might be under the control of different developmental regulation. Significantly, vertebrate lineages exhibit characteristic differences in the morphology of their lateral lines, and these differences have long contributed to the morphological character sets used to determine taxa, both extinct and extant. Thus, lateral lines provide a rich data set, evident in fossils as well as living forms, for studying the evolution of a sensory system. Furthermore, lateral lines are more broadly distributed in vertebrate phylogeny than many of the anatomical innovations often associated with the evolutionary successes of major subgroups within the clade. Examples include jaws, paired nostrils, and paired fins. Accordingly, the changes evident in this sensory network as it evolved in response to these radically transformed vertebrate anatomies are ripe for systematic investigation.

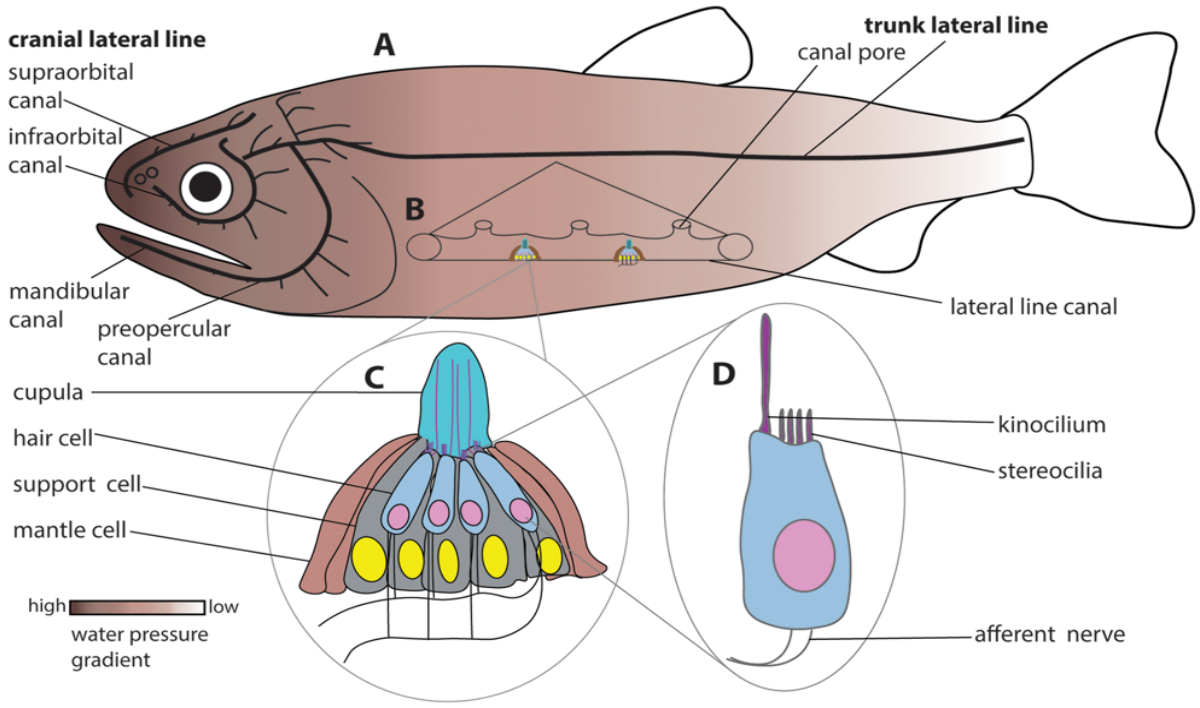

Figure 1-1: Basic structure of lateral lines

(A) Basic structure of lateral lines,with a model teleost fish adapted from Hilton (2002) showing components of cranial and trunk lateral line networks (black). Colour gradient indicates distribution of water pressure across body, after Mogdans *et al*., (2019). **(B)** Detail of trunk canal section illustrating neuromasts between pores opening externally. **(C)** Neuromast structure: hair cells surrounded by support cells, enveloped by layer of mantle cells; hair cell sensory cilia extend into jelly-filled cupula. **(D)** Single hair cell showing kinocilium and stereocilia, connected to afferent nerve.

Lateral line development

Mechanosensory lateral line systems (both neuromast receptors and their concomitant nerves) develop from ectodermal thickenings called placodes. Placodes are formed lateral to the neural crest in a domain called the pre-placodal ectoderm (Schlosser 2006). Apart from lateral line organs, vertebrate placodes form key sensory structures including the olfactory capsule, otic vesicle, lens of the eye, and parts of sensory

ganglia. These placodes can be broadly grouped into an anterior domain comprising the adenohypophyseal, trigeminal, lens, and olfactory placodes, and a posterior domain comprising the otic and lateral line placodes, along with the epibranchial placodes that form the ganglia of a subset of cranial sensory nerves (reviewed in Anselmi et al. 2024). Lateral line placodes flank the otic vesicle: the pre-otic and post-otic lateral line placodes form the anterior and posterior lateral line systems, respectively. Over the course of development, these placodes delaminate and migrate through the ectoderm as primordia of the lateral line. Primordia formed by pre-otic placodes migrate rostrally, while those formed by the post-otic placodes migrate caudally. At the same time, a deep component of each of these placodes develops into neuroblasts. These neuroblasts mature into bipolar sensory neurons, which send projections toward the hindbrain as well as axons that follow the migrating primordium. The lateral line is unique in being a placode-derived sensory system that forms receptors along the entire antero-posterior axis of the embryo and is the only placodal sensory system present on the trunk. Contrary to an early study (Collazo et al. 1994), which suggested that neural crest cells contribute to lateral line receptors, subsequent data have decisively shown that lateral line receptors are placode-derived in a wide variety of vertebrates (Modrell *et al*., 2011, Gillis *et al.,* 2012). Neural crest cells nevertheless likely contribute to the ganglia of lateral line systems, as has been demonstrated in zebrafish (Kague *et al.,* 2012). Northcutt (1989) suggested that vertebrates ancestrally possessed six lateral line placodes. However, this hypothesis has not been verified through embryological observation in evolutionarily relevant clades, in part owing to the difficulty of visualizing individual placodes.

Most of our current understanding of the molecular underpinnings of lateral line development comes from studies of the posterior lateral line in zebrafish (*Danio rerio*), which has served as an exemplar model of collective cell migration (reviewed by Baker & Piotrowski, 2014). In zebrafish, the posterior (trunk) lateral line primordium originates from a placode that develops just posterior to the otic vesicle. This placode and its derivatives all express the transcription factor gene *eya1*, a member of the *eyes-absent* family, throughout development (Sahly et al. 1999). Once formed around 19 hours post fertilization (hpf), the club-shaped posterior lateral line primordium begins to migrate caudally just beneath the skin, aligned with the horizontal myoseptum, reaching the caudal tip of the animal by 48 hpf (Dalle Nogare and Chitnis 2017). Its superficial location, coupled with the transparency of developing zebrafish embryos, has made the zebrafish lateral line system a superb candidate for real time *in vivo* imaging (e.g. Dalle Nogare et al., 2017). Moreover, transgenic lines have been developed that specifically label the zebrafish lateral line system, in particular the frequently used *CldnB:GFP* transgenic (Haas and Gilmour, 2006). Imaging studies have revealed, that during its migration, the primordium is divided into a distinct leading domain, composed of cells with a mesenchymal morphology, and a trailing domain, composed of epithelialized cells. The trailing domain forms rosettes of cells, which are periodically (once every five somites) ‘dropped off’, each ultimately becoming a neuromast. Although the primordium continues to proliferate, it becomes smaller as migration proceeds, and ceases to migrate at the tip of the embryo’s caudal peduncle.

The availability of genetic tools in the zebrafish system has helped uncover the molecular mechanisms that control the migration of the posterior lateral line primordium.

First, it was discovered that a chemokine, Cxcl12, is expressed along the horizontal myoseptum and plays a role in guiding the migration of the primordium (Haas & Gilmour, 2006). In mutants for *cxcl12* the primordium stops migration partway, and 'tumbles', reversing its direction. Directional movement of the primordium suggests the presence of a chemokine gradient. However, the chemokine is expressed in a continuous strip and not a gradient. These data corroborate classical studies using surgical fusion approaches, which we can now interpret as indicating that the chemokine is unlikely to form a gradient. Harrison (1903) surgically fused the heads of two differently pigmented frog embryos. If a chemokine had been expressed in an A-P gradient, the trunk primordium of one animal should have ceased migration at the point of fusion (since the gradient would be reversed here). Instead, the posterior primordium continued to migrate in its normal direction, even migrating on to the fused second head (Harrison, 1903). We now know that rather than following a polarized chemokine gradient, the primordium is instead polarized itself, with two different chemokine receptors, Cxcr7 and Cxcr4, expressed in leading and trailing domains respectively. Here, the receptor Cxcr7 acts as a local 'sink' to the chemokine, generating a local gradient (Boldajipour et al., 2008) within the primordium, thus giving it directionality. Further, there is a Wnt signalling domain in the leading edge of the primordium, which induces Fgf signaling in the trailing domain. Wnt and Fgf signalling mutually repress each other, producing separate Wnt and Fgf domains within the primordium (Aman and Piotrowski, 2008). Fgf signalling in the trailing zone in turn induces Delta/Notch signaling, which initiates epithelialization of cells, which then form rosettes (Dalle Nogare & Chitnis, 2017). As these rosettes leave the Wnt domain, they get dropped off

as proneuromasts. These proneuromasts then induce *atonal-1* expression in a central cell (mediated by lateral inhibition), which then matures into a hair cell of the neuromast. These genetic interactions have been extensively computationally modeled, and it has been shown that the number of cells in the initial primordium and the extent of Wnt and Fgf signaling determine the migratory speed, morphology and number of neuromasts (Dalle Nogare & Chitnis, 2017).

As ontogeny proceeds, the lateral line system gets greatly expanded, with the addition of both canal and superficial neuromasts. At approximately 48 hpf, a second primordium migrates along the horizontal myoseptum adding more trunk canal neuromasts (Sapède et al. 2002). Interneuromast cells which are initially deposited between the primary neuromasts later mature into neuromasts. This maturation is initially inhibited by signals from the glial cells that surround the posterior lateral line nerve. As the fish grows in size, the nerve moves further away from the string of interneuromast cells and this inhibition is reduced, inducing maturation at stage (Lopez-Schier & Hudspeth, 2005). Beginning at 3 days post fertilization (on the operculum), superficial neuromasts proliferate as “stitches” alongside the main trunk canal neuromasts (Wada et al., 2013). Further, new superficial neuromasts are added in the head as late as 15 days post fertilization (dpf) through a variety of mechanisms detailed in Chapter 4.

Though studies in zebrafish have provided extensive detail on the molecular underpinnings of posterior lateral line development, significant anatomical and taxonomic gaps remain. First, while posterior lateral line primordium migration is disrupted in the absence of chemokine signaling, the anterior lateral line in these

mutants develops normally, suggesting that anterior lateral line migration is under the control of different factors. Second, it has not been demonstrated whether Cxcl12 or a related chemokine mediates posterior lateral line development in other taxa. This is pertinent because the development of posterior lateral lines differs significantly in morphology in different organisms. While the zebrafish posterior primordium migrates, dropping neuromasts in its wake, in other taxa (e.g. chondrichthyans), the primordium elongates via cell division, forming a ridge along the flank of the embryo (for example in *Squalus acanthias,* Johnson, 1917). The ridge then fragments, forming individual neuromasts. Figure 1.2 contrasts the two modes of development: fragmentation and

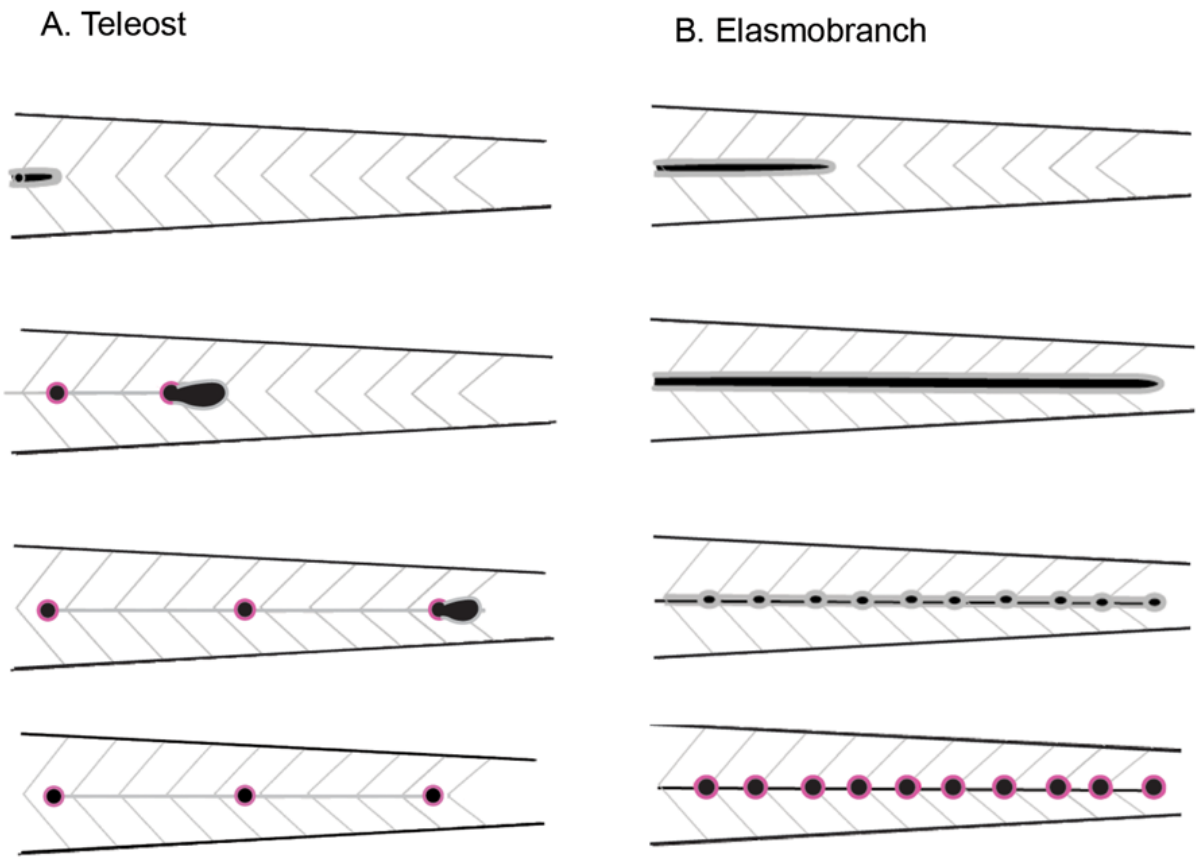

Figure 1-2: Contrasting modes of development (elongation and fragmentation) between the teleost and elasmobranch trunk line

migration. It was previously assumed that both head and trunk lines in chondrichthyans elongate and fragment, but this may not be the case. In Chapter 5, I discuss preliminary data suggesting that the pectoral line in skates may combine migratory and elongating primordia. Other taxa, e.g. amphibians, have elongating primordia on the head and migrating primordia on the trunk (Harrison 1903; Winklbauer & Hausen, 1985). Stone (1928) showed that when pre-otic and postotic primordia are interchanged, both primordia elongate and form a ridge, suggesting the trunk primordium is competent to elongate when on the head, but the head primordium does not have the competence to migrate like the trunk primordium, even when transplanted to the trunk. There are no data on the molecular underpinnings of elongating primordia, though it is possible that FGF and Wnt signalling again mediate their development, in a similar manner to the zebrafish migratory trunk primordium. It was further assumed that all teleost primordia—both head and trunk—are migratory (Lekander, 1949), but studies on the channel catfish have shown that head primordia in this taxon elongate and form ridges. In Chapter 3, I discuss my data indicating that cells of the infraorbital line in zebrafish also elongate into a ridge and coalesce to form neuromasts, as opposed to being migratory. In the absence of outgroup data from lampreys and hagfish, the phylogenetic signature of elongating and migrating primordia—what the plesiomorphic condition is— remains unclear.

Phylogeny of lateral lines: patterns of loss and modification

Fossil evidence of lateral lines dates back to the earliest known vertebrate whole-body fossils. The early vertebrates *Astraspis*, *Arandaspis* and *Sacabambapsis*, all had lateral lines embedded in their dermal skeletons (Janvier, 1996). Lateral lines are ancestrally

present in all major vertebrate clades, both jawless and jawed, and thus precede the evolution of jaws. Among extant lineages, some form of lateral line system is present in both clades of jawless vertebrates (hagfish and lampreys), cartilaginous fish including sharks, skates, rays and chimaeras, as well as bony fish including both ray-finned fishes and all three lineages of lobe- finned fishes (lungfish, coelacanths and amphibian tetrapods). The composition of the lateral line system however is different in various taxa. As previously mentioned, the lateral line can consist of both mechanosensory and electrosensory units. Among the cyclostomes, lampreys have both mechanosensory and electrosensory lateral line systems, while hagfish have likely lost just the electrosensory component. Available data (Braun & Northcutt, 1997) suggest that hagfish may possess mechanosensory cells, but the complete anatomy and peripheral innervation of these cells has not yet been described. Among jawed vertebrates, chondrichthyans possess both mechanosensory and electrosensory systems. Within tetrapods, electroreception is present in salamanders and caecilians (Roth et al., 1992). Among ray-finned fish, neopterygians (gars, bowfin, and teleosts) have lost electroreception. Some teleost lineages have secondarily evolved electroreception (reviewed in Piotrowski & Baker, 2014). All lateral lines, both mechanosensory and electrosensory have been lost within the amniote lineage, although the pattern of loss in this characteristically terrestrial lineage with the occupation of land remains unclear. The story is more complicated in lissamphibians. Stem lissamphibians seem to have lost the entire lateral line system at least in adult stages (eg *Balanerpeton,*Milner and Sequeira, 1993). It is however possible that the system evolved into a network of free neuromasts on the skin, which would not leave fossil evidence. However, some extant

lissamphibians such as axolotls and aquatic caecilians retain lateral lines well into adulthood. It is unclear if the lateral line system in these clades was secondarily evolved, or whether stem lissamphibians retained a larval lateral line, implying heterochrony in extant aquatic lissamphibians. Figure 1-3 summarizes the presence and absence of different lateral line components across vertebrate diversity. Lateral line-like systems have secondarily evolved in several amniote groups including the electrosensitive bills of platypuses (Gregory et al., 1987) and the trigeminal-innervated mechanosensory cells on the snouts of crocodylians (Leitch and Catania ,2012). However, there is no detectable lateral line placode in amniotes, and the aforementioned sensory systems are likely to have evolved convergently.

A key issue in understanding the evolutionary origin of the lateral line system is the difficulty in a recognizable outgroup pre-condition to lateral lines in vertebrates. All vertebrates (with the exception of amniotes) ancestrally have lateral lines, but no clear homologue of the system is visible in the nearest sister groups to vertebrates, the tunicates and cephalochordates. Recent data have suggested that a 'coronal sensory organ' in adult tunicates is composed of hair cells and support cells innervated by afferent and efferent nerves. This morphological similarity (Burighel et al., 2003) has been used to suggest that the coronal organ is a homologue of the lateral line system in vertebrates. Further bolstering this hypothesis, orthologues of vertebrate hair cell markers like *atonal1* have been identified in tunicates, but not localized to hair cells (Rigon et al., 2013). However, these genes are also conserved across bilaterians: for example, being expressed in the mechanosensory chordotonal organs in fruit flies (Jarman et al., 1993). Consequently, it is possible they are part of a more deeply conserved regulatory complex involved in multiple forms of mechanotransduction, being repurposed every time a

mechanosensory system evolves. In vertebrates, placodes are organized into an anterior domain (comprising the adenohypophyseal, trigeminal, olfactory and lens placodes) and a posterior domain (comprising the otic, lateral line and epibranchial placodes). Vertebrate hair cells develop exclusively from the posterior placodal domain, while the tunicate coronal sensory organ develops from an anterior placodal domain, casting doubt on whether the two might be homologous. It has been suggested that the ancestor of tunicates and vertebrates possessed the ability to form hair cells from both anterior and posterior placodal regions, and that this ability was differentially lost in both the groups. However, this hypothesis is yet to be tested, given that the nearest outgroup

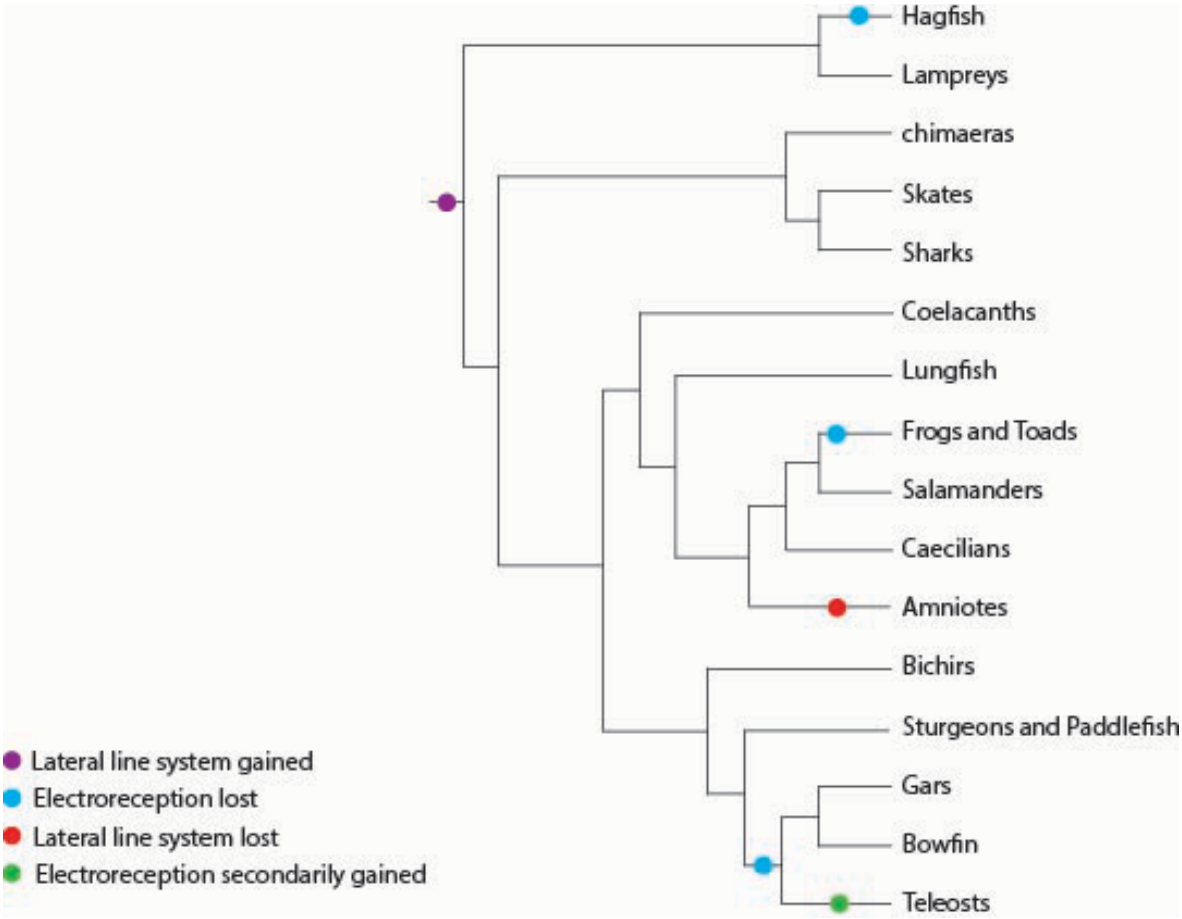

Figure 1-3: Phylogenetic signature of lateral line systems

to both tunicates and vertebrates—the cephalochordates—seems to have no hair cell-like structures.

Historical overview

A foundational question in sensory system research is reconstructing the ancestral morphological condition and delineating how this condition was modified in various groups across evolutionary morphological transitions. The most recent, integrative approach to answering this question with reference to the lateral line system, was by Northcutt (1989) who reconstructed a putative ancestral vertebrate condition based on inferences from both fossils and embryos. Northcutt was the first worker to take a cladistic approach to the question and compare lateral line morphologies in all major vertebrate clades. He hypothesized that the ancestral gnathostome had six lateral line branches, innervated by six lateral line nerves. This hypothesis was based on embryonic data from axolotls (Northcutt et al., 1994), the shovelnose sturgeon *Scaphirhyncus* (Gibbs and Northcutt, 2004) and the gar *Lepisosteus*, (Song and Northcutt, 1991). Northcutt also hypothesized that these six lateral line branches arose from a set of six independent placodes. Living vertebrate diversity is represented by jawed fishes which include Osteichthyes (bony fishes) and Chondrichthyes (cartilaginous fishes including sharks, rays and chimaeras) as well as jawless fishes (cyclostomes), represented by lampreys and hagfish. Embryological evidence supporting Northcutt's hypothesis of six ancestral placodes, however, used only the three osteichthyan species noted above, with no chondrichthyan or cyclostome representatives. Northcutt's detailed analysis combined developmental data from these three taxa with morphological information (the presence, absence and condition of different lateral line network components) from the fossil record to generate a

hypothesis of what the ancestral condition in jawed vertebrate lateral lines was. This was a maximalist inference, implying that the vast diversity of lateral line morphologies seen in different vertebrate clades arose as a result of differential loss, not independent gains. In essence, the ancestral gnathostome had more lines than found in any descendant lineages, with little room for innovation.

The value of Northcutt's study persists because of how it synthesized data drawn from two separate analytical frameworks. These frameworks were the comparative anatomical approach, primarily pursued by Anglo-American scientists including Westoll (1937; 1941), Watson (1937), Allis (1889; 1901; 1923), Moy-Thomas (1941), and Parrington (1949), which compared the lateral line morphologies of different adult forms in an evolutionary context, versus the approach taken primarily by members of the Stockholm school who used embryological data from a few select taxa to interpret adult variation and the fossil record. The latter was centered on the idea of an embryonic archetype or ground plan and includes monographic works by Stensio (1947), Holmgren (1942), and Holmgren & Pehrson (1949). Key papers of the former school include Westoll's survey of lateral lines on the cheek in teleosts (Westoll, 1937), Watson's survey of acanthodians (stem-sharks) (Watson,1937), Allis' studies of lateral line canals in several living taxa including the smooth-hound shark *Mustelus* (Allis, 1901), the bowfin *Amia* (Allis, 1889), the frilled shark *Chlamydoselachus* (Allis, 1923) and his synthetic work on vertebrate lateral lines (Allis, 1934), as well as Parrington's work on lateral line canals and dermal bones (Parrington, 1949). The Swedish school produced several detailed embryological studies including Holmgren's description of cranial development in sharks and rays (Holmgren, 1940; 1943) and Pehrson's description of

lateral line development in lungfish embryos (Pehrson, 1949). These embryological studies were synthesized by Holmgren (1942) and Stensiö (1947), with a subsequent synthesis and a response by Holmgren & Pehrson (1949). These embryological studies have had a long-lasting impact, being referenced in textbooks (Jarvik 1980) and also used in later analyses of lateral line development (eg., Northcutt, 1989).

The embryological studies of the Stockholm school were focused primarily on inferring the homologies of cheek lines in different fishes, and how lateral lines might have been modified across the agnathan-gnathostome transition. Vertebrate evolution was seen as a transformational series from 'lower' to 'higher' vertebrates, with taxa like *Chlamydoselachus* viewed as displaying primitive characters. For example, *Chlamydosleachus* has six gill slits, which was interpreted as a primitive character and not secondary. Stensiö used *Necturus* (mudpuppy) as a model embryo, while Holmgren and Pehrson used chondrichthyan embryos, particularly *Squalus* and *Torpedo*. Each study produced an embryonic placodal archetype, which was inferred to be modified in different groups through ontogeny (for a detailed analysis of the different morphotypes, see Northcutt, 1989). Fossils and adult forms were interpreted in light of these embryo archetypes. For example, the lateral lines in *Acanthodes* (a kind of early shark) were seen as a transformation of the lines in an embryonic *Squalus* (Fig 1-4). This interpretation was further bolstered by a reconstruction of lines in single embryo of *Chlamydoselachus*, which was interpreted as a primitive shark. *Chlamydoselachus* was thought to be primitive because it was seen to possess morphological characters representative of early vertebrates in the fossil record, including six gill arches. Further, fossil agnathans (particularly heterostracans) were compared to the only living jawless

vertebrates with lateral lines–lampreys– to deduce how lateral lines may have changed across the agnathan/gnathostome transition. Holmgren's works (e.g., Holmgren 1942; 1949) hypothesized that a gnathostome lateral line network arose by the modification and reduction of lines from a heterostracan-like ancestor. Heterostracans have more lateral line components than any other vertebrate lineage (Northcutt, 1989). These lines are also embedded deep in the dermal skeleton as canals, which implies a tractable fossil record of lateral lines. The Stockholm school argued that this represented the ancestral condition, and lateral lines in other, descendent, vertebrate lineages arose through loss or modification of such a heterostracan condition.

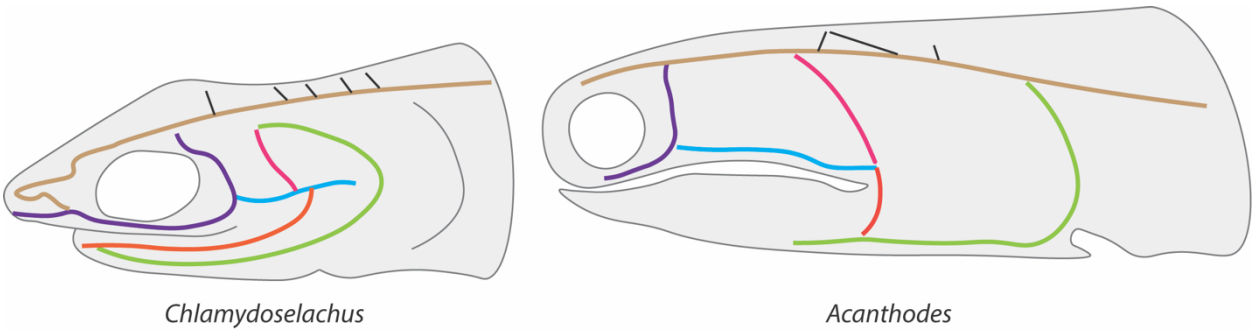

Figure 1-4: Homologization of lines between Chlamydoselachus and Acanthodes based on Holmgren 1942. Homologous portions between the two taxa indicated by the same colour

This hypothetical ancestor had a series of longitudinal lines extending antero-posteriorly along the body, connected by a series of segmental 'transversal' lines running dorso-ventrally (Holmgren, 1942). Lampreys were seen as primitive vertebrates, and interpreted in light of fossil jawless fishes, particularly heterostracans. Lampreys have a suprabranchial line running along the gill pores (Marinelli and Strenger, 1954) which Holmgren and Pehrson hypothesized to be homologous to the lateral of the two

longitudinal lines in heterostracans. Further, they hypothesized that the lamprey medial longitudinal line is homologous to the main trunk line in jawed vertebrates. With these morphological anchors in place, it was hypothesized, through a series of hypothetical transformational stages, that either a pair of the ventrally directed transverse lines (Holmgren, 1942) or two ventral longitudinal lines (Holmgren & Pehrson, 1949) extended on to the newly evolved mandibular territory. Most jawed vertebrates lost one of these two lines, though two mandibular lines on the jaws of some supposed primitive forms like the *Chlamydoselachus* or lungfish were considered holdovers of this evolutionary transition. Figure 1-5 schematizes this proposed transition from heterostracans to jawed vertebrates.

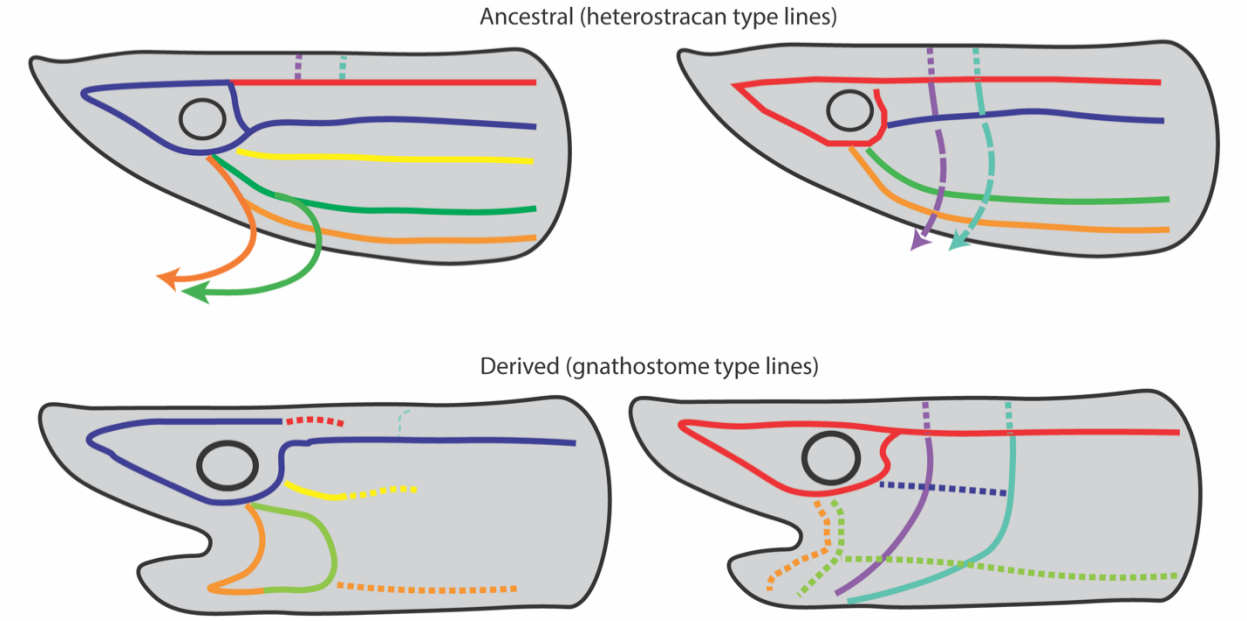

Figure 1-5:Schematized transitions from an ancestral (heterostracan) to a derived (gnathostome) type of lateral line configuration based on Holmgren and Pehrson, 1949 (left) and Holmgren, 1942 (right)

The idea that frilled sharks are primitive living ancestors was a holdover from previous descriptions and inferences (Bashford and Grudger, 1930). Modern

evolutionary understanding based on morphological (Villalobos-Segura et al., 2022) and molecular (Naylor et al., 2012) data has also shown that taxa like *Chlamydoselachus* are derived, like other sharks, and thus not fully representative of any ancestral condition. Further, though lampreys were compared to jawed vertebrates, there remains no information on the ontogeny of lamprey lateral lines. Finally, other workers have pointed out (e.g. Disler, 1961) that the descriptions of chondrichthyan embryos themselves might warrant reexamination.

The alternate approach to the Stockholm school was the one primarily taken by Anglo-American palaeontologists, who compared adult morphologies in fossil and living taxa. These studies were primarily concerned with the homology relationships of different components of vertebrate skulls and saw the lateral line as a useful criterion for determining such homologies. It was hypothesized by Westoll (1937) that bones carrying lateral lines were more stable through evolutionary time than other dermal bones, and this inference was used to homologize bones based on lateral line canal components in them.

The assumption that bones carrying lateral lines are more evolutionarily stable led to the speculation that sensory cells of the lateral line network might have an inductive effect on ossification processes. Moy-Thomas (1941) attempted to test this inductive relationship by ablating neuromasts on one side of a developing trout embryo and comparing ossification patterns on both sides. While his study showed that dermal bone developed normally regardless of neuromast ablation, the regenerative capability of neuromasts (Thomas et al., 2015) was unknown at the time, so it is possible that the ablations were incomplete. Further, an inductive potential of lateral lines was called into

question based upon the observation that ossification patterns remain consistent between clades that have lateral lines and clades that have completely lost them.

In an attempt to clarify any potential relationship between lateral lines and dermal bone, Parrington (1949) proposed a new synthesis. He suggested that lateral lines were not inducing dermal ossification, but that some 'morphogenetic field'— with its center correlating with a future center of ossification was guiding the migration of these canals. The hypothesis further suggested that the lateral lines may then induce ossification of these fields. However, these hypothetical fields have never been identified, nor has the hypothesis been tested.

Scope and aims of the thesis

This dissertation takes an integrative approach, combining anatomical, paleontological and developmental data to understand the evolution and development of the lateral line system. In chapter 2, I review the existing literature on lateral line morphologies in a variety of vertebrate taxa, both fossil and extant, and propose a novel synthesis describing the evolutionary trajectory of the system. This chapter also focuses on the relationship between other sensory systems and the lateral line, as well as the relationship between lateral lines and surrounding tissues. Key findings of this chapter include an evolutionary episode of reorganization and remodelling of the lateral line and the inference of a hierarchical relationship between different cranial sensory systems. Chapter 3 focuses on the role development plays in determining the anatomy of the lateral line in an exemplar model, the zebrafish. Focusing on the anterior lateral line of the zebrafish, this chapter aims to delineate the relationship between placodes (which form lateral lines) and another key vertebrate tissue, the neural crest. Examining the

relationship between placodes (which form lateral lines) and neural crest (which forms cranial dermal bone) is an empirical test of Parrington's 'morphogenetic field' theory described above. I show that neural crest cells are necessary for proper lateral line development, and experimental ablation of the neural crest results in stereotypical defects to the cranial lateral line. Chapter 4 focuses on postembryonic development and innervation of the lateral line in zebrafish. This chapter reveals novel patterns of innervation and post-embryonic growth of the lateral line system, including a hitherto undescribed mechanism of nerve-driven expansion of superficial neuromast number. Further, this chapter also includes functional tests of the relationship between nerves and lateral line receptors and shows that innervation is necessary for postembryonic lateral line development.

Chapter 5 synthesizes my findings on lateral line evolution and development. Here, I expand on my macroevolutionary hypotheses from Chapter 2, focusing on specific groups and important evolutionary transitions, particularly the advent of jaws and the vertebrate colonization of land. I explore gnathostome phylogeny in greater detail, focusing on osteostracans- the nearest sister group to crown jawed vertebrates- and stem tetrapods. I explore the phylogenetic patterns of lateral line change and loss in the tetrapod crown: stem amniotes and lissamphibians. I further expand on the different modes of lateral line development, centered around my preliminary findings in a chondrichthyan model, the little skate *Leucoraja erinacea*. I use the skate model to evaluate the placodal origins of some cranial lines. Further, I compare and contrast the developmental morphology of lateral lines between different lineages such as teleosts and batoids. I also speculate on the molecular mechanisms that could underlie lateral

line development and crest-placode interactions in zebrafish anterior lines. I conclude with a discussion of future directions, building primarily on my pilot data from skates.

CHAPTER TWO: RE-MAKE, RE-MODEL: EVOLUTION AND DEVELOPMENT OF VERTEBRATE CRANIAL LATERAL LINES

Summary

Lateral lines are placodally derived mechanosensory systems on the heads and trunks of many aquatic vertebrates. There is evidence of lateral lines in the earliest known vertebrate fossils, and they exist in organisms with widely different craniofacial morphologies – including the presence or absence of jaws, external or internal nostrils, and variable positions of the cranial cartilages with respect to eyes and braincase. Consequently, the lateral lines make an ideal study system to understand how morphological variation in a deeply conserved sensory system responds to overall evolution of the head. However, palaeontological and developmental data have not been integrated to elucidate the history of this system in the context of evolving vertebrate crania. The emergence of new imaging techniques and molecular methods to study ontogeny in non-model systems provides unique opportunities for such a study. This review examines open questions in light of new fossil discoveries that have altered our understanding of vertebrate evolution as well as new insights on the development of non-model taxa. We find that the diversity of lateral lines is not the result of simplification from a complex ancestral condition as previously supposed. Rather, the anterior lateral line systems of living gnathostomes result from an evolutionary episode of reduction and reassembly, both preceding and overlapping the origin of jawed vertebrates. This event is coupled to a marked postorbital to orbital–preorbital shift in the territorial elaboration of the lateral line systems, and we argue that this spatial move likely signals functional change, coinciding with a major enhancement of the gnathostome vestibular system. A version of this article has been published as:

Venkataraman V, Lopez M, Prince VE, Coates MI. Re-make, re-model: evolution and development of vertebrate cranial lateral lines. *Biol Rev Camb Philos Soc*. 2025. doi: 10.1111/brv.70045

I. Introduction

As discussed in the previous chapter, both cranial and trunk lateral lines develop from a suite of cranial neurogenic placodes. These lines are present in all lineages of aquatic vertebrates with the exception of amniotes. This system is composed of specialized receptive organs called neuromasts, which are contained within canals or grooves or embedded superficially in the skin, bones, and scales of the head and trunk (Fig 1-1 A). These neuromasts consist of specialized hair cells surrounded in some cases by support cells (Fig. 1-1 B, C). The hair cells have a prominent kinocilium and a series of smaller stereocilia projecting into a jelly-filled cupula (Fig. 1-1 D). These neuromasts are exposed to water in a lateral line canal, or in a groove, or directly from the surface of the skin in shallow pits. Different neuromasts on different parts of an organism's body contain hair cells polarized in characteristic orientations. Water currents deflect the cilia differentially and this deflection is then transduced as nervous impulses, transmitted from the neuromast organ to the hindbrain *via* afferent nerves.

Fishes use lateral line systems to perceive hydrodynamic stimuli at macro- and microscales. These systems have traditionally been implicated in schooling and orientation to water currents: fish that have had their lateral line network ablated are unable to orient themselves to the direction of bulk water movement. Species-specific adaptations of the lateral line can also filter out mechanosensory stimulation by strong currents, allowing the fish to detect high-frequency stimuli like approaching predators

(Herzog et al., 2017). However, recent functional studies have also shown that this mechanosensory system is part of a broader multimodal 'bioacoustic' network working in concert with the ear to detect auditory signals in the water (Higgs and Radford, 2013).

The study of lateral lines has attracted the interest of three distinct research programmes: palaeontologists and comparative anatomists concerned primarily with the *pattern* and disparity of lateral lines across vertebrate lineages (Northcutt, 1989), functional biologists and neuroscientists researching how lateral line input is processed and behaviours modified in response (Liao, 2006) and developmental biologists concerned with the *process* generating lateral line morphologies in a few easily accessible model taxa (Dambly-Chaudière et al., 2007). Developmental studies have primarily been concerned with the posterior or trunk lateral line, i.e., the component posterior to the otic vesicle. By contrast, palaeontological and functional studies have primarily been focused on the anterior or cranial lateral lines that occupy the skull and head shield. Importantly, data from all three programmes are reciprocally informative. Given our rapidly changing picture of early vertebrate evolution – thanks to new fossil discoveries, new imaging tools and new methods of phylogenetic reconstruction – developmental data gleaned from extant taxa can be used to improve our understanding of lineage-specific patterns of developmental bias or phylogenetic constraint. Reciprocally, comparative embryological approaches in a phylogenetic framework can reveal the developmental mechanisms underlying varied lateral line morphologies. This review focuses on these two approaches: evolution and development of cranial lateral lines.

Palaeontologists have a long-standing interest in lateral lines because of the high likelihood of their preservation within the dermal skeletons of early vertebrates. Furthermore, lateral lines exhibit considerable morphological variation across different lineages. Thus, lateral lines provide a data-rich window on sensory system evolution within the context of major morphological transitions. Examples of these transitions include the advent of jaws and changes in jaw position, changes in the number and location of nostrils, and changes in cranial proportion and position of the eyes. Further, vertebrates have also undergone major ecological transformations: from benthic to nektonic to marginal habitats and from demersal to pelagic and emergent lifestyles. Finally, lateral lines have been linked to hypotheses of dermal bone homology (Moy-Thomas, 1941; Parrington, 1949; Rizzato et al., 2020; Westoll, 1941) and thus feed directly into analyses of phylogenetic relationships.

In parallel, lateral lines are of great interest to developmental biologists. This is largely because the posterior or 'trunk' lateral line cells of zebrafish (*Danio rerio*) provide a tractable model for the study of collective cell migration (Haas and Gilmour, 2006; Chitnis et al., 2012; Dalle Nogare et al., 2017). The molecular mechanisms underlying the migration and morphogenesis of posterior lateral line neuromast primordia have been delineated through myriad studies. However, the more complex and variable anterior (or head) lateral lines have received much less attention (Iwasaki et al., 2020). This is especially significant because current data indicate that the head and trunk lines, at least in zebrafish, are patterned by different developmental mechanisms. But, the zebrafish is just one of nearly 35,000 species of extant teleost fishes (Froese & Pauly, 2024) separated from other bony fishes and cartilaginous fishes by nearly half a billion

years of evolution (Zhu et al., 2022). Given this evident dearth of comparative embryological data, the general *versus* derived modes of lateral line patterning and development across the vertebrates present an area ripe for exploration.

The goals of this review are to re-examine the evolution of the lateral line system in light of new phylogenies and data, both morphological and developmental. We include a discussion of how major evolutionary changes such as the occupation of the water column, the advent of predation, and transformations of cranial anatomy are linked to the origin and disparity of lateral line systems in living taxa. Further, we highlight gaps in the comparative data – taxonomic, morphological and developmental – with a view to setting an agenda for future research. Finally, we identify avenues of study in lateral line evolution that could be answered *via* an integrative approach combining comparative embryology, functional studies, digital visualization, and new phylogenetic analyses.

II. Vertebrate lateral line diversity

(1) General conditions

The disparate patterns of lateral line networks in major extant and extinct vertebrate groups are summarized in Fig. 2-1. This figure is a synthesis of several representative published descriptions for each group and shows an inferred general condition for each. Morphological features of the various kinds of heads have been abstracted to show the relationship of lateral lines to major landmarks including the eyes, nose, and the mouth (Fig. 2-1 A, B). The order of taxa displayed in Fig. 2-1 follows their relative familiarity rather than phylogenetic convention, hence, teleosts are presented first.

The general condition in extant jawed vertebrates, as seen for example in a representative teleost (Figs 1-1A, 2-1C), consists of one main trunk canal running from behind the head to the caudal fin, often referred to as the posterior lateral line. Anteriorly, this line extends as several branches coursing around various cranial openings like the orbits (Figs 1-1A, 2-1C), the nostrils and the operculum, as well as extending along the jaw. These anterior lines are consequently termed the orbital, nasal, pre-opercular and mandibular branches of the lateral line network. This basic pattern is modified or elaborated in different lineages. For example, teleosts, in addition to having elaborated lines (Webb, 1989), can have accessory lines of superficial neuromasts flanking the main head canals (Northcutt et al., 2000)(Fig. 2-1C), and cartilaginous fishes often have additional canals and loops as seen in the rostrum of holocephalans (Didier, 1995)(Fig. 2-1D) or the pectoral fins of batoids (Abe et al., 2012). In some cases, like amphibians or bathypelagic fishes, all lateral lines are composed of neuromasts within grooves in the skin as opposed to canals. However, to understand fully the extent and evolution of vertebrate lateral line diversity, we need to delve into the fossil record.

A selection of exemplar fossil vertebrates is included in Fig. 2-1 to demonstrate the historical diversity of anterior lateral line systems. †'Placoderms' are the earliest jawed vertebrates. Use of a dagger in this context denotes an extinct taxon, and the use of inverted commas denotes uncertainty about whether 'placoderms' constitute a natural group or merely a grade of extinct vertebrates. Nevertheless, †'placoderms' are mostly characterized by the possession of cranial and thoracic skeletons consisting of large plates which preserve clear traces of their lateral line systems. These fishes had diverse

morphologies, ranging from large, predatory open-water swimmers like the arthrodires (for example, †*Dunkleosteus*) to small, benthic taxa including †antiarchs such as †*Bothriolepis* (Janvier, 1996). Recently discovered maxillate ‘placoderms’ (Fig. 2-1E), including the Silurian †*Entelognathus*, are inferred to be ‘†placoderms’ but are also considered to be the sister group of extant jawed vertebrates. Significantly, these are the only ‘placoderms’ known to have lateral lines on the lower jaw (Zhu et al., 2016). It follows that †*Entelognathus* occupies a key position in the transition from stem to crown jawed vertebrates, and the maxillate ‘placoderms’ have prompted a significant reappraisal of relationships among taxa close to the crown gnathostome node(Zhu et al., 2016; King et al., 2017; Li et al., 2021).

Importantly, beyond ‘placoderms’, the evolutionarily deeper stretches of the gnathostome lineage also include a host of jawless groups. Many of these jawless fishes also bear a head shield consisting of large plates and a tail covered in bony scales, thereby extending the total evolutionary record of lateral line system diversity. †Osteostracans (Fig. 2-1F) and †galeaspids (Fig. 2-1G) have dorsoventrally flattened crania, enclosing remarkably detailed internal morphology (Janvier, 1985; Gai et al., 2011). By contrast, †heterostracans, including †pteraspids (Fig. 2-1H), have head shields but no substantial endocranial remains (Moy-Thomas & Miles, 1971). This deficit in the quality of fossil material extends to the very earliest vertebrate body fossils, including †*Astraspis*, † *Arandaspis* and †*Sacabambaspis* (Fig. 2-1I), all from the Ordovician period (Ritchie and Gilbert-Tomlinson, 1977; Sansom et al., 1997; Gagnier et al., 1986; Pradel et al., 2006; Dearden et al., 2023).

From these data, we infer that the general condition for vertebrates is to have one or a series of longitudinal (or trunk) lines extending from approximately the otic region to the caudal end of the animal. Rostrally, extensions of these lines course around apertures in the skull, including the orbits, the nostrils, the mouth and gill openings. However, the eyes of the earliest vertebrates were positioned close to the front of the head (Gagnier et al., 1986). Thus, the lateral line system in these fossils consists of multiple longitudinal lines behind the orbits, often with multiple transverse extensions. These postorbital and dorsal networks are elaborated in †heterostracans and †galeaspids (Fig. 2-1G, H), where such lines may form complex reticulating networks (Janvier, 1996; Yang et al., 2024).

(2) Orbital lines

Orbital lines in modern jawed vertebrates generally consist of a supraorbital and infraorbital line coursing around the eye. Although the two lines are connected caudally in most extant jawed vertebrates, fossil data from early sarcopterygians (Qiao & Zhu, 2010) (Fig. 2-1J), actinopterygians (Gardiner,1984) (Fig. 2-1C) and '†acanthodians' (Fig. 2-1K) (early sharks) (Burrow 2021; Watson, 1937) demonstrate that the primitive condition is the two lines being disjunct caudally. In these cases, the supraorbital lines lie parallel to a stretch of an infraorbital line behind the eye (Fig. 2-1C). Therefore, in modern taxa, the connections between two orbital lines both behind and in front of the eyes represent a derived condition but it remains unclear how many times these connections evolved.

Orbits have been modified in both position and size during vertebrate evolution, and the supraorbital and infraorbital lines have shifted accordingly with respect to orbit

location as well as the position of a pineal opening. We note that infraorbital lines are the most consistently present component of the anterior lateral line system throughout vertebrate diversity. The earliest vertebrate condition, as revealed by †heterostracans, †galeaspids and †antiarch 'placoderms' is to have supraorbital lines converging behind the pineal opening (Fig. 2-1H,G, L). In †osteostracans, the pineal opening is located anteriorly, between the eyes, consequently reducing the space for a post pineal commissure, and correlates with a total absence of supraorbital lines (Fig. 2-1F). Similar instances occur in lampreys (Fig. 2-1M), where the pineal is also anterior to the eyes. However, the †anaspids (stem group cyclostomes) are poorly preserved showing few traces of a rudimentary line network (Fig. 2-1N). In living gnathostomes (osteichthyans and chondrichthyans: e.g., Fig. 2-1O, P), orbits are in a much more lateral position relative to the orbits of †osteostracans and †galeaspids and the supraorbital lines connect with the main trunk lines on their respective sides. In some cases, a medially directed supratemporal canal connects the trunk lines of both sides, forming an occipital commissure, posterior to the supraorbital canals.

Pit lines are short grooves in the skin that house superficial neuromasts. In extant forms, the pit lines are generally found in the parietal/postparietal domain. They also occur in extinct taxa, such as the lines found on the nuchal bones of '†placoderms' and the cheeks and jaws of early osteichthyans. The anterior pit line in modern osteichthyans is a short, open groove with superficial neuromasts positioned behind the caudal extremity of the supraorbital line. There are usually two other pit lines, termed the middle and posterior lines, radiating out from the crown of the head. Unlike the

anterior pit line, the middle and posterior pit lines do not bear any obvious spatial relationship to other parts of the anterior lateral line system.

(3) Cheek and jaw lines

The general condition for lines on the cheek of jawed vertebrates is a series of longitudinal and transverse lines posterior to the orbit. This includes, as seen in zebrafish, lateral lines on the preopercle as well as lines on the lower jaw: the mandibular line (Fig. 1-1A). Embryological evidence from several taxa including zebrafish supports morphological data that connect the lower jaw line to a preopercular line: one is a continuation of the other (Lekander, 1949; Iwasaki et al., 2020). The cheek region accommodates the jaw adductor muscles of gnathostomes and is therefore also a derived feature of the group (although rarely recognized as such). Lampreys and other jawless vertebrates do not have a well-defined cheek as such, so the relationship of their postorbital lines to those of jawed vertebrates is unclear. The mandible (lower jaw) is a feature of jawed vertebrates, but mandibular lines are not present in early members of the clade, hence the significance of the mandibular lateral line discovered in †*Entelognathus* (Zhu et al., 2013).

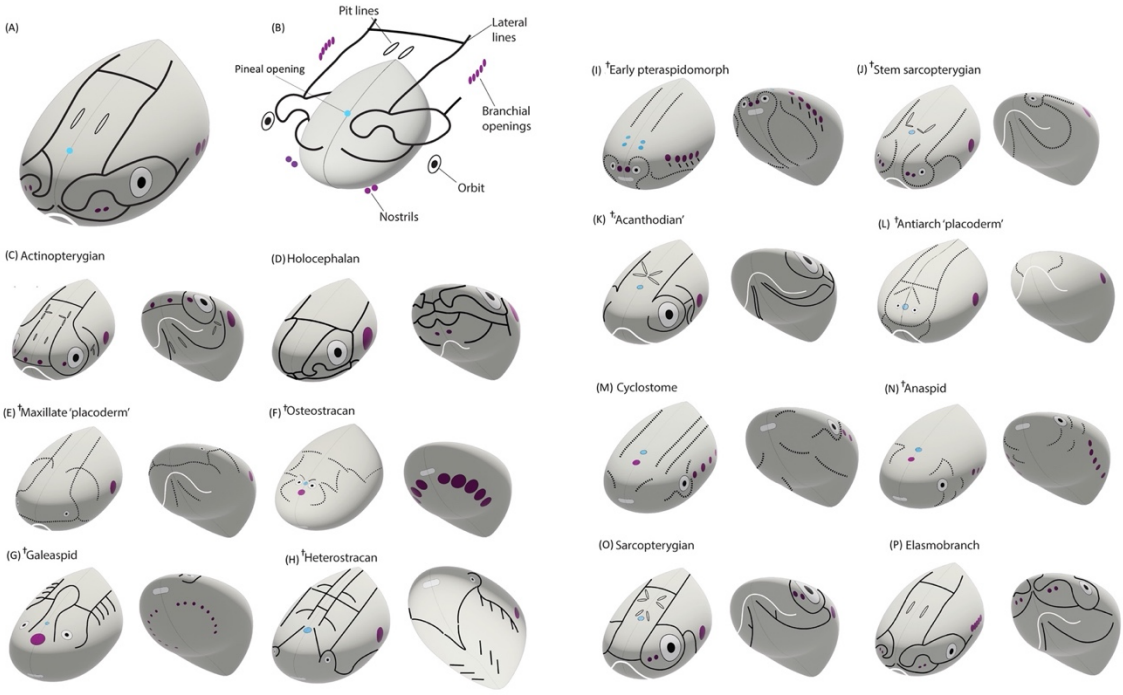

Figure 2-1:Extant and extinct vertebrate cranial models

Each is abstracted from multiple representatives of the taxon in question to illustrate features of the characteristic lateral line networks, highlighting system diversity. A and B provide key to panels C–P. Taxon panel order follows the sequence of taxa discussed in the main text. **(A)** Elasmobranch head in dorsolateral view. **(B)** Same head 'exploded' to show component parts. **(C)** Actinopterygian, after Gardiner (1984), with teleost pit-line pattern after Lekander (1949). **(D)** Holocephalan after Cole (1897). **(E)** Maxillate 'placoderm' after Zhu *et al*. (2016). **(F)** Osteostracan after Janvier (1974, 1985). **(G)** Galeaspid after Shan *et al*. (2020). **(H)** Heterostracan (cythaspid and pteraspid conditions) after Janvier (1996) and Randle *et al*. (2022). **(I)** Early pteraspidomorph (†Astraspid, †Arandaspid and †Sacabambaspid conditions) after Gagnier *et al.* (1986), Sansom *et al.* (1997) and Pradel *et al*. (2006). **(J)** Stem sarcopterygian (†*Guiyu* and †*Psarolepis* conditions) after Yu (1998), Zhu *et al*. (1999) and Qiao & Zhu (2010). **(K)** 'Acanthodian' generalized after Watson (1937). **(L)** Antiarch 'placoderm' after Graham-Smith & Parrington (1978). **(M)** Cyclostome (*Lampetra*) after Marinelli & Strenger, 1954. **(N)** Anaspid (stem-cyclostome) after Smith (1957). **(O)** Crown sarcopterygian *Gogonasus* (stem-tetrapod) after Long *et al*. (1997. **(P)** Crown elasmobranch (squalomorph), after Garman (1888) and Johnson (1917). Use of a dagger indicates an extinct taxon. Blue circles indicate pineal openings.

(4) Sensory system hierarchy and new morphologies

We note that there appears to be a hierarchy in sensory system patterning, with lateral lines shifting to accommodate the changing positions of other cranial sensory systems, particularly the olfactory, visual, and hearing systems. Novel and extreme morphologies help us to understand such apparent hierarchies. For example, body forms can be flattened either dorsoventrally or laterally. Dorsoventral compression may be restricted to the rostrum, as in sturgeons and paddlefish, or involve flattening of the entire body, as in the skates and rays. Lateral flattening can involve extreme asymmetry, as seen in flatfishes (pleuronectids). In each instance, the lateral line system invades new territory, although to different degrees in different lineages. In addition to skates and rays, several other chondrichthyan groups have evolved flattening, including angel sharks and wobbegongs (carpet sharks). In most cases, lateral lines have grown onto the expanded, flattened regions of the body, as seen for example in guitarfish (Garman, 1888). These extended lateral line branches, often misleadingly called scapular lines, run from the main trunk line and grow out laterally (Maruska, 2001). The most extensive flattening in skates and rays involves fusion of the pectoral girdle to the rostral tip of the snout, and in this unique instance, the cranial lateral line canals extend onto the pectoral fin (Ewart & Mitchell, 1895; Maruska, 2001). Notably, these pectoral lines are also unique in being the only example of a rostral (preotic) placode-derived lateral line growing in a posterior direction.

Elongate rostra, not always associated with elongate jaws, repeatedly evolved in both osteichthyans and chondrichthyans. In osteichthyan examples such as sturgeons

and paddlefish, and chondrichthyan examples such as sawfishes and sawsharks (Wueringer et al., 2011), the rostrum is elongate, but the mouth is in a sub-terminal position with the nostrils close to the face (Fig. 2-2A,B). However, despite these similarities in gross morphology, the distribution of the orbital lateral lines differs between these two groups. In sturgeons and paddlefish the infraorbital canal extends onto the ventral side of the snout, forming complex loops, but the supraorbital line terminates abruptly in a proximal position between the nostrils (Fig. 2-2A). By contrast, in sawfishes and sawsharks, both lines run to the anterior tip of the snout (Fig. 2-2B). It appears that nostril position dictates these different patterns of lateral line distribution. In sturgeons and paddlefish, the supraorbital line lies between the anterior and posterior nostril and is perhaps trapped in this proximal domain. In sawfishes and sawsharks, however, both nostrils lie outside the loop of the orbital lines, and therefore the lines are not restricted by nostril position. Conditions in garpike (Fig. 2-2C), another osteichthyan, corroborate this restriction scenario. Garpike have elongated rostra, but these fish have both nostrils positioned at the very tip of the snout. Here, both supra and infraorbital lines extend all the way to the distal extremity and loop around the nostrils. Taken together, these three conditions across two divisions of jawed vertebrates support the idea that lateral lines have their positions dictated by cranial openings such as nostrils. In this regard, the migrating orbits of pleuronectids might provide a further test of the generality of this scenario, in which lateral line network patterning is warped to match the location of other major sensory systems.

Flatfishes (pleuronectids, Fig. 2-2D) develop as bilaterally symmetrical larvae, but through ontogeny begin to lie on one side (the ‘blind side’) and move their orbits,

nostrils and mouth towards the side facing the water column (the ‘eyed side’). During this process, a conventionally symmetric larval lateral line system becomes asymmetric. Recent data (Duarte-Ribeiro et al., 2024) indicate that cranial asymmetry evolved once in flatfishes, and extensive studies (Neave, 1986; Harvey et al., 1992; Voronina et al., 2019) have demonstrated that all members of the group show varying degrees of asymmetry in lateral line positioning. While the morphological diversity of pleuronectiform lateral lines has been documented in detail, there is scant information on how developmental remodelling emerges within the system. It is unclear if neuromasts undergo apoptosis, with new ones arising within the transformed head, or if canals and neuromasts somehow relocate along with a shift of the dermis or change in cranial morphology.

Yet another example of the hierarchical relationship between lateral lines and other sensory systems is evident in the internalization of the posterior nostril in tetrapods, lungfishes, and holocephalans (also known by a variety of other names including chimaeras, ghost sharks, ratfish, and elephant sharks). The ancestral condition for lobe-finned osteichthyan lineages, as exemplified by the early tetrapod †*Tungsenia* (Lu et al., 2012) and early lungfish †*Porolepis* (Kulczycki, 1960; Chang, 1995), was for the orbital line to loop around and encompass both nostrils. However, in intermediate forms like the early tetrapod *Kenichthys*, where the posterior nostril is at the ventral border of the maxilla, the supraorbital line displays a kink, as if it were dragged down with the nostril (Zhu and Ahlberg, 2004). In the case of extant lungfishes both nostrils are internal, with the anterior nostril on the medial border of the lip. Here, both nostrils appear to have ‘broken through’ the loop of the supraorbital line, which

never connects with the infraorbital line. In holocephalans the posterior nostril is once again within the medial border of the upper lip (Howard et al., 2013) but in this instance both nostrils lie outside the loop of the orbital lines, thus no lines are altered or interrupted.

In summary, lateral lines appear to be subordinate or secondary to other sensory systems. The positioning of cranial openings for these systems, like the olfactory or optic, influences the course of the anterior lateral lines. It follows that the phylogenetic legacies of chondrichthyans and osteichthyans – the initial positions of their nostrils relative to the lateral lines – played a major role in determining lateral line morphology.

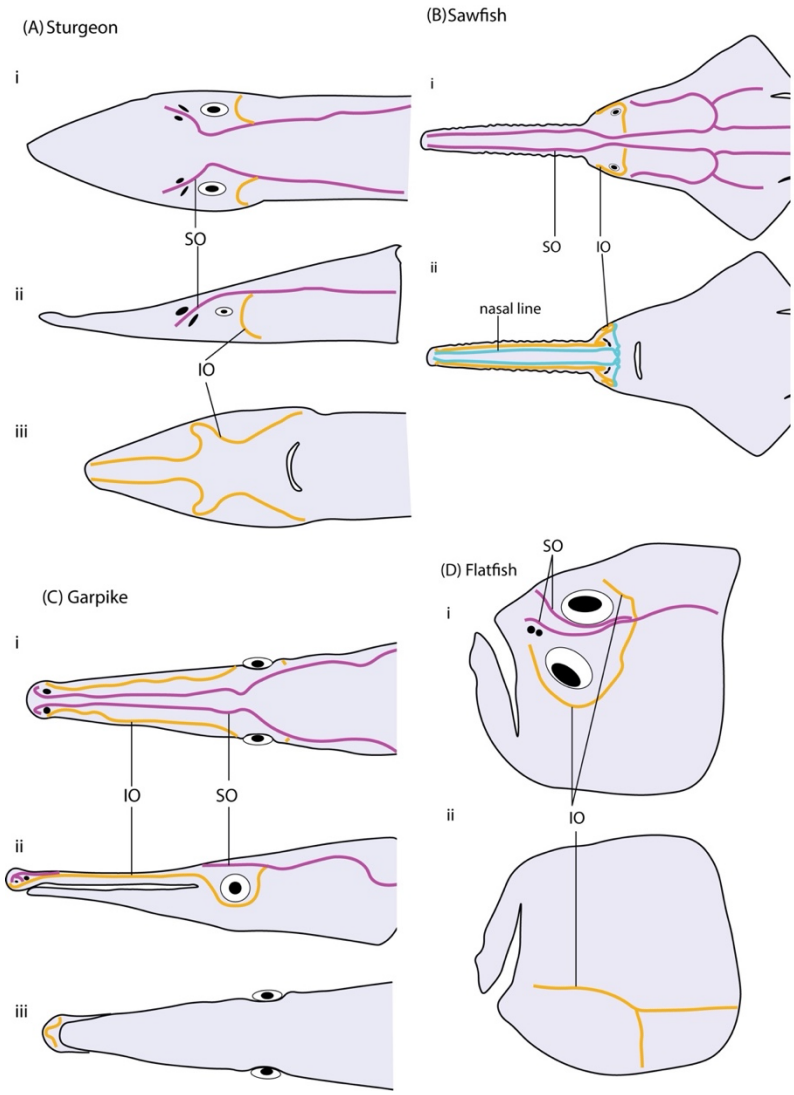

Figure 2-2: Orbital lines on extreme head shapes.

(**A–C**) Examples of rostral elongation showing the relationship of orbital lateral line canals to nostrils. (A) Sturgeon after Gibbs & Northcutt (2004); i, dorsal view; ii, lateral view; iii, ventral view. (B) Sawfish after Wueringer et al. (2011); i, dorsal view; ii, ventral view. (C) Garpike after Song & Northcutt (1991); i, dorsal view; ii, lateral view; iii, ventral view. (D) Flatfish (*Tephrinectes sinensis*) after Voronina et al. (2019); i, dorsal view; ii, ventral view. Supraorbital line (magenta, SO) terminates close to eyes in sturgeons, and extends to rostral tip in sawfishes and garpikes. Infraorbital line (yellow, IO) extends to rostral tip in all cases. Sawfishes have 'nasal' line characteristic of elasmobranchs (blue). Nostrils are shown in black throughout.

III. Lateral lines and surrounding tissues

Lateral lines derive from ectodermal thickenings or placodes in front of and behind the otic vesicle. The preotic placodes form primordia that migrate or elongate anteriorly to form the anterior lateral line network. By contrast, the placodes posterior to the otic

vesicle form primordia that elongate or migrate caudally to form the posterior or trunk lateral line system.

A long-standing area of research has focused on the relationship between lateral line systems and the surrounding dermoskeleton; for a recent review, see Hamm & Gross (2025). Westoll (1936, 1937) argued that the bones carrying lateral line canals were less morphologically variable than other dermal bones; he termed these non-canal bones ‘anamestics’ or filler bones (Hilton et al., 2011). This observation led to a suggestion that the lateral line system developmentally induces ossification of the surrounding dermal bones (Lekander, 1949; Holmgren & Pehrson, 1949). However, Moy-Thomas (1941) ablated the rudiments of the lateral line on one side of the head of an early larval rainbow trout (*Onchorynchus myskiss)* and reported the complete development of frontal bones on both the ablated and unablated control sides, implying that lateral lines are not necessary for dermal ossification to occur. However, neuromasts are known to regenerate after ablation (Williams & Holder, 2000). It is thus possible that neuromasts on the ablated side in Moy Thomas’ (1941) experiments regenerated to allow dermal ossification to occur normally.

Lateral lines might yet be found to influence morphogenesis of specific components of the cranial dermal skeleton. Studies dating back to Allis (1889) indicate that in many fishes the dermal skull bones are produced by two separate developmental modules: a flat, membrane-bone component and a separate cylindrical component surrounding the neuromasts (see Fig. 11 in Grande & Bemis, 1998). These two ossifications may fuse through ontogeny, forming a single dermal bone (Tarby & Webb, 2003; Webb & Shirey, 2003). The cylindrical component forms as the epithelium

underlying the neuromasts invaginates to form a gully, which may then enclose the neuromasts as the apices of the gully contact each other to form a closed tube or canal. Neuromasts might have some inductive potential on the ossification of these grooves and canals. Chang & Franz-Odendall (2014) laser-ablated developing infraorbital neuromasts of larval and juvenile zebrafish, then analysed ossification of the infraorbital bones after the neuromasts had regenerated. They found that canal wall ossification was significantly reduced in all cases, despite the fact that the neuromasts had regenerated, although the overall shape of the infraorbital bones remained unaffected. Based on these findings, the authors inferred that neuromasts have an early inductive effect on the later ossification of the canal wall, but development of the remaining dermal bone is independent of neuromast influence.

While many studies have examined the histological structure of fossil vertebrate dermal skeletons (Sansom et al., 1992; Donoghue, 2002; Giles et al., 2013; Keating & Donoghue, 2016), it is notable that there have been few studies on the histology of fossil lateral line canals or grooves. Further work is needed to explore the evolution of lateral line histology, including the taxonomic extent and history of separate lateral line canal ossifications.

In many chondrichthyans, which lack large dermal plates and have a dermal skeleton made of small scales, those scales abutting the lateral line canals are modified. In holocephalans, the only scales that remain on the trunk resemble incomplete curtain rings, forming a flexible gutter housing the lateral line (Cole 1897; von Lubitz, 1981; Didier et al., 2012). In many †'acanthodians' (early sharks), scales surrounding the lateral lines are larger than other scales of the flank and fins (Watson

,1937) and may be morphologically distinct (Hanke & Wilson, 2006;). All these data suggest that the lateral line might influence the development and morphogenesis of adjacent scales. We suggest this observation deserves further experimental evaluation.

Current comparative data are equivocal on whether canals or grooves were the ancestral condition for vertebrates: available fossil data are insufficient. However, for crown jawed vertebrates, canals appear to be the ancestral condition. But, once again, we do not know if canals evolved at the root of all vertebrates or among the earliest members of the gnathostome lineage. Resolution of this question is hindered by ongoing uncertainty concerning the monophyletic *versus* paraphyletic status of 'placoderms'. Furthermore, it remains unclear if a separate bony lining around the lateral line canals is an osteichthyan synapomorphy. Finally, experimental data (Chang & Franz-Odendaal, 2014), considered together with the observations on scale patterns in chondrichthyans, suggest a possible inductive relationship between lateral lines and mineralized portions of the dermoskeleton.

Embryological studies have explored the interaction between the lateral line and adjacent tissues early in development, particularly to test if the migratory substrate plays a role in guidance or patterning of lateral line systems. Smith et al.(1990) attempted to delineate a potential substrate-driven lateral line guidance mechanism in axolotl (*Ambystoma* mexicanum) embryos. They surgically manipulated the overlying epidermis in front of a migrating posterior primordium, turning it by 90º or 180º. When the epidermis was flipped by 180º, the primordium migrated indistinguishably from controls that had undergone sham surgeries, suggesting the rostrocaudal directionality of overlying tissues was unimportant. However, when the epidermis was turned by 90º, the

primordium ceased to migrate, or turned at the site of surgery and wandered until it encountered the path of another primordium, whereupon it followed the new path. This suggests that migrating primordia follow ‘tracks’ in the overlying substrate. A complete rostrocaudal flip of these supposed tracks does not change primordium migration, suggesting that the tracks are not polarized. While the molecular nature of these tracks and their interactions with the primordium remain unclear, extirpation of the underlying mesoderm (one somite) stalls primordium migration, even with no surgical flipping of the ectoderm. This suggests that the migration is influenced by both overlying epidermis and underlying mesoderm. We speculate that the track in the axolotl mesoderm might be of a chemokine molecule, as has been shown in zebrafish ((Haas and Gilmour, 2006); see below for details). A crucial limitation of these studies is that they have not been replicated for the head. Thus, while these classical embryological approaches have provided important insights into how the trunk lateral line system develops, we have a much more rudimentary understanding of anterior lateral line development.

It is already evident that head and trunk lines differ in their manner of development between different taxa. In zebrafish, both the head and trunk lateral lines develop as a migrating primordium deposits a series of neuromasts (Fig. 1-2A) (Iwasaki et al., 2020; Haas & Gilmour, 2006). By contrast, in a foundational study, Johnson (1917) showed that in a chondrichthyan (*Squalus acanthias*), both the head and trunk primordia elongate and subsequently fragment (Fig. 1-2B). This pattern of elongation and fragmentation is also found in the anterior lateral lines of a wide variety of non-teleost osteichthyans (Allis, 1889; Harrison,, 1903; Beckwith, 1907; Landacre and Conger, 1913; Winklbauer and Hausen, 1983; Northcutt et al., 1994; Modrell et al.,

2011). However, the trunk systems in these osteichthyans exhibit similar migration and deposition patterns to zebrafish. For these reasons, we argue that the general condition for teleosts is unclear, and further note that all relevant data on anterior lateral line development are limited to studies of a single teleost sub-group: the ostariophysans (Landacre, 1910; Lekander, 1949; Iwasaki et al., 2020).

The molecular mechanisms that underlie the development of lateral lines from primordia also remain unclear, with current knowledge derived exclusively from studies in zebrafish(Haas and Gilmour 2006; Dambly-Chaudière et al., 2007; Chitnis et al., 2012; Piotrowski and Baker, 2014; Neelathi et al.,, 2018). These studies have demonstrated that the zebrafish posterior lateral line develops from a migrating primordium (Fig. 1-2A). The primordium follows a track of the chemokine Cxcl12 (C-X-C Motif chemokine ligand 12) (Haas & Gilmour, 2006), which is laid down in a narrow stripe along the length of the underlying trunk paraxial mesoderm. Of note, the embryological experiments of Smith et al. (1990) suggest that a similar track may exist in axolotls, but in the overlying epidermis. Periodic deposition of neuromasts from the migrating primordium is dependent on a feedback loop between distinct Wnt (wingless related integration site) and Fgf (fibroblast growth factor) domains within the primordium (Aman et al., 2011). However, there are no data yet on whether trunk lateral lines in other taxa that are deposited by migrating primordia (e.g. in amphibians, see Smith *et al*., 1990) follow similar chemokine tracks, nor whether Wnt/Fgf signalling are involved. Elongating primordia (Fig. 1-2B) might use entirely different molecular mechanisms to achieve neuromast distribution, including specific spatiotemporal patterns of gene expression. Surprisingly, however, the classic embryological experiments of Stone

(1928) revealed that the head and trunk lateral line primordia of *Ambystoma punctatum* (axolotl) are functionally interchangeable (Fig. 2-3). However, it is unclear from figures 9 and 10 in Stone (1928) whether the anterior primordium, when transplanted to the trunk, migrated like a normal trunk primordium or instead elongated and fragmented. In either case, Stone's (1928) findings suggest that extrinsic signals from the surrounding cranial or trunk tissues must play a major role in patterning the placodal primordia and the lines that emerge from them.

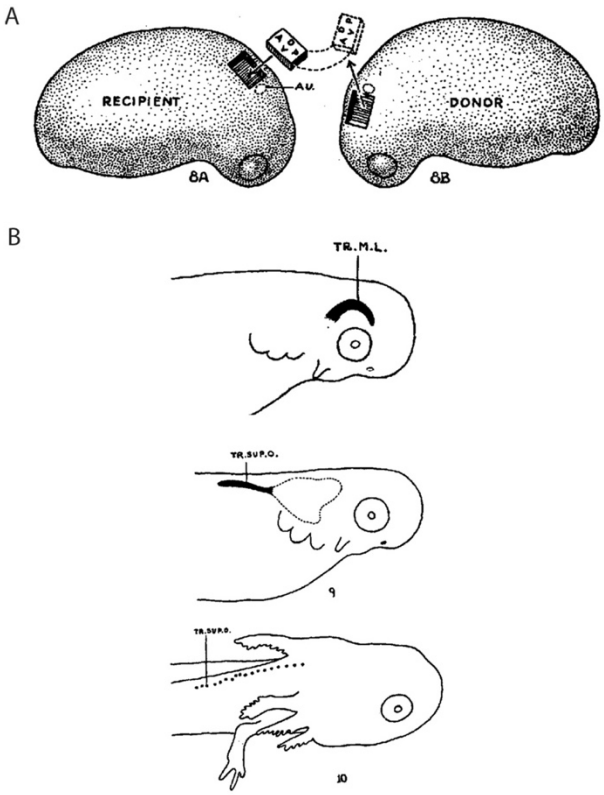

Figure 2-3: Stone's transplantation experiments

(A) Reproduction of figure 8 of Stone (1928) schematizing a reciprocal transplantation approach, moving placodal ectoderm from preotic to postotic domains and *vice versa* between embryos of spotted salamanders (*Ambystoma punctatum*). **(B)** Reproduction of figures 2 and 9 of Stone (1928) *camera lucida* drawings showing that the preotic ectoderm migrated posteriorly leaving behind rosettes of hair cells when transplanted to a postotic domain. Conversely, postotic ectoderm elongated and formed ridges around the

Fig 2-3 cont. eye when transplanted to a preotic domain. Stone (1928) concluded that placodal ectoderm migrates or elongates based on its local environment.

IV. Northcutt's paradigm

Northcutt (1989) provided the first cladistic and rigorously comparative analysis of lateral line evolution. His study combined embryological data from *Ambystoma mexicanum* with palaeontological and anatomical data from diverse sources (Northcutt, 1989; Northcutt et al., 1994) with the aim of reconstructing the ancestral gnathostome lateral line condition. Northcutt (1989) hypothesized an ancestral gnathostome with a set of orbital, mandibular and cheek lines (Fig. 2-4 A). He further argued that these lines arise from six placodes and are innervated by a corresponding set of six placodal nerves. Based on this posited ancestral condition, Northcutt (1989) hypothesized that all diversity evident in extant vertebrate lateral lines resulted from descent with differential loss.

In this respect, Northcutt's work developed ideas put forward in earlier studies (Holmgren, 1942; Holmgren and Pehrson, 1949). However, Holmgren & Pehrson (1949) based their evolutionary scenario on a †heterostracan ancestor extrapolated from a theoretical vertebrate archetype. At that time, †heterostracans provided the earliest available information on fossil vertebrate conditions, hence their significance in these mid-20th century studies. As noted in Section II (Fig. 2-1H), †heterostracan head shields bear a network of longitudinal and transverse lines. Therefore, they theorized that with the advent of a jaw, components of this network extended onto the new anatomical territory of the mandible. Holmgren (1942) and Holmgren & Pehrson (1949) connected their ancestral condition with 'advanced types', representing conditions in extant forms *via* a series of hypothetical intermediates. Unlike Northcutt's (1989)

hypothesis, they included no explicit arguments for gains or losses at nodes in the vertebrate phylogeny. Moreover, they were influenced by the idea that extant 'lower vertebrates', such as the frilled shark *Chlamydoselachus anguineus* and lungfishes, more closely approached these primitive or archetypical states of vertebrate anatomy (Allis, 1923).

By contrast, Northcutt (1989) aimed to reconstruct trait history, generate hypotheses of evolutionary developmental mechanisms, explore form–function relationships, and identify knowledge gaps, all within an explicit tree-based framework (Fig. 2-4B). It is important to note that at this time Northcutt had access to a limited set of fossil data (Moy-Thomas & Miles, 1971). However, since 1989, our best estimates of early vertebrate interrelationships and evolution have changed drastically (Fig. 2-4C). Over 30 years' worth of discoveries have filled gaps in the fossil record in unexpected ways, while generating new questions. New phylogenies of early vertebrates have changed our fundamental understanding of character evolution. The notion of 'higher' and 'lower' taxa has been jettisoned, and *C. anguineus* is neither a living fossil nor a living ancestor. Similarly, it is also clear that cyclostomes (lampreys and hagfish) are far from primitive. Nevertheless, several of the knowledge gaps identified by Northcutt (1989) remain unfilled such as information on the comparative innervation and development of cyclostome lateral lines.

Importantly, Northcutt's (1989) analysis provided an explicit, testable hypothesis: that lateral lines evolved *via* a pattern of gradual reduction, and that traces of this ancestral condition are manifest in the distribution of canals, pit lines, and superficial neuromasts of extant taxa. In the next section, we explore this hypothesis in the light of

updated phylogenies (Fig. 2-4C), acknowledging both stable and unstable areas of the evolutionary tree.

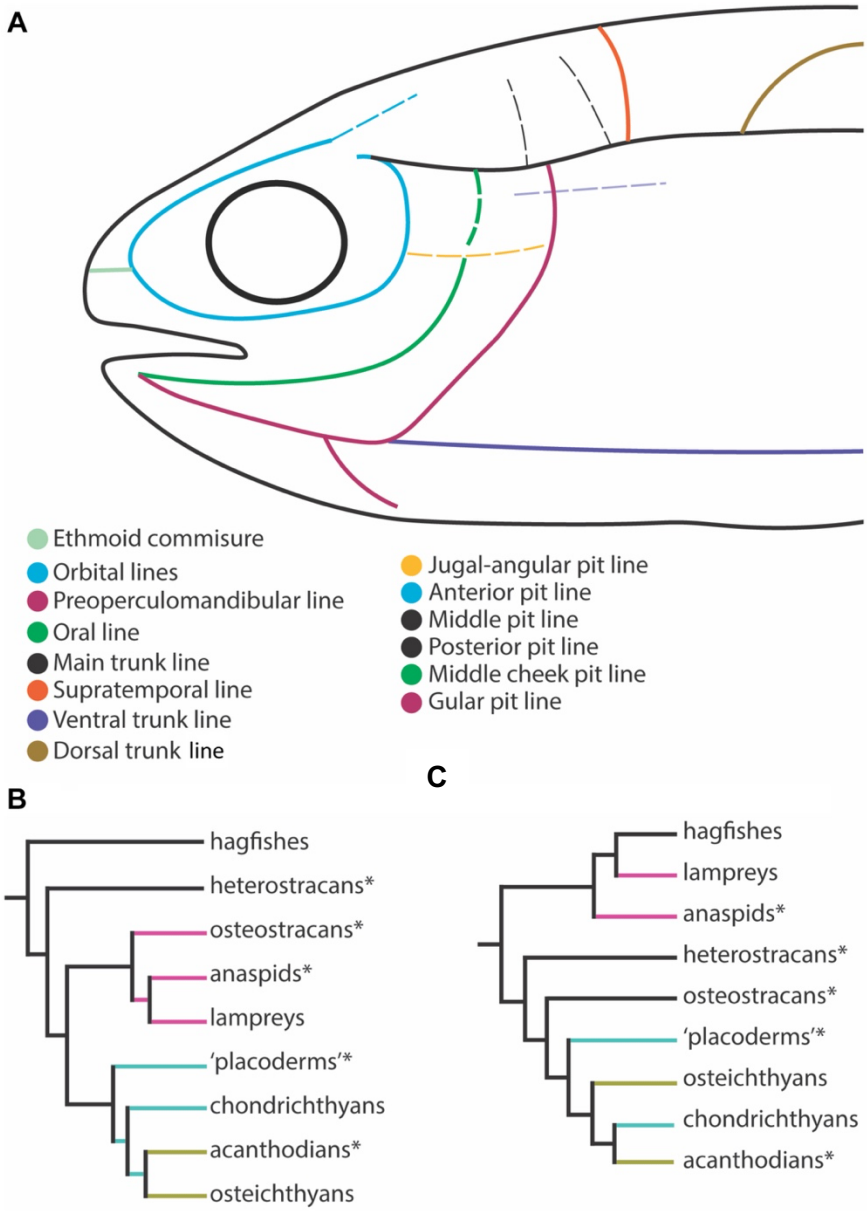

Figure 2-4: Ancestral gnathostome lines from Northcutt (1989).
(A) Northcutt's proposed morphotype for ancestral gnathostome head and trunk lateral lines [after Northcutt (1989), fig. 3.3D]. **(B)** Cladogram of fossil and living vertebrate relationships after fig. 3.1 in Northcutt (1989). **(C)** Taxa from B rearranged based on current phylogenetic consensus (Miyashita et al., 2019)

V. New tree, new synthesis

(1) Vertebrate phylogeny revised

Fig. 2-5 presents a summary of the most recent phylogenetic trees of early vertebrates. It is important to recognize that this is not a formal supertree (Gordon, 1986; Bininda-Emonds et al., 2002). Challenges to the consensus that underpinned Northcutt's phylogeny (Fig. 2-4B; fig. 3.1 in Northcutt, 1989) first emerged in Forey & Janvier (1993) and were further developed in Janvier's *Early Vertebrates* (see his 'odd trees' in fig 9.1 in Janvier, 1996). Changes cover all clades involved in this topology. To set the stage for our discussion of lateral line macroevolutionary patterns in Section V.3, we describe some important changes to the topology and identify some of the unresolved relationships.

In contrast to Northcutt's (1989) hypothesis (compare Fig. 6B and 7) †'acanthodians' are now recognized as early chondrichthyans (Brazeau, 2009; Davis et al., 2012; Coates et al., 2018). This discovery of a stem group has vastly enriched the entire chondrichthyan lineage but depopulated the osteichthyan stem. The few remaining stem osteichthyans are contentious in the sense that they have been equivocally interpreted as stem or crown group members, with either actinopterygian or sarcopterygian affinities (Basden et al., 2000; Lu et al., 2016).

†'Placoderms' (magenta box in Fig. 2-5) are the earliest jawed vertebrates in the fossil record. Taxonomically diverse and morphologically disparate, they might not

constitute a natural group. If instead †'placoderms' constitute a grade, meaning clades branching successively from the stem, then they can provide a series of snapshots of trait evolution leading to modern jawed vertebrates (Dupret et al., 2017; M. Zhu et al., 2016; Y. Zhu et al., 2022). Alternatively, if a large monophyletic rump group of †'placoderms' persists, then they represent an independent evolutionary radiation of early jawed fishes. In this case, they must have converged on several morphologies shared with modern clades. Both hypotheses are current – monophyly (natural group, see King et al., 2017) and paraphyly (Brazeau and Friedman, 2015; Brazeau et al., 2023); for this reason, we include polytomy A in Fig. 2-5.

†*Entelognathus* is the first maxillate †'placoderm', meaning it has a maxilla, like osteichthyans. But perhaps more significantly, it is also the first †'placoderm' found to have lateral lines on the jaws, thus bearing out Northcutt's predictions (Northcutt, 1989, p. 69). Among the †'placoderms', †*Entelognathus* and other maxillate forms are now hypothesized to be sister groups to the extant gnathostome evolutionary radiation.

In contrast to the instability of †'placoderm' relationships, cyclostome monophyly is now resolved on the basis of both molecular and morphological evidence (Kuraku et al., 1999; Furlong and Holland, 2002; Heimberg et al., 2010; Miyashita et al., 2019). As a consequence of this monophyly, early jawless fishes have been redistributed across cyclostome and gnathostome stems. The groups are shown in Fig. 2-5, although uncertainty persists (see polytomy B). *Contra* Northcutt (1989), †osteostracans (Stensiö, 1932; Janvier, 1985; Sansom, 2009) are now regarded as the sister group to jawed vertebrates (Forey, 1995; Donoghue and Smith, 2001; but see also Gai et al., 2011). †Heterostracans and their likely relatives (Fig. 7; blue box) provide additional and

abundant data on what appears to be an independent evolutionary radiation of stem-gnathostomes (Randle et al., 2022). †Thelodonts (Wilson and Caldwell, 1993; 1998; Wilson and Märss, 2009; Ferrón and Botella, 2017) remain the least fixed group in early gnathostome phylogeny, constituting a 'wild card' taxon (Nixon & Wheeler, 1992) because of their incomplete preservation, often consisting of little more than assemblages of scales.

The chronology of branching points is based on a series of minimum dates estimated from the fossil record, as determined by taxon ranges (Fig. 2-5; thick green lines). Recent discoveries (Zhu et al., 2022) have confirmed phylogenetic predictions (Brazeau & Friedman, 2015; Andreev et al., 2016; Coates et al., 2018) that crown gnathostomes date from at least the early Silurian (440 million years ago). This has consequences. Fig. 2-5 shows that a minimum hypothesis of the age of the last common ancestor of extant gnathostomes is pushed back in time, earlier than the earliest occurrences of the vast majority of †'placoderms' and most of their jawless outgroups. The key question now concerns the implied missing record of early vertebrates: how many groups of jawed and jawless fishes originated before or after the extinction event at the Ordovician–Silurian boundary (Harper et al., 2014; Servais and Harper, 2018)? Furthermore, how might these unknown groups transform our current best hypotheses of morphological evolution, including lateral lines?

(2) New hypotheses of lateral line evolution

The most arresting feature of cranial lateral line evolution depicted in Fig. 2-5 is the breakdown and reassembly of the lateral line networks near the origin of gnathostomes

(Fig. 2-5, yellow box). An overview of lateral line conditions in groups such as †heterostracans and †galeaspids reveals an abundance of reticulating lines with numerous twigs and branches ramifying across the dorsal surface in a distinctively postorbital position. The preorbital domain in most of these fishes is short and devoid of branching lateral lines. In jawed vertebrates, the situation is quite different: the body of the lateral line network has switched from a postorbital to an orbital/preorbital position. Lines circumnavigate the orbits, traverse the snout, and populate the cheek and jaws. Crucially, this evolutionary episode of reassembly, remaking and remodelling, starts before the origin of jaws.

Our evolutionary scenario shows early and divergent trajectories of sensory system elaboration. This contrasts with traditional narratives in which systems and characteristics evolve, usually towards humans, in a linear fashion. In Northcutt's (1989) framework, the path is one of descent with loss and modification. Most recently, Edens & Bronner (2025) reviewed the evolution of placodes and neural crest to reconstruct the serial assembly of peripheral sensory structures, but this too, is essentially a linear narrative.

Returning to Fig. 2-5, in our scenario, the earliest full elaboration of the anterior sensory line system is seen in †heterostracans and their relatives. This elaboration is also seen in the broad head shields of †galeaspids, but it is strikingly absent in the similarly shaped head shields of †osteostracans. Thus, †galeaspids and †osteostracans bracket the first signal of this transformation. In both, the general condition of the head shields is dorsoventrally flattened and broadly semi-lunate with dorsally positioned orbits. However, the lateral line networks and other sensory systems are strikingly

different. †Galeaspids show the elaborate, ramifying, postorbital patterns seen in †heterostracans and other allied groups, but †osteostracans have only a rudimentary array of superficial lines. And this signature persists in the earliest jawed fishes: the †'placoderms'. Here, the general pattern of lines radiates out from the centre of the postpineal domain, much like †galeaspids, but lateral line occupation of the cheek region and lower jaw regions is limited. Both of these territories are evolutionary novelties relative to jawless conditions. In this respect, †*Entelognathus* is unique among †'placoderms' in having lines on the lower jaw (Zhu et al., 2016 *contra* Stensiö,1947). These data suggest a 'phylogenetic lag': new domains are not immediately occupied by the lateral line system.

Switching focus to extant clades, our new synthesis signals that, *contra* Northcutt (1989), the lateral lines of extant gnathostomes are not the end products of serial reductions from a maximally lined common ancestor (Fig. 2-4,A). Instead, we propose that lateral line systems diversified independently in quite distinct trajectories among the jawless and jawed lineages. This raises the question of how this new scenario changes our estimates of general *versus* specialized conditions among the lateral lines of extant groups.

Among modern fishes and their extinct relatives, the infraorbital line emerges as the most stable component of the system. In living sharks and bony fishes, the infraorbital line consistently joins the supraorbital line behind the orbit (Figs 2-1 C, D, O, P and 7). But the introduction of fossils like †*Mimipiscis* and †*Falcatus* (Fig. 2-5) shows that this connection is a convergent phenomenon (as noted in Section II.2). By contrast, supraorbital lines are more evolutionarily labile. Most †'placoderms' such as

†arthrodires (Fig. 2-5) possess supraorbital and infraorbital lines indicating that these are likely a general feature for all jawed gnathostomes. Therefore, the absence of supraorbital lines in maxillate †'placoderms' (Zhu *et al*., 2013) such as †*Entelognathus* is probably derived.

The evolutionary hypothesis laid out in Fig. 2-5 also raises questions about lateral line placode evolution. Mandibular lines are considered a general feature of the cranial lateral line network. However, their first appearance in the lower jaws of taxa such as the maxillate †'placoderm' †*Entelognathus*, in the absence of any cheek canal, is likely important. In modern jawed vertebrates, the mandibular line is continuous with a preopercular line on the cheek (Fig. 1-1). Developmental data (Northcutt et al., 1994; Iwasaki et al., 2020) indicate that the mandibular and preopercular lines develop from a single anteroventral placode. This suggests a transformational hypothesis. First, the evolution of the mandible was followed by the *de-novo* condensation of a new placode. Next, the developmental derivative of this placode invaded the new territory of the cheek. Currently, there are no data on whether any homologue of an anteroventral placode exists in extant jawless cyclostomes (hagfishes and lampreys).

The macromeric skulls of osteichthyans, i.e., skulls comprising large plates, have been presented as the result of correlated evolution between lateral lines and the dermal skeleton (Westoll 1941; Pehrson 1922). These skulls were previously thought to have evolved from a micromeric skull composed of tiny scales (Romer, 1966; Schultze, 1993). However, this general scenario is no longer supported by current hypotheses and data. First, micromeric skulls are now recognized as a derived feature, and are not ancestral to macromeric skulls (Friedman and Brazeau, 2013). Second, major features

of the lateral line network persist through this shift from macromery to micromery. Third, in macromeric skulls such as our own, the general pattern of skull bones persists despite the complete and long-standing absence of a lateral line system. For these reasons we argue that the respective pattern stabilities of cranial bones and lateral lines are independent to a greater degree than previously appreciated.

(3) Functional implications and macroevolutionary pattern

Fig. 2-5 shows how extinction events (skull and crossbones) map through time relative to the taxon ranges and branching events in this summary of vertebrate phylogeny. The origin of all major clades – both jawed and jawless – dates back to at least the early Silurian, and the early radiation of these lineages might have occurred in response to the end-Ordovician extinction (Harper et al., 2014). Similarly, the foundations of extant vertebrate diversity, composed mostly of osteichthyans (tetrapods and actinopterygians) and chondrichthyans were laid in the aftermath of a pair of late Devonian extinctions, the Kellwasser and Hangenberg events (Sallan and Coates, 2010). Notably, both tetrapods and actinopterygians diversify into new body shapes, new abundance, and new habitats. The so-called ‘Age of Fishes’, formerly the Devonian ‘pre-tetrapod’ vertebrate world now ranges from the end-Ordovician to the end-Devonian, a span of some 80 million years. Moreover, throughout most of this period jawless and jawed fishes overlapped. There is no rapid elimination of jawless taxa, but quite how this ichthyological Eden was maintained remains to be determined.

The acquisition of crown gnathostome characters, including a heterocercal tail, muscular pectoral and pelvic fins, a third semicircular canal of the inner ear, a jaw, and dentition, enabled increasingly active swimming and a wider range of feeding strategies.

These changes are associated with the most successful of what appear to have been several ecological excursions into the water column by different early lineages, and likely underpinned the vertebrate component of the Devonian Nekton Revolution (DNR) (Klug et al., 2010; for alternative views of timespan and significance of the DNR see Whalen and Briggs, 2018). Crucially, all of these transformations accompany the major reorganization of the cranial lateral line network.

The DNR (Klug *et al*., 2010), encapsulating increased occupation of the water column by nektonic and demersal clades (invertebrate and vertebrate), fundamentally changed marine ecosystems and food webs. Aside from changes already outlined for vertebrates in general, this shift is also reflected in body cross-sectional outlines. Fig. 2-5 shows transitions from broad, dorsoventrally flattened conditions (blue half-circles) to more laterally compressed profiles (crimson circles). Among the jawless groups, both †anaspids and †thelodonts have bodies with round to laterally compressed cross sections (green ovals) suggesting life in the water column, and swimming modes in these taxa have been modelled as such (Ferrón and Botella, 2017; Ferrón et al., 2020; Ferrón and Donoghue, 2022). However, the extent to which these fishes could sustain occupancy of the water column, as well as their ability to evade predators, is unknown.

For other early jawless gnathostomes, such as †*Astraspis*, body shapes indicate that they experienced downward thrust, consistent with demersal (Fig. 2-5, taxa marked D) or strictly benthic (Fig. 2-5, taxa marked B) habits. All of these fishes likely fell victim to invertebrate predators that had already begun occupying the water column (e.g. †eurypterids and †radiodonts; Klug et al., 2010). For these reasons, we suggest that the extensive dorsal postorbital lines were adaptations for predator evasion and escape,

analogous to arthropod looming receptors (Rind et al., 2016). The general absence of lateral lines at the front of the head implies that these organisms were not gaining extensive sensory input from bulk water flow (Mogdans, 2019). Exceptions to this rule include heterostracans with extended rostra which very likely served as sensory arrays (e.g., *Errivaspis*; White, 1935). We acknowledge that many of these early jawless fishes have very little preorbital territory, but what is absent is a concentration of sensory lines and pits surrounding the orbitonasal and oral complex (e.g., *Sacabambaspis*). The lines in these cases are distributed evenly across the length of the headshield. The broadly limited sensitivity of these fishes to current strength and direction may have restricted swimming efficiency and sophistication (i.e., they were unlikely to have schooled or exhibited other coordinated group behaviours) and, by extension, limited their habitat occupation. By contrast, the evolution of complex mechanosensory systems located rostrally, combined with muscular paired fins, provided the capability to become fully pelagic (Fig. 2-5, taxa marked P), perform enhanced swimming manoeuvres, exhibit novel behavioural responses, and establish new ecological niches.

This sensory elaboration probably happened in a stepwise manner. †Osteostracans (Fig. 2-1F, Fig. 2-5) show that the evolution of at least one pair of muscular fins, a heterocercal tail, and large-scale remodelling of sensory systems preceded the advent of jaws. †Osteostracans and †galeaspids have similar body shapes (Janvier, 1996), but †osteostracans have exceptionally reduced lateral lines (Stensi,1932; Janvier, 1974). However, their peculiarly elaborated vestibular system is connected to large dorsal and rostral sensory fields. We suggest that these functioned similarly to the rostral lines of crown gnathostomes to perceive bulk water flow towards

the front of the head (Janvier, 1985). A similarly rudimentary lateral line system, but lacking any trace of sensory fields, is seen in †'placoderms' thought to represent primitive conditions (†antiarchs and †romundinids) (Denison, 1978). The modest jaws of these early branching clades precluded any possibility of macropredation, suggesting that jaws and teeth were only later co-opted for predatory behaviour. Notably, even the canal-bearing jaws of the maxillate †'placoderm'-grade antecedents of crown-group gnathostomes are toothless (Zhu et al., 2013). In summary, lateral lines are part of a major reorganization of sensory systems that both preceded and overlapped a vertebrate body plan that we now recognize as fundamental to modern gnathostomes.

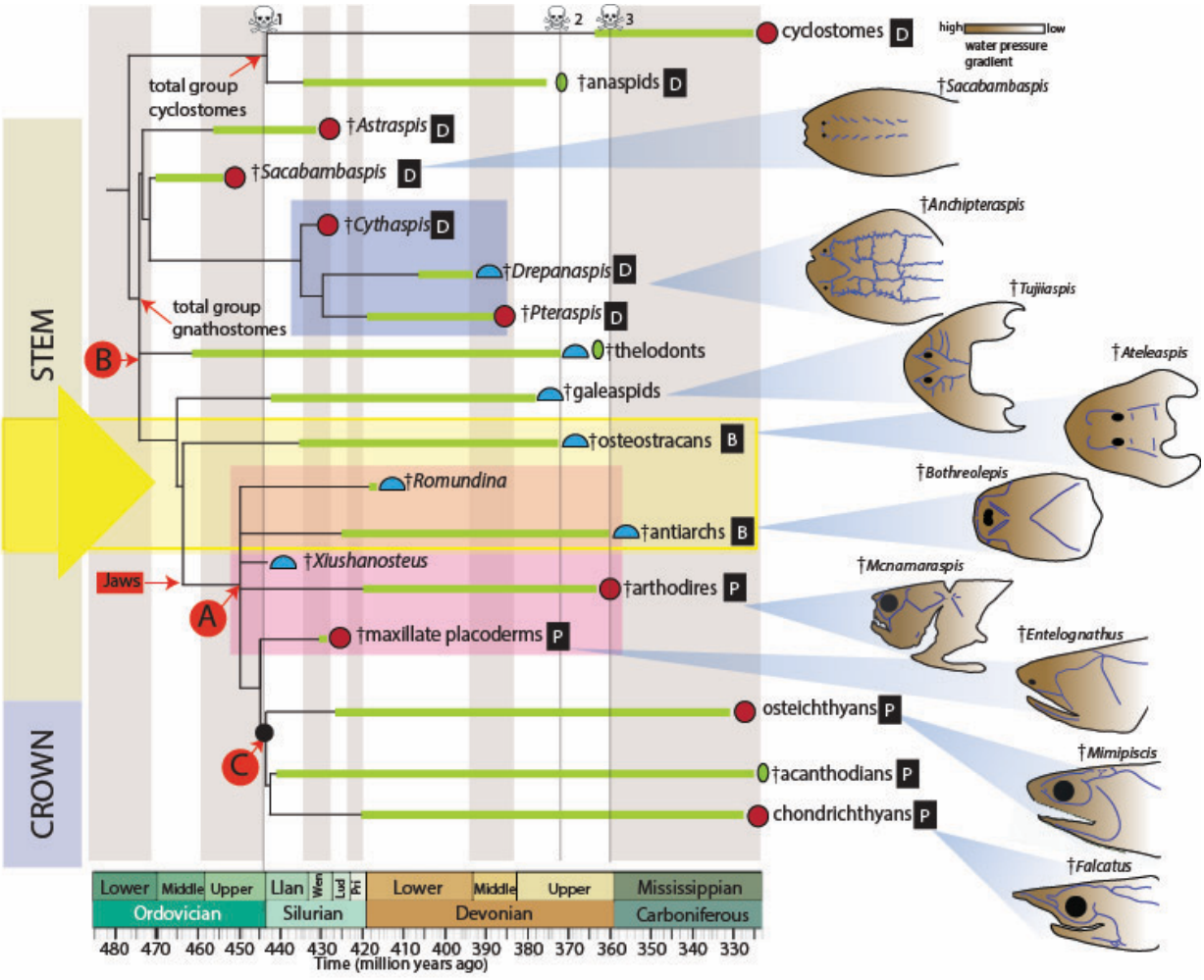

Figure 2-5: Early vertebrates and lateral line evolution

Figure 2-5 cont.: Time-calibrated phylogenetic synthesis after King *et al*. (2017), Miyashita *et al*. (2019) and Zhu et al. (2022). Crania sketched with lateral lines (blue) after Gagnier et al. (1986), Elliott & Mark-Kurik 2005), Gai et al. (2020), Stensiö (1932), Graham-Smith & Parrington (1978), Choo (2012), Long (1995) and Lund (1985). Colour shading on crania represents hypothetical water pressure gradients. Graded triangles connect crania to position on tree. Yellow arrowed box is zone of major remodelling of lateral lines. Thick green lines represent taxon ranges. Magenta box captures 'placoderms'; blue box captures heterostracans. Body shape indicated by symbols at branch tips: crimson circles are body shapes approximately circular in cross section; blue half circles are dorsoventrally flattened body shapes; green ovals are laterally flattened body shapes. Black boxed letters indicate inferred life habit (B, benthic; D, demersal; P, pelagic). Daggers represent extinct clades. Skull and crossbones denote extinction events: 1, End-Ordovician; 2, Kellwasser; 3, Hangenberg (End-Devonian). Black circle denotes crown node. Polytomies A and B (in red circles) represent unresolved branching within 'placoderms' and jawless stem gnathostomes, respectively. Advent of jaws (red box) as indicated. Simple calibration aligning taxon ranges to stratigraphic timescale is based on the International Commission on Stratigraphy, v 2023/09.

VI. Future directions: avenues for integrative research

An integrative approach, combining palaeontological, anatomical and developmental data is essential to fill the outstanding gaps in our understanding of lateral lines. Here we lay out an agenda of five themes deserving future work.

A key question is the relationship between lateral lines in jawless and jawed vertebrates: how do the lines in living agnathans relate to those in gnathostomes? Resolving this involves study of the only extant jawless vertebrates with extensive lateral lines: lampreys. While palaeontologists have attempted to address this question by comparing osteostracans and lampreys (Janvier, 1974), current phylogenetic consensus places these two lineages distant from each other. In addition, embryological evidence regarding the development of lateral lines in lampreys is lacking and would help reveal the placodal origins of lamprey lateral lines. This in turn would clarify the homologies between jawless and jawed vertebrate lateral lines and reveal whether lampreys have a precursor of the vertebrate anteroventral placode.

Another key area of research is the origin and development of lateral lines in fishes with extreme morphologies (see Section II.4). For example, it is unclear which

placode produces the novel pleural lines on batoid fins, nor do we know how they grow posteriorly. Molecular assays including antibody staining for proteins on large embryos (Masselink and Tanaka, 2023) and hybridization chain reactions (HCRs) to assay gene expression (Dirks and Pierce, 2004) would help trace the development of these lines at high resolution in fixed specimens. Combined with a vital dye labelling approach (e.g. using DiI(1,1′-dioctadecyl-3,3,3′,3′-tetramethylindocarbocyanine);(Gillis et al., 2012), this would illuminate the specific origin and homologies of these novel lines.

The relationship between the lateral line and the surrounding dermal skeleton (Section III) presents a further area ripe for investigation. While advances in tomographic imaging have vastly improved our knowledge of fossil dermal skeletons (Giles et al., 2013; Keating & Donoghue, 2016), none of these studies has focused on lateral lines. Moreover, experimental embryological evidence is needed to follow up on preliminary work looking at the relationship between the lateral line and other tissue types (Smith et al., 1990).

There are crucial gaps to fill within the fossil record, especially the missing Silurian ranges of jawless and jawed vertebrates (Section V.1). Resolution of †'placoderm' phylogeny, with further clarity on whether the clade forms a monophyletic group, will inform patterns of trait evolution in crown jawed gnathostomes. In particular, this would add detail to the evolutionary phase in which the lateral line system was remodelled to the condition at the base of extant jawed vertebrates (Fig. 2-5; yellow box).

The establishment of transgenes labelling zebrafish lateral lines (Haas & Gilmour, 2006) has allowed unprecedented access to spatiotemporal patterns of

development in this system. Using genetic, pharmacological or embryological approaches to ablate different tissue types in model systems like zebrafish or *Xenopus* would help explore the interaction between placodal lines and adjacent tissues like neural crest or underlying mesoderm. We lack a mechanistic understanding of how migrating *versus* elongating primordia are patterned. Antibody staining, combined with other morphological visualization techniques including scanning electron microscopy and paraffin histology would help advance our understanding of this difference.

Finally, vital dyes like TMRE (Tetramethylrhodamine, Ethyl Ester, Perchlorate) or DASPEI (2-(4-(Dimethylamino)styryl)-N-ethylpyridinium iodide) enable the visualization of maturing hair cells and thus neuromasts through the entirety of ontogeny in an unprecedented variety of vertebrates (Pisano et al., 2014; Esterberg et al., 2013).

CHAPTER THREE: DEVELOPMENT OF THE ZEBRAFISH ANTERIOR LATERAL LINE SYSTEM IS INFLUENCED BY UNDERLYING CRANIAL NEURAL CREST

Summary

The mechanosensory lateral line system of aquatic vertebrates comprises a superficial network of distributed sensory organs, the neuromasts, which are arranged over the head and trunk and innervated by lateral line nerves to allow detection of changes in water flow and pressure. While the well-studied zebrafish posterior lateral line has emerged as a powerful model to study collective cell migration, far less is known about development of the anterior lateral line, which produces the supraorbital and infraorbital lines around the eye, as well as mandibular and opercular lines over the jaw and cheek. Here we show that normal development of the zebrafish anterior lateral line system from cranial placodes is dependent on another vertebrate-specific cell type, the cranial neural crest. We find that cranial neural crest and anterior lateral lines develop in close proximity, with absence of neural crest cells leading to major disruptions in the overlying anterior lateral line system. Specifically, in the absence of neural crest neither supraorbital nor infraorbital lateral lines fully extend, such that the most anterior cranial regions remain devoid of neuromasts, while supernumerary ectopic neuromasts form in the posterior supraorbital region. Both neural crest and cranial placodes contribute neurons to the lateral line ganglia that innervate the neuromasts and in the absence of neural crest these ganglia, as well as the lateral line afferent nerves, are disrupted. Finally, we establish that as ontogeny proceeds, the most anterior supraorbital neuromasts come to lie within neural crest-derived frontal and nasal bones in the developing cranium. These are the same anterior supraorbital neuromasts that are

absent or mislocated in specimens lacking neural crest cells. Together, our results establish that cranial neural crest and cranial placode derivatives function in concert over the course of ontogeny to build the complex cranial lateral line system. A version of this article has been published as: Vishruth Venkataraman, Noel H. McGrory, Theresa J. Christiansen, Joaquin Navajas Acedo, Michael I. Coates, Victoria E. Prince, 2025. Development of the zebrafish anterior lateral line system is influenced by underlying cranial neural crest. *Developmental Biology* **525**, 102-121. Supplementary movies mentioned in this chapter are available with the online edition of the article.

Attributions

This project was done in close collaboration with undergraduate students Noel McGrory and Theresa Christiansen. I conceptualized the study, designed the experiments, interpreted results and worked on the manuscript, along with direct day-to-day supervision of NGM and TJC. JNA provided the time-lapse analysis shown in Fig. 3-1A-E and assisted with editing the manuscript; VEP generated the confocal images shown in Fig. 3-2, oversaw the project as a whole, and played a major role in the initial drafting of the manuscript as published at Developmental Biology; undergraduate student TC assisted in generating much of the data shown in Figs 3-3, 3-4, 3-6, 3-7, and 3-9 under my direct mentorship; undergraduate student NGM performed Nifupirinol drug treatments and acquired much of the data shown in Fig. 3-5, and also assisted with the initial establishment of the drug treatment protocol, again under my direct mentorship. The time-lapse analysis shown in Fig. 3-8 was kindly generated at the Marine Biological Laboratory by Carsten Wulf and Michael Wen.

I. Introduction

Aquatic vertebrates possess a mechanosensory lateral line system that gives organisms the ability to detect water movements in their environment. The lateral line system serves to orient an individual relative to flow direction, facilitate schooling behavior, enhance prey location, and contribute to predator evasion (Mogdans, 2019). Recent functional studies in goldfish have shown that this mechanosensory system is part of a broader multimodal 'bioacoustic' network, working together with the ear to detect auditory signals in the water (Higgs and Radford, 2013). The system includes the neuromasts—each comprising a core of sensory hair cells surrounded by support cells—and their afferent neurons, both of which are derived embryologically from discrete patches of thickened neurogenic epithelium termed lateral line placodes. The lateral line placodes form bilaterally on the sides of the developing head and each gives rise to a primordium and a sensory ganglion, which differentiate into the sense organs and nerves of the lateral line system, respectively.

The cellular and molecular bases of zebrafish posterior lateral line development have been studied in detail (reviewed by Chitnis et al., 2012; Piotrowski and Baker,, 2014; Olson and Nechiporuk, 2018). Briefly, the posterior lateral line initially develops from a post-otic primordium which migrates caudally along the trunk as a dynamic collective, depositing neuromasts in its wake at defined locations. At the same time, the primordium tows along its afferent nerve, which extends from the posterior lateral line ganglion (Haas & Gilmour, 2006). Key roles in this complex process have been established for chemokine signaling, which helps mediate directed migration, and for Fgf and Wnt signaling, which coordinate primordium proliferation and neuromast

deposition (reviewed by Piotrowski & Baker, 2014). Posterior lateral line development continues as a second primordium follows the first, depositing additional neuromasts (Navajas Acedo et al., 2019), with intercalary neuromasts emerging still later, through proliferation of interneuromast cells left behind by the migrating primordia (reviewed by Ghysen & Dambly-Chaudière, 2007).

We have a more limited understanding of zebrafish anterior lateral line development, derived primarily from two previous studies. A description of the anterior lateral line ganglia and nerves was published over two decades ago (Raible and Kruse, 2000) and, more recently, transgenic zebrafish lines were used to generate a detailed description of the deposition of anterior lateral line neuromasts, and their innervation, over the first 10 days of development (Iwasaki et al., 2020). We also know that the initial establishment of the placodes that form posterior versus anterior lateral line primordia is controlled by different signaling pathways: retinoic acid is necessary for formation of the posterior lateral line placode, while Fgf is necessary for formation of the anterior lateral line placode(Nikaido et al., 2017). While disruptions in chemokine signaling block migration of the posterior lateral line, they have not been reported to disrupt the anterior lateral line (David et al., 2002; Ghysen & Dambly-Chaudière, 2007).

The anterior lateral lines that extend above the eye (the supraorbital) and below the eye (the infraorbital) develop from an anterodorsal placode, which arises just anterior to the otic vesicle by 24 hours post fertilization (hpf). The lines that traverse the cheek and jaw develop from an anteroventral placode, which arises a little more ventrally around 36 hpf (Iwasaki et al., 2020; Raible & Kruse, 2000). Iwasaki and colleagues (2020) classified anterior lateral line neuromasts into four categories:

homegrown, which develop near their point of origin; migratory, which arise from a migratory primordium; budding, which form through outgrowth from already deposited migratory neuromasts; and intercalary, which arise from interneuromast cells, similar to the production of intercalary neuromasts in the posterior lateral line.

Cranial placodes, together with neural crest cells, are found exclusively in the vertebrates and these tissues have together allowed the evolution of complex vertebrate crania with their array of sensory structures (Gans and Northcutt, 1983). These two classes of cells develop from early primordia that lie in close apposition and are likely intermixed at the earliest stages (reviewed by Koontz et al., 2023; Rocha, Beirirger et al., 2020; Rocha, Singh et al., 2020; Steventon et al., 2014). As development continues, placode-derived and neural crest cells remain close together, allowing scope for interactions between these spatially associated cells in the assembly of cranial sensory structures (Steventon et al., 2014). Cranial neural crest cells are therefore a good candidate to influence the development of the anterior lateral line.

Functional interplay between neural crest and cranial placodes has been described in multiple species and situations, including in zebrafish posterior lateral line development, where neural crest-derived glial cells function to suppress premature formation of trunk intercalary neuromasts (Grant et al., 2005; López-Schier and Hudspeth, 2005; Lush and Piotrowski, 2014). In chick, as well as zebrafish, both neural crest and placode cells co-contribute to cranial ganglia (Covell Jr. and Noden, 1989; Hamburger, 1961; Kague et al., 2012). Chick neural crest cells also establish corridors for placode-derived neuroblast cells to migrate through, helping to establish stereotypical organization of their cranial sensory ganglia (Freter et al., 2013). Zebrafish

neural crest cells similarly promote assembly of epibranchial ganglia (Culbertson et al., 2011). Evidence of neural crest-placode interactions has also been found in a lamprey, *Petromyzon*, where CRISPR-mediated disruption of neural crest development results in changes to cranial ganglia morphology and positioning, but does not affect the total number of ganglia (Yuan et al., 2020). In *Xenopus*, the positioning of both the neural crest cells and the placodes is partially determined by a 'chase and run' dynamic. The neural crest cells 'chase' placode cells due to attraction by placode-secreted chemokines, whereas placode cells 'run' from neural crest cells in response to cell contact (Theveneau et al., 2013). Importantly, the zebrafish neural crest and anterior lateral line systems remain closely coupled throughout the entire course of ontogeny. The cranial neural crest gives rise to a subset of the zebrafish dermal bones that encase the adult cranium (Kague et al., 2012), and as bones form during ontogeny, the cranial lateral lines become enclosed by bony canals (Webb and Shirey, 2003).

The relationship between the lateral line and surrounding dermal bone was a topic of repeated interest over the last century, with multiple authors suggesting that lateral line neuromasts might influence ossification of surrounding dermal bones (Moy-Thomas, 1947; Pehrson, 1922; Stensiö, 1947). In response to that idea, but also to findings that called it into question, Parrington (1949) put forward an alternative model rooted in early development. Specifically, Parrington hypothesized that "the precursors of dermal ossifications influence the courses of the lateral lines". While Parrington did not mention neural crest, we now know that the neural crest cells are the source of many cranial dermal bones (Kague et al., 2012). Parrington's hypothesis, together with the many examples of functional interactions between neural crest and cranial placodes

(above), led us to test whether zebrafish neural crest cells might interact with the placode-derived anterior lateral line system to influence how the lateral lines navigate over the developing head.

Here, we have investigated zebrafish anterior lateral line development using confocal and Single Plane Illumination Microscopy (SPIM) of transgenic specimens, as well as immunolabeling, to build on previous descriptions of neuromast deposition and innervation (Iwaskaki et al., 2020, Raible & Kruse, 2000). Importantly, we have established that both the supraorbital and infraorbital anterior lateral lines develop directly adjacent to cranial neural crest cells, with neural crest cells also surrounding and contributing to anterior lateral line ganglia. To test the hypothesis that cranial neural crest influences anterior lateral line development we ablated neural crest cells using transgene mediated cytotoxicity. We found that absence of neural crest cells leads to absence of neuromasts in the most anterior (pre-orbital) part of the cranium. Supraorbital line extension stalls above the eye, while ectopic neuromasts often form in the posterior supraorbital region. The infraorbital line is severely reduced, and the mandibular and opercular lines are missing. We also explored the innervation of the zebrafish anterior lateral line system, demonstrating that both dorsal and ventral anterior lateral line ganglia have neural crest and placode cell contributions, and establishing that lateral line gangliogenesis and lateral line innervation are disrupted in the absence of neural crest cells. Finally, we exploited Cre-based lineage tracing of neural crest cells to reveal that the most anterior supraorbital neuromasts become encased in neural crest-derived bone. These same most anterior supraorbital neuromasts are the ones that fail to migrate to their normal positions in the absence of neural crest. Together,

our findings establish that developmental interactions between neural crest and placode-derived anterior lateral line cells prefigure anatomical interactions.

II. Materials and methods

(1) Animal husbandry

Zebrafish (*Danio rerio*) were maintained in accord with IACUC-approved protocols at the University of Chicago, the Stowers Institute, and the Marine Biological Laboratory. Embryos were maintained in E3 solution (5mM NaCl, 0.17mM KCl, 0.33mM Ca_2Cl_2, 0.33mM $MgSO_4$), which was supplemented with 0.3% 1-phenyl-2-thiourea (PTU; Sigma) to block pigment formation for analyses after 24 hpf, and staged according to standard guidelines (Kimmel et al., 1995; Parichy et al., 2009). Embryos were obtained from crosses of adult fish stocks of wild types (*AB line) and/r transgenics.

The following transgenic zebrafish lines were used in this study: *Tg(cldnB:GFP)*^{zf106}, a tight junction marker that labels the membranes of cells in the lateral line system, other placodes, and epithelia (Haas & Gilmour, 2006); *Tg(-8.0cldnB:H2AmCherry)*^{psi4Tg}, referred to in the text as *Tg*(*cldnB:H2AmCherry)*, is a nuclear localized red fluorescent version of the same marker (Peloggia et al., 2021); *Tg(dRA:GFP)*, a fortuitous insertion line that labels the lateral line primordia (provided by Parker and Krumlauf, who generated the line using methodology described in (Parker et al., 2014); *Tg(-7.2sox10:mRFP)*^{vu234}, referred to in the text as *Tg(sox10:mRFP)*, labels the membranes of neural crest cells as well as part of the otic vesicle (Kucenas et al., 2008)*; Tg(sox10:gal4;UAS:NTR-mCherry)*, which combines the *Tg(-7.2sox10:Gal4-VP16)*^{psi5} (Rosenberg et al. 2014) and *Tg(UAS-Eib:NfsB-mCherry)*^{jh17} (Parsons et al., 2009) transgenes, this line is referred to in the text as *Tg(sox10:NTRmCherry)*, and expresses

Nitroreductase enzyme in neural crest cells and the otic vesicle; *Tg(Hgn39d:EGFP)* is an enhancer trap insertion (Nagayoshi et al., 2008) into the *contactin associated protein 2a* gene, referred to in the text as *Tg(cntnap2a:EGFP)*, and exclusively labels lateral line afferent nerves (Faucherre et al., 2009; Pujol-Martí et al., 2012); *Tg(-28.5Sox10:cre;ef1a:loxP-dsRed-loxP-egfp*), referred to in the text as *Tg(sox10Cre;dsRed/EGFP*), uses Cre/Lox recombination to permanently label neural crest cells with EGFP, while other cells express dsRed (Kague et al., 2012).

(2) Single plane illumination microscopy (SPIM)

Transgenic embryos were mounted for SPIM in Fluorostore Fractional FEP Tubing (F018153-5) using a modified multilayer technique (Kaufmann et al., 2012). Embryos were immobilized using 0.3% agarose (Invitrogen UltraPure Low Melt Agarose Cat #16500) dissolved in E3 medium and 0.2 mg/ml tricaine, and the FEP tubing capped with a 1.2% agarose plug. Embryos were incubated at 28.5 °C during data collection. Images were captured with either a Zeiss Lightsheet Z.1 (with 20x objective) or a Zeiss Lightsheet 7 (with 10x objective) single-plane illumination microscope, each equipped with tandem PCO.edge sCMOS cameras (PCO.Imaging, Kelheim, Germany). Volumes were acquired every 10 minutes. Zeiss Zen software was used to acquire images, with post processing in FIJI (Schindelin et al., 2012) and Imaris (Oxford Instruments).

(3) Confocal image acquisition

For assays in fixed specimens, embryos were fixed in 4% paraformaldehyde (PFA; Sigma) at 4 °C overnight. Following overnight fixation, embryos were washed in 1X

Phosphate Buffered Saline (PBS) five times for 5 min each. For long-term storage of embryos, embryos were washed in 30%, 60% and 100% methanol (diluted in 1X PBS) and stored in 100% methanol at −20 °C. If stored in 100% methanol, embryos were progressively washed in 60%, 30% methanol as well as 1X PBS + 0.1%Tween-20 (Sigma) before mounting or staining. Static confocal images were collected on upright Zeiss LSM710 or LSM900 confocal microscopes with Plan-Apochromat 10x/0.45, 20x/0.8W, or 40x/1.W objectives. Time-lapse confocal microscopy of living specimens was performed on an inverted Zeiss 780 microscope using a 40x/1.1W Corr M27 objective in a climate-controlled chamber set at 28 °C. Embryos were anesthetized as described for SPIM and mounted in 0.8% low melt agarose in glass-bottomed dishes (MatTek, USA). Zeiss Zen software was used to acquire images, with post processing in FIJI (Schindelin et al., 2012).

(4) Nitroreductase mediated neural crest ablations

Double transgenic zebrafish specimens were acquired by crossing individuals of two different transgenic lines to generate *Tg(sox10:NTRmCherry;cldnB:GFP)* or *Tg(sox10:NTRmCherry;cntnap2a:EGFP*) embryos. The *sox10:NTRmCherry* transgene is expressed shortly after 9 hours post fertilization, so drug treatments were begun at this stage. To achieve drug-mediated ablation of Nitroreductase-expressing neural crest cells, 9 hpf embryos were transferred in their chorions into 1.25 μM Nifurpirinol (Sigma-Aldrich catalog # 32439) dissolved in E3 medium plus 1:1000 dimethyl sulfoxide (DMSO) and incubated in the dark. Controls were incubated in E3 medium plus DMSO carrier alone. Double transgenic embryos were sorted and dechorionated at 24 hpf, and single transgenic sibling specimens lacking *Tg(sox10:NTRmCherry)* also kept as

controls. The Nifurpirinol solution was replaced with fresh solution at the 48 hpf stage for specimens to be raised to later stages.

(5) Immunolabeling

Immunolabeling was performed as previously described (Prince et al., 1998) on specimens fixed in 4% PFA. The following primary antibodies were used: anti-Sox2 1:200 (anti-rabbit; GTX124477), anti-Sox10 1:250 (anti-rabbit; GTX128374), anti-HuC/D 1:200 (anti-mouse; Molecular Probes 16A11), anti-GFP 1:200 (anti-rabbit; Sigma A-6455), and anti-Otoferlin, 1:50 (anti-mouse; Developmental Studies Hybridoma Bank HCS-1). Secondary antibodies used were Alexa 488, 1:500 (Invitrogen anti-mouse A-11001; anti-rabbit A-11008), Alexa 546 1:500, (Invitrogen anti-rabbit A-11035), and Alexa 633, 1:300 (Invitrogen anti-mouse A-21052; anti-rabbit A-21070). The far-red Alexa 633 secondaries were coupled with HuC/D, Otoferlin and Sox2 antibodies.

For adult zebrafish staining, a CUBIC clearing and staining protocol was adapted from Pende et al. (2020). Specifically, we depigmented adult specimens in acetone overnight at -20 °C before lightly bleaching for 5-19 minutes in a 3% solution of hydrogen peroxide in 1% KOH. Specimens were then incubated overnight in Low Urea CUBIC I solution at 37°C for initial clearing. For immunolabeling, cleared specimens were blocked using goat serum at 25°C for 3-4 hours before primary and secondary incubation. Specimens were incubated in primary antibody at 37 °C for 2-3 days and subsequently in secondary antibody at 37 °C for 2 days, with *sox10Cre;EGFP* signal amplified using anti-GFP antibody. Specimens were placed in CUBIC R + (N) RI matching solution (Kubota et al., 2017) for at least 30 minutes prior to imaging. For TMRE live-dye labeling, larval zebrafish were incubated for 30 minutes in 5nM

Tetramethylrhodamine, Ethyl Ester, Perchlorate (TMRE; Invitrogen) in E3 medium (Esterberg et al., 2013; Mandal et al., 2021).

(6) Large format lightsheet microscopy

Adult specimens were imaged on a LaVision Large Format Lightsheet, using a 4x objective, and 2.0 µM excitation sheet in CUBIC R+ (N) imaging medium (Kubota et al., 2017).

III. Results

(1) The anterior lateral line system develops in close proximity to cranial neural crest

Throughout this study we have made use of *Tg(cldnB:GFP)* to visualize the dynamic process of anterior lateral line development. This tight junction marker labels the membranes of sensory placode cells including those of the lateral line system, as well as epithelial cells (Haas & Gilmour, 2006). Figure 3-1 A-E shows a series of still images from a confocal time-lapse analysis of a triple transgenic *Tg(cldnB:GFP;dRA:GFP;cldnB:H2AmCherry*) specimen. The *Tg(dRA:GFP*) line (provided by Parker & Krumlauf) is a fortuitous insertion, which labels the lateral line (yellow) and augments the *cldnB:GFP* signal (also yellow); nuclear localized *cldnB:H2AmCherry* (magenta) reveals the nuclei of lateral line and epithelial cells. Our analysis focused on the cranial region, specifically the region between the developing eye and the otic vesicle, from 25-42 hpf, with confocal maximum projection images shown in lateral view (Fig. 3-1A-E; Supplemental Movies 1, 2). As early as 25 hpf the primordia that will produce the supraorbital (SO) and infraorbital (IO) anterior lateral

lines can be observed beginning to migrate anterodorsally and anteroventrally, respectively (Fig. 3-1A, A', SOp and IOp). Shortly after this stage, a little before 29 hpf, the first two otic neuromasts are deposited (Fig. 3-1B, B', O1 and O2). These 'homegrown' neuromasts (Iwasaki et al., 2020) remain close to their points of origin, gradually shifting apart as development continues. At this same 28.7 hpf stage, the IO primordium consists of an elongated ridge of cells extending under the eye (Fig. 3-1B, B', IOp). The SO primordium deposits the SO2 neuromast at about 33 hpf (Fig. 3-1C, C'), and shortly after begins to bud, such that the SO line extends further anteriorly over and around the eye as development proceeds (Fig. 3-1D-E; and see also Fig. 3-1G-I', below). The IO primordium is maintained as a ridge, but gradually starts to condense to form neuromasts (e.g. Fig. 3-1E, IO4; and see also Fig. 3-1F-I', below).

To investigate a potential relationship between the developing anterior lateral line system and the cranial neural crest, we made use of *Tg(sox10:NTRmCherry)*, which—in common with other transgenes driven by *sox10* gene regulatory sequences—labels developing neural crest cells (Rosenberg et al., 2014). Figure 3-1F-I shows a series of still maximum projection images from a Single Plane Illumination Microscopy (SPIM) time-lapse analysis of a *Tg(cldnB:GFP;sox10:NTRmCherry)* double transgenic specimen. Our SPIM analysis allowed the entire cranial region to be imaged from 33 to 52 hpf, again presented in lateral view (Fig. 3-1F-1; and Supplemental Videos 3, 4). At 33 hpf the supraorbital primordium of the anterior lateral line is already migrating anterodorsally above the eye (Fig. 3-1F, F', SOp). By 37 hpf the SO2 neuromast has started to condense from the supraorbital primordium (Fig. 3-1G, G', SO2), and has begun to form SO1 (here labeled as SO1p, for primordium). The budding process

continues (Fig. 3-1H, H'), depositing the more anteriorly located SO1 neuromast close to the olfactory bulb (ob) by 45 hpf (Fig. 3-1I, I'). The infraorbital primordium, in contrast to the supraorbital, initially forms as an elongated ridge of cells (Fig. 3-1F, F', small arrowheads). The IO neuromasts gradually condense from this ridge, with IO2 beginning to appear by 37 hpf (Fig. 3-1G, G'), and the more anteriorly located IO1 by 45 hpf (Fig. 3-1I, I'). Over this same developmental period the homegrown otic neuromasts O1 and O2, remain dorsal and ventral to the anterior lateral line ganglion (gALL; which is also *cldnB:GFP*-positive), gradually shifting apart as development proceeds. Throughout the 33-52 hpf developmental time-period, the various lateral line components are in close proximity to neural crest cells that have already migrated out into the cranial region (Fig. 3-1F-I; Supplemental Video 4). Above the eye, the region into which SO2 buds to produce SO1 houses a layer of abundant neural crest cells (Fig. 3-1H; I; note locations of SO1p and SO1). Below the eye, where the IO line is developing, a dense domain of neural crest cells is present throughout the region (Fig. 3-1F-I').

In summary, confirming previous descriptions (Iwasaki et al., 2020), our confocal and SPIM time-lapse analyses demonstrate that the supraorbital lateral line forms via migration and budding of neuromasts. By contrast, we find that the infraorbital line forms from an initial elongated ridge of cells, with neuromasts then condensing from the ridge. Importantly, our analysis also reveals that anterior lateral line components are already in close proximity to cranial neural crest cells at the 33 hpf stage, a relationship that continues as the IO and SO lines continue to develop, including during the stages when the SO2 neuromast buds to generate SO1.

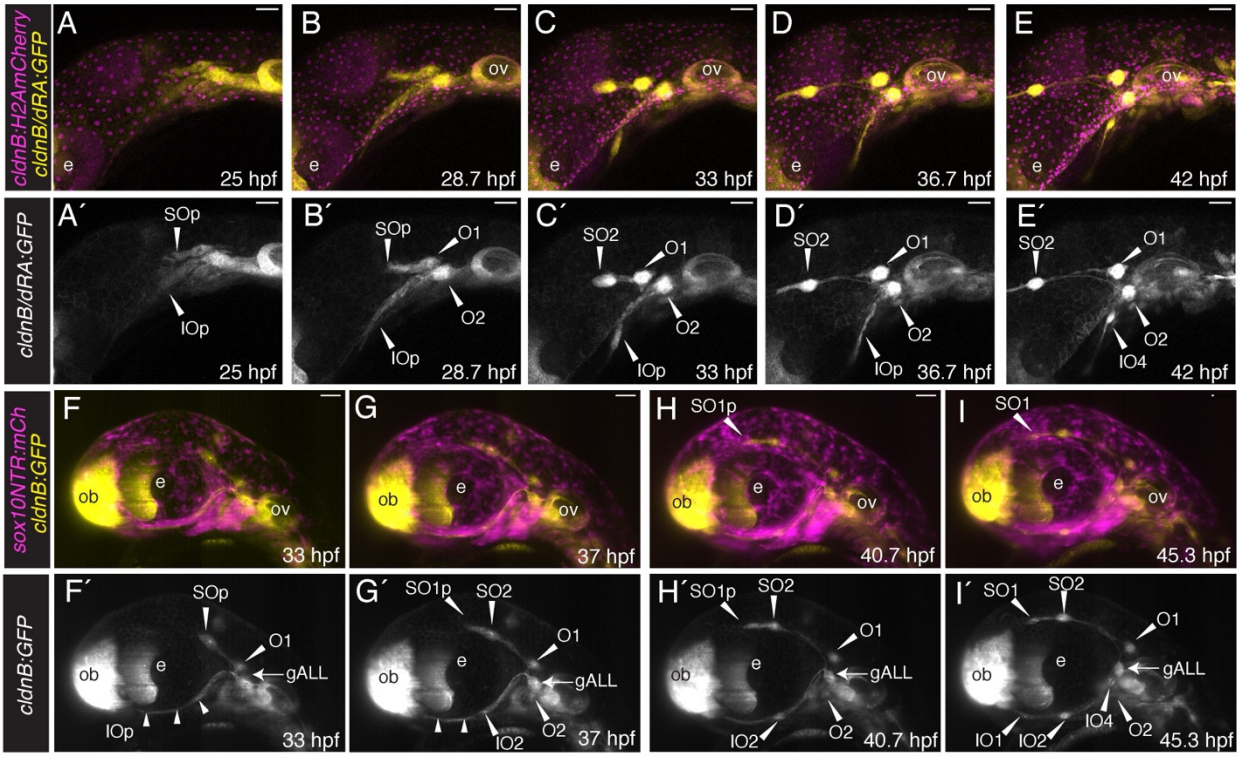

Figure 3-1:Time-lapse microscopy analysis reveals dynamics of anterior lateral line development and relationship to cranial neural crest cells.
(A-E) Confocal microscopy time-lapse images of the cranial region of a *Tg(cldnB:GFP;dRA:GFP;cldnB:H2A-mCherry)* triple transgenic specimen, in lateral view with anterior to the left. Maximum projections are shown at 25 hpf (A), 28.7 hpf (B), 33 hpf (C), 36.7 hpf (D), and 42 hpf (E). A′-E′ are single channel images of the lateral line (*cldnB:GFP* and *dRA:GFP*) alone. Neuromasts are indicated with white arrowheads and labeled (SO: supraorbital neuromast; IO: infraorbital neuromast; O: otic neuromast). The supraorbital and infraorbital primordia are indicated (SOp, IOp). **(F-I)** Single Plane Illumination Microscopy (SPIM) time-lapse images of the cranial region of a *Tg(sox10:NTRmCherry;cldnB:GFP)* double transgenic specimen, in lateral view with anterior to the left, allowing comparison of the development of the lateral line system (*cldnB:GFP*; yellow) and neural crest (*sox10:NTRmCh*; magenta) over developmental time. Maximum projections (imaged using the 20x objective) are shown at 33 hpf (F), 37 hpf (G), 40.7 hpf (H), and 45.3 hpf (I). F′-I′ are single channel images of the lateral line (*cldnB:GFP*) alone. Neuromasts are indicated with white arrowheads and labeled. Small white arrowheads in F′ and G′ indicate the elongating ridge of the infraorbital line, which can be seen condensing to form the IO2 neuromast in G′-I′. Note budding of the SO2 neuromast in G′ and H′, extending a primordium (SO1p) that then forms the SO1 neuromast, I'. Abbreviations are as follows: e: lens of the eye; ov: otic vesicle; ob: olfactory bulb. Scale bars are 50 μm.

To investigate the proximity of the anterior lateral line and cranial neural crest cells in more detail we returned to confocal microscopy. We once again used the *Tg(cldnB:GFP)* line to label the lateral line, but for this analysis used *Tg(sox10:mRFP)*,

which labels the membranes of neural crest cells (Kucenas et al., 2008), allowing more effective evaluation of cell-cell interactions between neural crest and placode-derived lateral line cells (Figure 3-2). Confocal imaging of 37 hpf specimens (Fig. 3-2A, A') again demonstrates that cells of the placode-derived lateral line system (*cldnB:GFP*, yellow) and neural crest (*sox10:mRFP*, magenta) are closely apposed. In Fig. 3-2A' the supraorbital and infraorbital regions are boxed, indicating the regions imaged at higher magnification in panels B and E, respectively. Fig. 3-2B shows the developing supraorbital region, with boxed regions on this panel indicating the locations of images focused on the SO1 neuromast primordium (C) and SO2 neuromast (D), displayed in subsequent panels.

Fig. 3-2C is a maximum projection of three z-slices (total z depth = 3.75 μm) in the plane of the SO1 primordium, revealing that the *cldnB:GFP*-expressing lateral line cells budding from SO2 (Fig. 3-2C'; SO1p) overlie *sox10:mRFP*-expressing neural crest cells (Fig. 3-2C"). An orthogonal yz reslice through the whole z-stack is shown on the right-hand side of Fig. 3-2C, confirming the close proximity of the two cell types. Fig. 3-2D is a maximum projection of three z-slices (total z depth = 3.75 μm) in the plane of SO2 and the supraorbital nerve (Fig. 3-2D', nADso), revealing that *sox10:mRFP*-expressing neural crest cells wrap around the *cldnB:GFP*-expressing SO nerve (compare Figs. 3-2D, D', D"; an orthogonal yz reslice through the whole z-stack is provided on the right-hand side of Fig. 3-2D). Fig. 3-2E shows a maximum projection of three z-slices in the infraorbital region (total z depth = 3.75 μm; an orthogonal yz reslice through the whole z-stack is provided on the right-hand side). The infraorbital, like the supraorbital, has *cldnB:GFP*-expressing lateral line cells (Fig. 3-2E') in close contact

with underlying *sox10:mRFP*-expressing neural crest cells (Fig. 3-2E"), confirming the close proximity of the two cell types. Finally, to address whether the close relationship between placode-derived and neural crest cells is present earlier in development, we performed a similar analysis at the 30 hpf stage, when the SO and IO primordia are first forming. Fig. 3-2F is a single z-slice (z depth 1.44 μm) that shows both the SO and IO primordia branching away from one another. Already at this stage, the *cldnB:GFP*-expressing lateral line cells (Fig. 3-2F') are directly overlying *sox10:mRFP*-expressing neural crest cells (Fig. 3-2F").

Together, our lightsheet and confocal microscopy analyses confirm that placode-derived anterior lateral line primordia develop in close proximity to cranial neural crest cells, from as early as 30 hpf.

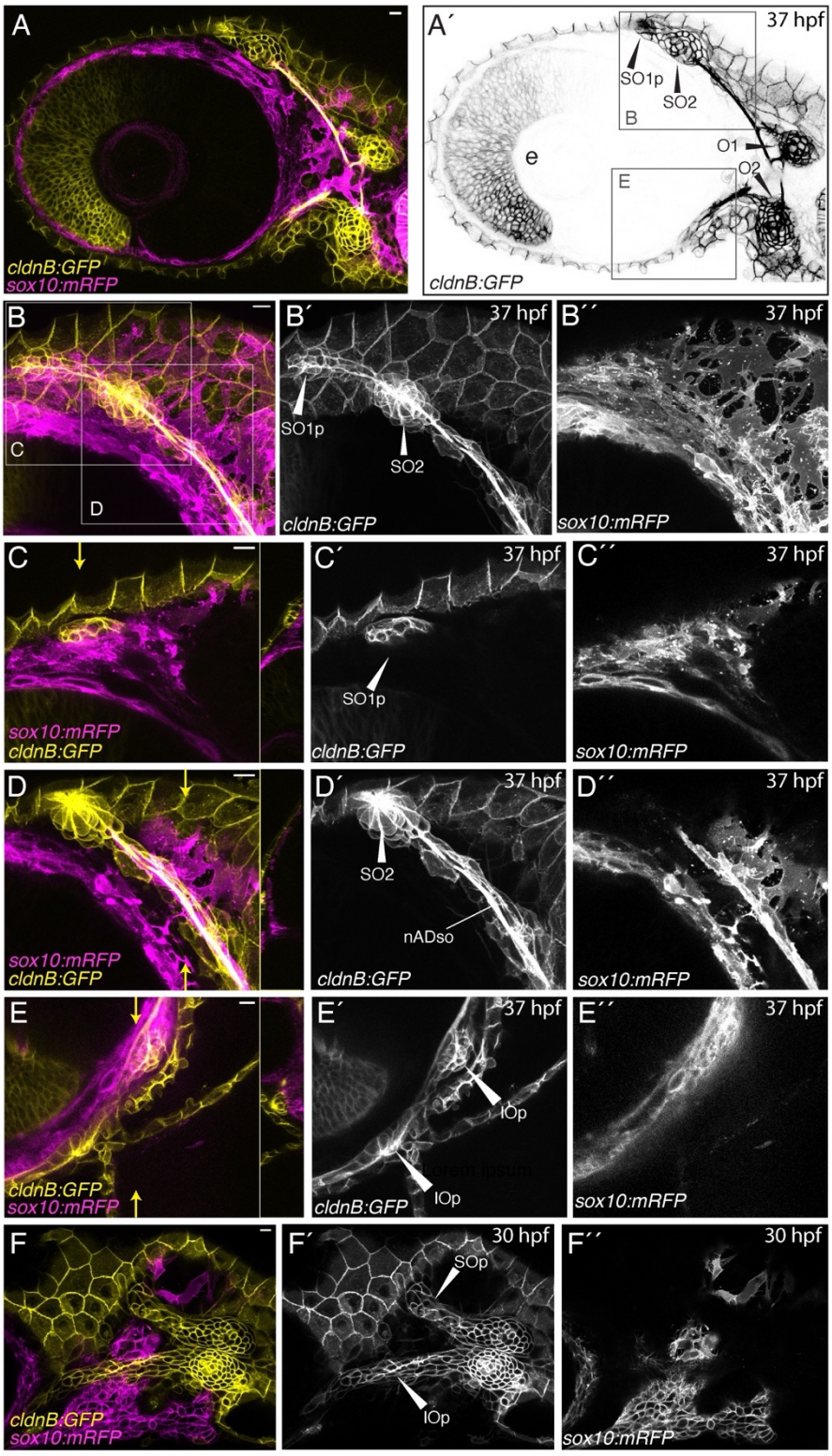

Figure 3-2:Confocal imaging reveals that cells of the anterior lateral line develop in close proximity to cranial neural crest cells.

Fig 3-2 cont.: (A) Lateral view of the cranial region of a 37 hpf *Tg(cldnB:GFP;sox10:mRFP)* double transgenic embryo, anterior to the left. Maximum projection of a 3 μm deep z-stack, imaged using the 10x objective, shows the juxtaposition of the developing anterior lateral line (yellow) with cranial neural crest cells (magenta). (A′) Single channel image (*cldnB:GFP*) of the same specimen, showing the developing lateral line system only. Neuromasts are labeled: SO2: supraorbital neuromast 2; SO1p: primordium of supraorbital neuromast 1 in the process of budding from SO2; O1, O2: otic neuromasts; e: lens of the eye. Boxed regions indicate the approximate regions imaged in panels B and E. **(B-E)** Maximum projections of a second 37 hpf *Tg(cldnB:GFP;sox10:mRFP)* specimen, imaged using the 40x objective. (B-B″) Maximum projection of a 30.75 μm deep z-stack, centered on the developing supraorbital region (see panel A′ for region). Hatched boxes indicate regions imaged at higher magnification in panels C and D. (C-C″) Maximum projection of a 3.75 μm deep sub-stack of the z-series from the specimen in B, in a focal plane showing the SO1 primordium (SO1p, indicated in C'; *cldnB:GFP*) budding over neural crest cells (C″; *sox10:mRFP*). An orthogonal yz reslice through the whole stack, in the plane indicated by a small yellow arrow, is provided to the right of C. (D-D″) Maximum projection of a 3.75 μm deep sub-stack of the z-series from the specimen in B, in a focal plane showing the SO2 neuromast and supraorbital nerve (nADso; D′). An orthogonal yz reslice through the whole stack, in the plane indicated by small yellow arrows, is provided to the right of D. Note the nSO nerve is wrapped in neural crest cells (D''; *sox10:mRFP*). (E-E″) Maximum projection of a 3.75 μm sub-stack of the larger z-series, in a focal plane showing the developing infraorbital region (see panel A′ for region). An orthogonal yz reslice through the whole stack, in the plane indicated by small yellow arrows, is provided to the right of E. IOp indicates the infraorbital primordium (E; *cldnB:GFP*) elongating over neural crest cells (E″; *sox10:mRFP*). **(F-F″)** A single (1.44 μm) z-slice of a 30 hpf *Tg(cldnB:GFP;Sox10:mRFP)* embryo, imaged using the 40x objective, showing supra- and infraorbital primordia (SOp and IOp) of the anterior lateral line diverging away from one another (F′) over a field of neural crest cells (F″; magenta). Scale bars are 10 μm throughout.

(2) Lateral line ganglia have a shared neural crest and placode origin

The lateral line system not only comprises the neuromast sensory organs, but also the ganglia and afferent nerves that innervate them. Moreover, all these components of the system derive from the same set of cranial placodes. We therefore turned our attention to investigating the anterior lateral line ganglia and their relationship with the neural crest cells.

Figure 3-3A-D'' shows lateral views of confocal maximum projections of the cranial region of *Tg(cldnB:GFP)* (yellow) specimens at 24 hpf, 30 hpf, 36 hpf, and 48 hpf. Specimens were immunolabeled with anti HuC/D antibody, a marker of differentiated neurons (cyan), and anti-Sox10 antibody, which marks neural crest cell

nuclei (magenta). The anterodorsal component (gAD) of the ALL ganglion is specified by 24 hpf (Fig. 3-3A-A''), adjacent to the acoustic ganglion (gVIII), and shifts anteriorly towards the trigeminal ganglion (gV) by 30 hpf, while rapidly growing in size (Fig. 3-3B-B''), as previously reported (Raible & Kruse, 2000). At 36 hpf and 48 hpf, the gAD retains a spherical shape and lies directly adjacent and posterior to the trigeminal ganglion (Fig. 3-3C-3D''). We were able to observe the first signs of neurons in the anteroventral component (gAV), specified ventromedially to the gAD, at 36 hpf (Fig. 3-3C-C''), a few hours earlier than the previously reported 40 hpf (Raible and Kruse 2000). Neurons of the lateral line ganglia (gAD, gAV, gP) can be identified by double labeling with HuC/D (cyan) and CldnB:GFP (yellow) (Fig 3-3A''-D''). Throughout the development of these lateral line ganglia, Sox10-positive neural crest cell nuclei are clustered around the gAD, gAV, and gP (Fig. 3-3A-D). We include a single z-slice inset (z depth 1.22 μm) in Fig. C'', which shows how neural crest cells (magenta) directly contact the clustered HuC/D-positive, CldnB:GFP-positive (cyan and yellow, respectively) cells of the gAD. We also observed that neural crest cells wrap around the supraorbital (nADso) and infraorbital (nADio) lateral line nerves of the gAD as early as 30 hpf (Fig. 3-3B''-D''), as well as the mandibular nerve (nAVmd) of the gAV once it is specified (Fig. 3-3D''').

Expression of Sox10 protein is down regulated rapidly in some migrating neural crest cells, such that anti-Sox10 antibody reveals only low levels of expression in those cells populating the developing pharyngeal arches (Fig. 3-3A-D''). By contrast, the membrane RFP signal provided by *Tg(sox10:mRFP)* is long-lasting, providing a more complete readout of neural crest cell localization. We therefore immunolabeled

Tg(sox10:mRFP) specimens with anti-HuC/D antibody, allowing a comparison of neural crest cell and neuron localization at 26 and 32 hpf (Fig. 3-3E-F''). At both stages, we find that the gAD is encased in a 'shell' of neural crest tissue.

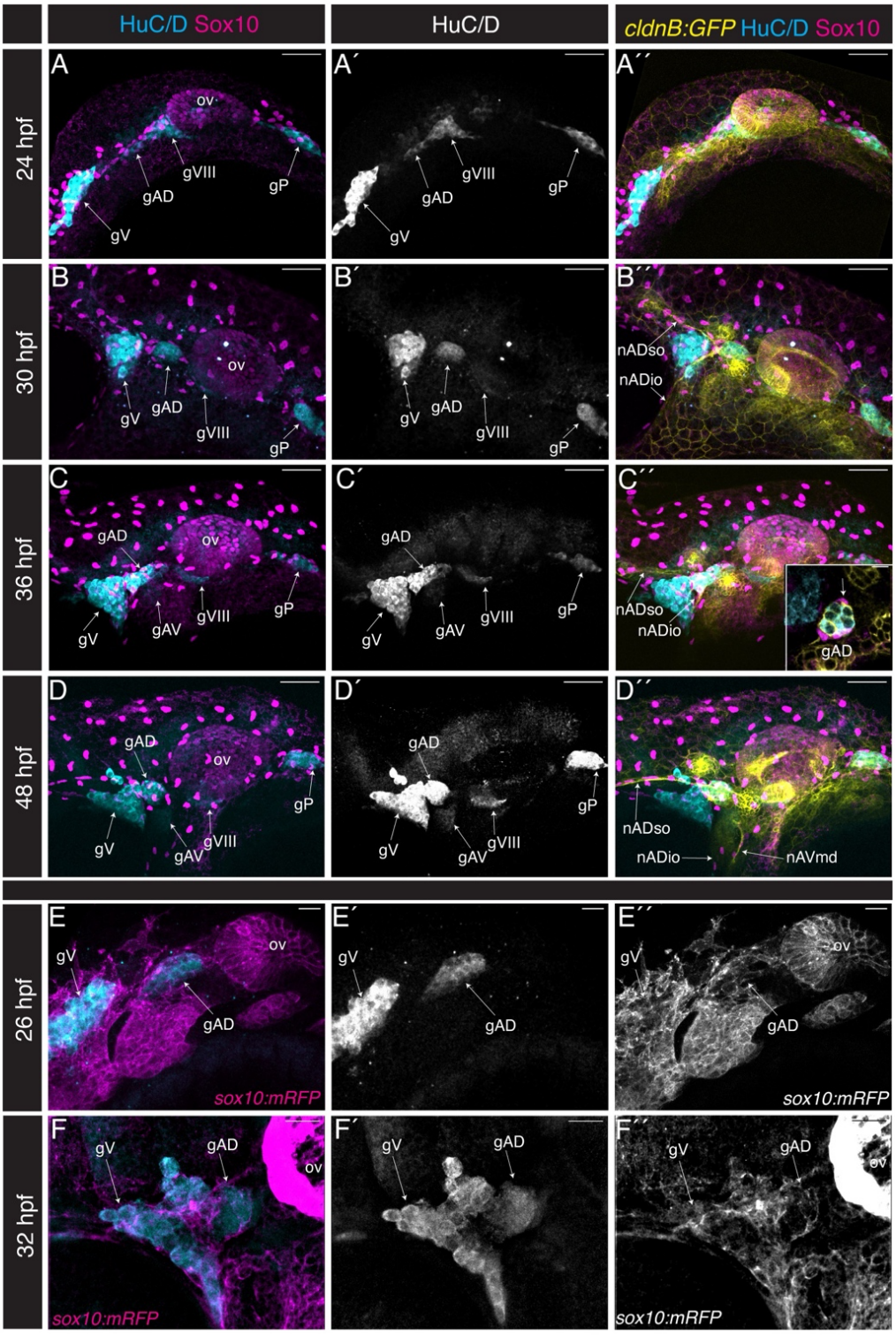

Figure 3-3: Lateral line ganglia form in close association with neural crest cells.

Fig 3.3 cont.: (**A-D″**) Confocal maximum projections in lateral view (40x objective), anterior to the left, of the lateral line ganglia of specimens co-labeled for differentiated neurons (anti HuC/D; cyan), neural crest cells (Sox10; magenta) and lateral line (*Tg(cldnB:GFP):* yellow); channels as indicated. In A (24 hpf), B (30 hpf), C (36 hpf), and D (48 hpf) neural crest cell nuclei are labeled with anti-Sox10 antibody. Inset in C″ is a single z-slice (z depth = 1.22 μm) showing neural crest cells (magenta) enveloping neurons in the anterodorsal lateral line ganglion (arrow; gAD; cyan). (**E-F″**) In E (26 hpf) and F (32 hpf) neural crest cell membranes are labeled by *Tg(sox10:mRFP)* (magenta) and differentiated neurons are labeled with anti HuC/D (cyan). The anti-HuC/D marker is shown in single channel in E′ and F'; *Tg(sox10:mRFP)* is shown in single channel in E″ and F″. Abbreviations: ov: otic vesicle; gV: trigeminal (Vth nerve) ganglion; gAD: anterodorsal lateral line ganglion; gAV: anteroventral lateral line ganglion; gVIII: acoustic ganglion; gPLL: posterior lateral line ganglion; nADso: supraorbital nerve; nADio: infraorbital nerve; nAVmd: mandibular nerve. Scale bars are 50 μm for A-D, 10 μm for the inset in C″, and 20 μm for E-F.

While data in Figure 3 indicate that lateral line gangliogenesis occurs in close proximity to the neural crest, it is unclear from this analysis whether neurons within the ganglia are neural crest cell-derived. To address whether there is a neural crest cell contribution to the anterior lateral line ganglion, we extended our analysis to later stages, shown in Figure 3-4. Fig. 3-4A shows a single high magnification confocal z-slice of a 72 hpf *Tg(sox10:mRFP)* specimen, immunolabeled with anti HuC/D antibody. In this single slice, two HuC/D-expressing ALL ganglion neurons can be seen to co-express mRFP (Fig. 3-4A-A"; arrowheads in Fig. 3-4A'). Cell counts (Fig. 3-4B) indicate a range of 3-6 neural crest derived neurons within the ALL ganglion at this stage. By 96 hpf, however, we were no longer able to detect mRFP signal in the ganglia of *Tg(sox10:mRFP)* specimens, presumably reflecting the down regulation of Sox10 in neural crest cells.

To facilitate longer term tracking of Sox10-expressing neural crest cells we made use of a two-transgene lineage tracing system previously employed by Kague et al. (2012): *Tg(-28.5Sox10:cre;ef1a:loxP-dsRed-loxP-egfp)*, for simplicity referred to hereafter as *Tg(sox10Cre;dsRed/EGFP*). The first transgene uses neural crest-specific *sox10* regulatory sequences to drive expression of Cre recombinase, and the second

transgene responds as a “switch”, with LoxP sites recombined by Cre to remove dsRed gene and bring EGFP under control of the *ef1a* ubiquitous promoter. Thus, despite the down regulation of Sox10 expression described above, once cells have expressed the *sox10*-driven Cre recombinase, they become genetically labeled by EGFP, a trait that is passed on to all that cell’s progeny.

As the *Tg(sox10Cre)* transgene is driven by different Sox10 regulatory sequences to those used in *Tg(sox10:mRFP)*, we began our analysis by confirming that *Tg(sox10Cre;dsRed/EGFP*) faithfully drives EGFP expression in Sox10 expressing cells. We compared *sox10Cre*-driven EGFP expression with anti-Sox10 antibody labeling in 22 hpf and 24 hpf specimens, stages selected to be early in neural crest cell migration while allowing sufficient time for the Cre recombinase to act. Fig. 3-4C-C” shows a lateral view of a confocal maximum projection of a 22 hpf *Tg(sox10Cre;dsRed/EGFP*) specimen. As expected, multiple cells are co-labeled with Sox10 antibody (yellow) and *Tg(sox10Cre;EGFP*) (magenta). The co-labeled cells (white arrowheads) are in the otic vesicle, the pharyngeal arches, and the pre-otic region where the ganglion will later form. In the ventrally-localized pharyngeal region, the Sox10 protein signal (Fig. 3-4C (yellow), C’) is already reduced, as expected due to down regulation of *sox10* gene expression, whereas the permanent EGFP signal (Fig. 3-4C (magenta), C”) is retained at high levels. Reciprocally, in dorsal regions, including the otic vesicle, some cells express high levels of Sox10 protein (Fig. 3-4C (yellow), C’) but are not yet EGFP-positive (Fig. 3-4C (magenta), C”). This reflects the expected temporal delay between the onset of Sox10 expression and *ef1a*-driven EGFP expression, which can only occur after completion of Cre/LoxP recombination. Results

were similar at 22 and 24 hpf, and, importantly, at both stages (n = 6) very few EGFP-expressing cells show no Sox10 protein expression and those that are present may have experienced transient Sox10 expression at an earlier stage. We conclude that *Tg(sox10Cre;dsRed/EGFP*) is a reliable reporter of neural crest cell identity and can therefore be used to investigate later neural crest cell contributions to the anterior lateral line ganglion.

Figure 3-4D shows a single high magnification confocal z-slice of a 96 hpf *Tg(sox10Cre;dsRed/EGFP)* specimen, immunolabeled with the HuC/D marker of differentiated neurons. At this stage, there are multiple EGFP-expressing (magenta) neural crest-derived cells co-labeled with HuC/D (cyan), in both the ALL ganglion and the adjacent trigeminal (gV) ganglion (Fig. 3-4D-D", arrowheads). Counts of neurons in the ALL ganglia at 96 hpf are provided in Fig. 3-4E. The finding of neural crest derived neurons in the ALL ganglion is consistent with our data using *Tg(sox10:mRFP)* at 72 hpf (Fig. 3-4A, B) and also confirms a previous report from Kague et al. (2012).

In Figure 3-4F we show a lateral view of a confocal projection of the broader cranial region of a 120 hpf *Tg(sox10Cre;dsRed/EGFP*) specimen, with the organization of the cranial ganglia again revealed by immunolabeling with the HuC/D marker of differentiated neurons (cyan). Fig. 3-4F shows the location of EGFP-labeled neural crest cells (magenta). Fig. 3-4G is a schematized version of Fig. 3-4F, indicating the locations of cranial ganglia and summarizing their placodal (cyan) or placode plus neural crest (hatched cyan/magenta) origins, based on our data. We find, again confirming the previous report by Kague et al. (2012), that the anterior lateral line, posterior lateral line, Vth/trigeminal, VIIth/facial, and VIIIth/acoustic ganglia (Fig. 3-4G:

gP, gV, gVII, and gVIII) each include neurons of mixed origins. In Figs 3-4H-K, we extend these previous findings, to demonstrate that both the dorsal and the ventral components of the anterior lateral line ganglion (gAD and gAV) share placode and neural crest cell contributions. Figures 4H and J are single high magnification confocal slices through the adjoining trigeminal (gV) and anterior lateral line ganglia (region boxed with red dashes in Fig. 3-4G). Panels H-H" show a single confocal z-slice through the superficial dorsal ganglion (gAD), whereas panels J-J" show a single confocal z-slice through the deeper ventral ganglion (gAV). Fig. 3-4I schematizes the relative locations of these slices. All neurons are HuC/D-positive (Figs 3-4H, H'' and J, J'') and a subset of the gV, gAD and gAV ganglia are EGFP-labeled (magenta) (Figs 3-4H', J'), revealing their neural crest origins. Counts of neurons in the ALL ganglia (both gAD and gAV) at 120 hpf are provided in Fig. 3-4E. The proportion of neural crest derived neurons in gALL increased from an average of 14% at 72 hpf to 25% at 120 hpf ($n = 5$ each, Wilcoxon test $p < 0.05$). In summary, both the anterodorsal and the later forming anteroventral components of the zebrafish anterior lateral line ganglion combine placode-derived and neural crest-derived neurons (schematized in Fig.3-4K).

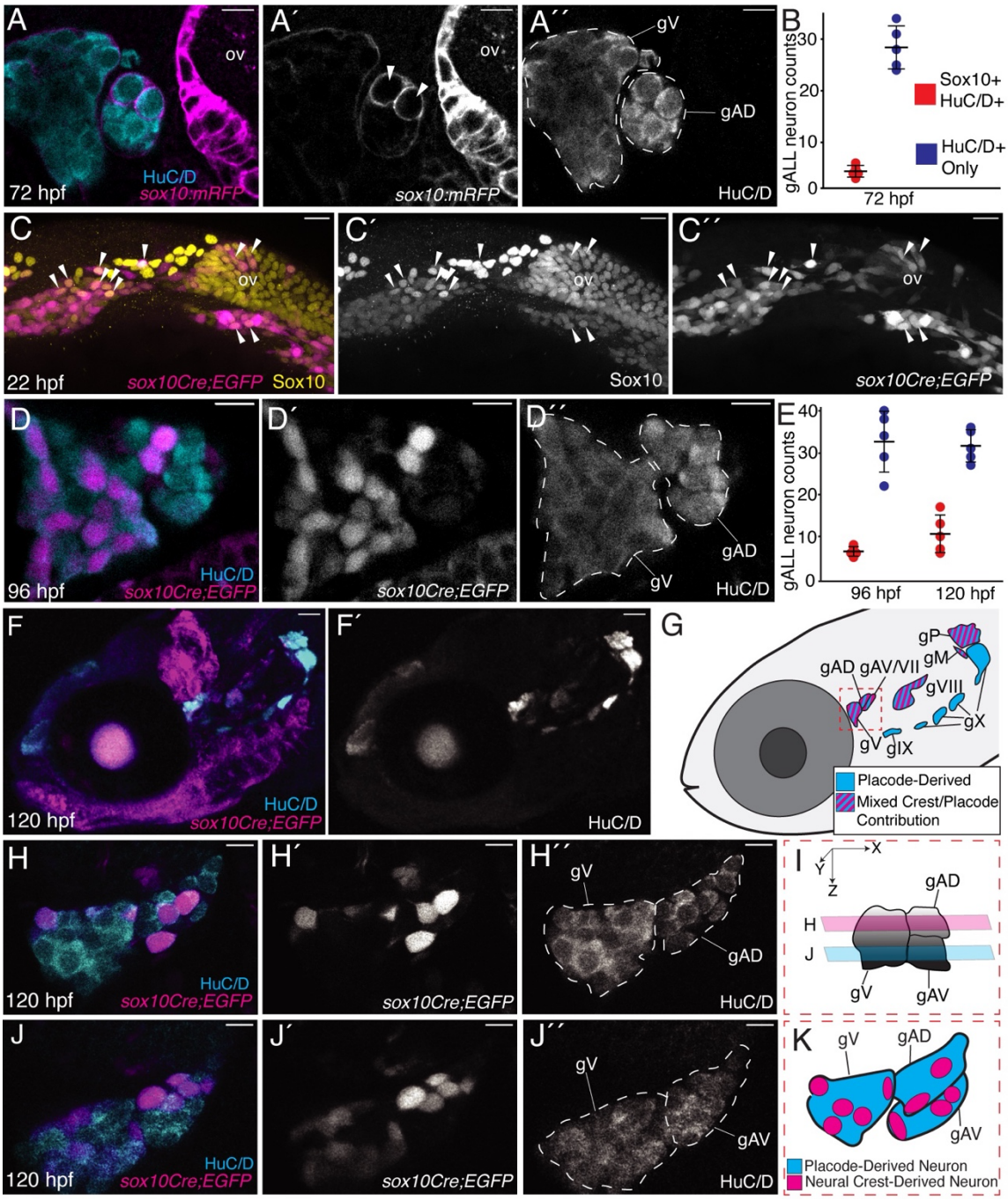

Figure 3-4:Lateral line ganglia have a shared neural crest and placode origin.

Fig 3-4 cont.: (**A-A″**) A single high magnification confocal z-slice (40x objective) through the anterior lateral line ganglion of a 72 hpf specimen (of n = 5). (A) Neural crest cell membranes are labeled by *Tg(sox10:mRFP)* (magenta) and differentiated neurons are labeled with anti HuC/D (cyan). (A′) *Tg(sox10:mRFP)* only; arrowheads indicate *sox10mRFP*-expressing neurons in the gALL. (A″) HuC/D-positive differentiated neurons only. (**B**) Quantification of *sox10:mRFP*-positive (Sox10+); HuC/D+ neurons (red) and *sox10:mRFP*-negative (Sox10-); HuC/D+ neurons (blue) in the ALL ganglia at 72 hpf (n = 5). Mean and standard deviation are indicated. (**C-C″**) Confocal maximum projection (40x objective), in lateral view with anterior to the left, of the pre-otic region of a 22 hpf *Tg(sox10Cre;dsRed/EGFP*) specimen immunolabeled with anti-Sox10 antibody (yellow) (of n = 6). (C) Sox10 antibody labeled neural crest cell nuclei (yellow) and *sox10Cre;EGFP* labeled cells (magenta). Co-labeled cells are indicated with white arrowheads. (C′) Sox10-antibody positive neural crest cell nuclei only. (C″) *sox10Cre;EGFP* labeled cells only. (**D-D″**) A single high magnification confocal z-slice (40x objective) through the anterior lateral line ganglion of a 96 hpf specimen (of n = 5). (D) Neural crest cells are labeled with *sox10Cre;EGFP* (magenta) and differentiated neurons are labeled with anti HuC/D (cyan). (D′) *sox10Cre;EGFP* only. (D″) HuC/D-positive differentiated neurons only. (**E**) Quantification of *sox10Cre;EGFP*-positive; HuC/D-positive (red) neurons and *sox10Cre;EGFP*-negative; HuC/D-positive (blue) neurons in the ALL ganglia at 96 hpf (n = 5) and 120 hpf (n = 5). (**F, F′**) Confocal maximum projection (10x objective), in lateral view with anterior to the left, of the cranial region of a *Tg(sox10Cre;dsRed/EGFP*) 120 hpf specimen immunolabeled with anti HuC/D (of n = 6). (F) HuC/D-positive neurons (cyan) together with *sox10Cre;EGFP* neural-crest derived cells (magenta). (F′) HuC/D-positive differentiated neurons only. (G) Schematic representation of panel F indicating placode and neural crest contributions to the cranial ganglia. (**H-J″**) Higher magnification views (40x objective) of the region boxed in G (red dashed line). (**H-H″**) A single z-slice (1.02 μM), in the plane of the anterodorsal lateral line ganglion and trigeminal ganglion. (H) Merge, neural crest-derived cells in magenta and HuC/D-positive neurons in cyan. (H′) neural-crest-derived cells (*Sox10Cre;EGFP*); (H″) HuC/D-positive neurons; (**J-J″**) A single z-slice (1.02 μM), in the plane of the anteroventral lateral line and trigeminal ganglion. (J) merge, neural-crest derived cells in magenta and HuC/D-positive neurons in cyan. (J′) neural crest-derived cells (*Sox10Cre;EGFP*); (J″) HuC/D-positive differentiated neurons only; (**I**) Schematic representation of the ganglia shown in H and J, indicating the z-planes imaged. (**K**) Schematic representation of panels H and J, showing the neural crest contribution (magenta) to the anterior lateral line ganglia and the trigeminal ganglion. Scale bars are 20 μm in A, C, D; 50 μm in F, and 10 μm in H, J. Abbreviations are as follows: ov: otic vesicle; gV: trigeminal (Vth nerve) ganglion; gALL: anterior lateral line ganglion; gAD anterodorsal lateral line ganglion; gAV: anteroventral lateral line ganglion; gAV/gVII: anteroventral lateral line ganglion fused with facial ganglion; gVIII: acoustic ganglion; gM: middle lateral line ganglion; gP: posterior lateral line ganglion, gIX: glossopharyngeal ganglion; gX: vagal ganglion

(3) Anterior lateral line development is disrupted in the absence of neural crest

Having confirmed a close physical relationship between cranial neural crest cells and all parts of the anterior lateral line system, we tested the hypothesis that neural crest cells play a functional role in anterior lateral line patterning and development. To remove neural crest cells, we turned to a commonly used method to ablate zebrafish cells conditionally: the genetic/pharmacological approach based on expression of the transgene-encoded bacterial enzyme Nitroreductase (NTR)(Curado et al., 2007).

(Genetically encoded NTR converts a prodrug into a cytotoxic compound that is strictly limited to the NTR-expressing cells, thus causing cell-specific apoptosis (White and Mumm, 2013). To achieve neural crest-specific cell death we used the *Tg(sox10:NTRmCherry)* transgene, which expresses NTR enzyme and mCherry fluorescent protein under control of the neural crest specific *sox10* regulatory sequences. By treating these transgenic specimens with the prodrug Nifurpirinol (NIF) we achieved effective ablation of the NTR-expressing neural crest cells without generalized toxicity, consistent with previous reports (Bergemann et al., 2018; Cavanaugh et al., 2015). We then used this approach to evaluate how depletion of neural crest cells impacts development of the anterior lateral line system.

Figure 3-5A-D' shows lateral views of confocal maximum projections of the crania of *Tg(sox10:NTRmCherry; cldnB:GFP)* double transgenic specimens, treated with DMSO carrier control, at 36 hpf, 48 hpf, 72 hpf, and 120 hpf. As expected, development of the lateral line system in the DMSO-treated controls was indistinguishable from that of unmanipulated specimens (compare Fig. 3-5A-B' with Figs 3-1 and 3-2). Fig. 3-5E-L shows *Tg(sox10:NTRmCherry;cldnB:GFP)* experimental specimens, which were treated with 1.25 μM NIF from the 9 hpf stage; a stage selected because it is immediately before the onset of *sox10* expression. In the experimental specimens, at 36 hpf and at all subsequent stages, we observed widespread neural crest cell death: apoptotic cells are distinguished by their reduced size and eventual degradation to puncta, accompanied by a dramatic reduction in mCherry signal. The absence of neural crest cells led to disrupted cranial morphology, with a complete absence of jaw structures apparent by 72 hpf. Despite a lack of neural crest cells, the

specimens remained generally healthy and continued to develop, although by 120 hpf they displayed dysmorphic hearts as previously reported in response to an equivalent manipulation (Cavanaugh et al., 2015). We also noted that the otic vesicle was reduced in size, consistent with expression of *Tg(sox10:NTRmCherry)* in this structure. We used the *cldnB:GFP* transgene to evaluate how the lateral line system was affected by the loss of neural crest cells. Fig. 5E-L shows two independent experimental specimens out of n =/> 10, at each of the four developmental stages.

At the 36 hpf stage there were only modest differences between the anterior lateral lines of control (Fig. 3-5A, A') and NIF-treated experimental (Fig. 3-5E, I) specimens. When neural crest cells were depleted, the supraorbital primordium exhibited a modest reduction in distance migrated above the eye, but otherwise appeared similar to control specimens. The infraorbital cell stream similarly exhibited a more limited extension relative to controls, and also appeared slightly broader. By the 48 hpf stage the phenotypes in experimental specimens were more pronounced. In 48 hpf control specimens (Fig. 3-5B, B') the SO1 neuromast had already begun to bud from SO2, and extended anteriorly, approaching the developing olfactory bulb (Fig. 3-5B', ob). By contrast, in the experimental specimens (Fig. 3-5F, J) the supraorbital line had not extended beyond the dorsal apex of the eye, with limited or scant SO2 budding (Fig. 3-5F, SO*; Fig, 3-5J). Additionally in 48 hpf control specimens, the infraorbital line had completely extended along the ventral edge of the eye (Fig. 3-5B, B'), and the IO2 neuromast had formed, whereas in experimental specimens the infraorbital was significantly underdeveloped, and in most cases had extended very little beyond its 36 hpf position with no IO2 neuromast in place (Fig. 3-5F, J). In some experimental

specimens an infraorbital neuromast appeared to have been displaced dorsally, up into the supraorbital region (e.g. Fig. 3-5F, IO*). Additional evidence supporting the assignment of such ectopic neuromasts to the infraorbital system came from our studies of innervation and time-lapse microscopy (see Figs 3-6 to 3-8, below).

The phenotype of restricted supra and infraorbital development continued through the 72 and 120 hpf stages in NIF-treated specimens (Fig. 3-5G, H, K, L). The supraorbital line rarely extended beyond the apex of the eye, never reaching the olfactory bulb region, while the infraorbital line remained drastically shortened with missing neuromasts (compare Fig. 3-5C, C' with Fig. 3-5G, K, and Fig. 3-5D, D' with Fig. 3-5H, L). To quantify the extension of the supraorbital line we measured the linear distance between the center of the O1 neuromast and the center of the furthest migrated (most anteriorly-located) SO neuromast at the 120 hpf stage. This distance averaged 322 mm in DMSO-treated control specimens (n = 9) compared with 243 mm in NIF-treated specimens (n = 13). This 25% reduction in supraorbital extension in specimens that lack neural crest cells was highly significant ($P < 0.0001$; Wilcoxon Test). At the 120 hpf stage, many experimental specimens had formed an additional infraorbital neuromast, to result in two total (compare Fig. 3-5H, L with D, D'), but we never observed more than three total IO neuromasts in experimental specimens (average number = 2.77; n = 13), whereas control specimens typically had four IO neuromasts (average number = 3.89; n = 9). This difference was also highly significant ($P < 0.0001$; Wilcoxon Test). Additionally, at these later stages, we observed emergence of ectopic supernumerary neuromasts in the posterior supraorbital region of 25% of the NIF-treated specimens analyzed (brackets, Fig. 5K, L), resulting in arrays of

closely clustered neuromasts. By 120 hpf the mandibular and opercular lines have begun to form in control specimens (Fig. 3-5D, D'). Both are entirely absent from the neural crest deficient specimens, consistent with major deficits in the neural crest-populated mandibular and hyoid arches.

In the absence of neural crest-derived glial cells, as occurs in several zebrafish mutants including those in the ErbB/Neuregulin pathway (Lush and Piotrowski, 2014), precocious intercalary neuromasts form in the posterior lateral line system. We found that our neural crest cell-deficient specimens similarly displayed supernumerary posterior lateral line neuromasts in the trunk, consistent with the predicted loss of glial cells. Figure 3-5M-P shows confocal projections of whole *Tg(sox10:NTRmCherry;cldnB:GFP)* larvae in lateral view at the 30 hpf and 72 hpf stages. DMSO-treated control specimens display typical posterior lateral line primordium migration at 30 hpf, with healthy neural crest cells (magenta) migrating ventrally in streams adjacent to each somite (Fig. 3-5M). By 72 hpf, 5-7 primary posterior lateral line neuromasts have been deposited at regular intervals along the trunk (Fig. 3-5N, this example has 6 trunk neuromasts). At 30 hpf the NIF-treated specimens showed normal primordium migration, although the most anterior neural crest cells—which were born earliest—are already rounding up and undergoing apoptosis (Fig. 3-5O). By 72 hpf all neural crest cells are either absent or dead, and supernumerary posterior lateral line neuromasts are present (Fig. 3-5P, this example has 13 trunk neuromasts). Importantly, despite the development of precocious neuromasts, the posterior lateral line migrates all the way to the posterior limit of the trunk when neural crest cells are absent (n = 10). We conclude that migration of the

posterior lateral line primordium is independent of neural crest cells, unlike the situation for the anterior lateral line system.

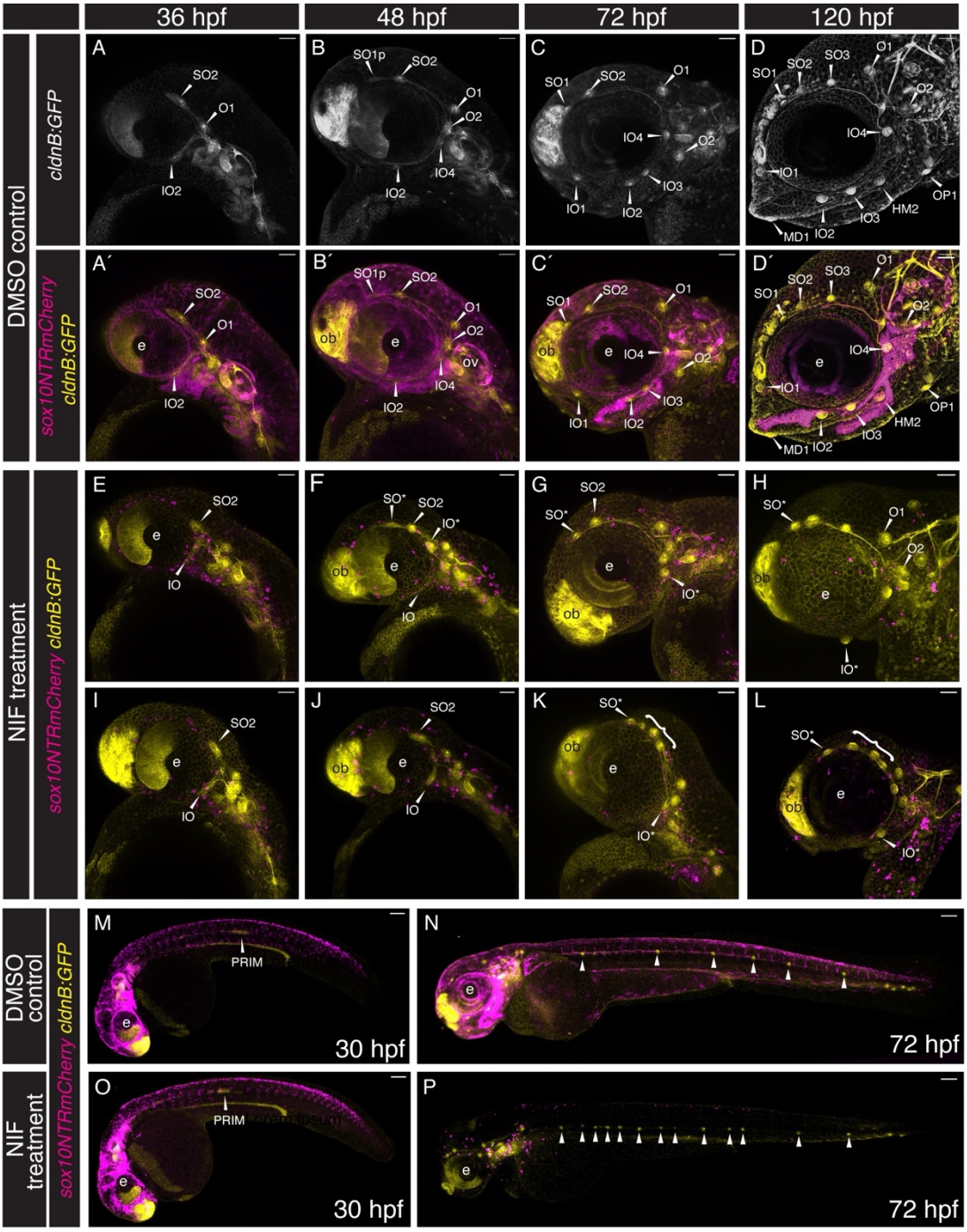

Figure 3-5: Anterior lateral line development is disrupted in the absence of neural crest cells.

Fig 3-5 cont.: (**A-L**) Confocal maximum projections, in lateral view with anterior to the left, of the cranial regions of *Tg(sox10:NTRmCherry;cldnB:GFP)* double transgenic specimens at 36 to 120 hpf. (**A-D′**): DMSO carrier-treated controls show normal development of the lateral line; stages are as indicated. A-D show the lateral line alone *(cldnB:EGFP)*; A′-D′ show both lateral line (*cldnB:EGFP*; yellow) and neural crest (*sox10:NTRmCherry*; magenta). (**E-L**) When neural crest (*sox10:NTRmCherry*; magenta) cytotoxicity is activated via Nifurpirinol (NIF) treatment, lateral line (*cldnB:GFP*; yellow) development is disrupted. Two different samples are shown at each stage (n = 14 at 36 hpf, n = 10 at 48 hpf, n = 10 at 72 hpf, n = 16 at 120 hpf). The dying *sox10:NTRmCherry*-positive neural crest cells show punctate fluorescence at all stages, with the number of remaining neural crest cells reducing over time. Lack of neural crest leads to disrupted morphogenesis of the anterior lateral lines. The anterior-most neuromast of the supraorbital line (SO∗) never reaches the olfactory bulb (ob), even at 120 hpf post fertilization. By 72 hpf we sometimes observe an array of ectopic neuromasts in the posterior supraorbital domain (brackets, K, L). Infraorbital lateral line development is severely truncated, with fewer than normal infraorbital neuromasts, often inappropriately positioned (IO∗), developing. (**M-P**) Low magnification, tiled, confocal maximum projections, in lateral view with anterior to the left, of entire *Tg(sox10:NTRmCherry;cldnB:GFP)* double transgenic specimens. (**M, N**): DMSO carrier-treated control specimens show normal development of the posterior lateral line (*cldnB:EGFP*; yellow) and trunk neural crest cells (*sox10:NTRmCherry*; magenta). (M) 30 hpf, the posterior lateral line primordium (PRIM; yellow) is migrating through the anterior trunk, and neural crest cells (magenta) are located in the dorsal neural tube and migrating ventrally in segmental streams. (N) 72 hpf, shows six evenly distributed trunk neuromasts (arrowheads). (**O, P**) Nifurpirinol (NIF) treatment causes neural crest (*sox10:NTRmCherry*; magenta) cytotoxicity and formation of supernumerary trunk neuromasts, but does not prevent the posterior lateral line from migrating fully along the trunk. (O) 30 hpf; shows the posterior lateral line primordium (PRIM; yellow) migrating normally through the anterior trunk, while neural crest cells (magenta) are starting to die. (P) 72 hpf; shows multiple supernumerary trunk neuromasts (arrowheads), while most neural crest cells (magenta) are now absent. Abbreviations are as follows: e: lens of the eye; ov: otic vesicle; ob: olfactory bulb; SO: supraorbital neuromast; IO: infraorbital neuromast; O: otic neuromast; OP: opercular neuromast; HM: hyomandibular neuromast; MD: mandibular neuromast. Scale bars are 50 μM throughout.

(4) Anterior lateral line gangliogenesis and innervation are disrupted in the absence of neural crest

As cranial neural crest cells contribute directly to the lateral line ganglia (Figs 3-3, 3-4) we predicted that absence of neural crest would cause disruptions to anterior lateral line gangliogenesis and potentially to innervation. We tested this prediction by once again taking advantage of *Tg(sox10:NTRmCherry)* specimens and NIF treatment to cause neural crest cell death. Figure 3-6A-C shows lateral views of confocal projections of the region surrounding, and posterior to, the developing eye of DMSO control-treated *Tg(sox10:NTRmCherry)* specimens at 48 hpf, 72 hpf, and 120 hpf. These specimens additionally carry *Tg(cntnap2a:EGFP)* (cyan), which is expressed exclusively in the afferent lateral line nerves (Faucherre et al., 2009; Pujol-Martí et al. ,2012), and are

immunolabeled with anti-Sox2 antibody (yellow), to mark neuromast support cells (Hernández et al., 2007); Figs 3-6A'-C' show *cntnap2a:EGFP* alone. At the 48 hpf stage (Fig. 3-6A, A') the dorsally located SO2 neuromast is innervated by the supraorbital nerve (nADso) and the ventrally located IO2 neuromast is innervated by the infraorbital nerve (nADio). Both the supraorbital and infraorbital nerves extend from the gAD ganglion. Two additional nerves emerge from gAD to innervate the otic neuromasts, O1 and O2, generating a characteristic 'X' pattern, which is maintained at 72 hpf and 120 hpf as development proceeds (Fig. 3-6B, B'; C, C'). By 72 hpf (Fig. 3-6B, B') the developing mandibular neuromasts are innervated by the mandibular nerve (nAVmd), which emerges from the recently formed ventral (gAV) anterior lateral line ganglion. By 120 hpf this nerve has branched to form the opercular nerve (nAVop), and the ventral ganglion (gAV) can now be visualized as a separate component of the anterior lateral line ganglion.

The DMSO-treated control specimens (Fig. 3-6A-C') are compared with two independent NIF-treated specimens (out of n = 10 at each stage; Fig. 3-6D-I). As early as 48 hpf, ectopic nerves could be visualized in the supraorbital region (arrows), frequently innervating misplaced neuromasts (indicated by asterisks; e.g. Fig. 3-6D, E, F). The dorsal translocation of the nADio nerve confirmed that an IO neuromast is often deposited in an unusually dorsal location to lie close to SO neuromasts (e.g. Fig. 3-6E). By 120 hpf, 8 of 10 NIF-treated specimens have multiple dorsally-directed projections (e.g. Fig. 3-6F, I; and see also Fig. 3-7F, ahead), suggesting that ectopic supernumerary neuromasts originate not only from the misdirected IO, but additionally from other sources, which might include precocious proliferation of interneuromast cells.

At the 120 hpf stage the lack of a separated gAV ganglion becomes apparent in the NIF-treated specimens, with the gAV-derived mandibular and opercular nerves missing altogether (Fig. 3-6F, I). In addition to reduced and missing ganglia, the nerves themselves are often thinner in the NIF-treated neural crest-deficient specimens, likely as a consequence of missing neural crest-derived neurons. We also noted that the nerves emerged from non-uniform points on the ganglia, relative to controls, and that the nerves are often defasciculated, as additionally shown ahead (see Fig. 3-7D). In some specimens, nerves extended erratically in the supraorbital region without innervating a neuromast (e.g. Fig. 3-6E).

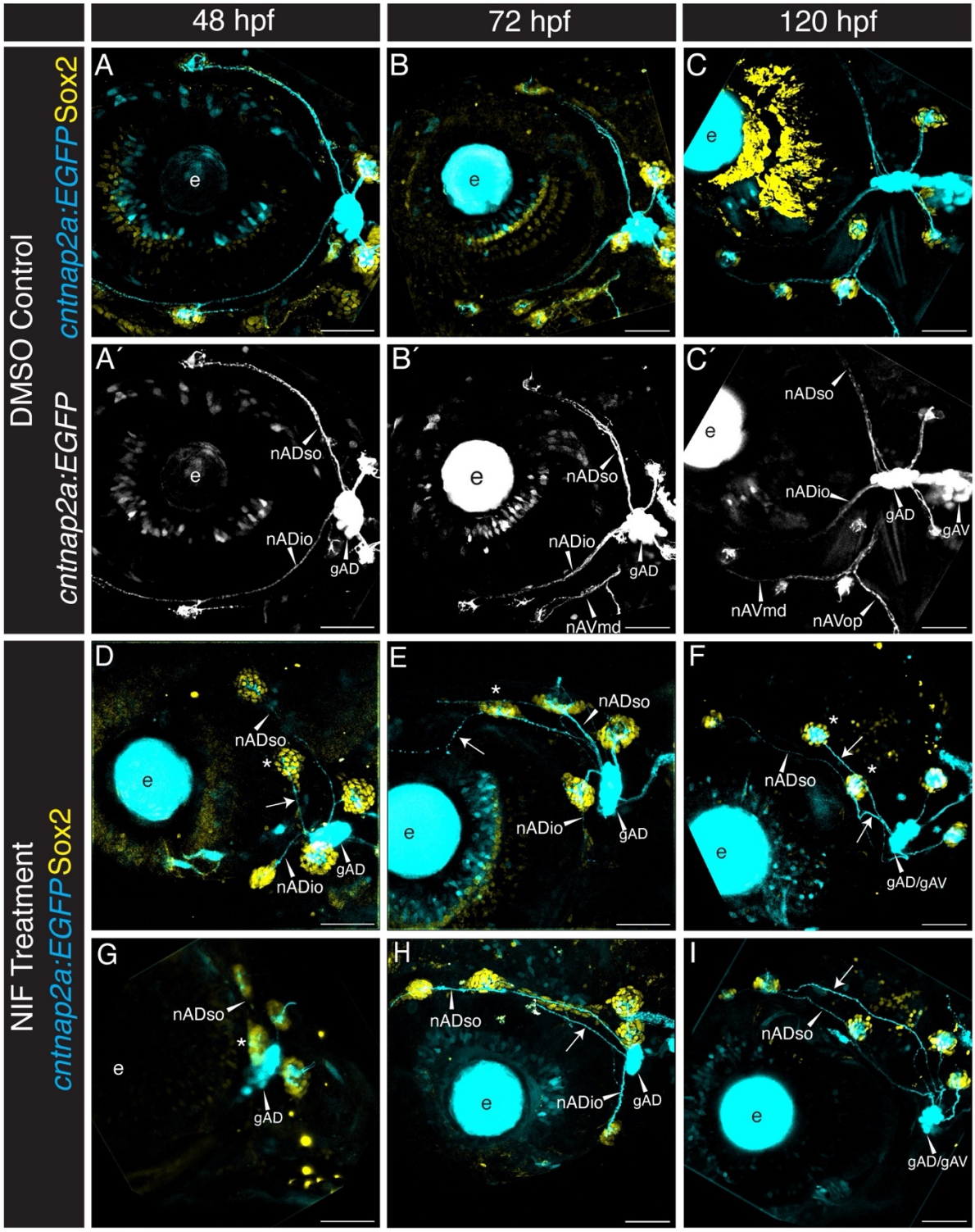

Figure 3-6:Lateral line innervation is disrupted in the absence of neural crest.

Fig 3-6 cont.: (**A-I**) Confocal maximum projections (40x objective), in lateral view with anterior to the left, of the cranial regions of *Tg(sox10:NTRmCherry;cntnap2a:EGFP)* double transgenic specimens at 48 to 120 hpf. The *cntnap2a:EGFP* transgene (cyan) labels afferent lateral line neurons and the lens of the eye. The specimens are also immunolabeled with the neuromast support cell marker anti-Sox2 (yellow). (**A-C**): DMSO carrier-treated controls show normal development of the lateral line nerves (*cntnap2a:EGFP*; cyan) and neuromasts (Sox2; yellow). (**A′-C′**) are the same specimens as A-C, shown in the *cntnap2a:EGFP* (cyan) channel alone. Stages are as indicated. (**D-I**) When neural crest (*sox10:NTRmCherry*; not shown) cytotoxicity is activated via Nifurpirinol (NIF) treatment, lateral line innervation (*cntnap2a:EGFP*; cyan) and neuromast organization (Sox2, yellow), are both disrupted. Two different samples, out of n = 10 at each stage, are shown. Innervation is disrupted, with gAV nerves nAVmd and nAVop failing to form by 120 hpf (compare F, I with C′). Nerves often project to misplaced neuromasts, although some fail to reach a neuromast and project ectopically (arrows). Nerves also make multiple supraorbital projections, often innervating ectopic or supernumerary neuromasts (D, E, F, G, asterisks), and tend to be defasiculated and contain fewer axons in comparison to DMSO-treated control specimens. Abbreviations are as follows: e: lens of the eye; nADso: supraorbital nerve; nADio: infraorbital nerve; nAVmd mandibular nerve; nAVop: opercular nerve. Scale bars are 50 μM throughout.

In Figure 3-7 we compare confocal maximum projections of high magnification lateral views, showing the anterior and posterior lateral line ganglia and the afferent nerves of untreated control (Fig. 3-7A), DMSO-treated control (Fig. 3-7B), and NIF-treated experimental (Fig. 3-7C) 120 hpf *Tg(sox10:NTRmCherry;cntnap2a:EGFP)* double transgenic specimens. Compared with the two control conditions, which show no significant differences from one another, NIF-treated specimens lack most of the posterior lateral line ganglion (gP) cells, and have a significant reduction in the anterior lateral line ganglia. Moreover, the gAD and gAV components of the anterior lateral line ganglia can no longer be distinguished in experimental specimens (gAD/gAV, Fig. 3-7C). While the controls show distinct axon projections from the gAD and gAV ganglia into the hindbrain, NIF-treated specimens lack the gAV projection and have thinner, defasciculated axons (compare Figs 3-7A, B, C, arrowheads). Fig. 3-7D shows an example of the defasciculation typical in neuromast-innervating nerves of neural crest-deficient specimens.

We next quantified aspects of these phenotypes. Fig. 3-7E is a Boxplot comparing counts of anterior lateral line ganglia neurons in DMSO-control specimens

(blue) with NIF-treated specimens (red), revealing a significant reduction in number of neurons when neural crest cells are missing. Fig. 3-7F quantifies the number of supraorbital nerve projections that innervate neuromasts in DMSO-treated control specimens (blue) versus NIF-treated specimens (red) at 48 hpf, 72 hpf, and 120 hpf. This analysis reveals that when neural crest cells are lacking there is a modest increase in the number of nerve projections at 48 hpf and 72 hpf, followed by a significant increase at 120 hpf. The increase in projections correlates with the increase in neuromasts, as shown in Fig. 3-7G, which quantifies the number of neuromasts in the supraorbital region of DMSO-treated control specimens (blue) versus NIF-treated specimens (red) at 48 hpf, 72 hpf, and 120 hpf. When neural crest cells are missing there is an increase in the number of neuromasts in the supraorbital region, which becomes significant at 120 hpf.

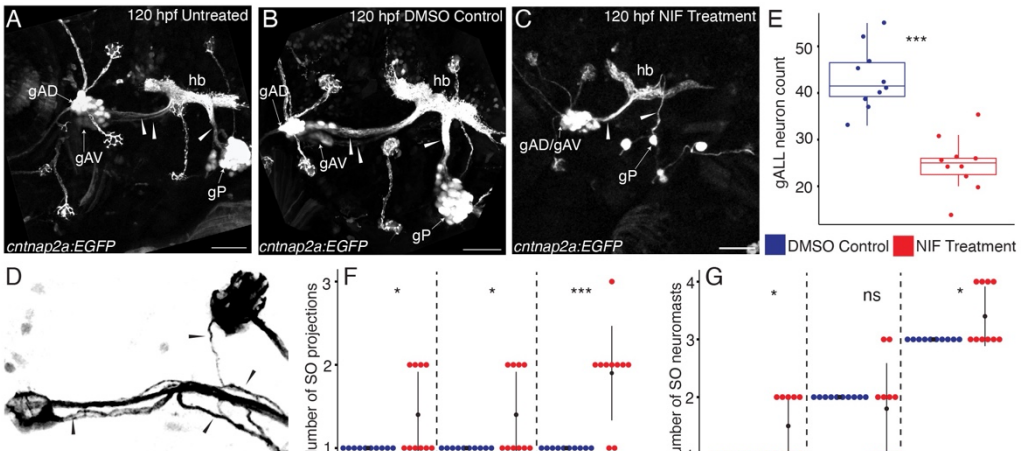

Figure 3-7:Lateral line patterning and gangliogenesis are disrupted in the absence of neural crest

(A-C) Confocal maximum projections (40x objective), in lateral view with anterior to the left, of the lateral line afferent system of *Tg(sox10:NTRmCherry;cntnap2a:EGFP)* specimens at 120 hpf; *(cntnap2a:EGFP)* shown in single channel. (A) Untreated specimen showing the locations of the gAD, gAV, and gP lateral line ganglia and their individual projections to the hindbrain (arrowheads). (B) DMSO carrier-treated control showing normal ganglia morphology and innervation patterns *(cntnap2a:EGFP)*. (C) When neural crest (*sox10:NTRmCherry*) cytotoxicity is activated via Nifurpirinol (NIF) treatment, lateral line ganglion morphology is disrupted.

Fig 3-7 cont.: The gAV and gAD ganglia are no longer separated, show altered density and shape, and make a shared projection to the hindbrain. The posterior ganglion has severe deficits. (**D**) Example of neuromast-innervating nerves (*cntnap2a:EGFP*, black) defasciculation (arrowheads) in the absence of neural crest cells. (**E**) Boxplot showing counts of HuC/D-expressing neurons, in both the dorsal and ventral parts of the anterior lateral line ganglia in DMSO control versus NIF-treated specimens at 120 hpf (n = 10 for each condition). (**F**) Stacked Histogram showing the number of supraorbital nerve projections to neuromasts in DMSO control versus NIF-treated conditions at 48 hpf, 72 hpf, and 120 hpf (n = 10 for each stage and condition). (**G**) Stacked Histogram showing the number of neuromasts in the supraorbital region of DMSO control versus NIF treated specimens at 48 hpf, 72 hpf, and 120 hpf (n = 10 for each stage and condition). Abbreviations are as follows: gAD: anterodorsal lateral line ganglion; gAV: anteroventral lateral line ganglion; gP: posterior lateral line ganglion; hb: hindbrain. Data are shown as the mean ± SD (E, F, G) ns $P > 0.05$, $*P < 0.05$, $***P < 0.001$ (Wilcoxon rank-sum test). Scale bars are 50 μM (A–C) and 20 μM (D).

Finally, to gain a more dynamic understanding of how inappropriately localized anterior lateral line neuromasts and disrupted nerves develop in the absence of neural crest cells, we again turned to SPIM time-lapse analysis. Figure 3-8 shows a series of still images taken from a time-lapse analysis of a NIF-treated *Tg(cldnB:GFP;sox10:NTRmCherry)* double transgenic specimen, imaged between 33 and 55 hpf (Fig. 3-8A-F; and Supplemental Videos 5, 6). By 33 hpf (Fig. 3-8A) the supraorbital (SOp) and infraorbital (IOp) primordia had split anterior to the otic vesicle (ov). However, unlike unmanipulated control specimens with a full complement of neural crest cells (Figs 3-1, 3-2), in this specimen a broad region of Cldn:GFP labeled tissue (asterisk) remained between the supraorbital and infraorbital branches.

By 34.7 hpf (Fig. 3-8B) the otic neuromasts O1 and O2 had condensed, while the supraorbital primordium SOp had continued to migrate dorsoanteriorly over the eye (e). Distinct from specimens with intact neural crest cells (Figs 3-1, 3-2 and Supplemental Movies 1-4), in this experimental specimen (Fig. 3-8B) the infraorbital primordium split into a dorsal branch (IOp*) as well as a ventral branch (IOp), as it approached the eye. By 37.9 hpf (Fig. 3-8C) the ectopic dorsal component of the infraorbital primordium (IOp*) had begun migrating parallel to the supraorbital primordium SOp, while the

ventral component of the infraorbital primordium (IOp) behaved as in unmanipulated specimens, migrating ventrally. The ventral component of the primordium started to condense into the first infraorbital neuromast by 42.7 hpf (Fig. 3-8D, IO4), while the dorsal component (IOp*) continued to migrate parallel to the supraorbital primordium (Fig. 3-8D, SOp). By 46.3 hpf (Fig. 3-8E), migration of the ventral infraorbital primordium had completely stalled, with IO4 now in place. The supraorbital primordium deposited neuromast SO2, and its migration stalled at the apex of the eye (Fig. 3-8E, SOp). The dorsal branch of the infraorbital primordium (IOp*) similarly stalled parallel to SO1p at the apex of the eye, after having dropped off an ectopic neuromast IO* (Fig. 3-8E). By 55 hpf (Fig. 8F), the supraorbital and ectopic dorsal branch of the infraorbital primordia (SOp and IOp*) had ceased to migrate, after having deposited neuromasts SO2 and IO*, respectively. Axons can be seen extending from the anterior lateral line ganglia (gALL) to the otic neuromast O1, the supraorbital neuromast SO2, the infraorbital neuromast IO4, as well as ectopic neuromast IO* (Fig. 3-8F). The region of ectopic Cldn:GFP labeled tissue between the supraorbital and infraorbital branches (asterisks, Fig. 3-8A-E) gradually reduced in size over developmental time, consistent with the possibility that these cells might become incorporated into the ectopic dorsally projecting IO primordium (IOp*).

In summary, we found that when neural crest cells are absent, there are not only disruptions in neuromast migration, number, and organization, but also related disruptions in their innervation and reductions in the size of the anterior lateral line ganglion.

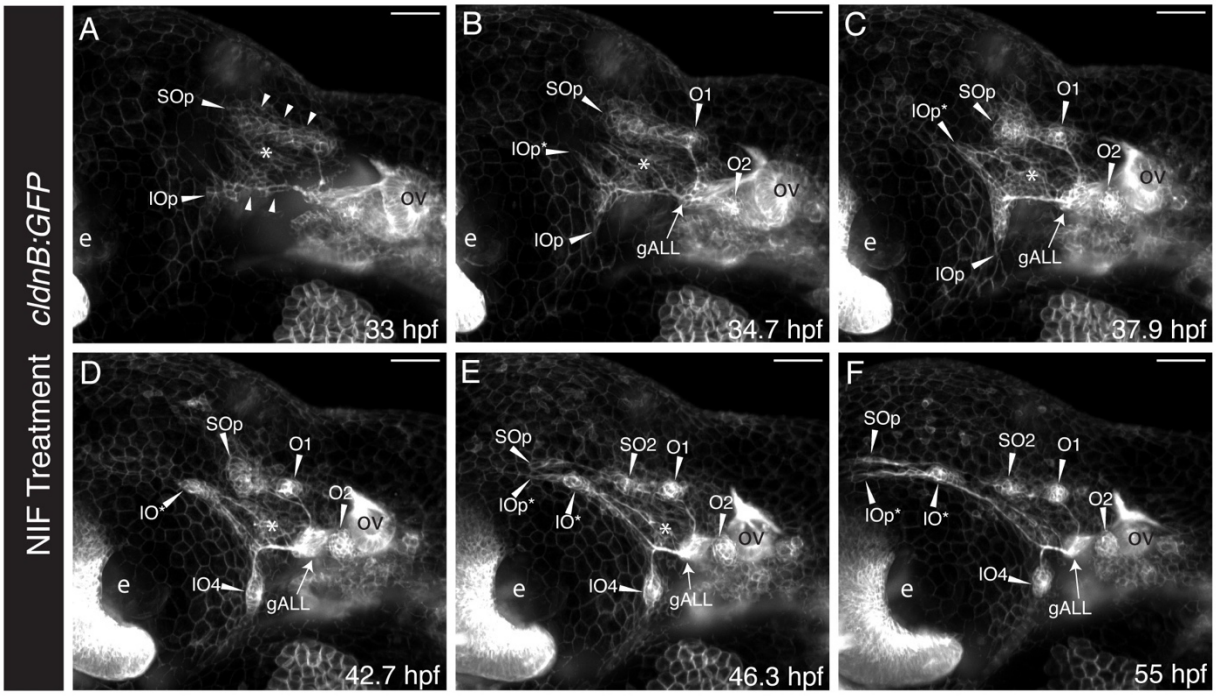

Figure 3-8:Time-lapse analysis of anterior lateral line development in the absence of neural crest cells.

(**A-F**) SPIM time-lapse images of the cranial region of a *Tg(sox10:NTRmCherry;cldnB:GFP)* double transgenic specimen, treated with Nifurpirinol (NIF), in lateral view with anterior to the left. Single channel maximum projections, imaged using the 10x objective, showing only the *cldnB:GFP* label are shown at (A) 33 hpf, (B) 34.7 hpf, (C) 37.9 hpf, (D) 42.7 hpf, (E) 46.3 hpf, and (F) 55 hpf. **(A)** Arrowheads indicate primordia of the supraorbital (SOp) and infraorbital (IOp) lines splitting anterior to the otic vesicle at 33 hpf, as they begin to migrate. **(B)** shows the infraorbital primordium splitting into two primordia at 34.7 hpf, a ventrally projecting branch (IOp) and an ectopic anterodorsally projecting branch (IOp∗); otic neuromasts O1 and O2 have formed. **(C)** shows that by 37.9 hpf the ectopic dorsal infraorbital primordium (IOp∗) has migrated parallel to the supraorbital primordium (SOp), while the ventral infraorbital primordium (IOp) has migrated ventrally to produce infraorbital neuromast IO4. **(E)** by 46.3 hpf SOp has dropped off the first supraorbital neuromast (SO2) and continued to extend, but without producing an SO1 neuromast. The anterodorsal IOp∗ primordium has dropped off an ectopic neuromast IO∗ and continued to migrate anteriorly, parallel to SO1p. **(F)** shows that ectopic neuromast IOp∗ is innervated by a nerve from the anterior lateral line ganglion gALL. The ventral IOp∗ stalls after producing IO4 and does not continue to migrate below the eye. Abbreviations are as follows: e: lens of the eye, ov: otic vesicle. Scale bars are 50 μm. Time-lapse analysis of anterior lateral line development in the absence of neural crest cells

(5) The most anterior neuromasts are encased in neural crest-derived bone in adult zebrafish

As zebrafish ontogeny proceeds, the lateral line system remains closely associated with neural crest cell-derivatives. Supraorbital canals, which will enclose the primary SO neuromasts, begin to develop in postembryonic specimens that are 10 mm standard length (around 4-6 weeks post fertilization; Parichy et al., 2009) (Webb & Shirey, 2003). By the time the developing fish are young adults of 22 mm in standard length, the process of canal enclosure of the neuromasts is close to complete (Webb & Shirey, 2003). Having observed early patterning defects in the most anterior components of the supraorbital system when neural crest cells were absent, we hypothesized that these same anterior components are the ones that ultimately lie in neural crest cell-derived bone.

The contributions of neural crest cells to the bones of the zebrafish cranium have previously been mapped out using the Cre-recombinase based two-transgene system described above (Kague et al., 2012). This analysis established that only the most anterior component of the frontal bone is neural crest derived, with the remainder being mesoderm-derived. The small nasal bone, which lies anterior to the frontal bone, is similarly neural crest derived (Kague et al., 2012). We exploited the same two-transgene Cre-based lineage tracing system to follow neural crest-derived cells into the bony elements of the cranium, to ask how these neural crest-derivatives correspond with supraorbital lateral line components.

We began our analysis by using *Tg(sox10Cre;dsRed/EGFP)* zebrafish to follow neural crest-derived cells into juvenile zebrafish. Fig. 3-9A shows a maximum projection

confocal image of the left side of the cranium, in dorsal view, of a 6 mm standard length (SL) (around 3 weeks post fertilization) juvenile specimen. For this analysis, we labeled the supraorbital neuromasts using the vital mitochondrial dye TMRE (yellow), and found that the anteriorly localized SO1 neuromast was now embedded in neural crest-derived, *sox10Cre;EGFP*-positive (magenta), tissue. We then extended our analysis to young adult stages (22 mm SL). Fig. 3-9B shows a low-magnification maximum projection large format lightsheet image of the right side of the cranium of a *Tg(sox10Cre;dsRed/EGFP)* specimen. This specimen is co-labeled with a hair cell marker, anti-Otoferlin antibody (yellow) (Goodyear et al., 2010), to reveal SO neuromasts, which now include the newly formed anteriorly-located SO1' neuromast (Webb & Shirey, 2003), as indicated. By this stage, the supraorbital canal has formed, and its large open pores are readily apparent, highlighted by edge effects that produce some non-specific fluorescent signal in these large specimens. To provide more context, Fig. 3-9C shows a schematic view of the entire cranial region of a 22 mm SL young adult specimen, again in dorsal view, indicating the supraorbital canals and the canal neuromasts within them (yellow), in relation to the neural crest-derived (magenta) and mesoderm-derived (blue) regions of the frontal bone. The small anterior nasal bones, which are also neural crest-derived, lie adjacent to the nostrils (nos). The region imaged in Fig. 3-9B-B'' is indicated by a dashed box.

The image in Fig. 3-9B is shown in single channels in Figs 3-9B' and 3-9B''. Confirming a previous report (Kague et al., 2012), Fig. 3-9B' (the *sox10Cre;EGFP* channel) shows that the anterior part of the frontal bone is neural crest cell-derived; note EGFP-positive puncta across the entire surface of the region to the left of the red

dashed line. Newly formed superficial neuromasts are also apparent at this late stage (Webb & Shirey, 2003). In common with the canal neuromasts (see below), the superficials include EGFP-positive puncta, reflecting innervation from neural crest cell-derived neurons. Fig. 3-9B''(the Otoferlin channel) allows individual canal neuromasts to be identified. The region surrounding each of these neuromasts (white dashed line boxes) is re-imaged using confocal microscopy at high magnification in Fig. 3-9D-G', with orthogonal (yz) views captured adjacent to each neuromast (plane indicated by yellow arrows), provided to the right of each image. Of note, at the level of each neuromast there are filamentous EGFP-positive structures, which are the tips of the neural crest cell-derived afferent nerves. Importantly, Figs 3-9D, D' and E, E' show that the bone surrounding supraorbital neuromasts SO1 and SO1' is EGFP-positive, confirming its neural crest origin. By contrast, Figs. 3-9F, F' and 3-9G, G' show that the bone surrounding SO2 and SO3 lacks a neural crest contribution.

In summary, our Cre-based lineage tracing has shown that the most anterior components of the supraorbital lateral line system, the SO1 neuromasts and the late forming SO1' neuromasts, lie in the neural crest-derived portion of the frontal bone and in the neural crest-derived nasal bone, respectively, while SO2 and SO3 are located in the mesoderm-derived portion of the frontal bone.

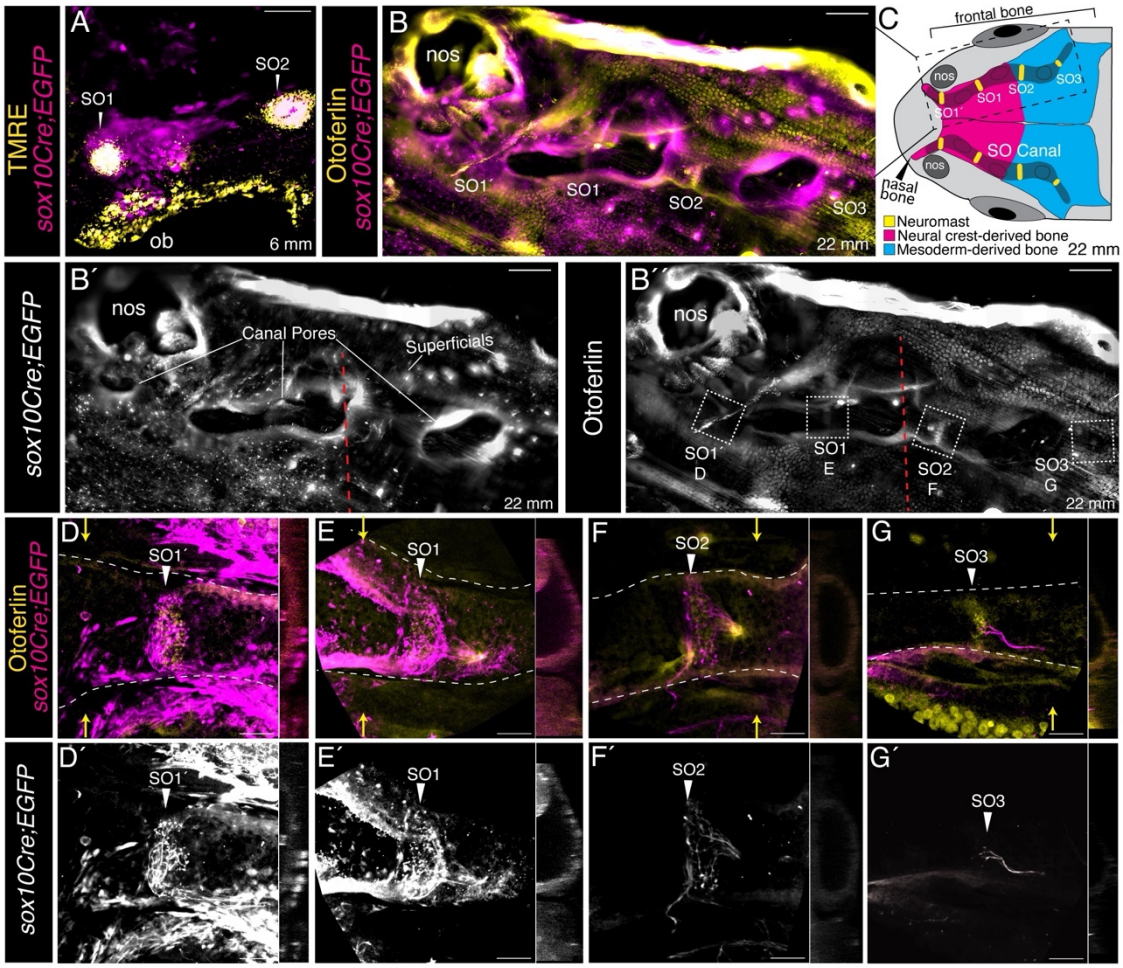

Figure 3-9:The most anterior supraorbital neuromasts are encased in neural crest-derived bone in adult zebrafish.

(**A**) Confocal maximum projection (40x objective), in dorsal view, of the left hand side of the anterior cranial region of a 6 mm SL *Tg(sox10Cre;dsRed/EGFP*) specimen labeled with the vital dye TMRE, a mitochondrial marker labeling neuromasts. Canal neuromasts SO1 and SO2 are shown (TMRE, yellow) alongside neural crest-derived tissue (*sox10Cre;EGFP*, magenta). Because TMRE is highly fluorescent in the rhodamine channel (546 nm), the *sox10Cre:dsRed* signal present throughout the specimen is not visible with the imaging parameters selected. ob = olfactory bulb. (**B**) Large format lightsheet (4x objective), maximum projection of the right hand side of the cranium (boxed area in C) of a 22 mm SL adult *Tg(sox10Cre;dsRed/EGFP*) specimen (of n = 5). Neural crest cell-derived tissue is labeled with *sox10Cre;EGFP* (magenta), neuromasts are labeled with anti-Otoferlin antibody (yellow), in dorsal view with anterior to the left. (**B′**) EGFP channel showing neural crest cell-derived tissue (to left of red dashed line). (**B″**) Otoferlin channel showing neuromasts (in white dashed-line boxes). (**C**) Schematic of the supraorbital canals and canal neuromasts (yellow) in an adult zebrafish. The large frontal and small anterior nasal bones (next to the nostrils, nos) are indicated. Cell-type contributions to the bones are as indicated, neural crest in magenta, mesoderm in blue. (**D-G′**) Confocal maximum projection (40x objective), in dorsal view with anterior to the left, of each of the canal neuromasts shown in B″ (boxed regions). The white dashed lines in D-G indicate the supraorbital canal; D′-G′ show the *sox10Cre;EGFP* channel alone. Orthogonal (yz) sections, taken adjacent to each neuromast (at level of yellow arrows), are provided to the right of each panel. Scale bars are 50 μm for panels A, D-G″ and 200 μm for panels B–B’’.

IV. Discussion

Our study has augmented understanding of zebrafish anterior lateral line system development and its relationship with the cranial neural crest. Importantly, we have documented a close physical tissue-tissue association between the developing placodally-derived anterior lateral line system and the underlying cranial neural crest cells. Further, we have tested the functional significance of this interaction: using transgene mediated cytotoxicity to kill neural crest cells, we have demonstrated that the zebrafish cranial neural crest plays a key role in the development of the overlying anterior lateral line. Both the supraorbital and infraorbital lines fail to extend into the anterior, pre-orbital, portion of the cranium in the absence of neural crest. Using genetic lineage tracing, we have established that later in ontogeny it is these same anterior supraorbital neuromasts that become encased in neural crest-derived bone. Taken together, our experiments have revealed that the cranial neural crest and cranial placode derivatives function in concert over the extent of ontogeny to build the complex anterior lateral line system.

Our analysis of anterior lateral line development during the first five days of zebrafish larval life is broadly consistent with a previous comprehensive description of neuromast deposition (Iwasaki et al., 2020). Like Iwasaki and colleagues (2020), we have documented migrating anterior lateral line primordia, neuromast budding processes, and the emergence of intercalary neuromasts from interneuromast cells. However, our SPIM time-lapse analysis has further revealed that migration and budding

in the supraorbital line are not entirely separate processes, with the budding of SO1 from SO2 beginning before SO2 has reached its final location (Fig. 3-1; Supplemental Videos 1-4). Moreover, our Single Plane Illumination Microscopy reveals that the infraorbital line initially forms as an elongated ridge of cells, with neuromasts subsequently emerging through condensation and proliferation of progenitor cells (Fig. 3-1; Supplemental Videos 3, 4). The existence of this ridge was not noted by Iwasaki et al. (2020), possibly reflecting the challenge of imaging cells that are located immediately below the developing orbit using standard confocal microscopy.

Migration of a primordium that deposits neuromasts in its wake has been described in great detail in the context of the zebrafish posterior lateral line, and is thus the more familiar process, but it is important to note that this might not be the general condition in jawed vertebrates. Rather, elongation and fragmentation of lateral line primordia occur in both crania and trunks of chondrichthyan species (Gillis et al., 2012; Johnson, 1917), as well as in the crania of many non-teleost osteichthyan species (Modrell et al., 2011; Northcutt et al., 1994; Stone, 1928; Winklbauer & Hausen, 1983). As noted by Iwasaki et al. (2020) evolution of different modes of neuromast deposition might reflect relatively modest changes in specific cellular properties. Ultimately, a full understanding of lateral line system evolution will require documentation of these varying deposition mechanisms across the vertebrates, including in a wider range of teleosts.

Our analysis of lateral line gangliogenesis and afferent nerve development is in agreement with the seminal study of Raible and Kruse (2000), as well as with the recent detailed transgenic analysis of Iwasaki and colleagues (2020). We focused in particular

on the relationship of developing lateral line ganglia and nerves with the neural crest cells. Confirming a report from Kague et al. (2012) we documented that the neurons in the anterior lateral line ganglion derive from both placodes and neural crest. We extended their findings to confirm that both the dorsal (gAD) and the later developing ventral (gAV) components of the anterior lateral line ganglia include neurons of both origins. We also established that when the lateral line ganglia first develop from the placodes they are surrounded by a 'shell' of neural crest cells, which may serve as progenitors for the neurons that will subsequently populate the ganglia. Other neural crest cells—presumably developing glia—interact closely with the developing anterior lateral line nerves.

When neural crest cells were removed by transgene-mediated cytotoxicity we found that anterior lateral line development was dramatically disrupted. In the absence of neural crest cells the migration of the supraorbital primordium 'stalls' above the apex of the eye, such that no anterior supraorbital neuromasts are deposited in their typical anterodorsal locations relative to the eye. Similarly, the infraorbital primordium fails to extend ventrally below the eye, leading to a similar absence of anterior neuromasts in their typical anteroventral locations relative to the eye. In addition, supernumerary neuromasts often develop in the absence of neural crest, producing an unusually condensed array of neuromasts in the posterior supraorbital region. Potential sources of these supernumerary neuromasts are discussed below.

As neural crest cells contribute directly to the lateral line ganglia, it is not surprising that we find alterations in both gangliogenesis and lateral line innervation when neural crest cells are missing. While not a primary focus of this study, we note

that the posterior lateral line ganglion (gP) is severely reduced in size and highly disorganized in the absence of neural crest cells (as exemplified by Figure 3-7C). Despite this, we find that the posterior lateral line primordium migrates successfully to the terminus of the trunk, consistent with previous reports that innervation is not required for its migration (López-Schier & Hudspeth, 2004). While the anterior lateral line ganglion shows less dramatic deficits, our quantification reveals that the number of neurons in the ganglion is significantly reduced by 120 hours post fertilization, with the anteroventral (gAV) component of the ganglion either absent or drastically reduced in size, and the projection from gAV into the hindbrain lacking altogether (Figure 3-7). Of note, it is this late developing gAV component of the ganglion that innervates the mandibular and opercular lines, which are completely missing when neural crest is absent, presumably reflecting the absence of the tissue in which they would normally form.

In addition to reduced gAD ganglion size when neural crest cells are absent, the anterior lateral line nerves are thin, defasciculated, and often make ectopic projections (Figures 3-6, 3-7). These ectopic projections frequently, but not always, connect with ectopic neuromasts in the supraorbital region. On occasion, the nerve that typically projects anteroventrally to the infraorbital line (nADio) instead—or in addition—projects more dorsally, raising the possibility of dorsal translocation of a single IO neuromast into the posterior supraorbital domain. Consistent with this hypothesis, our SPIM time-lapse analysis (Figure 3-8; Supplemental Videos 5, 6) has captured an example of such aberrant dorsal migration. Thus, at least in some instances, ectopic neuromasts in the supraorbital region might be misplaced infraorbital neuromasts that are following

supraorbital cues and migrating above the eye. Overall, the deficits we have found in lateral line gangliogenesis and innervation are consistent with previous descriptions of roles for neural crest in ganglion condensation and establishment of neural connections (reviewed by Steventon et al. 2014), including a requirement for chondrogenic—but not glial—neural crest in the initial assembly of zebrafish epibranchial ganglia (Culbertson et al., 2011).

Our results raise questions about the source of the other ectopic neuromasts in the posterior supraorbital region of neural crest-deficient zebrafish larvae. One possibility is that the ectopic neuromasts derive from cells which would normally form the mandibular or opercular neuromasts. Another possibility, by analogy with posterior lateral line phenotypes in the absence of neural crest-derived glia, is that these additional cranial neuromasts represent prematurely or ectopically developing intercalary neuromasts, or both. We have observed neural crest cells in close proximity to the projecting supraorbital nerves (Figures 3-2, 3-3), and these 'wrapping' cells are presumably myelinating Schwann cells (Lyons et al., 2005). In the absence of the Schwann cells, nearby interneuromast cells might proliferate precociously and condense to form new neuromasts, much as occurs in the trunk. However, it should be noted that a previous study of *ngn1* and *sox10/colourless* mutants, both of which lack glial cells, did not reveal ectopic cranial neuromasts at 6 days post fertilization (López-Schier & Hudspeth, 2005). Nevertheless, a more detailed future exploration of a potential role for Schwann cells in suppressing intercalary neuromast development in the anterior lateral line system is warranted. If Schwann cells prove to play non-equivalent roles in the cranium and trunk, with respect to suppressing precocious

neuromast formation, this does not rule out a similar role for other cranial neural crest-derived cells.

We have found that both the neuromasts and the lateral line nerves show disrupted localization in the absence of neural crest. While the anterior lateral line neuromasts and their nerves develop together and in concert in specimens with intact neural crest, we have found that when neural crest cells are lacking the lateral line nerves project from non-uniform points on the ganglia, and then tend to wander, not always innervating a target neuromast. These observations suggest that neural crest cells influence nerve outgrowth from the ganglia. It remains to be resolved whether the relevant neural crest cells lie in the outlying tissue, wrap around the ganglia, contribute neurons to the ganglia, or are in some combination of these locations. A possible explanation for the increased number of projections from the ganglia is that in the absence of surrounding neural crest cells the placode-derived neurons put out disorganized projections which do not properly fasciculate. Neural crest cells play a somewhat similar role as 'boundary cap' cells, which help to organize the entry and exit points of peripheral nerve roots (Maro et al., 2004). Subsequent axon guidance may also be influenced by neural crest-derived cells, particularly glia. Consistent with such a model, it has been shown that glial-derived neurotrophic factor (GDNF) is required for proper extension of the posterior lateral line nerve, although in that instance it is the posterior lateral line primordium itself that serves as the GDNF source (Schuster et al., 2010).

The precise nature of the interaction between neural crest and placode-derived lateral line cells deserves further attention. While the neural crest is a highly migratory

cell type, our time-lapse analyses reveal that neural crest cells neither tow nor chase (Theveneau et al., 2013) the anterior lateral line primordia. Rather the neural crest cells are already in place, although still proliferating and far from static (Supplemental Videos 2 and 4), at the stages when the supraorbital and infraorbital primordia are migrating over them. The neural crest cells might, however, be providing a physical substrate on which the anterior lateral line primordia migrate and bud, and our confocal analysis has revealed close apposition of the two cell types, compatible with such a model. Alternatively, the neural crest cells might serve as the source of one or more localized signals. Available data (reviewed by Piotrowski & Baker, 2014) suggest that anterior lateral line development does not require chemokine signaling—in distinct contrast to the situation in the posterior lateral line—but one or more different short-range signals could potentially be at work.

Iwasaki et al. (2020) uncovered a role for local tissue-tissue interactions in the specific instance of hyomandibular neuromast progenitors; these respond to R-spondin2 emanating from mesenchyme of the second pharyngeal arch, which in turn activates Wnt/beta-catenin signaling to activate progenitor proliferation. The lack of a requirement for R-spondin2 in the development of other cranial neuromasts is consistent with a model in which multiple different localized molecular signals, or cues, serve to pattern the varied components of the anterior lateral line system. We hypothesize that one such cue (or set of cues) is followed by the supraorbital primordium as it initially migrates dorsoanteriorly to the position where SO2 is deposited. The relatively normal initial migration of the supraorbital primordium in the absence of neural crest cells suggests that this particular cue must emanate from non-

neural crest derived tissue. Moreover, we observed that when neural crest cells are missing, a dorsally mis-placed infraorbital primordium can migrate adjacent to the supraorbital primordium, presumably following the supraorbital cue(s) (Figure 3-8; Supplemental Movies 5, 6). A candidate for this supraorbital cue is Fgf signaling. Simultaneous knockdown of Fgf3 and Fgf10a disrupts supraorbital neuromast deposition, with the sources of these Fgfs identified as the mesoderm/endoderm and the anterior lateral line itself, respectively (McCarroll and Nechiporuk, 2013).

Our study has focused on the anterior lateral line system, which was already understood to use distinct developmental mechanisms relative to those of the better studied posterior lateral line system (Piotrowski & Baker, 2014). However, our data have uncovered another important difference between the head and trunk lines: we have demonstrated that in the absence of neural crest cells the anterior lateral lines fail to reach their destinations, yet the posterior lateral line completes its full migration to the caudal terminus of the trunk (Figure 3-5). Intriguingly, the posterior lateral line system, despite its destination being the trunk, is nevertheless derived from a cranial placode, and could be viewed as a 'head' structure (Northcutt and Gans, 1983). Nevertheless, this post-otic placode derivative responds very differently to adjacent neural crest cells than does the pre-otic anterior line placode. It remains unclear to what extent these differences are driven by intrinsic differences between the placodes, for example differential Hox gene expression status, versus extrinsic differences. Classical embryology experiments performed by Stone (1928) in the axolotl suggested that extrinsic differences play a major role. Stone swapped the anterior and posterior lateral line placodes, and found that these swapped placodes responded much as the correct

ones to their new environments. The powerful molecular genetics and imaging opportunities now available in the zebrafish provide opportunities to continue to explore the molecular underpinnings of both intrinsic and extrinsic aspects of lateral line patterning, including the bases of the differences between the anterior and posterior systems.

The placode-derived lateral line system and the neural crest cells are two vertebrate specific cell types that are key to vertebrate evolution (Hall 1998; Northcutt & Gans, 1983; Gans & Northcutt, 1983). The relationship between these cell types begins at the earliest developmental stages with their shared embryonic origins from nearby or overlapping non-neuroepithelial ectoderm (reviewed by Koontz et al., 2023; Rocha, Beiriger, et al., 2020; Rocha, Singh, et al., 2020; Steventon et al., 2014). The relationship continues with multiple functional interactions, now including those we describe in this study in which the neural crest cells influence anterior lateral line patterning. This relationship then culminates with elements of the lateral line system becoming embedded in the dermal bone that derives from this same neural crest population (this study, Webb & Shirey, 2003). The contributions of neural crest to different components of the cranial dermal skeleton have changed through the course of vertebrate evolution (Rocha, Beiriger et al., 2020), as have the morphologies of lateral lines (Northcutt, 1989). New comparative data will be needed to elucidate how the relationship between placode-derived lateral lines and cranial neural crest has been modified over evolutionary time scales to produce the numerous different lateral lines patterns that we find in different vertebrate groups (Northcutt, 1989).

As discussed in the introduction, Parrington (1949) hypothesized that the precursors of dermal ossifications—which we now know include neural crest cells—might influence the 'courses' of the lateral lines. Parrington also noted that the test of his hypothesis must "rest eventually on experimental evidence". Three-quarters of a century later, our study now provides that evidence, validating Parrington's insightful model and confirming that there is an intimate and ongoing functional relationship between the cranial neural crest cells (which include precursors of dermal bones) and placode-derived anterior lateral lines.

CHAPTER FOUR: INNERVATION DRIVES POSTEMBRYONIC EXPANSION OF THE ZEBRAFISH ANTERIOR LATERAL LINE SYSTEM

Summary

Lateral lines are an essential sensory system used by aquatic vertebrates to sense environmental hydrodynamic information. The system comprises distributed sense organs called neuromasts and their innervating ganglia, which are organized into anterior lateral lines around the eye and jaw and posterior lateral lines (LL) on the trunk. At postembryonic stages, early forming neuromasts expand in size and sink into bony canals, while late-forming superficial neuromasts are added to maintain sensory density. Unlike the well-studied zebrafish posterior LL, details of anterior LL postembryonic development remain unknown. Here, we have characterized developmental mechanisms and innervation patterns driving expansion of the zebrafish anterior LL. Using tissue-clearing to observe neuromast and nerve markers through ontogeny, we demonstrate continuous neuromast addition in the anterior LL, with peak rates at larval stages of 6-10 mm standard length (SL). Superficial neuromast lines form parallel to existing canal lines as late as 7 mm SL, with new neuromasts added through migration of new primordia, budding, intercalation, and a novel cross-placodal mechanism. Despite some canal lines being innervated by the anterodorsal ganglion, all superficial lines are innervated by the anteroventral ganglion. Anterior LL ganglion ablation reveals that denervation abrogates superficial neuromast formation – including via the novel cross-placodal mechanism – and limits canal neuromast growth. While the anterior and posterior LL have disparate developmental strategies, innervation is critical to expansion of both systems. Our findings demonstrate that the anterior LL

undergoes a “developmental switch” at 7 mm SL, where innervation becomes necessary for a secondary phase of sense organ development.

Attributions

This work was done in close collaboration with undergraduate student Theresa J Christiansen, who generated much of the data in panels 4-1 to 4-7 under my direct supervision. I conceived of the study and performed preliminary literature reviews and developed the modified CUBIC and TMRE imaging protocols, performed immunolabeling and helped with optimizing confocal microscopy. TJC did the neuromast counts using vital dye labelling, large format lightsheet microscopy, additional immunolabelling and CUBIC stains, laser ablations and performed quantitative analyses. VEP played a major role in developing the manuscript for publication, coordinated the project and funding acquisition.

I. Introduction

The lateral line is a sensory system found in fishes and amphibians that allows them to sense hydrodynamic information from their aquatic environment. The system is essential to complex behaviors such as schooling, hunting, and predator evasion. The lateral line comprises distributed lines of mechanosensory organs called neuromasts innervated by afferent nerves, which relay sensory input to the lateral line ganglia and then to the dorsal octavolateral nucleus of the hindbrain (Raible and Kruse, 2000). Each neuromast comprises a cluster of sensory hair cells and their surrounding support cells, with the hair cells projecting sensory cilia into an overlying jelly-like cupula that interacts directly with the water stream. These neuromasts are embedded in canals—open to the water via pores—or located superficially on the dermis (reviewed

by (Venkataraman, Lopez et al., 2025). Adult patterns of neuromast distribution are complex and vary widely, even between closely related species (Webb, 2014). These variations may be adaptations to varied flow environments (Mogdans, 2019).

The neuromast receptors and their associated nerves develop from ectodermal thickenings, the cranial placodes. While cranial placodes give rise to a variety of sensory systems, including the olfactory, optic and auditory capsules, a separate series of 'dorsolateral' placodes gives rise to lateral line receptors and their nerves (Baker and Bronner-Fraser, 2001) The dorsolateral placodes lying just anterior to the otic vesicle produce the anterior lateral lines (anterior LL) that populate the head, while placodes just posterior to the otic vesicle produce the posterior lateral lines (posterior LL) that populate the trunk. The ontogeny of neuromast patterning has been described for several teleost species, including both the anterior and posterior LL systems of the cichlid genera *Tramitichromis* and *Aulanocara* , the anterior and posterior LL systems of rainbowfish (family Melanotaeniidae) , the anterior LL of the brook trout and the goby genus *Elacitinus* , and the posterior LL of lab strains of medaka and zebrafish (Ledent, 2002).

Much of our knowledge of lateral line development comes from the zebrafish (*Danio rerio*), where the early development of the posterior LL has been thoroughly characterized at a molecular and cellular level during embryogenesis (the first three days post fertilization; dpf) (reviewed by Aman & Piotrowski, 2011; Dalle Nogare & Chitnis, 2017; Piotrowski & Baker, 2014). Recently, the systems level development of the more complex zebrafish anterior LL has also been described up to 10 dpf (Iwasaki et al., 2020). This work built on a seminal study on the innervation of the zebrafish

lateral line system (Raible & Kruse, 2000), which described both anterior and posterior placodal systems. Raible & Kruse (2000) established that the lateral line nerves have stereotypical entry points into the hindbrain, where the anterior LL enters with the facial (VIIth) motor nerve root, while the posterior LL enters with the glossopharyngeal (IXth) nerve. Moreover, they found that the zebrafish anterior LL system comprises separate anterodorsal (AD) and anteroventral (AV) systems, which originate from adjacent placodes located anterior to the otic vesicle. Each placode gives rise to a migrating primordium of neuromast progenitor cells (which later deposit neuromasts at stereotyped locations) as well as the ganglion that innervates these cells. The early larval AD system consists of the supraorbital and infraorbital neuromast lines, above and below the eye, respectively, innervated by the anterodorsal ganglion (gAD). The AV system consists of the continuous preopercular and mandibular lines along the jaw, and the anteroventral ganglion (gAV). The overall organization of the anterior LL is schematized in Figures 1A, A'.

Raible and Kruse's study (2000) focused specifically on the embryonic and early larval stages of zebrafish development, up to 5 dpf, with Iwasaki and colleagues (2020) extending our knowledge out to 10 dpf. Following the embryonic establishment of lateral lines from primordia, we know from studies of the posterior LL that additional neuromasts are added via budding from parent neuromasts, or form between existing neuromasts via proliferation and condensation of interneuromast progenitors, a process termed 'intercalation' (reviewed by Ghysen & Dambly-Chaudière, 2007). Similar mechanisms were described by Iwasaki et al. (2020) in the first 10 days of anterior LL development. However, the entire lateral line system expands enormously during

subsequent ontogeny. As the animal continues to grow from larval stages to adulthood, early forming canal neuromasts increase in size and become enveloped in grooves that ossify into canals. Simultaneously, hundreds of smaller superficial neuromasts emerge to form complex patterns on the surface of the skin (Webb and Shirey, 2003; Ghysen and Dambly-Chaudière, 2004). The developmental mechanisms underlying the addition of these superficial neuromasts remain unknown. However, for the posterior LL system it has been shown that innervation is dispensable during embryonic development but becomes necessary by adult stages for the budding process that produces orthogonal "stitches" of superficial (or "accessory") neuromasts. When the posterior LL ganglion is unilaterally ablated from juvenile zebrafish, the budding process fails to occur, such that no superficial neuromasts develop along the flank on the experimental side (Wada et al., 2013). In the anterior LL, only the superficial opercular line has had neuromast ontogeny described in detail (Wada et al., 2010), and the ontogeny of complete adult anterior LL innervation has not been described for any teleost to date.

Here, by combining live imaging of transgenic markers with CUBIC clearing and immunostaining methods, we visualized zebrafish anterior LL development from early larval to adult stages at high spatiotemporal resolution. We find that late-forming superficial anterior lateral lines form parallel to canal lines during early larval development, with each superficial line innervated by a new branch of the AV ganglion. Many of the newly forming superficial neuromasts develop through previously documented strategies: primordium migration, budding, and intercalation. However, in the case of the supraorbital superficial line, we describe a novel, cross-placodal mechanism of superficial neuromast line formation that combines neuromast tissue from

the AD system with innervation from the AV system. Using laser ablation of the ganglia, we establish that functional removal of anterior LL innervation decreases superficial neuromast number and restricts patterning. Specifically, canal neuromast growth is limited, and neuromasts formed by the newly described cross-placodal mechanism are absent. Together, our findings reveal that innervation acts as a 'developmental switch', becoming broadly required for anterior LL development only at late larval stages.

II. Materials and methods

(1) Animal Husbandry

Zebrafish (*Danio rerio*) were maintained in accord with IACUC-approved protocols at the University of Chicago. Embryos and early stage larvae were maintained in E3 solution (5mM NaCl, 0.17mM KCl, 0.33mM Ca_2Cl_2, 0.33mM $MgSO_4$), which was supplemented with 0.3% 1-phenyl-2-thiourea (PTU; Sigma) to block pigment formation for analyses between 24 hpf and 7 dpf, and staged according to standard guidelines (Kimmel et al., 1995). Later stage larvae (up to 10 mm SL), juveniles (11-22 mm SL) and adults (>3 months and >22 mm SL) were staged by measuring standard length (SL). SL was measured from the tip of the snout to the caudal peduncle (Parichy et al., 2009), providing a more accurate measure of developmental stage than days post fertilization, because growth rates differ between individuals (see Table 1 for stages analyzed in this study). Embryos were obtained from crosses of adult fish stocks of wild type (*AB line) and/or transgenic lines. The following transgenic lines were used: *Tg(cldnB:GFP)^{zf106}* is a tight junction marker that labels cell membranes in the lateral line system, other placodes, and epithelia (Haas and Gilmour,

2006); *Tg(Hgn39d:GFP)*^{nkhgn39dET} is an enhancer trap insertion (Nagayoshi et al., 2008) into the *contactin associated protein 2a* gene, which specifically labels lateral line afferent nerves as well as the lens (Faucherre et al., 2009; Pujol-Martí et al., 2012).

(2) Vital Dye Labeling and Live Imaging

For TMRE live-dye labeling, zebrafish were incubated in 5 nM Tetramethylrhodamine Ethyl Ester, Perchlorate (TMRE; Invitrogen) in E3 medium. Larvae were incubated for 30 minutes and adults for up to 1 hour (Esterberg et al., 2013; Mandal et al., 2021). After incubation, the specimens were washed repeatedly in E3 medium to remove excess TMRE. Specimens were anesthetized using 0.08-0.1% tricaine in E3 for a maximum of one hour after TMRE treatment to allow imaging. Fish were monitored continuously and immediately removed from the tricaine solution if opercular movements, indicative of respiration, stopped. TMRE-labeled specimens were live imaged using a Leica M205A epifluorescent microscope with an AmScope MU500-PB10 5MP USB Camera or a Zeiss LSM 900 confocal with the Plan-Apochromat 10x/0.3W or 40x/1W objectives. For epifluorescent imaging, specimens were positioned in a 35 mm petri dish of E3 medium containing a lateral or dorsal zebrafish larval body shape agarose mold. Custom 3D printed mold blocks were designed in Tinkercad and printed with the Ultimaker 3 printer in PVA material (gift from Elaine Kushkowski). Molds were made by placing the mold blocks in 1-1.5% agarose for 30 minutes before carefully removing them with forceps. Confocal imaging was performed on larvae embedded in 0.7-1% agarose (Invitrogen UltraPure Low Melt Agarose Cat #16500) dissolved in E3 medium containing 0.08-0.1% tricaine cooled to 37°C in 60 mm glass bottom dishes (MatTek, USA). Larvae mounted in agarose were

carefully positioned and removed from the agarose after imaging using a wire tool. Larvae that were previously stained with TMRE were then housed in separate tanks. Images were acquired using the Zeiss Zen software and image post-processing was performed in FIJI (Schindelin et al., 2012)

(3) CUBIC clearing and immunolabeling

For adult zebrafish immunolabeling, a CUBIC clearing and staining protocol was adapted from Pende et al (2020) on specimens fixed in 4% paraformaldehyde (PFA; Sigma). Adult specimens were depigmented in cold acetone overnight at -20°C before lightly bleaching for 5-20 minutes in a 3% solution of hydrogen peroxide in 1% KOH in water. Specimens were incubated overnight in Low Urea CUBIC I (Pende et al., 2020) solution at 37°C for initial clearing. For immunolabeling, cleared specimens were blocked using goat serum at 25°C for 3-4 hours before primary and secondary incubation. Primary and secondary solutions were centrifuged for 5 minutes to remove aggregates immediately prior to incubation. Primary incubation time varied from 1-4 days at 37°C depending on specimen size, followed by secondary incubation from 1-3 days at 37°C. Specific incubation times based on specimen size were as follows:- 4-6 mm SL: 1 day primary, 1 day secondary; 6-10 mm SL: 2 days primary, 1-2 days secondary; 10-22 mm SL: 3 days primary, 2-3 days secondary. To preserve transgenic fluorescence of *Tg(Hgn39d:GFP)* specimens, bleaching was limited to <10 minutes. Cleared and stained specimens were deskinned with forceps to remove unwanted signal from epithelial tissue before imaging. Specimens were placed in CUBIC R + (N) RI matching solution (Kubota et al., 2017) for at least 30 minutes prior to imaging and mounted between two glass coverslips. Cleared and stained specimens

were imaged on either a Zeiss LSM 900 microscope or a LaVision Large Format Lightsheet microscope.

For embryonic and early larval stages, immunolabeling was performed as previously described (Prince et al., 1998)on specimens fixed in 4% PFA. The primary antibodies used were anti-Sox2 1:200 (anti-rabbit; Genetex GTX124477; RRID AB_1117806), anti-GFP 1:200 (anti-rabbit; Thermo Fisher Cat # A-6455; RRID: AB_221570), and anti-acetylated alpha-tubulin, 1:200 (anti-mouse; Sigma-Aldrich Cat# T7451; RRID_AB_609894). Secondary antibodies used were Alexa 488, 1:500 (Invitrogen anti-mouse A-11001; anti-rabbit A-11008), Alexa 546 1:500, (Invitrogen anti-mouse A-11003; anti-rabbit A-11035), and Alexa 633, 1:300 (Invitrogen anti-mouse A-21052; anti-rabbit A-21070). Specimens were mounted in 1% agarose in 60 mm dishes and imaged on the Zeiss LSM 900 confocal with the Plan-Apochromat 10x/0.3W or 40x/1W objectives.

(4) Large Format Lightsheet Imaging

Juvenile and adult specimens were imaged on a LaVision Large Format Lightsheet, using a 4x objective, and 2.0 µM excitation sheet in CUBIC R+ (N) imaging medium (Kubota et al., 2017).

(5) Laser Ablations

A confocal microscope (either Zeiss LSM 900 or LSM 710) at 40x magnification was used to unilaterally ablate the anterior lateral line ganglion (both dorsal and ventral components) of *Tg(Hgn39d:GFP)* specimens. *Tg(Hgn39d:GFP)* specimens were selected for ablation at 4 dpf based on bright GFP signal in the ganglia coupled with

strong swimming ability, indicative of healthy and robust specimens. Larvae were anesthetized and mounted as described above. The side to be ablated was selected at random. A 405 nm laser was used on 60%-75% power to ablate 2-4 cells at once (Morsch et al., 2017). Cells were identified and the zoom feature in Zen used to magnify them by 20x (800x total magnification) before exposing them to the laser in 6 bursts of 30 seconds, using the photobleaching module in Zeiss Zen software. In successful ablations, all signal from the ganglion cells was permanently removed and degradation of the lateral line nerves could be visualized immediately. Specimens were maintained as described above through larval stages. Ablated specimens were raised in groups of ≤ 6 in small tanks of ~200 ml water volume with daily water changes of 5-10%. Specimens were stained with TMRE each week as described above until sacrifice for final analysis at 6 weeks of age or a minimum length of 11 mm SL. During analysis, superficial neuromasts in the nasal line were not included in the total counts, due to consistent ectopic reinnervation of ablated side nasal neuromasts by control side nerves.

(6) Image Processing

Lateral line tissue was segmented out from epithelia in selected confocal image stacks (used in Figures 4-4 and 4-5) of transgenic *Tg(CldnB:GFP)* or *Tg(CldnB:GFP;Hgn39d:GFP)* larval specimens using the software FIJI. Image stacks were thresholded and converted to binary. The 'analyze particles' tool was used to generate masks of image features 50 μm^2 or larger. Masks were manually edited to exclude lateral line tissue using the 'watershed' and 'flood fill' tools and enlarged using

the ‘dilate’ tool. To remove the epithelial tissue signal, masks were subtracted from the original image stack using the image calculator tool. To compare signal intensity between control and ablated specimens in Figures 4-6 and 4-7, images were taken at the same laser power and processed using identical parameters. In specimens immunolabeled with Sox2, canal neuromast length was measured transverse to the canal and width was measured parallel to it, as described by (Webb and Shirey, 2003), to establish aspect ratios.

III. Results

(1) The zebrafish anterior lateral line expands by addition of superficial neuromast lines

The ontogeny of zebrafish anterior lateral lines at late larval and juvenile stages has not been described in detail. This gap in knowledge reflects the challenge of visualizing structures such as cranial nerves in juvenile zebrafish that become increasingly opaque through development. In this study, we have visualized zebrafish anterior lateral line (ALL) development in larval, juvenile, and young adult specimens at high temporal and spatial resolution by combining live imaging of transgenic markers with CUBIC clearing and immunolabeling methods. To map out the postembryonic development of the ALL, we documented changing neuromast patterns and their innervation in larvae of 3 mm standard length (SL) (7 days post fertilization; dpf) through juvenile stages and on to adults of 22 mm SL (approximately 3 months post fertilization; mpf), as shown in Figure 4-1.

As schematized in Fig. 4-1A, in 3 mm SL larvae there are just four lines of neuromasts present: the mandibular (MD) canal line (including the hyomandibular (HM) neuromasts) (1), the infraorbital (IO) canal line (2), the supraorbital (SO) canal line (3),

and the superficial otic series (O) (4). By contrast, in the 22 mm SL adult an additional nine superficial lines or series of neuromasts are present (Fig. 4-1A', lines 5-13; Table 2). The superficial lines include three that parallel the original canal lines (the MD (5), IO (6), and SO (7) superficial lines), as well as neuromast series that form at the anterior ends of the IO and MD canals via neuromast budding (8-9) (Table 2).

The data that underlie these schematics are shown in Fig. 4-1B-E. These images are confocal (Fig. 4-1B-C') or lightsheet (Fig. 4-1D-E) maximum projections of specimens cleared using CUBIC to allow the visualization of deep structures that are immunolabeled for the neuromast marker Sox2 (magenta; (Hernández et al., 2007) Genetex GTX124477, RRID AB_1117806) and the nerve marker acetylated alpha-tubulin (cyan, (Chitnis & Kuwada, 1990), Sigma-Aldrich Cat# T7451, RRID_AB_609894) (Fig. 4-1B-E). At the larval starting point (3 mm SL; Fig. 4-1B), there are stereotypically fourteen neuromasts, connected by simple lateral line nerves. By late larval stages (10 mm SL; Fig. 4-1C, C') the system has expanded dramatically to include approximately 100 neuromasts and increasingly branched cranial nerves. At this stage, developing canal neuromasts are easily distinguished from superficial neuromasts by their larger size (Brown et al., 2023; Webb & Shirey, 2003). In Fig. 4-1C', the individual canal neuromasts of the infraorbital (IO) system are labeled in blue, and those in the preopercular/mandibular canal (hereafter referred to as the mandibular (MD) canal) are labeled in yellow.

By early adulthood (22 mm SL), the number of superficial neuromasts has increased further and the mature canal neuromasts have become enclosed by epithelial grooves that have begun to ossify into canals (Fig. 4-1D, E; yellow dotted outlines

indicate the canal boundaries). In Fig. 4-1E, the canal neuromasts of the supraorbital (SO) system, SO1*-SO3, are indicated (white arrows; note that SO1* buds from existing neuromast SO1). Typically, the canal neuromasts lie at the bottom of the bony canals, curving upward along the sides of the canal, and elongating along the length of the canal as the fish grows (Webb & Shirey, 2003). By contrast, superficial neuromasts are significantly smaller and lie adjacent to the canals on the surface of the skin (SO superficial neuromasts are indicated, Fig. 4-1E). There are also much smaller clusters of cells labeled by Sox2, which we tentatively assign as cutaneous touch receptors, unrelated to the anterior LL system (Fig. 4-1E, yellow arrows; Brown et al., 2023; Webb & Shirey, 2003).

We quantified the total anterior LL neuromast count on one side of the head between 3 mm and 22 mm SL stages, using the vital dye hair cell label Tetramethylrhodamine Ethyl Ester, Perchlorate (TMRE) to label the neuromasts repeatedly as ontogeny proceeded (Fig. 4-1F; n = 10). Throughout ontogeny there is a consistent increase in total neuromast number with body size, with variation in neuromast number between specimens increasing over time. Notably, there is a sharp increase in neuromast addition rates at late larval stages (7-10 mm SL) (Fig. 4-1F; gray panel). Canal neuromasts and superficial neuromasts making up superficial neuromast lines are added with different kinetics, as shown in Fig. 4-1G. About half of the adult canal neuromasts are added at stages between 4 mm and 9 mm SL, with the last forming canal neuromasts developing just before the onset of formation of the bony canals beginning at 10-11 mm SL (Webb & Shirey, 2003). Across the superficial lines, the broad coordination in neuromast addition likely reflects consistent growth of the

underlying dermal structures. Notably, the spike in superficial neuromast addition rates at 7-10 mm SL occurs across all major superficial lines (Fig. 4-1G; gray panel).

Our neuromast quantifications allowed us to track the ontogeny of each canal neuromast and neuromast line; these data are summarized in Table 2. As noted by Webb & Shirey (2003), not all neuromasts that form at embryonic stages are destined to become canal neuromasts, as exemplified by the early-forming superficial otic series and neuromast MD1. In the adult zebrafish, anterior LL canal neuromasts were described by Webb & Shirey (2003) as being organized into four neuromasts of the supraorbital canal, five neuromasts of the infraorbital canal, and five neuromasts of the mandibular canal, with pores in the canal bones lying in between adjacent neuromast organs and thus connecting the canal with the external environment. By contrast, we found about seven infraorbital and about seven mandibular canal neuromasts. This discrepancy likely reflects, at least in part, our finding that canal neuromasts are present at the open ends of each canal, in addition to those located between the pores. It is also possible that different zebrafish lab strains might exhibit differences in canal neuromast number. Of relevance, we find some variation in canal neuromast number between individuals, and in adults we have found that canal neuromasts sometimes split into two adjacent structures (e.g. Fig. 4-1D, asterisks).

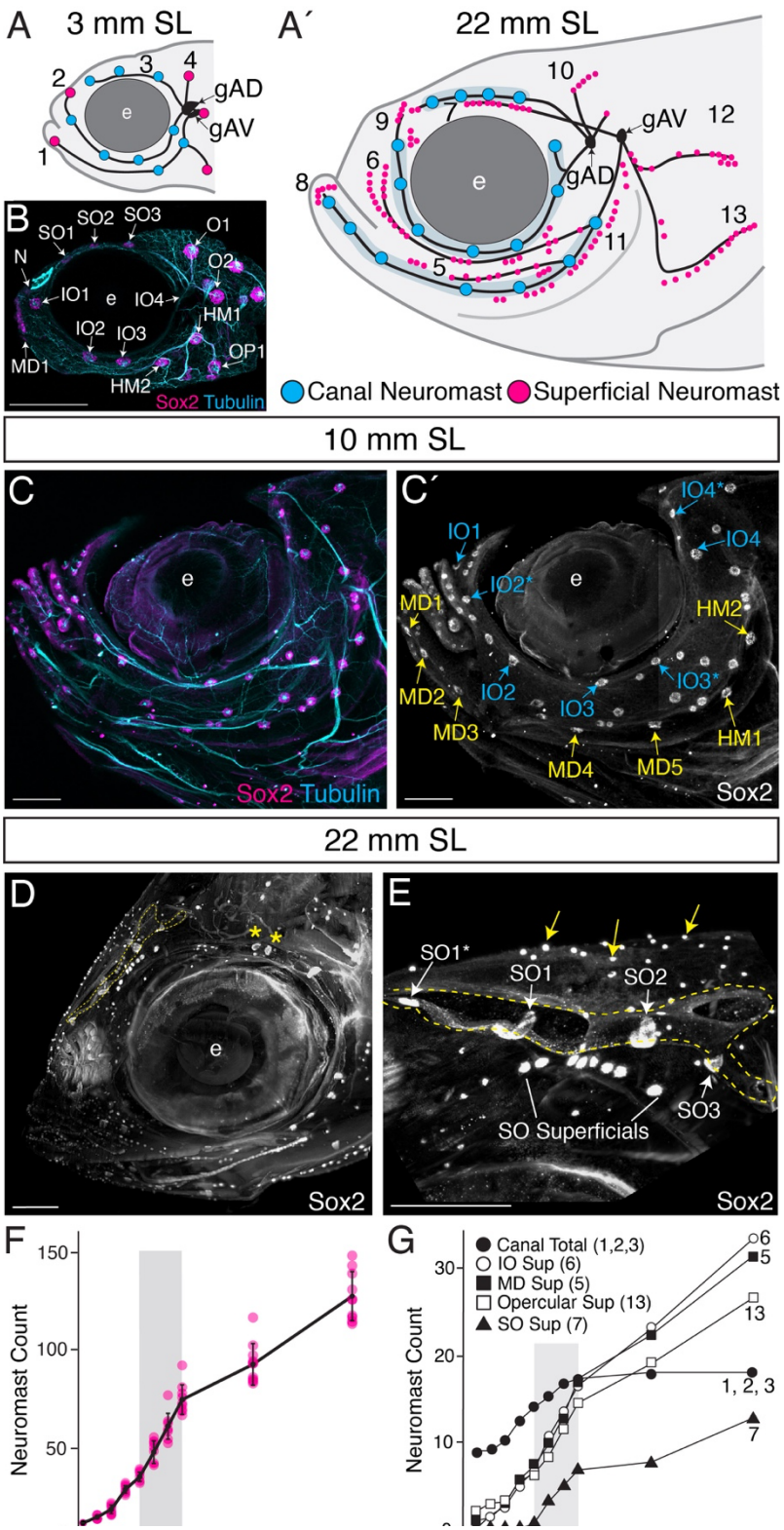

Figure 4-1: Development of neuromast patterning in the zebrafish anterior lateral line from early larval to adult stages (3-22 mm SL).

Fig 4.1 cont. (**A-A'**) Summary schematic of patterning changes between 3 mm SL / 7dpf larvae and 22 mm SL adults. The number and size of canal neuromasts (blue) increases and hundreds of superficial neuromasts (magenta) are added. Each canal line and superficial neuromast series found in the adult is labeled 1-13. **(A)** At 3 mm SL, the mandibular (MD) canal line (1); infraorbital (IO) canal line (2); supraorbital (SO) canal line (3); and otic series (4) are present. **(A')** At 22 mm SL, nine additional superficial lines are present: the MD superficial line (5), which runs parallel to the MD canal line; the IO superficial line (6), which runs parallel to the IO canal; the SO superficial line (7), which runs parallel to the SO canal line; the MD series (8) at the anterior end of the MD canal; the nasal series (9) at the anterior end of the IO canal; the anterior pit line (10), which buds dorsally from O1; the hyomandibular superficial line (11); the dorsal opercular line (12); and the opercular line (13). (**B-E**) Anterior LL neuromast pattern through ontogeny; e = eye. **(B)** Cranial region of a 3 mm SL specimen immunolabeled with Sox2 (magenta) and acetylated alpha-tubulin (cyan), Scale = 200 μm. **(C)** Cranial region of a 10 mm SL specimen immunolabeled with Sox2 and acetylated alpha-tubulin. **(C')** Single channel split of the specimen in (C) showing the Sox2 label. Infraorbital (IO) canal neuromasts are labeled in cyan and hyomandibular/mandibular (HM/MD) canal neuromasts are labeled in yellow. Scale = 200 μm. **(D)** Cranial region of a 22 mm SL young adult specimen stained with Sox2. Image was processed with IMARIS. The SO canal boundaries are highlighted (yellow dotted line). Yellow asterisks indicate an example of 'splitting' of a canal neuromast. Scale = 100 μm. **(E)** Close up of the supraorbital (SO) canal of the same specimen. The canal boundaries are highlighted (yellow dotted line) and canal neuromasts SO1*-SO3 are indicated with white arrows and labeled. The SO superficial neuromasts are also indicated. Examples of non-neuromast Sox2 expression are indicated by yellow arrows. Scale = 100 μm. (**F-G**) Quantification of neuromast patterning over ontogeny (3-22 mm SL). Region showing neuromast counts from 7-10 mm SL specimens is emphasized (gray rectangle). **(F)** Neuromast count vs. Standard Length (mm) for (n=10 each) of 3-10 mm, 15 mm, and 22 mm SL specimens. Brackets = standard deviation. **(G)** Neuromast count by line (total canal, IO superficial, MD superficial, opercular, and SO superficial) vs. Standard Length (mm).

We next described the second essential component of the anterior LL system, its sensory innervation from the anterodorsal (gAD) and anteroventral (gAV) ganglia. Figure 4-2 shows confocal and lightsheet maximum projections of cleared and stained specimens that reveal the ontogeny and adult pattern of anterior LL innervation in *Tg(Hgn39d:GFP)* specimens. *Tg(Hgn39d:GFP)* is a transgenic line that selectively labels lateral line afferent nerves (Faucherre et al., 2009; Pujol-Martí et al., 2012), with individual neuromasts recognizable by the complex dendritic arbors that contact the hair cells (Faucherre et al., 2009). Adult specimens were cleared with CUBIC and immunolabeled with anti-GFP antibody (Thermo Fisher Cat # A-6455; RRID: AB_221570) to enhance the endogenous *Tg(Hgn39d:GFP)* signal. Anterior LL innervation is divided into the anterodorsal (AD) system, innervated by gAD, and the anteroventral (AV) system, innervated by gAV.

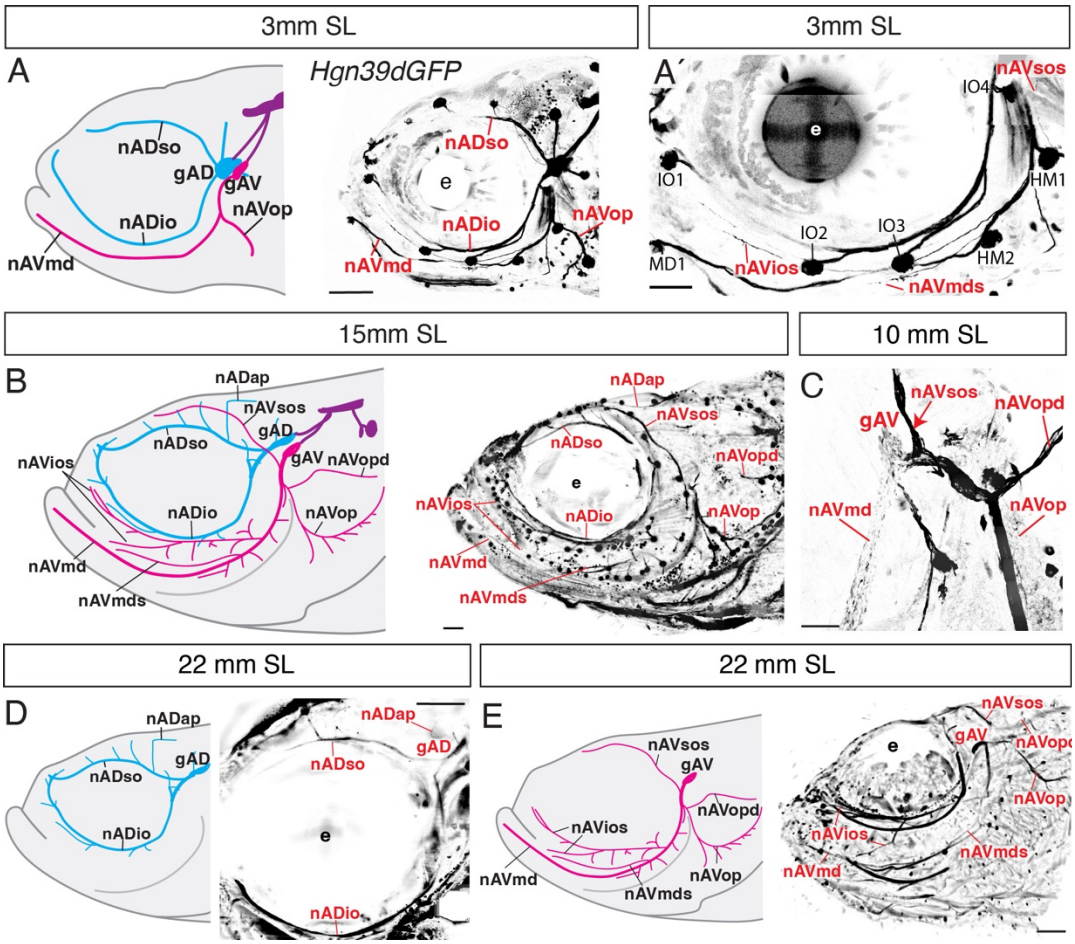

Figure 4-2: Description and development of adult zebrafish anterior lateral line innervation.

(**A-A´**) Innervation map at early larval stages (3 mm SL / 7 dpf). (A) 3 mm SL nerve map schematic, based on adjacent image of anterior lateral line afferent innervation of a 3 mm SL specimen immunolabeled for anti-GFP against *Tg*(*Hgn39d:GFP*) (confocal maximum projection). The schematic shows the anterodorsal nerves and ganglia in cyan (nAD supraorbital (so) and infraorbital (io) and the anteroventral nerves in magenta (nAV mandibular (md) and opercular (op). Axonal projections to the hindbrain are indicated in purple. (A') Close up of late forming superficial nerves (red labels) in the infraorbital region, running parallel to canal nerves, and neuromasts (black labels) at 3 mm SL. (**B**) 15 mm SL nerve map schematic showing the mature anterodorsal system (cyan: nAD supraorbital, infraorbital, and anterior pit (ap) and anteroventral system (magenta: nAV mandibular, mandibular superficial (mds), infraorbital superficial (ios), opercular, opercular dorsal (opd), and supraorbital superficial (sos), based on adjacent image of innervation of a 15 mm SL specimen immunolabeled for anti-GFP against *Tg*(*Hgn39d:GFP*) (lightsheet maximum projection). (**C**) 10 mm SL specimen, showing nerve branch points at the anteroventral ganglion (confocal maximum projection at high magnification). The nAVsos branch point is indicated with a red arrow. Scale = 50 µm. (**D-E**) Innervation map at adult stages (22 mm SL) immunolabeled for anti-GFP against *Tg*(*Hgn39d:GFP*). (D) Lightsheet maximum projection of orbital region of the cranium showing the anterodorsal ganglion and nerves (cyan in adjacent schematic). (E) Light sheet maximum projection of lateral-ventral view of a 22 mm SL specimen showing the anteroventral nerves (magenta in adjacent schematic). Scale = 100 µm.

In 3 mm SL specimens, the AD innervation is relatively simple, as schematized in Fig. 4-2A and shown by the adjacent Hgn39dGFP nerve map. The embryonic AD system (cyan in Fig. 4-2A) consists of branches innervating the SO and IO canal lines. The embryonic AV system (magenta in Fig. 4-2A) innervates the MD and Op (opercular) lines. Both ganglia project axons into the central nervous system at the level of the hindbrain (purple) (Fig. 4-2A). Fig. 2A' shows a higher magnification view of the 3 mm SL specimen, revealing the first developing nerve fibers for late-forming superficial lines that will branch from the gAV (red labels). Note that in the descriptions that follow, we use the terminology established by Raible & Kruse (2000), and in addition, we use the designation "s" for the newly forming nerves that will innervate superficial lines of neuromasts. In the 3 mm SL specimen, nAVios (**n**erve from the **AV** ganglion projecting to the **i**nfra**o**rbital **s**uperficial line) branches from near neuromast HM1 and runs parallel to the IO nerve; the nAVmds branches anteriorly from neuromast HM2 and runs part of the way down the MD nerve; and the nAVsos branches dorsally from the gAV root above neuromast HM1. We use the nomenclature of HM1 and HM2, based on Iwasaki et al. (2020), to describe the embryonic neuromasts that will eventually become canal neuromasts in the preopercular portion of the mandibular canal.

By juvenile stages (15 mm SL), all branches of adult innervation have been established (Fig. 4-2B). The organization of the anterodorsal system (cyan) remains very similar to that of 3 mm SL specimens (compare schematics in Figs 4-2A, B). By contrast, the anteroventral system (magenta) is significantly expanded at this later stage. New nerves have been added running parallel to each of the existing canal lines,

and a secondary dorsal branch of the opercular line (nAVopd) has formed (Fig. 4-2B). By these juvenile stages, superficial nerve nAVios has split into a dorsal branch, which innervates superficial neuromasts parallel to the infraorbital line, and a ventral branch, which innervates superficial neuromasts parallel to the mandibular line. The early origins (up to 10 dpf) of two of these nerves, nAVopd and nAVios (designated as nAVmx), were previously noted by Iwasaki et al. (2020). Fig. 4-2C shows a close-up view of the root of the anteroventral system dividing into several branches at late larval stages (10 mm SL), confirming that late forming nerves such as the nAVsos (red arrow) originate from the gAV. The AD (Fig. 2D) and AV (Fig. 4-2E) systems are separately shown in a 22 mm SL adult, with accompanying schematics highlighting the relative elaboration of each system's innervation. The expansion of the anterior lateral line occurs primarily due to the addition of AV-innervated superficial neuromast lines at larval stages.

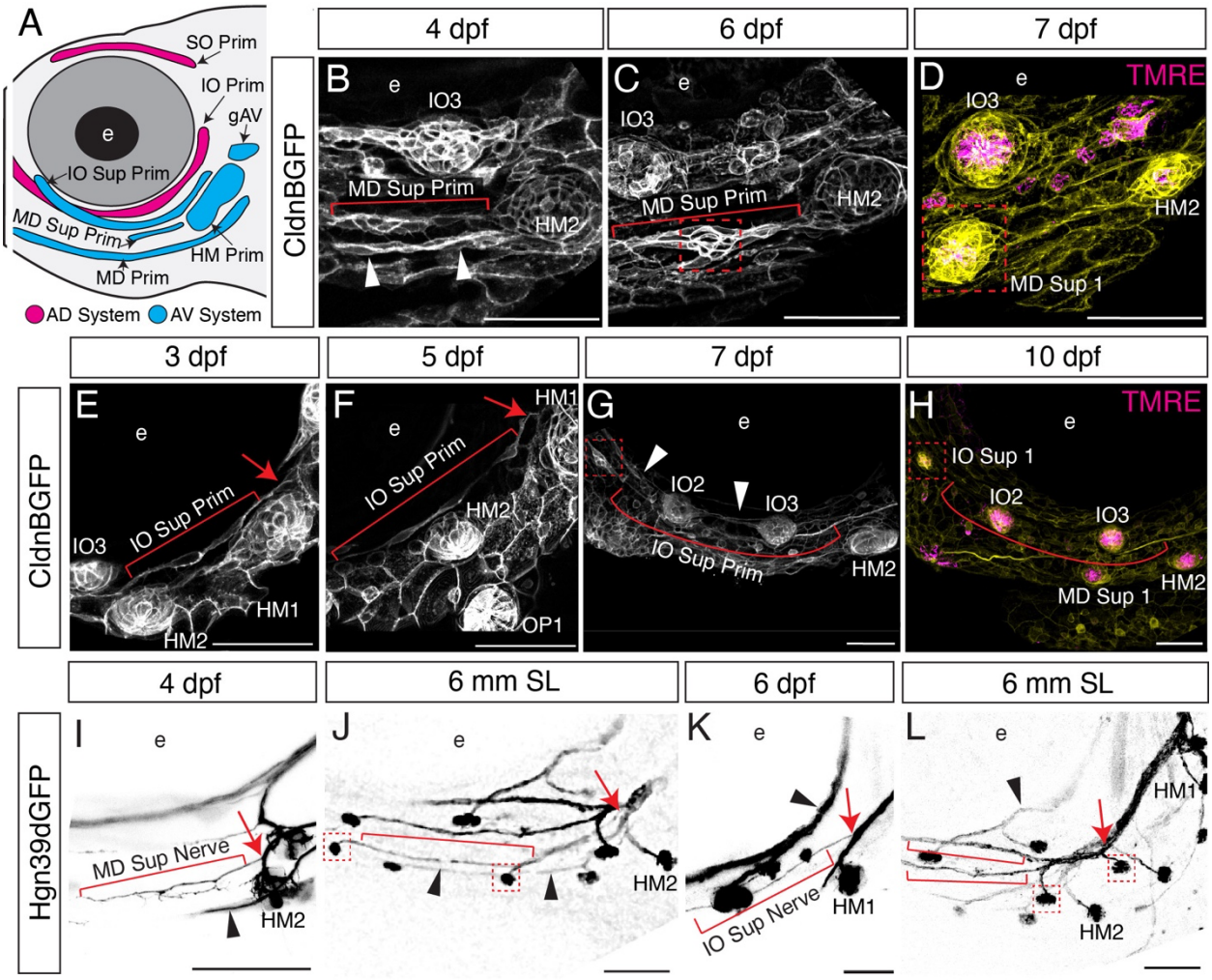

Figure 4-3: Mechanisms of postembryonic superficial neuromast formation from late forming primordia.

(**A**) Schematic of CldnB-labeled lateral line primordia derived from AD (magenta) and AV (cyan) placodes. (**B-H**) Confocal images of live *Tg(CldnB:GFP)* specimens. (**B-D**) Development of the mandibular superficial line from its migrating primordium (MD Sup Prim) at (B) 4 dpf; (C) 6 dpf; and (D) 7 dpf. (B) The mandibular superficial primordium (red bracket) extends from HM2 by 4 dpf, parallel to the mandibular primordium (white arrowheads). (C) By 6 dpf the primordium has begun to condense into a protoneuromast (red box). (D) At 7 dpf the first neuromast of the MD superficial line is in place (MD Sup 1; red box); *CldnB:GFP* (yellow); TMRE (magenta) labels hair cell mitochondria within the neuromast. (**E-H**) Development of the infraorbital superficial line from its migrating primordium (IO Sup Prim). Extension of the IO superficial primordium (red bracket) adjacent to HM1 at (E) 3 dpf; (F) 5 dpf; (G) 7dpf; and (H) 10 dpf; where it condenses into the first neuromast of the IO superficial line (IO Sup 1; red box). (E) The infraorbital superficial primordium originates adjacent to HM1 (red arrow)and extends a few cells ventrally. (F) At 4 dpf, the primordium has extended past HM2, running parallel to the IO canal line. (G) At 7 dpf, the primordium has extended parallel to the IO canal line (white arrowheads) to its terminal location adjacent to the eye between IO1 and IO2 (red box), where the terminus has condensed into a protoneuromast. (H) At 10 dpf, this terminus (red box) has differentiated into the first neuromast in the IO superficial line, labeled with *CldnB:GFP* (yellow) and neuromast hair cell marker TMRE (magenta). (**I-H**) Confocal images of live (I, K) and fixed (J, H) *Tg(Hgn39D:GFP)* specimens immunolabeled for GFP. (I) The innervating MD superficial nerve (red bracket) is shown at 4 dpf, branching from gAV near HM2 (red arrow), and running parallel to the MD canal nerve (black arrowhead). (J) At 6 mm SL the MD superficial nerve (red arrowheads) has extended anteriorly to innervate neuromasts in the mandibular superficial line

Fig 4-3 cont. (red boxes), continuing to run parallel to the MD canal nerve (black arrowheads). (K) The innervating IO superficial nerve (red bracket) branches off from gAV near HM1 (red arrow) and runs parallel to the IO canal nerve (black arrowhead). (L) At 6 mm SL the IO superficial nerve (red arrow) has formed a ventral branch, with both the original and ventral branches (red brackets) running parallel to the IO canal nerve (black arrowhead) and innervating neuromasts in the infraorbital superficial line (red boxes). e = eye.

(2) Neuromasts are added by re-use of embryonic mechanisms at later ontogenetic stages

Next, we investigated the mechanisms that drive the formation of the superficial lines that lie parallel to the canal lines, as well as the proliferation of superficial and canal neuromasts at larval stages. Postembryonic descriptions of the zebrafish posterior lateral line have described three different mechanisms by which late forming neuromasts can develop. The first mechanism relies on migration of new primordia: the posterior LL forms secondary primordia (prim II and primD) at 48 hpf that migrate parallel to the original line ventrally and dorsally, respectively, dropping off superficial neuromasts in their wake (Sarrazin et al., 2010). The second mechanism, intercalation, occurs in larval stages beginning at 3-4 dpf. In this mechanism, interneuromast progenitors, which are deposited between existing neuromasts during the initial migration of the primordia, proliferate and condense into new neuromasts (Ledent, 2002). The third mechanism is budding, where cells from a parent neuromast proliferate, extend, and then round up to condense into a daughter neuromast. In the posterior LL, budding occurs sequentially beginning at 10 mm SL to form dorsoventral "stitches" that lie orthogonal to the original line, increasing the number of neuromasts in each of the lateral lines (Ledent, 2002; Wada et al., 2013). For both the caudal neuromasts of the tail and the opercular superficial line of the anterior LL, neuromasts are added by a similar sequential budding process beginning at early larval stages and

occurring in the direction of growth of the underlying dermal bone (Wada et al., 2010). We asked if, when, and how each of these mechanisms might be used in the zebrafish anterior lateral line system, as well as whether there are any anterior LL-specific mechanisms of superficial neuromast formation.

Figure 4-3 documents the emergence of superficial lines from newly emerging primordia. By 3 dpf the mandibular, infraorbital, and supraorbital primordia of the canal lines have migrated to their final locations. Next, the superficial lines start to develop from newly emerging superficial primordia, all of which derive from the AV system (schematized in Fig. 4-3A; blue). Figs 4-3B-H show maximum confocal projections of lateral line tissue in living zebrafish specimens, imaged using *Tg(CldnB:GFP*), a transgenic line that marks tight junctions of epithelial cells and is enriched in the lateral line system (Haas & Gilmour, 2006). Fig. 4-3B-D documents the emergence of the mandibular superficial line, which runs parallel to the mandibular line, from a newly emerging strand of CldnB-labeled primordium cells that extends anteriorly from the AV-derived hyomandibular system at relevant stages (n = 5 specimens). Fig. 4-3B shows a 4 dpf specimen with a new primordium splitting off the anterior end of the HM primordium (red bracket), parallel to the mandibular line (white arrowheads). By 6 dpf (Fig. 4-3C), this MD superficial primordium has extended part way along the length of the MD line and cells are beginning to condense into a protoneuromast (red box). At 7 dpf (Fig. 4-3D) the first MD superficial neuromast (MD Sup 1; red box) is in place, with mitochondria-rich hair cells labeled by vital dye TMRE (magenta) now present.

Fig. 4-3E-H documents the similar emergence of the infraorbital superficial line (n = 5). At 3 dpf (Fig. 4-3E), a new strand of CldnB-labeled primordium cells (red bracket)

extends anteriorly from a location adjacent to the AV-derived hyomandibular system (red arrow). This IO superficial primordium was described by Iwasaki et al. (2020) as forming the “maxillary line” and our findings corroborate their previous description: we find that the primordium elongates parallel to the IO line (Fig. 4-3G, white arrowheads) at 5 dpf (Fig. 4-3F), and by 7 dpf (Fig. 4-3G) extends anteriorly (red bracket) to an enlarging endpoint (red box), beyond neuromast IO2, where the tissue begins to proliferate and condense into the first new infraorbital superficial neuromast (IO Sup 1, red box; Fig. 4-3H) by 10 dpf.

We also used the *Tg(Hgn39d:GFP)* transgene to visualize innervation during the development of the MD and IO superficial neuromast lines (Figs 4-3I-L). Fig. 4-3I, J show the emergence and later development of the mandibular superficial nerve (nAVmds). Fig. 4-3I shows the nerve (red bracket) branching off from the same location on the nAVhm nerve (red arrow) as its primordium, at 4 dpf. By the 6 mm SL stage (Fig. 4-3J), the nerve (red bracket) extends to innervate multiple MD superficial neuromasts (red boxes). Fig. 4-3K, L show the similar emergence and later development of the infraorbital superficial nerve (nAVios). Fig. 4-3K shows the new nerve branching from the same location on the nAVhm nerve as the newly forming superficial IO line primordium. By the 6 mm SL stage (Fig. 4-3L), the nerve extends to innervate multiple IO superficial neuromasts (red boxes) and has formed a ventral branch that innervates superficial neuromasts parallel to the MD line. In conclusion, the initial establishment of the mandibular and infraorbital superficial lines occurs over several days, with the system continuing to elaborate throughout ontogeny.

Following the establishment of canal and superficial lines by migrating primordia, many additional neuromasts are added. In Figure 4-4, we document the stereotyped development of superficial neuromasts via the previously described mechanisms of budding and intercalation, using confocal maximum projections of live specimens (n = 5 per mechanism). Neuromast maturation was tracked using the vital dye TMRE, which labels mitochondria-rich hair cells, indicative of mature functional neuromasts. By repeated co-labeling of live developing *Tg(CldnB:GFP)* specimens with TMRE, neuromast formation (GFP-positive; yellow) and subsequent maturation (TMRE-positive; magenta) were traced over time.

Fig. 4-4A-C tracks an example of the budding mechanism over a 5-day period. In this 5 mm SL specimen, the IO1 neuromast is just starting to bud at Day 0 (Fig. 4-4A; white box), to produce a new *CldnB:GFP*-labeled superficial protoneuromast at Day 3 (Fig. 4-4B), with TMRE-positive (magenta) hair cells developing within the newly formed neuromast by Day 5 (Fig. 4-4C). In Fig. 4-4D, we used *Tg(Hgn39D:GFP)* to document the expansion of innervation associated with the budding process; a direct projection branches (red arrow) from the parent to the daughter neuromast (red box). Fig. 4-4E-G tracks a HM superficial neuromast (white arrow) in the process of developing between two mature canal neuromasts, HM1 and HM2, via intercalation. Fig. 4-4E shows a 5 mm SL specimen in which expansion of *CldnB:GFP* interneuromast progenitors between the mature canal neuromasts is just beginning (Day 0; white arrow). By Day 2 a protoneuromast has formed (Fig. 4-4F; white arrow). By Day 7, TMRE-expressing hair cells are present in the newly formed superficial neuromast (Fig. 4-4G, white arrow). In Fig. 4-4H, we again used

Tg(Hgn39D:GFP) to document the expansion of innervation associated with the intercalation process; here, a new projection branches (red arrow) from the HM nerve to the newly formed superficial neuromast (red box). Fig. 4-4I and Fig. 4-4J show schematics of neuromast formation by budding and intercalation, respectively.

Taken together, the data we present in Figures 4-3 and 4-4 indicate that the increasingly complex patterning of the anterior LL system can be explained, at least in part, by the re-use of embryonic developmental mechanisms at varied locations and developmental stages.

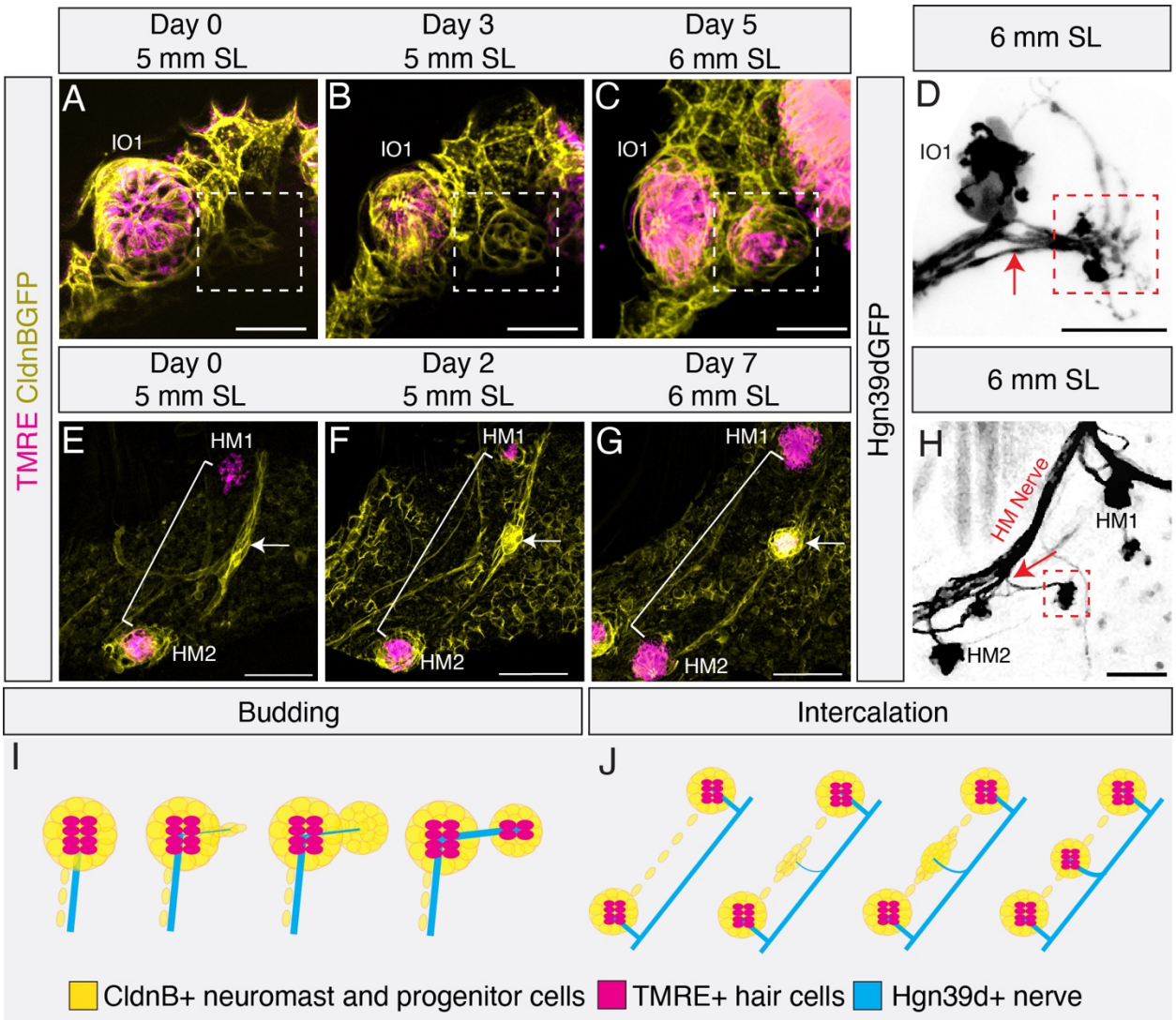

Figure 4-4: Development of anterior lateral line superficial neuromasts by budding and intercalation mechanisms.

Fig 4-4 cont. (**A-C**) High magnification confocal time series of lateral line tissue (CldnB:GFP; yellow) and mature neuromasts (TMRE; magenta) showing the budding mechanism of neuromast formation in a single live specimen from 5-6 mm SL. (A) At day 0, canal neuromast IO1 extends a posterior projection of a few CldnB:GFP labeled cells (white box). (B) By day 3, the cells from the posterior projection have proliferated to form a protoneuromast (white box). (C) By day 5, this tissue has differentiated into a mature daughter neuromast expressing TMRE (white box) lying directly posterior to parent neuromast IO1. (**D**) Confocal image of a live *Tg(Hgn39D:GFP)* 6 mm SL specimen showing a direct nerve branch (red arrow) extending from the ganglion, which also innervates the parent neuromast (IO1), to the daughter (red box) neuromast. (**E-G**) High magnification confocal time series of the lateral line tissue (CldnB:GFP; yellow) and mature neuromasts (TMRE; magenta) showing the intercalation mechanism of neuromast formation in a single live specimen from 5-6 mm SL. These images were manually segmented to remove unwanted signal from superficial epithelial tissue. (E) At day 0, a HM superficial neuromast is beginning to form (white arrow) from a thickening of interneuromast tissue (white bracket) between two mature canal neuromasts, HM1 and HM2. (F) At day 2, the interneuromast tissue has proliferated into a rosette shape (white arrow). (G) By day 7, the interneuromast tissue has differentiated into a mature superficial neuromast with TMRE signal (white arrow). (**H**) Confocal image of a live *Tg(Hgn39D:GFP)* 6 mm SL specimen showing a new nerve branch (red arrow) extending from the main HM nerve between the HM1 and HM2 branches to innervate the newly formed HM superficial neuromast (red box). (**I-J**) Schematics of neuromast formation processes: CldnB:GFP-labeled neuromast and progenitor cells (yellow), TMRE+ hair cells (magenta), and Hgn39d+ nerves (cyan). (**I**) Schematic of budding process. (**J**) Schematic of intercalation process.

(3) A novel lateral line formation mechanism with a mixed placodal origin

Unlike the primordium-driven mode of development described above for the MD and IO superficial lines, there is no primordium tissue initially associated with the developing supraorbital superficial nerve, which has emerged by 7 dpf (3 mm SL) (nAVsos; Fig. 4-2A'). To investigate the origins of the neuromast-producing lateral line tissue of the SO superficial line, we traced the development of the region immediately caudal to the eye between the 3 mm SL stage, when the nerve first appears, and the 8 mm SL stage, when the first SO superficial neuromast has formed over the apex of the eye (Fig. 4-5). Panel 5A is a low magnification view showing the AV-derived canal neuromast HM1, as well as AD-derived neuromasts IO4 and O2. We next visualized this region in high magnification confocal maximum projections, in living specimens, using the *Tg(CldnB:GFP;Hgn39d:GFP)* double transgenic, which labels both lateral line

progenitor tissue and lateral line afferent nerves with GFP (yellow), together with TMRE vital dye to mark mature neuromasts (magenta).

A caveat of using *Tg(CldnB:GFP;Hgn39d:GFP)* double transgenic specimens is that both lateral line progenitors and innervation are labeled with the same fluorophore, making it challenging to discriminate lateral line cells from either epithelial cells or the nerves at late stages. To rectify this issue, we immunolabeled some fixed specimens with anti-Sox2 antibody (Genetex GTX124477, RRID AB_1117806), a label of lateral line primordia and interneuromast cells (Hernández et al., 2007). While Sox2 is a transcription factor, and the antibody therefore labels nuclei of progenitors as expected, we find that this antibody additionally labels emerging lateral line nerves (confirmed by co-labeling with acetylated alpha-tubulin). Sox2 labeling thus clarifies whether cells visualized with the double transgene marker are lateral line cells, nerves, or neither. Fig. 4-5B-B' confirms that the Sox2-positive supraorbital superficial nerve does not have any lateral line primordium cell nuclei directly associated with it (magenta; red arrowheads), and that *CldnB:GFP*-positive cells extending from existing neuromasts are interneuromast cells with Sox2-positive nuclei (white arrowheads).

Fig. 4-5C-F shows a time series of SO superficial lateral line formation in a representative single living specimen (n = 5). Fig. 4-5C shows that at 5 mm SL the newly forming nAVsos nerve extends dorsally (white arrowhead) past the level of neuromasts IO4 and O2. Each of these neuromasts extends a strand of *CldnB:GFP* labeled interneuromast cells (brackets) that meet to form a "bridge" of tissue, which the extending nerve intersects (intersection indicated by white box). A few days later, at 6 mm SL (Fig. 4-5D), the nerve has extended beyond the bridge of tissue, and up over

the eye (out of frame in this panel). By this stage, additional primordium tissue is present along the nerve, at points beyond (i.e. dorsal to) the intersection with the tissue bridge (white arrowhead: Fig. 4-5D). By the 7 mm SL stage (Fig. 4-5E), the SO superficial nerve has extended fully, to reach a location above the apex of the eye, and the cells along the nerve are beginning to proliferate and condense into the first SO1 superficial neuromast. In addition, at this same stage, the tissue extending dorso-anterior from IO4 loses contact with the SO superficial line, and this tissue now establishes a 'bud' from IO4. This tissue goes on to form new canal neuromast IO4* (Fig. 4-5F). By 8 mm SL, the first SO supraorbital superficial neuromast (SO Sup 1) has matured to become fully TMRE-positive (Fig. 4-5F). Staining this 8 mm SL endpoint for Sox2 (magenta) and acetylated alpha-tubulin (cyan) confirms that the tissue projecting from IO4 and O2 to the nAVsos nerve is composed of interneuromast cells (Fig. 4-5F-F'), and that neuromast progenitor cells are not present along the nerve prior to its intersection with the AD-derived neuromast progenitor cells.

Fig. 4-5G-J shows representative confocal images of fixed specimens labeled with Sox2 (magenta) and acetylated alpha-tubulin (cyan) antibodies, which trace a cross-placodal mechanism of supraorbital superficial line development through a series of steps: (1) At 5 mm SL the naked nAVsos nerve extends (white arrowhead) to meet the tissue "bridge" made by the interneuromast cells of AD-derived neuromasts IO4 and O2 (Fig. 4-5G, brackets). (2) At 6 mm SL the nerve "catches" interneuromast tissue, which is now seen running parallel to the nerve after the initial intersection point (Fig. 4-5H, white box). (3) At 7 mm SL the nerve and interneuromast tissue are migrating together up and over the eye towards their final position above the apex of the eye (Fig.

4-5J; white arrowhead). (4) Interneuromast cells proliferate, with the first neuromast of the SO superficial line forming above the apex of the eye (Fig. 4-5J; SO Sup 1). Figure 4-5K is a schematic of the steps of the mechanism described in Fig. 5G-J, with the origin of each neuromast labeled as AV-derived (magenta) or AD-derived (cyan). This novel, cross-placodal, mechanism of neuromast formation is particularly significant because it combines a nerve from one placode and neuromast tissue from another to form a new neuromast line without the use of a shared primordium. Of note, this is the latest of all the anterior lateral lines to form, with development of the first supraorbital superficial neuromast completed at 8 mm SL. Additional superficial neuromasts will be added along this line throughout ontogeny.

Each of the mechanisms of larval stage neuromast formation generates characteristic innervation patterns. Thus, the adult innervation patterns allow us to infer how any given neuromast developed. For neuromasts formed by migrating primordia (Fig. 4-3) and the new cross-placodal mechanism (Fig. 4-5), a new branch extends directly from gAV. Because neuromasts that are innervated by a common nerve usually originate from the same primordium, 'daughter' neuromasts that descend from 'parent' neuromasts by budding will be directly connected to their parent neuromast by a new nerve branch (Fig. 4-4D, I). Consistent with this observation, a previous analysis of the development of the opercular line showed that superficial neuromast budding creates a 'pedigree pattern' (Wada et al., 2010). In contrast, we observe that neuromasts that form by intercalation between two existing neuromasts are innervated by a new nerve branch from the original, primary line (Fig. 4-4H, J). Analyzing the innervation patterns of 22 mm SL adult specimens (Fig. 4-2; Table 2) shows that superficial neuromasts are

added primarily by budding and intercalation during larval stages, while the founder neuromasts of each superficial line are established by migrating primordia and the novel cross-placodal mechanism.

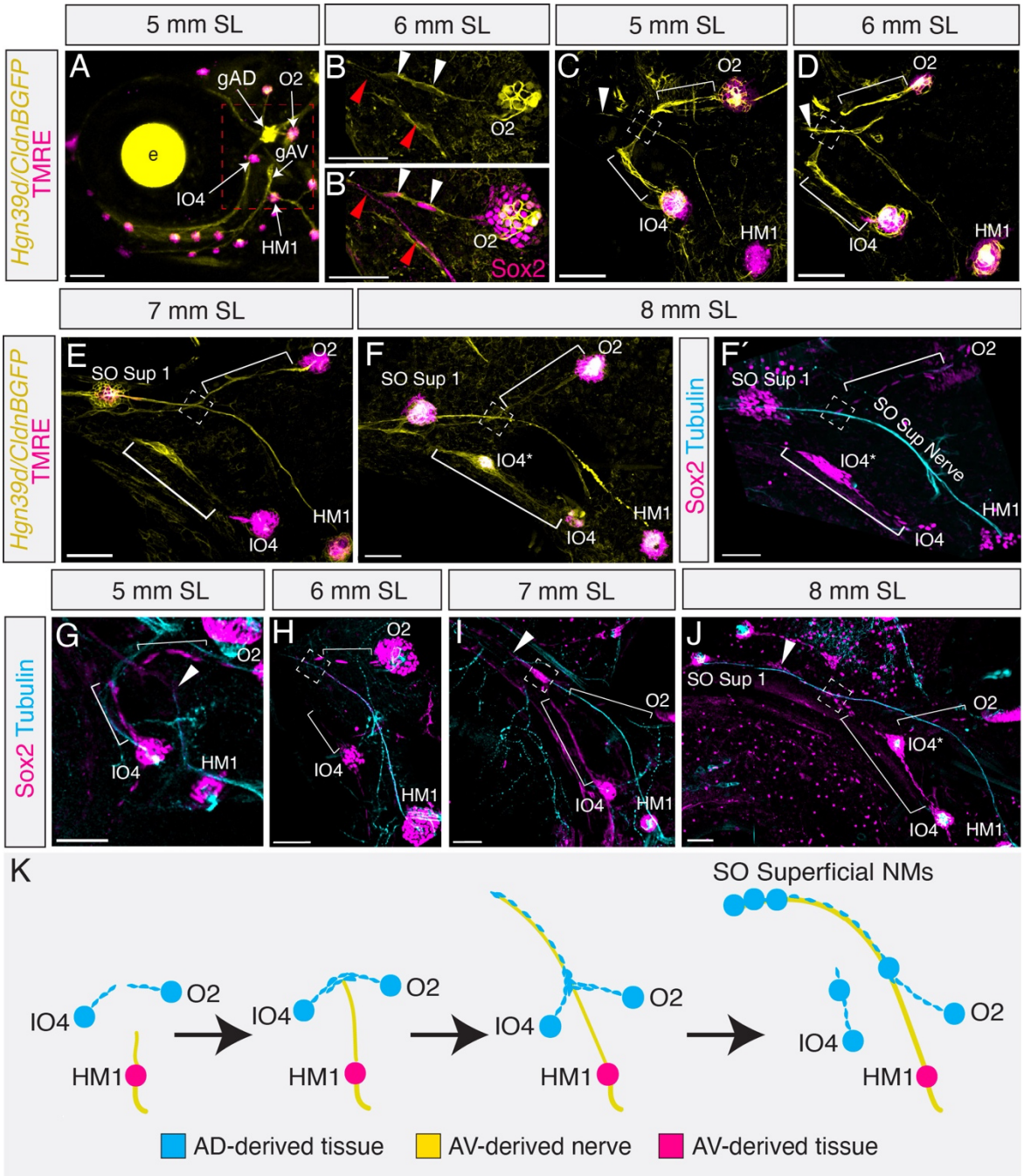

Figure 4-5: The supraorbital superficial line is of mixed placodal origin and is formed by a novel cross-placodal mechanism.

Fig 4-5 cont. (**A**) Low magnification (10x objective) confocal image of nerves (*Hgn39dGFP*; yellow) and mature neuromasts (TMRE; magenta) at 5 mm SL with the area of interest behind the eye indicated (red box). (**B-B'**) Comparison of (B) *Tg(CldnB:GFP)* (yellow) and (B') Sox2 (magenta) expression at the connection between neuromast O2 and the SO superficial nerve (red arrowheads) in 6 mm SL specimen. Note that the nerve is also Sox2-positive. CldnB:GFP-positive cells extending from existing neuromasts are interneuromast cells with Sox2-positive nuclei (white arrowheads). Scale = 20 μm. (**C-F**) Live time series images of a single *Tg(CldnB:GFP/Hgn39d:GFP)* (yellow) specimen labeled with TMRE (magenta). In all images, neuromasts HM1, IO4, and O2 are labeled. The intersection between the nerve originating from HM1 (white arrowhead) and strands of interneuromast cell-derived primordial tissue originating from IO4 and O2 (white brackets) is noted with a white box. Scale = 50 μm. (C) Initial intersection of the nerve and primordia at 5 mm SL. The SO superficial nerve extending from HM1 (white arrowhead) has no lateral line tissue along it and intersects (white box) with the CldnB:GFP-labeled primordium extensions (yellow) from O2 and IO4 (white brackets). (D) Adherence of primordium tissue to SO superficial nerve at 6 mm SL. The SO superficial nerve (white arrowhead) now has lateral line tissue running parallel to it on the portions of the nerve that extend past the intersection point (white box) with the O2 and IO4 primordia (white brackets). (E) Proliferation of primordium tissue in the SO superficial line at 7 mm SL. The primordium extending from O2 (white bracket) still intersects (white box) with the SO superficial line, while the primordium from IO4 is beginning to condense into canal neuromast IO4. The first neuromast of the SO Superficial line (SO Sup 1) has begun to condense beyond the intersection point. (F) Differentiation of a supraorbital superficial neuromast by 8 mm SL. Both SO Sup 1 and canal neuromast IO4* have differentiated into mature neuromasts with functional hair cells (magenta), and neuromast O2 remains permanently connected to the SO superficial line (white bracket; white box). (F´) Same view as (F) showing the same specimen immunolabeled for neuromast marker Sox2 (magenta) and nerve marker acetylated alpha-tubulin (cyan). The innervating gAVsos nerve (SO Sup Nerve) is labeled. (**G-H**) Representative images of SO supraorbital development in specimens stained for Sox2 (magenta) and acetylated alpha-tubulin (cyan) at (G) 5 mm, (H) 6 mm, (I) 7 mm, and (J) 8 mm SL. Annotations as in panels C-F. Scale = 50 μm. (K) Schematic of the cross-placodal mechanism of SO superficial line formation at the imaged stages 5-8 mm SL with placodal origin indicated.

Table 2 integrates data from Figures 4-1 to 4-5 to summarize the mechanisms of neuromast formation for each canal neuromast and for each superficial line or series. In the supraorbital line, canal neuromasts SO1-3 are initially deposited during embryonic development, with neuromast SO1* budding from SO1 at 5 mm SL. In the infraorbital line, canal neuromasts IO1, IO2, and IO4 form during embryonic development, with IO3 added shortly after in 4 dpf larvae, and three additional neuromasts forming during later larval stages, two by budding (IO2* and IO4*) and one by intercalation (IO3*). The mandibular line forms later, with only two mandibular canal neuromasts deposited by 3 mm SL (HM1 and HM2). By adult stages, another five mandibular neuromasts have formed by intercalation from the interneuromast progenitors along the mandibular canal. The first neuromasts of the superficial lines in general originate later — up to 8

mm SL in the case of the SO Superficial line — and each of the superficial lines continues to add neuromasts up to and during adulthood (> 22 mm SL). Our analysis reveals that a large proportion of both canal neuromasts and superficial line neuromasts originate during larval stages.

(4) Innervation is necessary for anterior lateral line development

In the posterior LL, innervation is necessary for the formation of superficial neuromasts via the budding mechanism (Wada et al., 2013). However, the role of innervation in the development of the anterior LL is unknown. Based on the prominence of innervation in the newly described 'nerve forward' cross-placodal mechanism of SO superficial anterior LL formation, we hypothesized that innervation might be required for the development of this superficial line. In addition, we wished to evaluate whether innervation is necessary for the development of additional components of the system, such as neuromasts formed through intercalation, or for canal neuromast maturation.

Figure 4-6 shows the neuromast patterns of zebrafish specimens in which we performed a unilateral ablation of both the gAD and gAV ganglia. In these specimens, all gAD and gAV neurons of *Tg(Hgn39d:GFP)* specimens were ablated at 4 dpf (a stage at which both dorsal and ventral ganglia are present and can be visualized) using a high-power UV laser to kill the neurons and thus remove innervation. The contralateral side of each ablated specimen serves as an internal control. Ablated specimens were raised to 6 weeks post fertilization (wpf), representing a range of stages between 11 and 15 mm SL. At these stages, all superficial lines have formed and canal neuromasts have sunk into ossifying canal grooves (Webb & Shirey, 2003). Those specimens that received a sham surgery of intense UV laser light applied immediately

adjacent to the anterior LL ganglia showed no change in neuromast or innervation patterns at the 6 wpf endpoint (n = 5).

In successful ablations (n = 10), the signal from both the gAD and gAV ganglia was completely and permanently removed, and the anterior LL neuromasts began to denervate immediately, as shown by confocal maximum projections in Fig. 4-6A-A'. We found no evidence for regeneration of either the ganglia or their nerves in these ablations. For each ablated specimen, the control and ablated side were imaged with an epifluorescent microscope and assayed using the live dye TMRE (Fig. 4-6B-C'), followed by clearing and staining for the neuromast marker Sox2 for a higher resolution confocal assay of the neuromast pattern (Fig. 4-6D-D'). Fig. 6B shows a dorsal view (anterior to the top) of the change in neuromast pattern in a single specimen between the control and the ablated side. While each of the SO canal neuromasts (yellow arrows) are present on the ablated side, the SO superficial line is completely absent (red brackets), and the anterior pit line is missing neuromasts (red asterisks). Importantly, in 8/8 ablated specimens assayed, all the neuromasts that lie adjacent to the SO canal line were missing at 6 wpf, indicating that the SO superficial line did not form. This finding confirms that the novel cross-placodal mechanism that forms the SO superficial line does indeed require innervation.

Observing the crania of our ablated specimens in lower magnification views, we found a dramatic reduction in the number of superficial neuromasts across the entire ablated side. Figure 4-6C compares lateral views of the control (Fig. 4-6C) and ablated (Fig. 4-6C') sides of the same specimen shown in Fig. 6B, with yellow arrowheads indicating locations where superficial neuromasts have been drastically reduced in

response to ablation. Neuromasts on the ablated side also show a decrease in TMRE intensity compared to posterior LL neuromasts on the same side, or control neuromasts on the contralateral side, suggesting a decrease in the number of functional hair cells per neuromast (Fig. 4-6B-C'). Close observation of the superficial neuromast pattern reveals that both the IO superficial and MD superficial lines are present at their full lengths, but they comprise fewer total neuromasts. Another example of reduction in superficial neuromast number is found in the opercular line, where in this specimen the control side (Fig. 4-6D) has 14 neuromasts (yellow arrowheads), but the ablated side (Fig. 4-6D') has only 7 neuromasts (yellow arrowheads), which are more widely spaced. This observation is consistent with a previous description of opercular line development, in which the line forms through sequential budding but proliferates further as the animal grows and the original neuromasts move apart (Wada et al., 2010), indicating that innervation becomes required for this secondary phase of development.

Notably, quantification reveals that the total number of canal neuromasts is not significantly different in ablated specimens relative to unablated or sham ablated controls, suggesting that innervation is not required for canal neuromast formation (Fig. 4-6E). The average number of total neuromasts decreased significantly, from 83.8 to 42.3, with this reduction almost entirely explained by the average reduction in number of superficial neuromasts from 65.7 to 24.9 (Fig. 4-6F). Moreover, the phenotype is very consistent, with all specimens showing a significant decrease in superficial neuromast number and similar disruptions to their complex neuromast patterns. We conclude that innervation is required for a significant proportion of the larval-stage formation of superficial neuromasts, regardless of the specific patterning mechanism used.

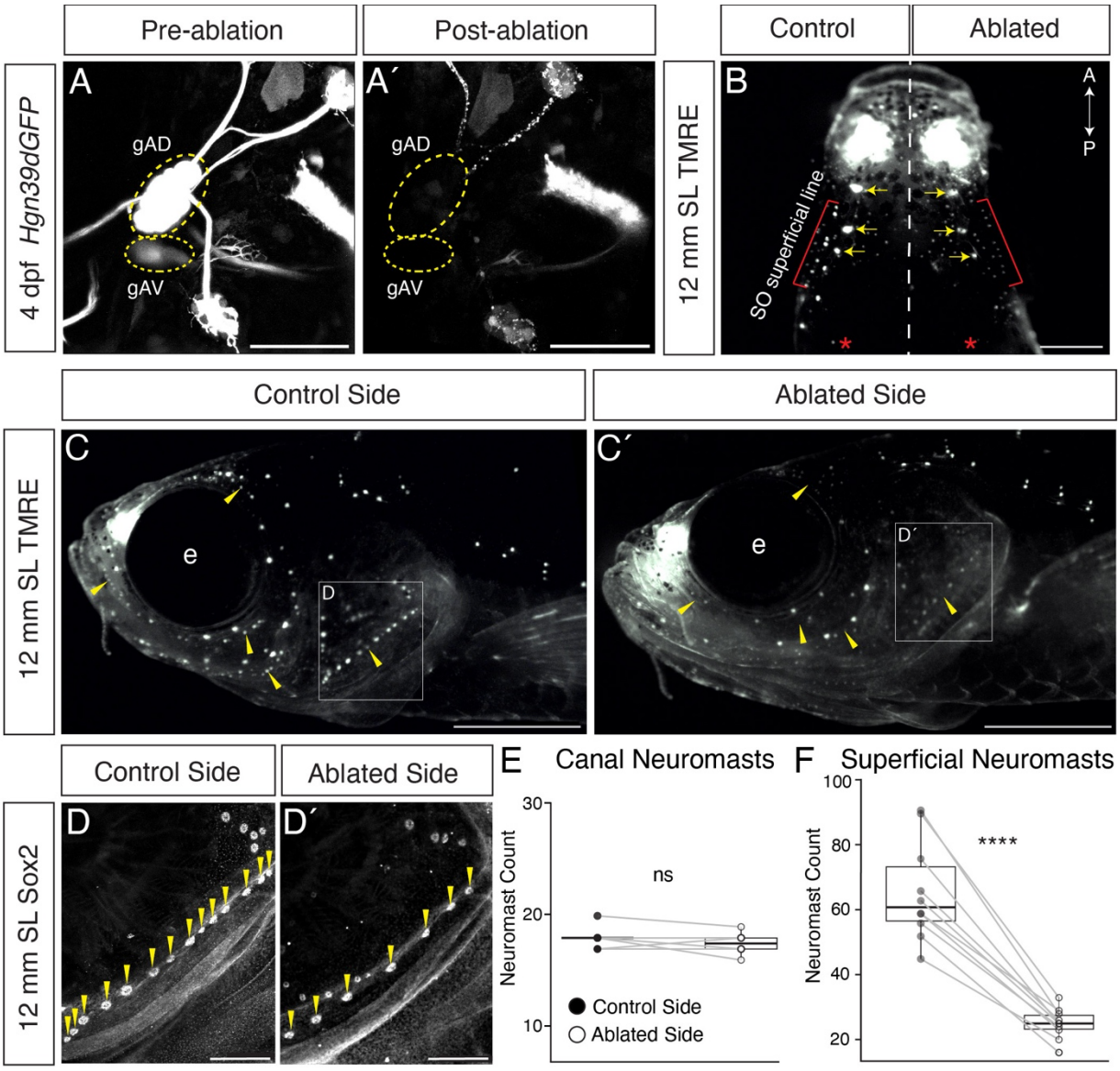

Figure 4-6: Superficial neuromast pattern and number is severely disrupted in the absence of innervation.

(**A-A´**) The anterior LL anterodorsal (gAD) and anteroventral (gAV) ganglia labeled by *Tg(Hgn39d:GFP)* (yellow ovals) before (A) and immediately after (A´) laser ablation at 4 dpf. (**B-D'**) Images of a representative single 12 mm unilaterally ablated specimen. (B) Dorsal view showing both control and ablated sides labeled with TMRE. The supraorbital superficial line (red bracket) is labeled parallel to the supraorbital canal line (yellow arrows) along with the anterior pit line (red asterisk). (**C-C´**) Lateral views showing control (C) and ablated (C´) sides. Yellow arrowheads indicate areas where superficial neuromast patterning was strongly reduced compared to the control side. The white boxes indicate the area magnified in (D-D'). (**D-D´**) Higher magnification confocal (10 x objective) view of the opercular superficial neuromast line in the same specimen immunolabeled for Sox2 showing control (D) and ablated (D') sides. Neuromasts are indicated with yellow arrowheads. (**E**) Box plot showing change in canal neuromast number between the ablated side and internal unablated control side (n = 10). (**F**) Box plot showing change in superficial neuromast number between the ablated side and unablated control side (n = 10). Gray lines indicate paired values. A Shapiro-Wilk test was performed on all data to confirm normality before performing a paired t-test. Not significant (ns) = $p > 0.05$; **** = $p < 0.0001$.

While loss of innervation does not reduce the number of canal neuromasts, it does disrupt canal neuromast size and morphology, as shown in Figure 4-7. Fig. 7A-D' shows confocal maximum projection images of canal neuromasts on the control and ablated sides of the same specimen. Figs 4-7A, A' compare a dorsal view of the supraorbital canal on control and ablated sides in a 12 mm SL specimen, cleared and stained for Sox2. On the ablated side, neuromast SO3 is similar in size to the control side, and neuromast SO2 is slightly smaller than its counterpart. There is a much more striking difference for SO1 and SO1*, where the neuromasts on the ablated side are a fraction of the size on the control side, and express Sox2 at lower levels. Similar morphological changes can be observed in the IO and MD canals. For example, on the ablated side, IO3 and IO3* show a strongly reduced Sox2 signal, are closer to the size of superficial neuromasts, and are more elongated than the circular control side neuromasts (compare Figs 4-7B, B').

To visualize changes in canal neuromast morphology in more detail, we also stained 11-15 mm SL specimens for acetylated alpha-tubulin, which labels innervating nerves as well as the soma and kinocilia of sensory hair cells (López-Schier and Hudspeth, 2005) (Fig. 4-7C-D'). On the control side, the overall shape of neuromast SO1 is round, with a large circle of sensory hair cells (magenta; white outline) located in the center of the support cells (yellow; Fig. 4-7C). By contrast, the SO1 neuromast on the ablated side is significantly smaller and more elongated; it appears to have lost its sensory hair cells and is composed entirely of support cells (Fig. 4-7C'). Canal neuromast SO3 on the control side has very similar morphology to SO1 (Fig. 4-7D), while its ablated

counterpart is slightly smaller, expresses Sox2 at a lower level (yellow), and appears to have fewer hair cells (magenta; white outline) (Fig. 4-7D'). During regeneration, it has been shown that Sox2 is necessary for both the turnover of neuromast support cells and the differentiation of hair cells from progenitors (Hernández et al., 2007). In neuromasts lacking innervation, we observe a decrease in Sox2 expression, as well as reduced canal neuromast size and fewer hair cells, as revealed by a decrease in both tubulin and TMRE signal. These findings are consistent with a potential role for Sox2 in developing canal neuromast support cell proliferation and hair cell differentiation. While canal neuromast morphology is altered in the absence of innervation, the canals themselves appear to be properly induced and patterned. In the posterior LL, neuromasts are required for canal formation ((Wada et al., 2014); by contrast, the presence of normal canals in the cranial region of our manipulated specimens suggests that loss of innervation, and resultant changes in neuromast morphology, do not disrupt cranial canal ontogeny.

To quantify the changes in canal neuromast morphology we calculated the area of each canal neuromast in control versus ablated specimens ($n \geq 6$) by measuring neuromast length (parallel to canal) and width (perpendicular to the canal). In all three canals, the area of the canal neuromasts was reduced significantly in the ablated condition (Fig. 4-7E). In zebrafish, canal neuromast maturity is described by the increasing width of the canal neuromasts with growth (Webb & Shirey, 2003), such that neuromast aspect (width/length) ratio increases as ontogeny proceeds. Comparison of the aspect ratio between the control versus ablated specimens ($n = 6$), reveals a significantly lower ratio on the ablated side, suggesting that these canal neuromasts

show arrested growth compared to their innervated counterparts (Fig. 4-7F). These results show that while innervation is not required for canal neuromast formation or canal induction, it does become required for proper canal neuromast morphology and growth.

Building on the consistency of the ablation phenotype, we sought to better characterize the developmental stage at which a developmental switch occurs, such that innervation becomes required for anterior LL patterning. Specimens that had undergone the ablation procedure at 4 dpf were incubated in TMRE once each week to assay neuromast counts on both the control and ablated sides (Fig. 4-7G). At 2 wpf (4 mm SL; n = 6) and 3 wpf (5-6 mm SL; n = 6), the number of neuromasts is nearly identical between the control and ablated conditions, showing that innervation is not required for anterior LL development during early larval stages. There are only small standard deviations in the overall neuromast counts at these stages, in line with the data collected from unmanipulated controls (compare with Fig. 1F). However, by 4 wpf (7-8 mm SL; n = 6), the number of neuromasts on the control side is significantly higher, and we observe noticeable differences in patterning, e.g., the first neuromasts of the SO superficial line failing to form. After this stage, the number of neuromasts on the ablated side plateaus, while neuromasts continue to be added on the control side. This quantification reveals a sharp developmental switch at 4 weeks post fertilization (7-8 mm SL), at which stage innervation becomes required for further superficial neuromast formation by any mechanism.

In summary, our results have established that innervation is required for the addition of superficial neuromasts by any mechanism, including the cross-placodal

development of the SO superficial line, as well as the growth and morphology of canal neuromasts, after approximately 7 mm SL.

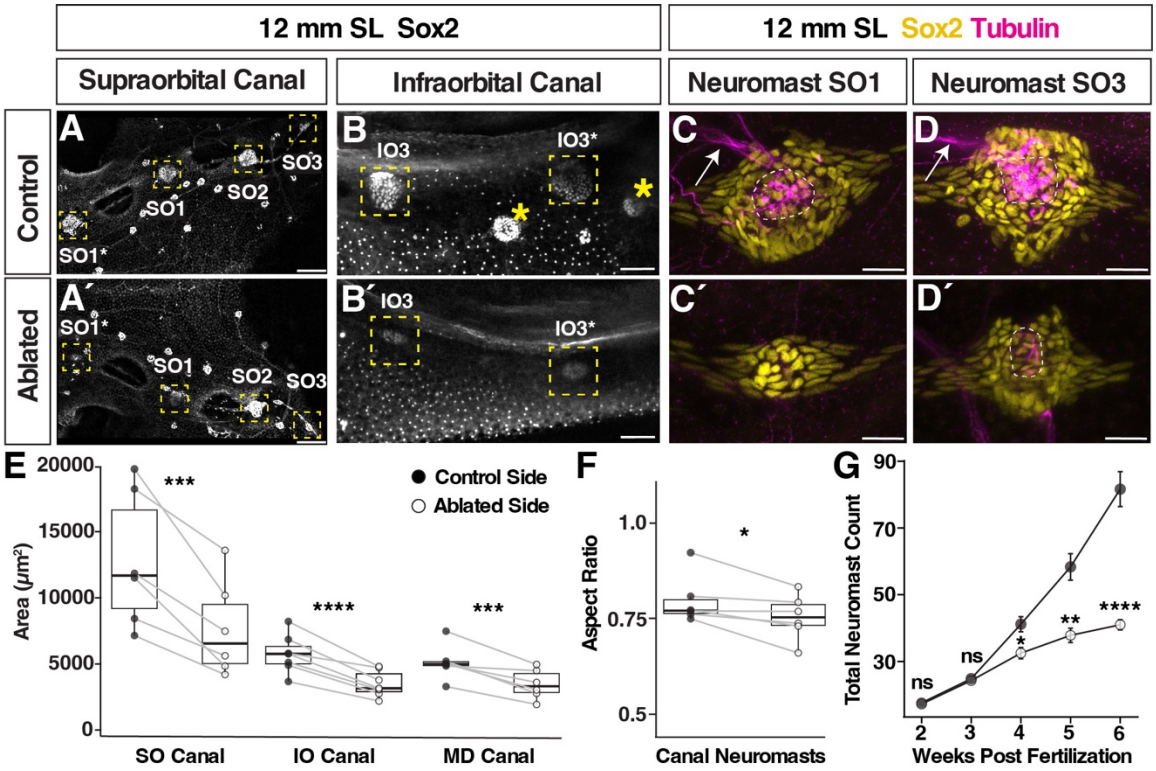

Figure 4-7: Loss of innervation disrupts canal neuromast size and morphology.

(**A-D'**) Comparison of canal neuromasts on the control and ablated sides of a 12 mm ablated specimen, immunolabeled with Sox2 (white, yellow) and acetylated alpha-tubulin (magenta). (A, A') dorsal view of canal neuromasts SO1*-SO3 (yellow boxes). (B, B') Lateral view of canal neuromasts IO2 and IO3 in the same specimen; yellow boxes indicate canal neuromasts, yellow asterisks indicate superficial neuromasts. Scale = 50μm. (C, C') Dorsal high magnification views showing morphology of canal neuromast SO1 on unablated control (C) vs. ablated side (C'). (D, D') Dorsal high magnification views showing morphology of neuromast SO3 on unablated control (D) vs. ablated side (D'). Scale = 20 μm. (**E-F**) Quantifications of canal neuromast area and aspect ratio. Gray lines indicate paired values. (E) Dot plot showing the difference in average canal neuromast area for the supraorbital (n = 6), infraorbital (n = 7), and mandibular (n = 6) canals in the control (solid circle) and ablated (open circle) conditions. (F) Dot plot (n = 6) showing the average canal neuromast aspect ratio for control and ablated conditions. (**G**) Total neuromasts vs. weeks post fertilization on the control and ablated sides of specimens at 2 wpf (n = 6), 3 wpf (n = 6), 4 wpf (n = 6), 5 wpf (n = 6), and 6 wpf (n = 8). A Shapiro-Wilk test was performed on all data to confirm normality before performing a paired t-test., * = $p < 0.05$ ** = $p < 0.01$ *** = $p < 0.001$ **** = $p < 0.0001$.

IV. Discussion

Here, we provide the first description of the patterning of the zebrafish anterior lateral line sensory neuromasts and their innervation at stages between 10 days post fertilization and adulthood. We find that the anterior LL system undergoes significant secondary development during larval stages, when three major superficial lines are established that run parallel to existing canal lines. By 22 mm SL, when the fish are considered adult, the system has expanded dramatically, in large part due to the development of three gAV-innervated superficial lines that run parallel to the three existing canal lines. These superficial neuromasts are added through the migration of new primordia, intercalation, budding, and by our newly described cross-placodal mechanism (summarized in Table 2). At around 4 wpf/7 mm SL, innervation becomes required for neuromast formation: when the anterior LL ganglia are ablated almost no superficial line expansion occurs after 4 wpf/7 mm SL, but the underlying dermal bones continue to expand, leading to increasingly sparse neuromast distribution. In addition, innervation is necessary for proper canal neuromast growth and morphology. Importantly, the peak in neuromast addition rates at late larval stages, seen in normal ontogeny, coincides with the developmental switch to innervation dependence, showing that innervation drives a distinct secondary phase of anterior lateral line development.

In the zebrafish posterior LL, all canal neuromasts and superficial lines have originated by the end of embryonic development at 3 dpf (Ledent 2002). By contrast, the cranial anterior LL generates half of its canal neuromasts and all its major superficial lines at larval stages, showing both temporal and mechanistic differences from the development of the comparatively simpler trunk posterior LL. This difference correlates

with the requirement that the complex cranial anterior LL system must navigate around a variety of morphological features, unlike the obstruction-free structure of the trunk.

We find that the anterior LL neuromasts formed during larval and adult stages following superficial line formation are added through the re-use of embryonic budding and intercalation mechanisms—mechanisms that are also used in the expansion of the posterior LL. During this process, both superficial and canal neuromasts are added to the anterior LL system, to maintain sensory density with growth. However, it is unclear how neuromasts acquire “canal” versus “superficial” identity. The superficial line neuromasts can only produce more superficial neuromasts. By contrast, when canal neuromasts bud they can produce daughter neuromasts of either canal or superficial identity. Moreover, the identity of these daughter neuromasts does not appear to correlate with either the time or the general location of their formation. For example, at 6 mm SL, canal neuromast IO1 buds off superficial neuromast daughters, while adjacent canal neuromast IO2 buds to form the canal neuromast daughter IO2*. Despite their proximity, these anterior LL neuromasts are spatially distributed, such that differential signaling from the local tissue environment or adjacent neuromasts might regulate daughter fate. In a related project we have established that cranial neural crest cells are required for aspects of early anterior LL patterning, providing an example of how a local tissue environment can influence neuromast development (Venkataraman, McGrory et al., 2025).

In addition to the previously described mechanisms of superficial neuromast formation, we have uncovered a novel mechanism that drives the development of the supraorbital superficial line. In this cross-placodal mechanism, a nerve from the AV

system interacts with interneuromast cells extending from AD-derived neuromasts, and the extending nerve and primordial neuromast cells then migrate together dorsally, towards the apex of the eye. Moreover, using a ganglion ablation strategy, we have demonstrated that this nerve is required for the migration and proliferation of these interneuromast cells. This mechanism is unique because it generates a superficial lateral line in which neuromast progenitor tissue originates from one placode (AD), whereas the nerve that innervates those neuromasts originates from another placode (AV). In all other described mechanisms, the nerve associates closely with the tissue of the relevant anterior LL primordium immediately after its formation, such that these other lines have a consistent placodal origin ((Wada et al., 2010) and this study).

Paralleling the formation of neuromasts by the cross-placodal mechanism, we have observed that in experimental situations the anterior LL nerves from one placode have the capacity to promiscuously innervate nearby neuromasts from another line or placode. In almost all fully ablated specimens (13/14), innervation crossed over from the control side to innervate the nasal line neuromasts of the ablated side. In a small proportion of our ablated specimens (4/14), the middle ganglion of the posterior LL (Raible & Kruse, 2000) ectopically reinnervated the anterior LL, with multiple nerve fibers contacting both superficial and canal neuromasts of the anterior LL system and partially rescuing neuromast patterning (data not shown). This observation supports a model in which innervation can induce the development of superficial neuromasts after interacting with proximal interneuromast progenitor tissue through an inefficient neurotropic effect. We speculate that the more developmental mechanisms the lateral line system has in its 'toolbox' the more permutations of patterning are possible,

suggesting mechanistic underpinnings for the remarkable diversity of lateral line patterns across teleost species (Wada et al., 2008).

While this study has uncovered differences in development of the anterior and posterior LL systems, it has also revealed commonalities. Both the zebrafish anterior LL (this study) and posterior LL (Wada et al., 2013) show innervation-dependent budding of superficial neuromasts at late developmental stages. For example, ablation of the posterior LL ganglion blocks the formation of posterior LL superficial neuromast clusters that form by the budding mechanism from an embryonic founder neuromast, beginning at approximately 10 mm SL (Wada et al., 2013). Moreover, in these posterior LL ganglion ablated specimens, the founder neuromast shows an initial extension of tissue, suggesting that innervation is required only for the later steps of proliferation and differentiation in the budding process. In addition to budding, we have established that innervation is required for other mechanisms of superficial neuromast patterning in the anterior LL. Specifically, superficial neuromasts that are added by the intercalation mechanism no longer form after approximately 7 mm SL in ablated specimens. The superficial supraorbital line, which forms via a previously undescribed cross-placodal mechanism, also fails to form in the absence of innervation. Understanding how the nerve modulates the proliferation of lateral line tissue at a molecular level will be essential to gain further understanding of this potentially instructive nerve-organ relationship.

Previous work suggests that Wnt/beta-catenin signaling is a prime candidate to direct neuromast expansion. Wnt/beta-catenin signaling in the leading edge of migrating posterior LL primordia is the driving force of primordial proliferation and

neuromast formation (reviewed by Dalle Nogare and Chitnis, 2017). At larval stages, the Wnt effector protein Lef1 is expressed in proliferating cells during neuromast budding and this expression is strongly reduced in the absence of innervation (Wada et al., 2013). The underlying mechanism that nerves use to induce superficial neuromast proliferation may thus be direct local activation of Wnt signaling. In support of such a model, Iwasaki et al. (2020) have shown that nerve-derived Rspo2/Wnt signaling is required for proliferation and subsequent budding of some posterior LL superficial neuromasts, as well as for embryonic development of HM1/2 neuromasts.

We have established that innervation is also required for proper growth of anterior LL canal neuromasts. Reporter lines for the Wnt effector protein Lef1 indicate that canal neuromasts strongly upregulate Wnt signaling during canal formation (13-15 mm SL), while the signal is undetectable in mature superficial neuromasts, suggesting that continuous Wnt expression promotes canal neuromast growth (Wada et al., 2014). We also observed that both the size of canal neuromasts and the number of hair cells decreased in the absence of innervation, which is consistent with the decrease in hair cells observed in denervated superficial neuromasts of the posterior LL (Wada et al., 2013). We suggest that future studies should investigate whether nerves in the anterior LL produce a ligand that induces Wnt signaling in both superficial and canal neuromasts.

The innervation-driven development of the lateral line system represents a striking reversal of the typical ‘organ-first’ relationship observed in sensory system development. Generally, nerves are dispensable for development, with sense organs differentiating from their placodes prior to innervation. For example, in the mammalian

inner ear, sensory tissue develops autonomously and later attracts axons through neurotrophic factor secretion (Fritzsch et al., 1997). Similarly, during embryonic posterior LL development, the primordium produces glial cell line-derived neurotrophic factor (GDNF), which is required for the extension of GDNF receptor-expressing nerves (Thomas et al., 2015). Our findings have revealed that the anterior LL undergoes a novel developmental switch from sensory tissue guiding innervation to the requirement of innervation for superficial neuromast proliferation.

What might be the functional purpose of this developmental switch for aquatic vertebrates? First, nerves may represent an efficient mechanism to drive neuromast proliferation as body size increases. Rather than relying on collective primordium migration over increasingly large distances, a single neuron already innervating a neuromast could locally release signaling molecules to stimulate proliferation. Second, a two-step system could allow the lateral line to perform adaptive functions across life stages. For rapidly developing aquatic vertebrates, fast, primordium-driven early development ensures that hatchlings have the sensory function needed for survival. As ontogeny proceeds, slower, cross-placodal proliferation during secondary development may permit diversification of adult neuromast patterns according to species-specific sensory needs (Wada et al., 2013).

While we have provided a detailed account of the late patterning of the anterior LL in zebrafish, comparative studies will be required to address how diverse neuromast patterns are established across species. Our review of previous studies documenting lateral line innervation patterns reveals that the expanded gAV innervation system that we have described for zebrafish is a common teleost feature (Asaoka et al., 2012; 2014;

Münz, 1979; Nakae et al., 2006; 2021; Nakae and Sasaki, 2010; Northcutt et al., 2000). However, a gAV-innervated supraorbital superficial line has not been previously documented, raising the question of whether lateral lines form with mixed placodal origin in other species. Fortunately, the wholemount clearing and immunostaining methods that we have described in this work are applicable to a variety of aquatic vertebrate species. Ultimately, comparisons of not only adult neuromast patterns, but also innervation patterns and developmental mechanisms, will clarify which aspects of late anterior LL development are zebrafish novelties, versus which aspects are conserved features of patterning systems fundamental to aquatic vertebrate development.

The evolution of vertebrate jaws, together with other associated characteristics, enabled increasingly active swimming and thus a broader range of feeding strategies coupled with exploration of new ecological territory. This dramatic expansion of fishes up into the water column has been referred to as the Devonian Nekton Revolution (Klug et al., 2010). Importantly, this phase of vertebrate evolution was accompanied by a radical transformation of the lateral line system, as lateral line networks occupied newly available head territory (Venkataraman, Lopez et al., 2025) . The heads of gnathostomes (jawed vertebrates) are remarkably diverse, allowing for a wide variety of feeding strategies. It is possible that the evolution of the gnathostome head apparatus was accompanied by the evolution of novel developmental mechanisms to pattern sensory structures, including the lateral line system. Our finding of multiple developmental mechanisms patterning lateral lines in a single teleost, the zebrafish, now prompts examination of developmental mechanisms patterning the broad diversity

of lateral lines across widely varied head shapes and structures, including those of basal ray-finned fishes, cartilaginous fishes, and jawless fishes.

Table 1: Zebrafish stages of ontogeny analyzed in this study
Based on Parichy et al., 2009 and our observations

Standard Length (SL)	Approx. time in weeks post-fertilization (wpf)	Phase
3 mm	~1 wpf	Larval
4 mm	~2 wpf	
5 mm	~3 wpf	
6 mm	3-4 wpf	
7 mm	4-5 wpf	Late larval
8 mm	~5 wpf	
9 mm	~5-6 wpf	
10 mm	~5-6 wpf	
11 mm	~6 wpf	Juvenile
12 mm	~6-7 wpf	
15 mm	~7-8 wpf	
22 mm	~11-12 wpf	
>22 mm	>12 wpf	Adult

Table 2: Larval ontogeny of canal and superficial neuromast development

Canal Neuromast	Stage of formation	Mechanism of formation	Where described
SO1*	Larval; 5mm SL	Buds from SO1	Webb and Shirey 2003

			Mechanism described in this study
SO1	Embryonic; 2 dpf	Buds anteriorly from SO2	Iwasaki et al.,2020
SO2	Embryonic; 1.5 dpf	Forms from migrating SO primordium	Iwasaki et al.,2020
SO3	Larval; 4 dpf	Intercalates behind SO2	Iwasaki et al.,2020
IO1	Embryonic; 3 dpf	Intercalates between IO2 and superficial neuromast N	Iwasaki et al.,2020
IO2*	Larval; 6 mm SL	Buds anteriorly from IO2	**This study**
IO2	Embryonic; 1.5 dpf	Forms from migrating IO primordium	Iwasaki et al.,2020
IO3	Larval; 4 dpf	Intercalates between IO3 and O2	Iwasaki et al.,2020
IO3*	Larval; 10 mm SL	Intercalates between IO3 and IO4	**This study**
IO4	Embryonic; 3 dpf	Forms from migrating IO primordium	Iwasaki et al.,2020
IO4*	Larval; 8 mm SL	Buds dorsally from IO4	**This study**
HM1	Embryonic; 3 dpf	Forms in place from HM primordium	Iwasaki et al., 2020

HM2	Embryonic; 3 dpf	Forms in place from HM primordium	Iwasaki et al., 2020
MD5	Larval; 9 mm SL	Intercalates along MD line	**This Study**
MD4	Larval; 8 mm SL	Intercalates along MD line	**This study**
MD3	Larval; 6 mm SL	Intercalates along MD line	Webb and Shirey 2003 **Mechanism described in this study**
MD2	Larval; 5 mm SL	Intercalates along MD line	Webb and Shirey 2003 **Mechanism described in this study**
MD1	Larval; 7 mm SL	Intercalates along MD line	Webb and Shirey 2003 **Mechanism described in this study**
Superficial Neuromast Line	**Stage of formation**	**Mechanism of formation**	**Where described**
IO superficial	Primordium by 3 dpf; first neuromast 4 mm SL/10 dpf	Primordium splits from HM prim	Iwasaki et al.,2020; termed 'maxillary' line **Larval development described this study**
MD superficial	Primordium by 4 dpf; first neuromast 4 mm SL/ 11 dpf	Primordium splits from HM prim	**This study**
SO superficial	First neuromast 7 mm SL	Tissue from IO4 and O2; See Figure 5	**This study**

Opercular Line	First neuromast by 3 dpf	Budding along subopercular bone growth axis	Full ontogeny of main branch described in Wada et al., 2010; dorsal branch described by Iwasaki et al., 2020
Nasal Line	First neuromast by 3 dpf	Medial budding from superficial neuromast N	N described by Iwasaki et al.,2020 **Mechanism described in this study**
Mandibular series	First neuromast by 3 dpf	Medial budding from superficial neuromast MD1	Series noted in Webb and Shirey 2003 **Mechanism described in this study**
Anterior Pit Line	First neuromast by 8 mm SL	Buds dorsally from O1	**This study** Analogous to anterior pit line seen in other ray-finned fishes (Actinopterygii), including the teleost catfish (Northcutt et al., 2000)

CHAPTER FIVE: DISCUSSION AND FUTURE DIRECTIONS

In this dissertation I have used an integrative approach combining palaeontology, developmental biology and comparative anatomy to understand the evolutionary developmental mechanisms underpinning the cranial lateral line system. In chapter 2 (Venkataraman, Lopez et al., 2025), I examined existing hypotheses regarding the macroevolutionary trajectory of lateral lines across the vertebrates and posited a new synthesis, suggesting a major episode of breakdown before the advent of jaws, followed by an episode of gradual reorganization and elaboration of the system with the origin of jawed vertebrates. This synthesis suggests that contrary to previous ideas of evolutionary descent with simplification of a more complex ancestral agnathan pattern in gnathostomes, different lineages of agnathans and gnathostomes elaborated their lateral line systems independently. These differences in patterning are likely related to differences in ecological and behavioral modes. In particular, I posit that the increased occupation of the water column by gnathostomes led to a relocation of the most elaborate parts of the cranial lateral line system to an anterior domain. This reorganization was likely functionally related to the occupation of a pelagic habitat concurrent with an increased focus on the location of patchy, discontinuous sources of nutrition. This was in contrast to a post-orbital elaboration of lateral lines seen in jawless vertebrates optimized for predator avoidance in a benthic habitat. In addition, I also suggested that there is a developmental sensory system hierarchy in the head, with lateral line systems changing in accordance with changes to other sensory systems like eyes or nostrils. In chapter 3 (Venkataraman, McGrory et al., 2025), I examined the relationship between development of the lateral line system and a an important tissue,

the neural crest. Using experimental manipulations and imaging in the zebrafish system, I showed that the neural crest is essential for lateral line development, and that alteration or arrest of neural crest development leads to stereotypical deficits in lateral line formation, particularly in the orbital and mandibular systems. In chapter 4, I identified the patterns and processes by which lateral line development proceeds through zebrafish larval and adult stages. I demonstrated that the lateral line undergoes significant expansion in postlarval stages, and that the expansion is primarily driven by a proliferation of superficial neuromasts. I also showed that superficial neuromast formation at late stages in zebrafish happens through a variety of modalities, including a novel nerve-dependent mechanism in the superficial supraorbital line. Using experimental ablation, I demonstrated that innervation is indispensable for this mechanism. In this final chapter, I will examine the broader implications of my findings to our understanding of different aspects of lateral line evolution and development, and suggest avenues for future work to address key questions generated by this research.

I. The agnathan-gnathostome transition

Crown gnathostomes share a characteristic complex of circumorbital, cheek and lower jaw lines and pit lines. This raises the question of what components of the general gnathostome anterior lateral line network are derived, and which are primitive, i.e. conserved from patterns established in the stem group, as discussed in chapter 2.

Both chondrichthyans and osteichthyans possess circumorbital lines, transverse lines on the cheek continuing on to the lower jaw and a variable number of pit lines on the dorsal surface of the head and on the side of the cheek. Fossil members of these

clades provide a test of the hypothesis that these lines in the two groups are homologous with respect to each other. As reviewed in chapter 2, two traditionally recognized major clades or grades of extinct jawed vertebrates, the acanthodians and placoderms, have been related to the crown group (osteichthyans and chondrichthyans) in various configurations. Current phylogenies place acanthodians on the chondrichthyan stem and placoderms on the gnathostome stem. Acanthodians share with living chondrichthyans a similar lateral line pattern with distinctive features such as orbital and preoperculo-mandibular lines. Available fossil data from the osteichthyan clades, sarcopterygians and actinopterygians, suggest that the general osteichthyan condition is to have orbital, cheek and lower jaw lines. However, how these lines relate to those on placoderms, or which of these lines are conserved from a placoderm condition and which are unique to crown jawed vertebrates remains an open question.

The aim of this section is to identify further steps/goals in this emerging research program.

(1) The 'placoderms'

To determine what parts of the lateral line patterns in jawed vertebrates are unique to the crown clade requires understanding conditions in the sister group to crown gnathostomes. The morphologically diverse placoderms are the first vertebrates with jaws and form a series of plesions (*sensu* Patterson & Rosen, 1977) on the stem of crown jawed vertebrates. While there are several contending hypotheses of placoderm interrelationships, seven well-recognized placoderm groups preserve good evidence of lateral line canals and will be the subject of this discussion. Fig (5-1) shows abstracted representations of the lateral line patterns in these major groups. The sister groups to all

other placoderms are either the antiarchs, the acanthothoracids or the brindabellaspids (Trinajstic and Roelofs, 2019; Dupret et al., 2017 but see also Zhu et al., 2021). More nested are the petalichthyds and sparsely armoured ptyctodonts, and both these groups are sister to the well-known arthrodires. Regardless of placoderm monophyly (King et al., 2017) or paraphyly (Zhu et al., 2013;2016), the maxillates- consisting of taxa like *Entelognathus,* and *Quilinyu* are consistently resolved as sister to all crown jawed vertebrates. Placoderm monophyly would position these taxa outside of the placodermi as the sister group to crown gnathostomes.

All placoderms with the exception of antiarchs and maxillates, preserve evidence of supra and infraorbital lines (seen in Fig 5-1). However, unlike extant gnathostomes, these lines do not connect with each other caudal to the eye. Such disjunct orbital lines in acanthodians and stem osteichthyans suggest that this connection likely evolved independently in chondrichthyans and osteichthyans (Northcutt, 1989). The maxillate placoderm *Entelognathus* is the only placoderm to have lines on the lower jaw (Zhu et al., 2013). This suggests an evolutionary lag- lateral lines did not immediately occupy the newly-evolved jaw territory. However, the possibility that a superficial lower jaw line evolved with the advent of a jaw and became incorporated into the dermal bone only in maxillates must nevertheless be considered. Another feature shared amongst all placoderm groups is very sparse lateral line occupation of the cheek. It bears repeating that the cheek, as a territory for the attachment of jaw closing muscles, is itself a gnathostome novelty. In most groups, the sole line on the lateral cheek surface is a single ‘post-marginal’ line, branching from either the main lateral line or the infraorbital line (marked in red, figure 5-1). Acanthothoracids, arthrodires and maxillates have

independently evolved a supraoral line on the upper jaw. The maxillate supraoral line may be a homologue of the maxillary line seen in extant gnathostomes (and described in detail in Chapter 4). Thus, a complex of lines seen on the cheek (and extending on to the lower jaw) evolved within the gnathostome crown group. A key placoderm characteristic is for several lines on the head to converge toward a central zone in the parietal/postparietal region. Lines converging here include the supraorbitals, a dorsal extension of the infraorbital line (commonly called the central line) and pit lines. This morphology is most clearly represented by the petalichthyds, which have a characteristic x-shaped commissure between supraorbital and central lines (e.g. Castiello and Brazeau, 2018). This pattern of convergence is only visible in some examples of the dorsal pit lines of crown gnathostomes, suggesting that there was a lateral shift of the orbital lines with the advent of the gnathostome crown.

Resolving placoderm phylogeny will have important implications for our understanding of the assembly of crown gnathostome lateral line characters. For example, antiarchs like *Bothriolepis* possesses fewer lines that other placoderm lineages (Graham-Smith and Parrington, 1978; see Fig 2-5), and characteristically do not have clear evidence of a supraorbital line, similar to the condition in osteostracans (Janvier, 1974). If placoderms are paraphyletic (Brazeau and Friedman, 2015) and antiarchs are resolved as sister to all other jawed vertebrates, antiarchs may indeed retain an ancestral condition shared with jawless osteostracans, with a supraorbital line being a novelty that evolved closer to the crown in other placoderm lineages. If placoderms are monophyletic however (King et al., 2017), antiarchs may represent a

secondary simplification of a more complex lateral line pattern related to their extremely dorsalized eyes (which provide little space for supraorbital lines).

A second question is the relationship of (sparse) cheek lines on placoderms to those in crown gnathostomes- are the supraoral and marginal lines in placoderms related the preopercular or other cheek lines in crown gnathostomes? Resolution of this question requires evaluating available criteria for homology including connectivity (or innervation). While most placoderms don't preserve detailed evidence of innervation patterns, exceptional specimens like *Romundina* (Dupret et al., 2017) or *Brindabellaspis* (Zhu et al., 2021) do. Combined with modern high-resolution imaging techniques, innervation patterns in these fossils can be compared to those in extant jawed vertebrates.

Finally, the relationship between morphology and function in placoderms is ripe for exploration. Placoderms are morphologically and ecologically diverse, spanning multiple body size ranges and ecological habitats, from the benthos or nearshore marine environments to the open ocean. Functional analyses of jaw morphology also suggest they had varied diets, ranging from possibly phytophagous antiarchs (Lebedev et al., 2022) to the macropredatory arthrodires (Anderson and Westneat, 2007). A key question is whether lateral line morphologies were conserved in groups spanning these different regimes (suggesting some underlying developmental constraint), or whether they varied based on diet and habitat. My preliminary examination of lateral line patterns across the entire group –as seen in figure 5-1– suggests the former but a systematic examination is warranted. For example, large macropredatory arthrodires like

Dunkleosteus do not show any unique profusion of rostral lateral lines related to their inferred predatory behaviors (Engelman, 2024).

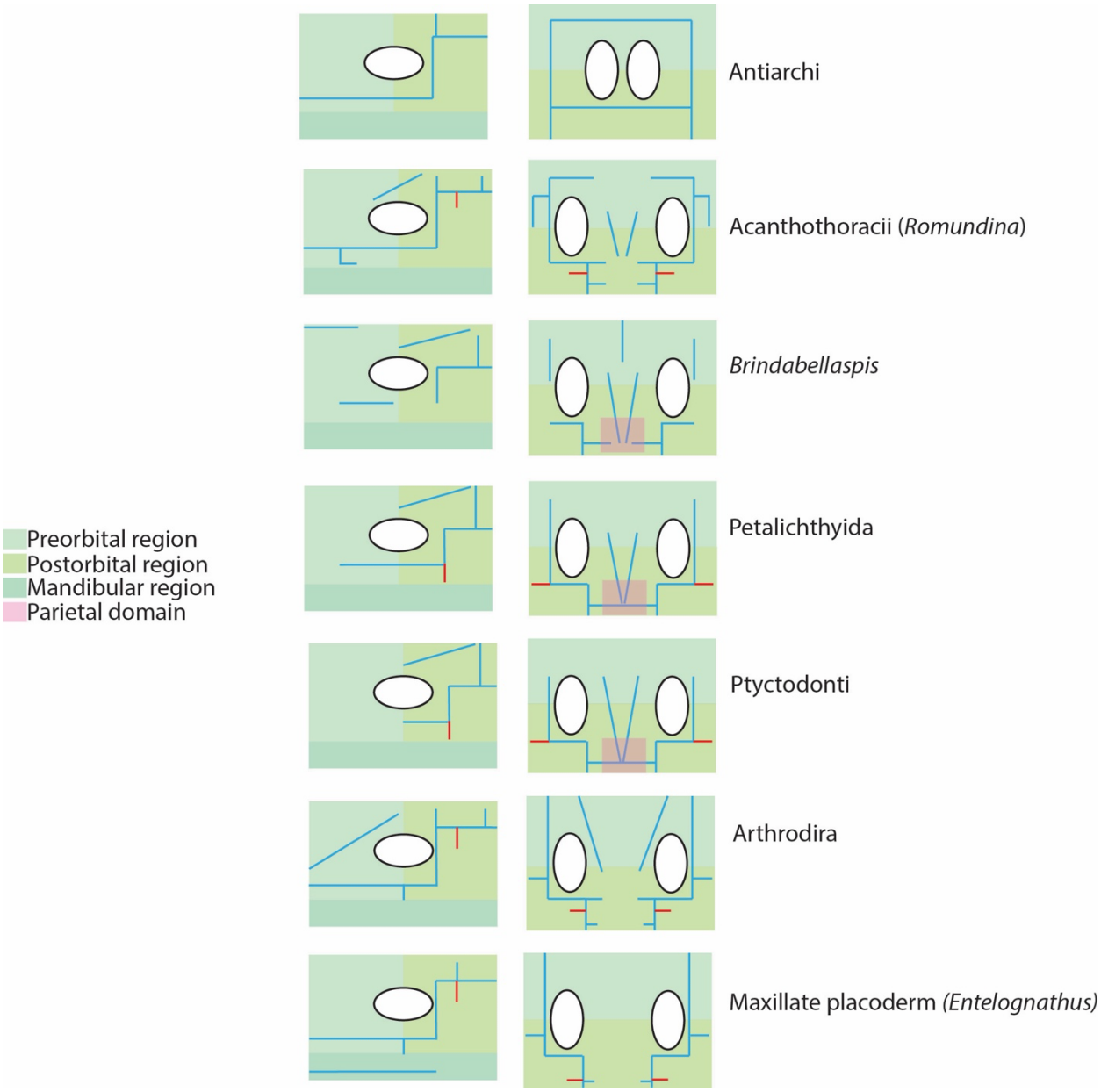

Figure 5-1: generalized morphology of lateral line patterns in major placoderm groups

Figures adapted from Denison (1978) and (Zhu et al., 2013) showing lateral (left) and dorsal (right) views. Different colours indicate preorbital, postorbital and mandibular domains. Lateral line grooves indicated by blue lines except for the supraoral line which is in red. Parietal domain with converging grooves indicated by magenta box.

(2) The agnathans

Understanding the relationship of lateral lines between jawless and jawed groups presents a much greater challenge owing to the great anatomical gulf between these two groups. Gnathostome evolution comprised not only the advent of a jaw, but also other major morphological shifts - from a single to split nostrils and the formation of a new cheek territory, to name a few. Consequently, the territory occupied by lateral lines underwent a major change, prompting the question of how lateral lines were modified accordingly. Living jawless fishes comprise the lampreys and hagfish. Of these, the former have a discontinuous distribution of superficially located neuromast lines (Gelman et al., 2008; Marinelli and Strenger, 1954). Eptatretid hagfishes have a possible homologue of lateral lines (Braun and Northcutt, 1997). However, there is no data on the peripheral innervation of these systems, and hypotheses regarding their homology with gnathostome lateral line components remain untested. Living cylcostomes are however phylogenetically remote from jawed vetebrates with a plethora of fossil forms separating the two groups (Miyashita et al., 2019). Anaspids are inferred to be stem cyclostomes, with a variety of other jawless fishes positioned on the gnathtostome stem. Osteostracans branch off as the jawless fishes sister to the first jawed vertebrates. Osteostracans have a simple, sparse and superficial distribution of lateral lines. They show no evidence of a supraorbital line, and have a short, discontinuous infraorbital line. The rest of the system consists of small transverse lines behind the eyes, and a ventral line close to the base of their head shield (Stensiö et al., 1932; Janvier, 1985). Despite the diversity of osteostracan body shapes and sizes,

ranging from horseshoe shaped *Ateleaspis* which had a complement of paired pectoral fins (Ritchie, 1967) to the smaller, barrel shaped *Trematapsis* which lacked paired fins (Patten, 1902), this pattern of lateral lines is broadly conserved across the group (Stensiö et al., 1932; Janvier, 1996). This lateral line pattern differs drastically from other agnathan groups, in particular, the heterostracans and galeaspids which have elaborate lateral line networks embedded deep in the dermal skeleton (Fig 2-5). In both these groups, the lateral line system consists of a reticulating network on the head shield, conspicuously in a postorbital domain, in contrast to the gnathostome condition. As detailed in chapter 2, this suggests a shift from a postorbital to a preorbital domain of lateral line elaboration, with a radical breakdown and rebuilding of the system. Osteostracans represent an episode of this breakdown and remodelling, with a secondary simplification of their lateral lines. As previously hypothesized, their elaborate sensory fields connected to the vestibular system may have compensated for reduced mechanosensation from lateral lines (Miyashita et al., 2025).

To understand how lateral line systems were transformed across the agnathan-gnathostome transition first requires evaluating which lines are homologous between cyclostomes and jawless and jawed members of the gnathostome total group. The primary step in this direction demands a detailed, comparative description of lateral line patterns in agnathans preserving evidence of lateral lines. Osteostracans, galeaspids and heterostracans comprise approximately 200 (Sansom, 2009), 70 (Zhu and Gai, 2007) and 300 (Randle et al., 2022) species described so far (blue wedges, fig 5-2). There has however been no examination of their lateral lines employing a comparative phylogenetic framework to understand intra-group lateral line diversity. For example, as

mentioned previously, the osteostracans span a wide variety of body shapes, with different morphologies of the sensory fields. It remains unclear (given that the sensory fields may compensate for reduced lateral lines) whether changes in the morphology of these fields correlate with changes in the morphology of lateral line patterns. Further, osteostracans and galeaspids preserve good evidence of cranial nerve tracts. New high resolution imaging techniques have the potential to reveal unprecedented morphological detail in these taxa (Gai et al., 2011; Miyashita et al., 2025), and thus reveal peripheral innervation of lateral line components. These data could be used in conjunction with neuroanatomical studies of extant gnathostomes and agnathans to establish homologies between different parts of the lateral line network using the criterion of connectivity. Current phylogenies also recover anaspids to be on the cyclostome stem (Miyashita et al., 2019). However, the anaspid fossil record, especially with regard to lateral line data, is sparse. Future studies on this group, hopefully aided by more fossil discovery, would aid our understanding of the assembly of the living agnathan lateral line pattern. Finally, developmental data from agnathans will be necessary to understand the placodal homologies of lateral lines between agnathans and gnathostomes, and these directions are discussed below.

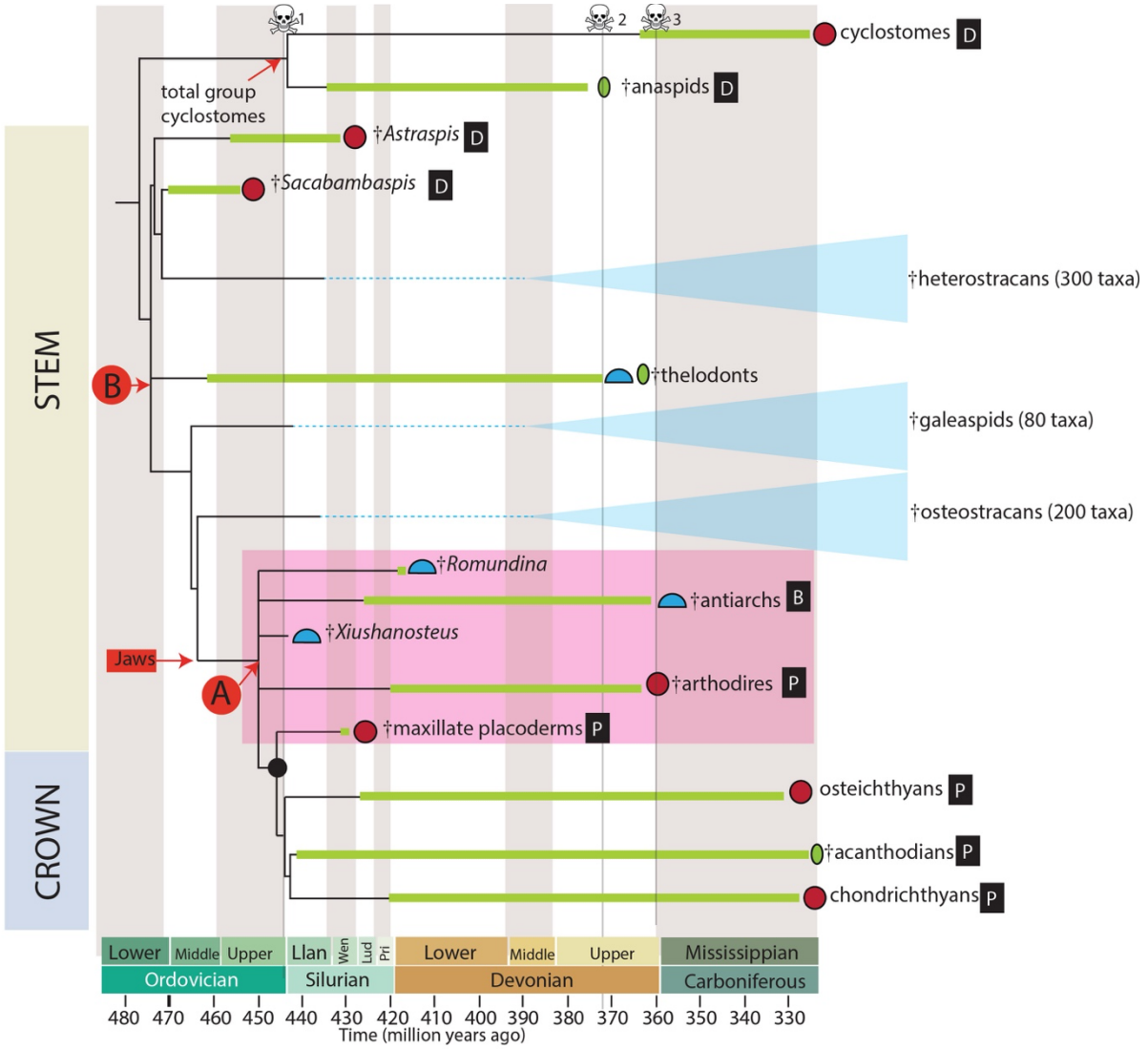

Figure 5-2: Vertebrate phylogeny indicating major clades requiring examination of lateral line characters (blue wedges) showing numbers of described taxa, respectively. For other symbols, refer to figure 2-5.

II. The water-land transition and lateral line loss

(1) Lissamphibia

The previous section dealt with the assembly of lateral line patterns leading to the gnathostome crown. Here, I discuss the prime example of reduction and loss in the system–within tetrapods. Extant tetrapods include amniotes and the lissamphibia (salamanders, frogs and caecilians). No extant amniotes have any lateral lines but amphibians show a myriad of conditions. Lissamphibians occupy a wide variety of ecological habitats and display a range of reproductive modes, from indirect to direct developers and completely aquatic to terrestrial inhabitants. Most lissamphibians however have aquatic larvae, and go through metamorphosis to inhabit a quasi-terrestrial or entirely aquatic habitat (Schoch and Witzmann, 2024). In all cases of indirect developers, larval stages have lateral lines present as a complex of superficial neuromasts (Northcutt et al., 1994; Hetherington and Wake, 1979; Quinzio and Fabrezi, 2014). Those that remain in aquatic habitats through the adult stages, like the cryptobranchid salamanders or aquatic frogs like *Xenopus* retain superficial lateral lines throughout their lives, while those that have terrestrial adult habits lose lateral lines at metamorphosis (Roth et al., 1992). Entirely aquatic direct developers like the Suriname toad *Pipa pipa* also retain lateral lines through adulthood (Perez-Rojas and Jerez, 2022), while direct developing terrestrial amphibians, like the frog *Eleuthrodactylus* or plethodontid salamanders never develop lateral lines (Roth et al., 1992). Thus, there seems to be a direct correlation between aquatic habitats and the presence of lateral

lines within the living amphibia. Notably, there is no aquatic amphibian without either an electrosensory or mechanosensory lateral line system.

Most phylogenies (Ruta and Coates, 2007; Pardo et al., 2017) suggest the crown group lissamphibians as nested within a large, diverse fossil clade called the Temnospondylii. Recent fossil discoveries (Kligman et al., 2023) have also confirmed that all three extant clades of lissamphibians branch off from within the temnospondyl sub-group called the dissorophoids. An examination of the temnospondyl fossil record (fig 5-3, adapted from Schoch, 2013) suggests that there was a patchy distribution of lateral lines amongst different groups, leading to the question of whether crown lissamphibian lateral lines represent a conserved ancestral condition, or a derived feature of the clade. A key question in this regard is the evolution of metamorphosis within the temnospondyls. Schoch and Witzmann (2024) argue that temnospondyl groups evolved different degrees of metamorphosis, but almost all had aquatic larval forms. This suggests that all temnospondyls likely possessed lateral lines in larval stages, and lost them to different degrees with the advent of terrestrialization. The dendrerpetontids (*Balanerpeton* and *Dendrerpeton*) have been perceived as terrestrial taxa in the adult stages, and did not have any semblance of lateral lines (Milner and Sequeira, 1993; Holmes et al., 1998). Other groups like the diminutive dvinosaurs or the large, crocodile-like stereospondyls (represented in the figure by *Archegosaurus, Trematosaurus* and *Mastodonsaurus*) had aquatic adult forms with good evidence of lateral lines preserved as grooves on the dermal skeleton (Moodie, 1908; Schoch, 2019; Witzmann, 2005; Schoch and Witzmann, 2024). The presence of lateral lines on *Archegosaurus* is historically important, since this character was used by Owen to

describe *Archegosaurus* as a key ‘transitional form’ between fishes and tetrapods (Owen, 1859) However, the group forming the sister to crown lissamphibians, the amphibamids, have no evidence of lateral lines preserved. Amphibamids, which are generally small, have been described as terrestrial insectivores with well-documented aquatic larval stages bearing external gills (Schoch, 2022). While evidence of lateral lines in these larval specimens remains missing, this is likely a consequence of superficially placed neuromasts, which would not preserve an osteogenic signature. Different degrees of neoteny have been documented in the dissorophoids (the larger group containing amphibamids), such as the case of the aquatic branchiosaurs, which retained larval characteristics into adulthood (Sanchez et al 2010). In essence the closest fossil relatives of extant lissamphibians have been documented as having a terrestrial adult condition, and it is likely that extant lissamphibians re-evolved persistent aquatic habits in some cases, while retaining larval lateral lines through adulthood as exemplified in some lineages such as *Xenopus*. Nevertheless, absence of evidence of lateral lines in fossil skulls is not evidence of absence of lateral lines altogether. It is possible that the groups that have no osteological remnants of lateral lines may have simply shifted them to a superficial location (akin to extant lissamphibians), so care must be taken in using the absence of lateral lines as definitive evidence for a terrestrial habitat. The presence or absence of lateral lines must be used in conjunction with other traits, such as the presence of external gills or limb structure to infer aquatic vs terrestrial habitats.

A major gap in our knowledge of lissamphibian lateral lines remains in the case of the caecilians. These enigmatic amphibians, least diverse of the living clades, span the

gamut from terrestrial, fossorial forms to entirely aquatic taxa, with either direct or indirect developing larvae (Wake, 1992). Previous studies have documented that indirect developing taxa with terrestrial adults (such as the Ichthyophiidae (Hetherington & Wake, 1979) have larval lateral lines lost at metamorphosis. Vivaparous, entirely aquatic caecilians of the Typhlonecticdae paradoxically never develop neuromasts, but retain electroreceptive ampullary organs throughout adulthood, making them unique amongst all gnathostomes (Roth et al., 1992). The study of caecilian lateral line development has been primarily hampered by their sparse, uniquely tropical distribution, difficulties in culturing all but a couple of species under laboratory conditions, and an exceptionally sparse fossil record. Further descriptions of lateral lines within this group are warranted to explain the relationship between lateral lines, ecology and developmental modes in this enigmatic group of lissamphibians.

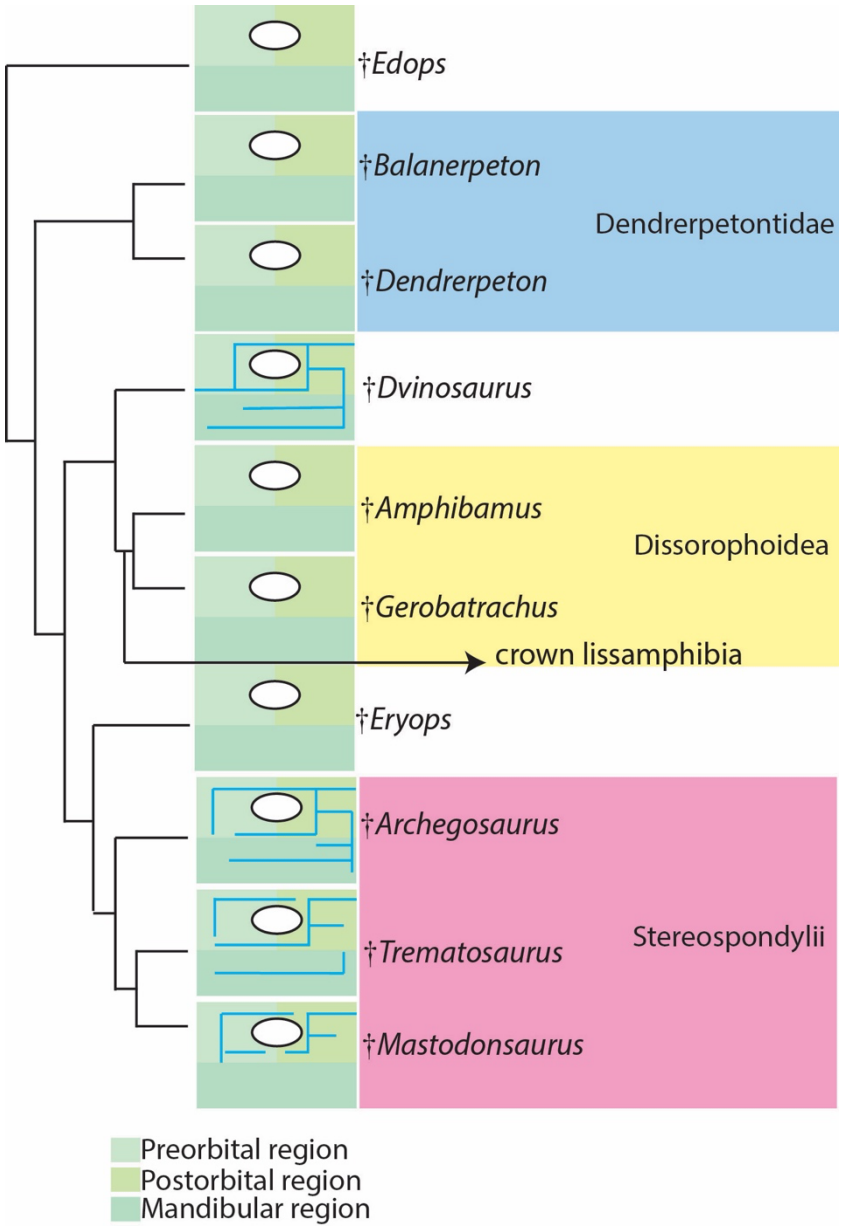

Figure 5-3: Lateral line patterns in temnospondyls

General morphology of the head in lateral view, anterior to the left. Lateral line grooves indicated by solid blue lines. Phylogeny adapted from Schoch 2013. Coloured boxes indicate major groups.

(2) Amniotes

No extant amniotes have any semblance of lateral lines at any point in ontogeny. This is likely related to the evolution of a terrestrial habitat (where lateral lines are of no use), internal fertilization and a cleidoic egg, which avoided the necessity for aquatic larval forms. Extant amniotes, consequently, are all direct developers. The immediate sister groups to crown amniotes, such as the diadectomorphs and seymouriamorphs also do not display any evidence of having lateral lines and have been reconstructed as being primarily terrestrial (Bazzana et al., 2020). Some analyses (Ruta & Coates, 2007) have suggested that the anthracosaurs which have well-developed lateral line sulci (Holmes 1984) are nested within the amniote total group, though other studies have moved them outside (Pardo et al., 2007). Phylogenetic analyses suggest that the lepospondylii, a diverse group of fossil tetrapods which had several aquatic forms with some lateral line grooves, such as the aistopods or the nectrideans (Pardo et al., 2007), are closely related to the amniotes. Consequently, it remains unclear where on the amniote stem lateral lines were completely lost. Some seymouriamorphs (closely related to crown group amniotes) have been inferred to have lateral line systems at least in larval stages, as exemplified by *Discosauriscus* (Klembara, 1994). Lateral lines are definitely lost in the cladde comprising the diadectomorphs and crown group amniotes. The issue is further compounded by lack of evidence as to where on the amniote stem the cleidoic egg evolved. Our earliest evidence of cleidoic eggs are the hard-shelled eggs of dinosaurs (Reisz et al., 2012), well into the amniote crown, and therefor uninformative as to conditions on the stem. The resolution to the problem will likely come from sites where extraordinary conditions permit the fossilization of soft-tissue structures, such as leathery, non-mineralized cleidoic eggs and fossils providing ontogenetic data about stem-amniotes.

(3) Stem-tetrapods

Tetrapods are nested within a clade of the sarcopterygians called the tetrapodomorpha, which includes lobe-finned fishes like *Eusthenopteron* and *Osteolepis* (Ahlberg and Johanson, 1998). Analysis of conditions outside the tetrapod crown, as shown in Fig 5-4, adapted from (Pardo et al., 2017) indicates that the plesiomorphic condition for stem tetrapods was to have a complex of lateral line canals embedded within the dermis, opening out to the surface through pores (e.g. *Panderichthys*), shared with tetrapodomorph fishes like *Osteolepis* (Westoll, 1936). However, there appears to be a gradual trend of change from canals to a mixed condition of canals and open grooves, as exemplified by taxa like *Acanthostega* (Clack, 2002) or *Whatcheeria* (Lombard and Bolt, 1995). Another major trend is the discontinuity of the supraorbital lines. This may be related to flattening of the skull, expansion of orbit size and reduction in inter-orbital space (MacIver et al., 2017). A potential behavioral or ecological cause for this reduction might also be that with the expansion of visual range, the eyes and top of the head were habitually above the water meniscus, where lateral lines would not be useful. Possibly in support of this, the mandibular canal is retained most consistently amongst stem tetrapods, likely again because the lower jaw and bottom of the skull were below the water surface. However, it must be noted that the very presence of (even some) lateral lines indicates that there was no necessary trend ‘towards’ terrestrialization, and these taxa were at least for the most part aquatic. Once again, other anatomical characters like the presence of gill skeletons in *Acanthostega* lend support to the idea that these sarcopterygians were not incipiently heading towards a terrestrial habitat (Coates and Clack, 1991), though they were likely spending increasing time in the shallows.

While there is no evident trend of lateral line loss with the advent of the tetrapod crown, there is nevertheless a change from enclosed canals to open grooves. In most temnospondyls, for example (fig 5-3), lateral lines are open grooves. The functional or ecological consequences of this shift remain unclear. Physiologically, superficial (or exposed) neuromasts function as velocity detectors that detect laminar flow and local water movement, particularly in standing or slow moving water, while enclosed canal neuromasts serve to sense pressure gradients and acceleration caused by other moving bodies or fast currents (Mogdans, 2019). It remains to be tested whether this shift from enclosed canals to open grooves within the tetrapod crown is related to a habitat shift towards still or slower moving water. However, it is unclear if neuromasts in open grooves are similar in physiology to completely superficial neuromasts (such as those seen in living lissamphibians). A similar trend is seen in lungfish, where two of the three living lineages exhibit a shift towards open grooves from an ancestral condition of enclosed lateral lines (Webb and Northcutt, 1997). Mathematical modelling of lateral line parameters including canal diameter, network topology and depth of the groove or canal from the dermal surface could be used to understand the different flow regimes that different types of lateral lines were optimized to sense. Such modelling has been done so far only on the canals of extant teleost fishes (Scott et al., 2023). Northcutt (1997) proposed that the shift from enclosed canals to open grooves happened as a result of a heterochronic shift. All neuromasts begin superficially on the dermis, and those destined to be canal neuromasts sink into ridges and get enclosed in bony or soft tissue canals. Northcutt (1997) suggested that at different points in the phylogeny, this ontogenetic trajectory was arrested at different stages, producing either superficial or enclosed

neuromasts. However, this hypothesis requires further testing, since data from zebrafish shown in chapter 4 indicate that superficial and canal neuromasts are entirely distinct both in morphology and in their ontogenies. In essence, neuromasts destined to become canal neuromasts are distinct at all stages (even when they are initially superficial), and do not resemble actual superficial neuromasts at any point in development.

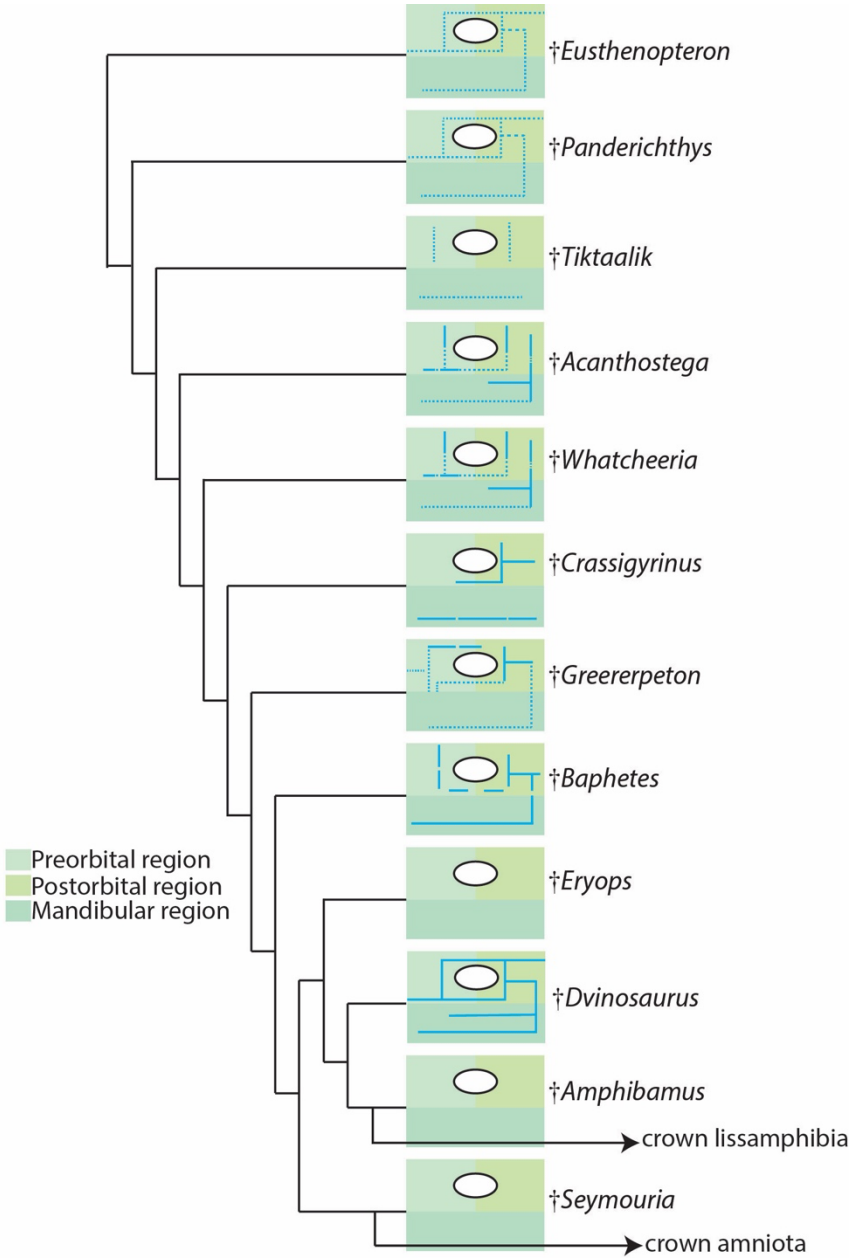

Figure 5-4: Lateral lines in stem-tetrapods

Fig 5-4 cont. Phylogeny adapted from Pardo et al., (2017). Heads shown in lateral view, anterior to the left, head regions as in fig 5-1. Enclosed lateral line canals indicated by dotted blue lines, open lateral line grooves indicated by solid blue lines.

In essence, there is no clear trend of lateral line loss or reduction within the tetrapod stem, though there is a trend towards open grooves rather than enclosed canals. Future systematic treatment of lateral line morphologies in this group is key to understanding the ecological and behavioral shifts that were happening within the tetrapod stem in the Devonian and Carboniferous. However, most morphological studies of stem-tetrapods are focused on identification of crown tetrapod characters associated with terrestrialization (hence the focus on, for example, limb or girdle evolution) and not on characteristics reflecting the more aquatic habits of this clearly aquatic group.

III. Lateral lines and the dermoskeleton

Chapter 2 briefly discussed another area ripe for exploration: the relationship between lateral lines and the surrounding dermal skeleton. Dermal skeletons vary widely in histological structure between different vertebrate groups. Recent studies (Keating and Donoghue, 2016) have substantiated the idea that the vertebrate dermal skeleton is composed of distinct, osteogenic and odontogenic layers producing bones or dentine, respectively (Smith & Hall, 1990). The diversity of vertebrate dermal skeletons is seen as different combinations of these modules in different groups (reviewed in Rocha et al., 2020). For example, it has been suggested that chondrichthyans reduced the entire osteogenic layer, while retaining an odontogenic component in their micromeric skeletons (Gillis et al., 2017). These data are founded on palaeontological evidence,

which indicates that a macromeric skeleton was the ancestral condition in gnathostomes (Friedman & Brazeau, 2013). However, the relationship between lateral lines and these various dermoskeletal modules remains unclear. Lateral lines vary regarding where in the dermal skeleton they are found; for example, heterostracan and galeaspid lateral lines are found in deep canals, while osteostracan lines are in shallow grooves (Janvier, 1996). Placoderms show a combination of these conditions, with lateral line grooves in most cases, but partially enclosed canals in some groups like the ptyctodonts. The functional and behavioural implications of lateral line position remain broadly unstudied. Further, there are no clear data on which part of the dermal skeleton (or which layer) lateral lines run through in different groups. This is especially pertinent in some groups that have complex, multi-layered dermal skeletons. For example, osteostracans and some sarcopterygians convergently evolved an elaborate system of pore canals in the dermis. These pore canals were once thought to be part of an electrosensory or mechanosensory system (Thomson, 1975; Meinke, 1984), but this hypothesis has since been questioned (Bemis & Northcutt, 1992). However, how lateral line canals connect with (if at all) these elaborated pore canals is not known.

The relationship between lateral lines and dermal skeletons is also interesting from a developmental point of view. As I have shown in chapter 3, in the teleost zebrafish the anterior lateral lines develop in close proximity to, and are at least partially dependent upon, the cranial neural crest. My data corroborate previous findings that neural crest is the source for some of the zebrafish dermal skeleton (Kague et al., 2012). Moreover, I find that in the absence of properly developing neural crest, it is those neuromasts that would normally become embedded in the neural crest-derived

bone that are absent. Parrington (1949), in an attempt to clarify the relationship between lateral lines and dermal bones, posited morphogenetic fields that would influence the course of the lateral lines, with their centers located at the centres of ossification of dermal bones. As demonstrated in chapter 3, the neural crest is now a clear candidate to be the source of such a morphogenetic field. In this case, how else might lateral lines interact with the diversity of dermal skeletons seen throughout vertebrate evolution, which might have some neural crest-derived components? For instance, it has been demonstrated that dentine is almost certainly a neural crest derivative (Rocha et al., 2020; Stundl et al., 2023). The dermal skeletons of fossil vertebrates are often covered in dentinous layers on the head and trunk, suggesting neural crest involvement. Description of the developmental morphology of lateral lines and (neural crest-derived) denticles in chondrichthyans would be a suitable test of the hypothesis that neural crest derived dentine influenced lateral line development. Further, osteichthyans also have characteristic tubes of dermal bone surrounding lateral line canals. It remains unclear, however, if this canal bone is neural crest-derived, and if neural crest and cranial placodes interact in this scenario. A detailed histological analysis of the dermal skeletons surrounding lateral lines in different groups would begin to shed light on this issue.

IV. Integrating development

All aspects of this dissertation can be aided by the integration of comparative embryological and developmental data, and further study of the fossil record would in

turn complement our understanding of vertebrate sensory system development. Here, I consider three primary future directions: an embryological interpretation of the agnathan-gnathostome lateral line transition, the placodal origin of conserved and novel lateral lines within gnathostomes, and the molecular underpinnings of anterior lateral line development in teleosts.

(1) Gnathostome placodes and lateral lines

Despite the general conservation of gnathostome lateral line patterns described above, there are nevertheless taxon-specific differences in the morphology of the network in different living jawed vertebrates. For example, there are more lines in chondrichthyans than in osteichthyans (see Fig 2-1), and there are lines that occupy the elongate rostra of taxa like gars, sturgeons or sawsharks in different manners (Fig 2-2). However, all the lateral lines derive from cranial neurogenic placodes. A key question then is how placodal development was modified in different groups to produce the diversity of lines seen in living forms. To answer this question, one must first clarify the relationship between individual placodes and specific lateral line components across diverse taxa.

Northcutt (1989) hypothesized that the ancestral gnathostome lateral line system was derived from six placodes, which gave rise to all the lines on different heads (Fig 2-4). In various lineages, placodes were either lost or may have fused, producing the variety of lines we see in extant taxa. However, this idea has not been comprehensively evaluated across vertebrate diversity. For example, Raible and Kruse (2000) showed that the zebrafish lateral line system is derived from anterior and posterior placodal domains (with the anterior further splitting into anterodorsal and anteroventral portions). However, it is important to note that the six placodes were only part of a hypothetical

ancestor, and not found specifically in any living vertebrate taxon. Further, Northcutt used innervation as a criterion to determine placodal development. For example, Northcutt (1989) suggest that a middle pit-line in gnathostomes was innervated by a middle lateral line nerve and so must have come from a middle placode. However, in Chapter 4 I demonstrated that nerves emanating from a placode may innervate neuromasts coming from a wholly different placode, so this criterion is not always reliable.

A detailed analysis of placode-line relationships across different groups is necessary to determine how many placodes exist in gnathostomes and how they may be related between different lineages. An ideal approach to pursue this question is to trace the development of placodes to their respective lateral line branches. This can be achieved by lineage tracing using vital dyes like DiI to inject the putative placodal regions (identified by immunolabelling) and identifying remnant components of the dye in different lateral line canals or grooves later in ontogeny (Gillis et al. 2012). While most work on lateral line development has focused on osteichthyans (primarily teleosts like the zebrafish), little attention has been paid to the other major lineage of jawed vertebrates - cartilaginous fishes. Chondrichthyans possess well-developed lateral line systems and vary vastly in morphology, ecology, diet and habitat, making them an ideal candidate for studying the evolution of lateral line development. A key taxon that proves useful for these studies is the little skate *Leucoraja erinacea*. Skates are oviparous, providing easy access to the developing embryo, and can be easily cultured under laboratory conditions (Gillis et al. 2022).

As a first step towards such analysis, I used immunolabelling in skates against the transcription factor Sox2 (expressed in neuromast support cells in teleost lateral lines; Hernández et al., 2007) at different stages, to describe overall embryonic development of the lateral lines (Fig 5-5). To trace the origin of lines to placodes, and as a proof-of-concept, I injected the anterodorsal placode in skate embryos at stage 27 with DiI (Gillis et al., 2022) (Fig 5-6, A, A'). The embryos were then allowed to grow until stage 32 (Maxwell et al., 2008) (by which time most lateral line branches are well-developed) and then sectioned (Fig 5-6 B,B',B''). I was able to identify the presence of DiI in a portion of the supraorbital canal, demonstrating that the SO canal in skates is derived from the anterodorsal placode, making it homologous with the SO canal in teleosts like zebrafish. Future studies involving injection of other placodal regions and tracing them to their respective lines, especially when done across a variety of representative taxa, would help identify homologous branches of the line across species, and help reconstruct the ancestral gnathostome lateral line condition.

Such an approach can also help shed light on lineage-specific novelties. For example, skates and rays possess unique 'pleural' and 'scapular' lines on the pectoral fin. This is the only recorded instance of a lateral line being present on a pectoral appendage in any vertebrate (Ewart & Mitchell, 1895). While scapular lines clearly branch from the main trunk lateral line (see Fig 5-6), the homology of the pleural line remains unclear. Is it a branch of one of the existing lateral lines in other vertebrates, or is it a de-novo condensation of an entirely new placode? Preliminary immunolabeling (with the marker Sox2) has indicated the presence of an as yet undocumented placode like region on the mandibular arch. Future DiI injections into this placodal domain would

help to establish if this is indeed a new placode, and if it gives rise to the novel pleural line. An ideal experiment would be to do DiI injections in skates in parallel with a tractable, closely related group like sharks– for example, the catshark *Scyliorhinus*, to determine if the pleural line is a novelty in skates arising from a new placode versus a modification of an existing line in chondrichthyans.

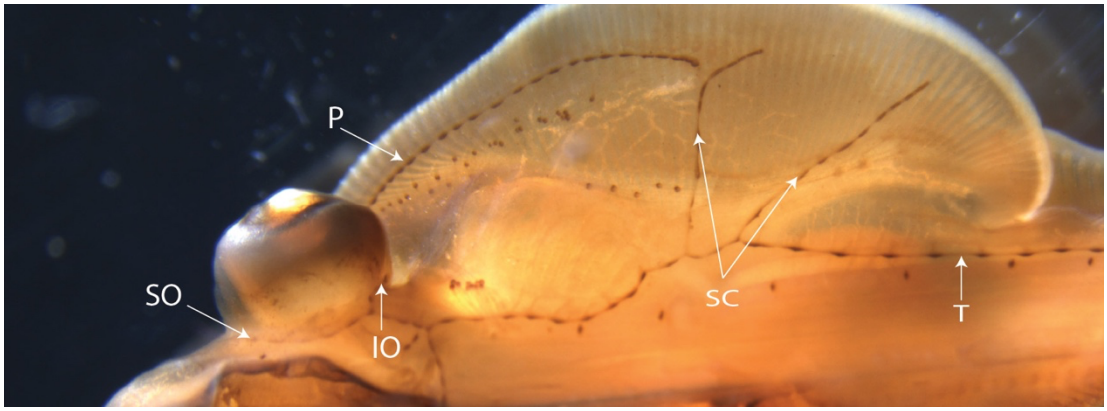

Figure 5-5: Sox-2 immunolabelling of a stage 32 skate showing major lateral line branches

Dorsal view, anterior to the left. Abbreviations: SO- supraorbital, P-pleural, IO- infraorbital, SC- scapular, T- main trunk line. Stain utilized Genetex Sox2 rabbit polyclonal antibody (GTX 12447) and was developed using DAB post amplification using Vectastain Elite avidin-biotin reaction (PK-6103)

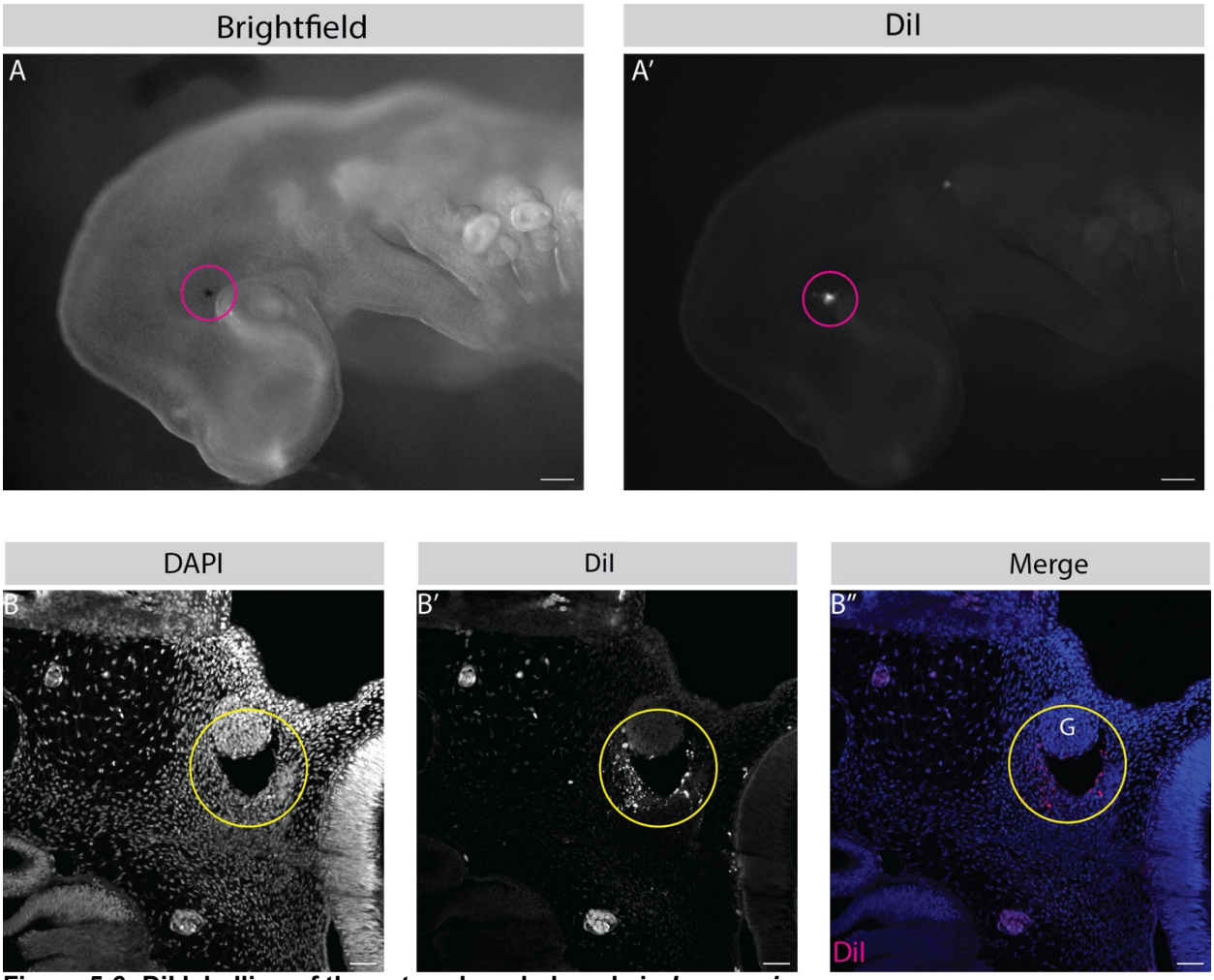

Figure 5-6: DiI labelling of the anterodorsal placode in *Leucoraja*

Fig 5-6 cont. A, A' showing brightfield and DiI views respectively of DiI injected above the eye in a st.27 skate (magenta circle), anterior to the left. B, B', B'' showing DAPI, DiI and merged views of the same specimen, sectioned at st.32. Imaged on an LSM 700 confocal microscope. Supraorbital canal indicated by yellow circle. G- anterodorsal ganglion. B' and B'' indicate presence of DiI in the supraorbital canal, proving it is derived from the anterodorsal placode.

(2) The agnathan-gnathostome transition: developmental insights

As detailed previously, a major gap in our understanding is how the lateral line system was modified with the advent of jaws. A key piece of this puzzle is testing the (taxic) homologies between living agnathans and gnathostomes. Section IV (2) described the identification of a conserved pattern of embryonic placodal development across gnathostomes. The methods used to establish this conservation (including lineage tracing and immunolabelling) could similarly be used on representative extant agnathans (ideally, lampreys). This approach could identify homologies between lateral lines in jawless and jawed groups (using a developmental criterion) and reveal how placodal development was altered across a major anatomical transformation, i.e., the advent of jaws and the concomitant re-organization of lateral line patterns (as discussed in chapter 2). As an example, we can consider the mandibular line. It has been noted that the maxillate placoderm *Entelognathus* is the only placoderm with a mandibular line, and, in living gnathostomes, the mandibular line is derived from an anteroventral placode (demonstrated for example in zebrafish, see Chapter 4) and innervated by an anteroventral nerve. Understanding the distribution and development of placodes in extant agnathans would help us to understand if an existing agnathan anteroventral placode was modified to form the gnathostome mandibular line, versus whether the gnathostome mandibular line was formed by the de-novo condensation of a new placode.

Chapter 2 details the significant shift of lateral lines from a postorbital to a preorbital cranial domain across the agnathan/gnathostome transition. A major component of craniofacial development, both in agnathans and gnathostomes is the cranial neural crest. The neural crest forms the frontonasal region between the nostrils and the cheek in gnathostomes. The pattern of neural crest migration differs markedly between agnathans and gnathostomes (Kuratani 2005). In Chapter 3 I have demonstrated that the neural crest is necessary for lateral line development in gnathostomes. However, it is not known if this relationship also exists in agnathans like lampreys. Integrating findings from chapters 2 and 3, with studies on the differences in cranial neural crest migration between agnathans and gnathostomes, would shed light on whether this post-pre orbital lateral line shift was associated with a change in neural crest migration, mediated via the creation of new neural crest territory - such as the inter-orbital, or inter-nasal spaces, or the cheek. It is consequently possible that the change in lateral line patterns that occurred in gnathostomes was a result of new anatomical territory enabling modified neural crest migration patterns, which in turn influenced lateral line development.

(3) Anterior lateral lines in teleosts: a more thorough molecular picture

Chapters 3 and 4, which focus on the development and innervation of lateral lines in the zebrafish system, each lead to several avenues for future study. First, Chapter 3 demonstrated that the anterior lateral line system is dependent on neural crest tissue for proper morphogenesis, but the specific nature of local molecular (or mechanical) cues underlying this relationship remain unknown. Intensive study of the zebrafish posterior lateral line has demonstrated that the system is patterned via a self-organizing posterior

lateral line primordium (Dalle Nogare and Chitnis, 2017). This primordium expresses mutually exclusive Wnt and FGF signalling domains that divide it into a leading edge with a mesenchymal morphology and a trailing edge with an epithelial morphology. As the primordium migrates, Wnt signaling promotes cell proliferation, and Fgf signaling promotes the formation of the epithelial rosettes that become neuromasts, such that the migrating primordium deposits appropriately spaced neuromasts in its wake. Confocal and lightsheet imaging shown in Chapter 3 have shown that the zebrafish supraorbital primordium is morphologically similar to the posterior lateral line primordium. However, it remains to be investigated if Wnt/FGF domains are operating in this primordium, similar to the trunk, or if anterior lateral line primordia are under the control of other developmental regulatory mechanisms. This is especially interesting given that the migrating posterior lateral line primordium follows a 'track' of the chemokine Cxcl12, which is localized along the horizontal myoseptum of the somitic mesoderm (Haas & Gilmour, 2006). Absence of chemokine expression (in mutant fish; David et al., 2002; Ghysen & Dambly- Chaudiere, 2007) does not affect anterior lateral line development. Thus, even if the supraorbital primordium requires Wnt/FGF expression, similar to the posterior lateral line primordium, then the molecular or mechanical cues this primordium follows around the head will still need to be identified. Pharmacological manipulations, for example using Wnt or FGF inhibitors or agonists, could help ascertain if these signalling pathways are involved in development of the ALL. As discussed in Chapter 3, previous studies have documented a role for FGF signalling in the anterior lateral line, with loss of FGF signaling resulting in an elongate, ridge-like supraorbital primordium (McCarroll and Nechiporuk, 2013). Moreover, a previous study has also shown that R-

spondin2, an activator of Wnt signalling is required for the development of a subset of neuromasts in the head (Iwasaki et al., 2020). Future studies using the above-mentioned techniques can begin to dissect which parts of the cranial lateral line system require which signalling pathways for proper development.

A related question in zebrafish lateral line development (both anterior and posterior) is what leads to the initiation of primordium migration. In mutants that lack chemokine expression, the posterior lateral line primordium nevertheless begins migrating for a short period before stalling (Haas and Gilmour, 2006). Mediated by the Wnt/FGF axis, the receptors Cxcr4 and Cxcr7 set up a sink for the chemokine, driving its migration through most of the trunk, but how the primordium begins to migrate onto the trunk in the first place remains to be seen. Similarly, in the absence of neural crest cells, the supraorbital primordium nevertheless begins migration, suggesting that there may be molecular signals to initiate migration derived from non-neural crest tissues.

Another possible avenue of research is the development of the infraorbital lateral line system in zebrafish. In Chapter 3 I have demonstrated that the infraorbital primordium is morphologically distinct from the supraorbital and posterior lateral line primordia, developing as an elongated ridge of cells that then condenses into distinct neuromasts, rather than as a migrating cluster of cells that deposits neuromasts in its wake. The elongating ridge mechanism used by the IO line in zebrafish appears similar to the mechanism of lateral line development used in other taxa, including elasmobranchs and the cranial lines of amphibians (Johnson, 1917; Winklbauer & Hausen, 1989). Currently, there are no data on the molecular underpinnings of the elongation and condensation mechanism of lateral line development in any system.

Future studies of gene expression and primordium migration in mutant zebrafish with aberrant Wnt/FGF signalling (such as the *apc* mutant, see Aman and Piotrowski 2008) would serve to inform the developmental mechanisms underpinning the infraorbital line. These data can be combined with assays of gene expression and pharmacological inhibition (Brooks et al., 2024) in other taxa that have elongating lateral lines to identify the molecular underpinnings of these lines, and test the hypothesis that zebrafish are redeploying developmental mechanisms seen in other vertebrates. This could further be complemented by computational methods to model the infraorbital line and its relationship to signalling factors as previously performed for the PLL (Dalle Nogare & Chitnis, 2017)

Chapter 4 has identified innervation patterns and novel mechanisms of neuromast development in larval stages. However, these studies represent data from just one teleost, the zebrafish *Danio rerio*. While such innervation patterns (specifically a supraorbital superficial nerve coming from an anteroventral placode) have not been documented in any other taxa in previous studies (Lekander, 1949; Landacre, 1910; Song and Northcutt, 1991; Northcutt et al., 2000), this may merely be due to limitations of the descriptive methods used. Both the CUBIC protocol and the live imaging protocol utilizing TMRE described in chapter 3 can be used on a wide range of representative organisms. The CUBIC protocol is able to render high resolution images of thin nerve branches, while live imaging with TMRE can track the proliferation of superficial and canal neuromasts through time in the same specimen. These methods can thus be used to identify if the newly described innervation patterns and neuromast development mechanisms occur in other teleosts, as well as if they represent a more conserved

vertebrate-wide pattern. Utilizing CUBIC clearing on fixed specimens of key representative taxa- elasmobranchs, amphibians and lampreys- would help reveal conserved and apomorphic patterns of innervation across vertebrate lineages.

Within the teleosts, catfish and medaka would represent ideal candidates for further examination for several reasons. First, they would phylogenetically bracket zebrafish to establish if any of these innervation patterns are conserved across teleosts, are an ostariophysan synapomorphy (since both catfish and zebrafish are ostariophysans), or are unique to cypriniforms. Second, both these species are genetically tractable, providing the ability to generate transgenics (e.g. using CRISPR 'knock-ins'; (Elaswad et al., 2018; Ansai and Kinoshita, 2014). Transgenics akin to zebrafish *Tg(Hgn39d),* the enhancer trap insertion (Nagayoshi et al., 2008) into the *contactin associated protein 2a* gene used in chapters 3 and 4, could potentially provide markers specific to the lateral line afferent nerves to allow imaging at high resolution, while also providing an opportunity to track the development of lateral line nerves and neuromasts in vivo. Such transgenic lines would also enable functional tests of the nerve-neuromast relationship as demonstrated in zebrafish via ablation of the lateral line ganglia.

Catfish are an especially interesting candidate for investigation because they are not only closely related to zebrafish as ostariophysans but have also been described to have superficial neuromast lines on the head and trunk in a pattern different from those of the zebrafish (Northcutt et al., 2000). Further, based on the one taxon examined (*Ictalurus,* Northcutt et al., 2000) catfish anterior lateral lines develop via elongating ridges, which differs from previous accounts of teleost anterior lateral line development

(except for the zebrafish infraorbital line, see chapter 3). They are also ideal candidates for integrating macroevolutionary studies, due to a well-established fossil record dating at least to the Late Cretaceous (Brito et al., 2024) and their widely variant ecologies. Catfish have also secondarily evolved electroreception, and have a profusion of approximately 4000 ampullary receptor organs scattered throughout the body. Data from other bony fishes (Modrell et al., 2011) have shown that ampullary receptors are derived from lateral line placodes. However, this previous finding suggests that it is only anterior lateral line placodes that can form electroreceptors. If this is the situation in catfish, there remains the question of how anterior placode derived ampullary organs (and their associated nerves) proliferate and migrate throughout the body.

Developmental approaches and data can help complement paleontological and comparative anatomical understanding of head evolution and diversification. As described in Chapter 2, the evolution of the gnathostome cranium and associated structures enabled the occupation of new ecological niches and facilitated a sea change in prevalent feeding behaviors. Embryological analyses can help identify molecular mechanisms involved in this reorganization, and how they maybe related to overall craniofacial development. For example, developmental data can help elucidate if and how closely related fish living in different environments have modified developmental pathways to produce contrasting lateral line morphologies. Ideal candidates to address the latter question would be the sighted and blind variants of the cavefish *Astyanax* which have a surface form with eyes and blind cave-dwelling forms. These two morphs have differences in their craniofacial skeletons, in neuromast number and position as well as the behaviour of their neural crest (Gross and Powers 2023; Powers et al., 2018;

Yoshizawa et al., 2018). Like the zebrafish, cavefish are a genetically tractable system (Sifuentes-Romero et al. 2023), allowing the approaches discussed earlier to be used to address if the expanded neuromast numbers of blind cave-dwelling morphs result from differences in neural crest migration or from changes in later neuromast expansion. Cavefish would provide an ideal candidate for synthesizing data on lateral line development, function (and its relation to ecology) and evolution- a model system for 'eco-evo-devo' studies.

In conclusion, the anterior mechanosensory lateral line is an excellent system for the integrative study of vertebrate evolution and development. This dissertation has elucidated several examples of studies taking such an approach, focusing on macroevolution of the lateral line and its relationship to major changes in the vertebrate craniofacial skeleton, the role of tissue interactions in shaping lateral line development and mechanisms driving postembryonic elaboration of the system. Future comparative studies expanding on these lines of inquiry would provide a window into understanding the complex interplay between morphology, ecology and development that shapes vertebrate sensory system evolution.

REFERENCES

Abe, Yoshikatsu, Ryu Asaoka, Masanori Nakae, and Kunio Sasaki. 2012. 'Ambiguities in the Identification of Batoid Lateral Line Systems Clarified by Innervation'. *Ichthyological Research* 59 (2): 189–92. https://doi.org/10.1007/s10228-011-0261-z.

Ahlberg, Per E., and Zerina Johanson. 1998. 'Osteolepiforms and the Ancestry of Tetrapods'. *Nature* 395 (6704): 792–94. https://doi.org/10.1038/27421.

Allis, Edward Phelps. 1889. 'The Anatomy and Development of the Lateral Line System in Amia Calva'. *Journal of Morphology* 2 (3): 463–566. https://doi.org/10.1002/jmor.1050020303.

Allis, Edward Phelps. 1901. 'The Lateral Sensory Canals, the Eye-Muscles, and the Peripheral Distribution of Certain of the Cranial Nerves of Mustelus Lævis'. *Journal of Cell Science* s2-45 (178): 87–236. https://doi.org/10.1242/jcs.s2-45.178.87.

Allis, Edward Phelps. 1934. 'Concerning the Course of the Latero-Sensory Canals in Recent Fishes, Pre-Fishes and Necturus'. *Journal of Anatomy* 68 (Pt 3): 361–415.

Allis jr., Edward Phelps. 1923. 'The Cranial Anatomy of Chlamydo-Selachus Anguineus'. *Acta Zoologica* 4 (2–3): 123–221. https://doi.org/10.1111/j.1463-6395.1923.tb00161.x.

Aman, Andy, Minhtu Nguyen, and Tatjana Piotrowski. 2011. 'Wnt/β-Catenin Dependent Cell Proliferation Underlies Segmented Lateral Line Morphogenesis'. *Developmental Biology* 349 (2): 470–82. https://doi.org/10.1016/j.ydbio.2010.10.022.

Aman, Andy, and Tatjana Piotrowski. 2008. 'Wnt/Beta-Catenin and Fgf Signaling Control Collective Cell Migration by Restricting Chemokine Receptor Expression'. *Developmental Cell* 15 (5): 749–61. https://doi.org/10.1016/j.devcel.2008.10.002.

Anderson, Philip S.L, and Mark W Westneat. 2007. 'Feeding Mechanics and Bite Force Modelling of the Skull of Dunkleosteus Terrelli, an Ancient Apex Predator'. *Biology Letters* 3 (1): 76–79. https://doi.org/10.1098/rsbl.2006.0569.

Andreev, Plamen, Michael I. Coates, Valentina Karatajūtė-Talimaa, et al. 2016. 'The Systematics of the Mongolepidida (Chondrichthyes) and the Ordovician Origins of the Clade'. *PeerJ* 4 (June): e1850. https://doi.org/10.7717/peerj.1850.

Ansai, Satoshi, and Masato Kinoshita. 2014. 'Targeted Mutagenesis Using CRISPR/Cas System in Medaka'. *Biology Open* 3 (5): 362–71. https://doi.org/10.1242/bio.20148177.

Anselmi, Chiara, Gwynna K. Fuller, Alberto Stolfi, Andrew K. Groves, and Lucia Manni. 2024. 'Sensory Cells in Tunicates: Insights into Mechanoreceptor Evolution'. *Frontiers in Cell and Developmental Biology* 12 (March): 1359207. https://doi.org/10.3389/fcell.2024.1359207.

Asaoka, Ryu, Masanori Nakae, and Kunio Sasaki. 2012. 'The Innervation and Adaptive Significance of Extensively Distributed Neuromasts in Glossogobius Olivaceus (Perciformes: Gobiidae)'. *Ichthyological Research* 59 (2): 143–50. https://doi.org/10.1007/s10228-011-0263-x.

Asaoka, Ryu, Masanori Nakae, and Kunio Sasaki. 2014. 'Innervation of the Lateral Line System in Rhyacichthys Aspro: The Origin of Superficial Neuromast Rows in Gobioids (Perciformes: Rhyacichthyidae)'. *Ichthyological Research* 61 (1): 49–58. https://doi.org/10.1007/s10228-013-0373-8.

Baker, Clare V.H., and Marianne Bronner-Fraser. 2001. 'Vertebrate Cranial Placodes I. Embryonic Induction'. *Developmental Biology* 232 (1): 1–61. https://doi.org/10.1006/dbio.2001.0156.

Basden, Alison M., Gavin C. Young, Michael I. Coates, and Alex Ritchie. 2000. 'The Most Primitive Osteichthyan Braincase?' *Nature* 403 (6766): 185–88. https://doi.org/10.1038/35003183.

Bazzana, Kayla D., Bryan M. Gee, Joseph J. Bevitt, and Robert R. Reisz. 2020. 'Postcranial Anatomy and Histology of Seymouria, and the Terrestriality of Seymouriamorphs'. *PeerJ* 8 (March): e8698. https://doi.org/10.7717/peerj.8698.

Beckwith, Cora J. 1907. 'The Early Development of the Lateral Line System of Amia Calva'. *Biological Bulletin* 14 (1): 23–34. JSTOR. https://doi.org/10.2307/1535645.

Bemis, W. E., and R. Glenn Northcutt. 1992. 'Skin and Blood Vessels of the Snout of the Australian Lungfish, Neoceratodus Forsteri, and Their Significance for Interpreting the Cosmine of Devonian Lungfishes'. *Acta Zoologica* 73 (2): 115–39. https://doi.org/10.1111/j.1463-6395.1992.tb00956.x.

Bergemann, David, Laura Massoz, Jordane Bourdouxhe, et al. 2018. 'Nifurpirinol: A More Potent and Reliable Substrate Compared to Metronidazole for Nitroreductase-Mediated Cell Ablations'. *Wound Repair and Regeneration* 26 (2): 238–44. https://doi.org/10.1111/wrr.12633.

Bininda-Emonds, Olaf R. P., John L. Gittleman, and Mike A. Steel. 2002. 'The (Super)Tree of Life: Procedures, Problems, and Prospects'. *Annual Review of Ecology, Evolution, and Systematics* 33 (Volume 33, 2002): 265–89. https://doi.org/10.1146/annurev.ecolsys.33.010802.150511.

Boldajipour, Bijan, Harsha Mahabaleshwar, Elena Kardash, et al. 2008. 'Control of Chemokine-Guided Cell Migration by Ligand Sequestration'. *Cell* 132 (3): 463–73. https://doi.org/10.1016/j.cell.2007.12.034.

Braun, Christopher B., and R. Glenn Northcutt. 1997. 'The Lateral Line System of Hagfishes (Craniata: Myxinoidea)'. *Acta Zoologica* 78 (3): 247–68. https://doi.org/10.1111/j.1463-6395.1997.tb01010.x.

Brazeau, Martin D. 2009. 'The Braincase and Jaws of a Devonian "acanthodian" and Modern Gnathostome Origins'. *Nature* 457 (7227): 305–8. https://doi.org/10.1038/nature07436.

Brazeau, Martin D., Marco Castiello, Amin El Fassi El Fehri, et al. 2023. 'Fossil Evidence for a Pharyngeal Origin of the Vertebrate Pectoral Girdle'. *Nature* 623 (7987): 550–54. https://doi.org/10.1038/s41586-023-06702-4.

Brazeau, Martin D., and Matt Friedman. 2015. 'The Origin and Early Phylogenetic History of Jawed Vertebrates'. *Nature* 520 (7548): 490–97. https://doi.org/10.1038/nature14438.

Brito, Paulo M., Didier B. Dutheil, Pierre Gueriau, et al. 2024. 'A Saharan Fossil and the Dawn of Neotropical Armoured Catfishes in Gondwana'. *Gondwana Research* 132 (August): 103–12. https://doi.org/10.1016/j.gr.2024.04.008.

Brooks, Paige M., Parker Lewis, Sara Million-Perez, et al. 2024. 'Pharmacological Reprogramming of Zebrafish Lateral Line Supporting Cells to a Migratory Progenitor State'. *Developmental Biology* 512 (August): 70–88. https://doi.org/10.1016/j.ydbio.2024.05.003.

Burighel, Paolo, Nancy J. Lane, Gasparini Fabio, et al. 2003. 'Novel, Secondary Sensory Cell Organ in Ascidians: In Search of the Ancestor of the Vertebrate Lateral Line'. *Journal of Comparative Neurology* 461 (2): 236–49. https://doi.org/10.1002/cne.10666.

Burrow, C. 2021. *Acanthodii, Stem Chondrichthyes*. Handbook of Paleoichthyology. Verlag Dr. Friedrich Pfeil. https://books.google.com/books?id=lDzyzgEACAAJ.

Castiello, Marco, and Martin D. Brazeau. 2018. 'Neurocranial Anatomy of the Petalichthyid Placoderm Shearsbyaspis Oepiki Young Revealed by X-Ray Computed Microtomography'. *Palaeontology* 61 (3): 369–89. https://doi.org/10.1111/pala.12345.

Cavanaugh, Ann M., Jie Huang, and Jau-Nian Chen. 2015. 'Two Developmentally Distinct Populations of Neural Crest Cells Contribute to the Zebrafish Heart'. *Developmental Biology* 404 (2): 103–12. https://doi.org/10.1016/j.ydbio.2015.06.002.

Chang, Carolyn T., and Tamara Anne Franz-Odendaal. 2014. 'Perturbing the Developing Skull: Using Laser Ablation to Investigate the Robustness of the Infraorbital Bones in Zebrafish (Danio Rerio)'. *BMC Developmental Biology* 14 (1): 44. https://doi.org/10.1186/s12861-014-0044-7.

Chang, Mee-mann. 1995. 'Diabolepis and Its Bearing on the Relationships between Porolepiforms and Dipnoans'. *Bulletin Du Muséum National d'Histoire Naturelle, 4e Série, Section* 17 (January): 235–68.

Chitnis, Ajay B., Damian Dalle Nogare, and Miho Matsuda. 2012. 'Building the Posterior Lateral Line System in Zebrafish'. *Developmental Neurobiology* 72 (3): 234–55. https://doi.org/10.1002/dneu.20962.

Choo, Brian. 2012. 'Revision of the Actinopterygian Genus Mimipiscis (=Mimia) from the Upper Devonian Gogo Formation of Western Australia and the Interrelationships of the Early Actinopterygii'. *Earth and Environmental Science Transactions of The Royal Society of Edinburgh* 102 (2): 77–104. https://doi.org/10.1017/S1755691011011029.

Clack, J. A. 2002. 'The Dermal Skull Roof of Acanthostega Gunnari, an Early Tetrapod from the Late Devonian'. *Earth and Environmental Science Transactions of The Royal Society of Edinburgh* 93 (1): 17–33. https://doi.org/10.1017/S0263593300000304.

Coates, M. I., and J. A. Clack. 1991. 'Fish-like Gills and Breathing in the Earliest Known Tetrapod'. *Nature* 352 (6332): 234–36. https://doi.org/10.1038/352234a0.

Coates, Michael, John Finarelli, Ivan Sansom, et al. 2018. 'An Early Chondrichthyan and the Evolutionary Assembly of a Shark Body Plan'. *Royal Society of London. Proceedings B. Biological Sciences* 285 (1870). https://doi.org/10.1098/rspb.2017.2418.

Cole, Frank J. 1897. 'XIX.—On the Cranial Nerves of Chimæra Monstrosa (Linn. 1754); with a Discussion of the Lateral Line System, and of the Morphology of the Chorda Tympani'. *Earth and Environmental Science Transactions of The Royal Society of Edinburgh* 38 (3): 631–80. https://doi.org/10.1017/S0080456800033433.

Collazo, A., S. E. Fraser, and P. M. Mabee. 1994. 'A Dual Embryonic Origin for Vertebrate Mechanoreceptors'. *Science (New York, N.Y.)* 264 (5157): 426–30. https://doi.org/10.1126/science.8153631.

Covell Jr., David A., and Drew M. Noden. 1989. 'Embryonic Development of the Chick Primary Trigeminal Sensory-Motor Complex'. *Journal of Comparative Neurology* 286 (4): 488–503. https://doi.org/10.1002/cne.902860407.

Culbertson, Maya D., Zachary R. Lewis, and Alexei V. Nechiporuk. 2011. 'Chondrogenic and Gliogenic Subpopulations of Neural Crest Play Distinct Roles during the Assembly of Epibranchial Ganglia'. *PLOS ONE* 6 (9): e24443. https://doi.org/10.1371/journal.pone.0024443.

Curado, Silvia, Ryan M. Anderson, Benno Jungblut, Jeff Mumm, Eric Schroeter, and Didier Y.R. Stainier. 2007. 'Conditional Targeted Cell Ablation in Zebrafish: A New Tool for Regeneration Studies'. *Developmental Dynamics* 236 (4): 1025–35. https://doi.org/10.1002/dvdy.21100.

Dalle Nogare, Damian, and Ajay B. Chitnis. 2017. 'A Framework for Understanding Morphogenesis and Migration of the Zebrafish Posterior Lateral Line Primordium'. *Mechanisms of Development* 148 (December): 69–78. https://doi.org/10.1016/j.mod.2017.04.005.

Dalle Nogare, Damian, and Ajay B Chitnis. 2020. 'NetLogo Agent-Based Models as Tools for Understanding the Self-Organization of Cell Fate, Morphogenesis and Collective Migration of the Zebrafish Posterior Lateral Line Primordium'. *Seminars in Cell & Developmental Biology*, Regeneration of vertebrate organs edited by Jia-Qiang HeCell migration edited by Michelle Starz-Gaiano, vol. 100 (April): 186–98. https://doi.org/10.1016/j.semcdb.2019.12.015.

Dambly-Chaudière, Christine, Nicolas Cubedo, and Alain Ghysen. 2007. 'Control of Cell Migration in the Development of the Posterior Lateral Line: Antagonistic Interactions between the Chemokine Receptors CXCR4 and CXCR7/RDC1'. *BMC Developmental Biology* 7 (1): 23. https://doi.org/10.1186/1471-213X-7-23.

David, Nicolas B, Laure Saint-Etienne, Michael Tsang, Thomas F Schilling, and Frédéric M Rosa. 2002. 'Requirement for Endoderm and FGF3 in Ventral Head Skeleton Formation.' *Development (Cambridge, England)* 129: 4457–68.

Davis, Samuel P., John A. Finarelli, and Michael I. Coates. 2012. 'Acanthodes and Shark-like Conditions in the Last Common Ancestor of Modern Gnathostomes'. *Nature* 486 (7402): 247–50. https://doi.org/10.1038/nature11080.

Dean, Bashford, Bashford Dean, and E. W. Gudger. 1930. *The Bashford Dean Memorial Volume : Archaic Fishes*. [American Museum of Natural History]. https://doi.org/10.5962/bhl.title.48528.

Dearden, Richard P., Agnese Lanzetti, Sam Giles, et al. 2023. 'The Oldest Three-Dimensionally Preserved Vertebrate Neurocranium'. *Nature* 621 (7980): 782–87. https://doi.org/10.1038/s41586-023-06538-y.

Didier, Dominique A., Jenny M. Kemper, and David A. Ebert. 2012. 'Phylogeny, Biology, and Classification of Extant Holocephalans'. In *Biology of Sharks and Their Relatives*, 2nd ed. CRC Press.

Didier, Dominique Anne. n.d. 'Phylogenetic Systematics of Extant Chimaeroid Fishes (Holocephali, Chimaeroidei)'. Ph.D., University of Massachusetts Amherst. Accessed 28 May 2024. https://www.proquest.com/docview/304010544/abstract/F7BBFC74F459428DPQ/1.

Dirks, Robert M., and Niles A. Pierce. 2004. 'Triggered Amplification by Hybridization Chain Reaction'. *Proceedings of the National Academy of Sciences* 101 (43): 15275–78. https://doi.org/10.1073/pnas.0407024101.

Disler, N. 1961. 'On the Structure of the Laterosensory System in Sharks and Rays'. *Acta Zoologica* 42 (1–2): 163–75. https://doi.org/10.1111/j.1463-6395.1961.tb00062.x.

Donoghue, Philip C. J. 2002. 'Evolution of Development of the Vertebrate Dermal and Oral Skeletons: Unraveling Concepts, Regulatory Theories, and Homologies'. *Paleobiology* 28 (4): 474–507. https://doi.org/10.1666/0094-8373(2002)028<0474:EODOTV>2.0.CO;2.

Donoghue, Philip C. J., and M. Paul Smith. 2001. 'The Anatomy of Turinia Pagei (Powrie), and the Phylogenetic Status of the Thelodonti'. *Earth and Environmental Science Transactions of The Royal Society of Edinburgh* 92 (1): 15–37. https://doi.org/10.1017/S026359330000002X.

Duarte-Ribeiro, Emanuell, Ulises Rosas-Puchuri, Matt Friedman, et al. 2024. 'Phylogenomic and Comparative Genomic Analyses Support a Single Evolutionary Origin of Flatfish Asymmetry'. *Nature Genetics* 56 (6): 1069–72. https://doi.org/10.1038/s41588-024-01784-w.

Dupret, Vincent, Sophie Sanchez, Daniel Goujet, and Per Erik Ahlberg. 2017. 'The Internal Cranial Anatomy of Romundina Stellina Ørvig, 1975 (Vertebrata, Placodermi, Acanthothoraci) and the Origin of Jawed Vertebrates—Anatomical Atlas of a Primitive Gnathostome'. *PLoS ONE* 12 (2). https://doi.org/10.1371/journal.pone.0171241.

Edens, Brittany M., and Marianne E. Bronner. 2025. 'Making Sense of Vertebrate Senses from a Neural Crest and Cranial Placode Evo-Devo Perspective'. *Trends in Neurosciences* 48 (3): 213–26. https://doi.org/10.1016/j.tins.2024.12.008.

Elaswad, Ahmed, Karim Khalil, David Cline, et al. 2018. 'Microinjection of CRISPR/Cas9 Protein into Channel Catfish, Ictalurus Punctatus, Embryos for Gene Editing'. *Journal of Visualized Experiments : JoVE*, no. 131 (January): 56275. https://doi.org/10.3791/56275.

Elliott, David. 2005. 'A Review of the Lateral Line Sensory System in Psammosteid Heterostracans'. *Revista Brasileira De Paleontologia - REV BRAS PALEONTOLOGIA* 8 (August): 99–108. https://doi.org/10.4072/rbp.2005.2.02.

Engelman, Russell K. 2024. 'Reconstructing Dunkleosteus Terrelli (Placodermi: Arthrodira): A New Look for an Iconic Devonian Predator'. *Palaeontologia Electronica* 27 (3): 1–79. https://doi.org/10.26879/1343.

Esterberg, Robert, Dale W. Hailey, Allison B. Coffin, David W. Raible, and Edwin W. Rubel. 2013. 'Disruption of Intracellular Calcium Regulation Is Integral to Aminoglycoside-Induced Hair Cell Death'. Articles. *Journal of Neuroscience* 33 (17): 7513–25. https://doi.org/10.1523/JNEUROSCI.4559-12.2013.

Ewart, J. C., and J. C. Mitchell. 1895. 'VI.—On the Lateral Sense Organs of Elasmobranchs. II. The Sensory Canals of the Common Skate (Raia Batis)'. *Earth and Environmental Science Transactions of The Royal Society of Edinburgh* 37 (1): 87–105. https://doi.org/10.1017/S008045680003252X.

Faucherre, Adèle, Jesús Pujol-Martí, Koichi Kawakami, and Hernán López-Schier. 2009. 'Afferent Neurons of the Zebrafish Lateral Line Are Strict Selectors of Hair-Cell Orientation'. *PLOS ONE* 4 (2): e4477. https://doi.org/10.1371/journal.pone.0004477.

Ferrón, Humberto G., and Héctor Botella. 2017. 'Squamation and Ecology of Thelodonts'. *PLOS ONE* 12 (2): e0172781. https://doi.org/10.1371/journal.pone.0172781.

Ferrón, Humberto G., and Philip C. J. Donoghue. 2022. 'Evolutionary Analysis of Swimming Speed in Early Vertebrates Challenges the "New Head Hypothesis"'. *Communications Biology* 5 (1): 1–8. https://doi.org/10.1038/s42003-022-03730-0.

Ferrón, Humberto G., Carlos Martínez-Pérez, Imran A. Rahman, Víctor Selles de Lucas, Héctor Botella, and Philip C. J. Donoghue. 2020. 'Computational Fluid Dynamics Suggests Ecological Diversification among Stem-Gnathostomes'. *Current Biology* 30 (23): 4808-4813.e3. https://doi.org/10.1016/j.cub.2020.09.031.

Forey, P. L. 1995. ‘Agnathans Recent and Fossil, and the Origin of Jawed Vertebrates’. *Reviews in Fish Biology and Fisheries* 5 (3): 267–303. https://doi.org/10.1007/BF00043003.

Forey, Peter, and Philippe Janvier. 1993. *Agnathans and the Origin of Jawed Vertebrates*. 361.

Freter, Sabine, Stephen J. Fleenor, Rasmus Freter, Karen J. Liu, and Jo Begbie. 2013. ‘Cranial Neural Crest Cells Form Corridors Prefiguring Sensory Neuroblast Migration’. *Development* 140 (17): 3595–600. https://doi.org/10.1242/dev.091033.

Friedman, Matt, and Martin D. Brazeau. 2013. ‘A Jaw-Dropping Fossil Fish’. *Nature* 502 (7470): 175–77. https://doi.org/10.1038/nature12690.

Fritzsch, B., I. Silos-Santiago, L. M. Bianchi, and I. Fariñas. 1997. ‘The Role of Neurotrophic Factors in Regulating the Development of Inner Ear Innervation’. *Trends in Neurosciences* 20 (4): 159–64. https://doi.org/10.1016/S0166-2236(96)01007-7.

Furlong, Rebecca F., and Peter W. H. Holland. 2002. ‘Bayesian Phylogenetic Analysis Supports Monophyly of Ambulacraria and of Cyclostomes’. *Zoological Science* 19 (5): 593–99. https://doi.org/10.2108/zsj.19.593.

Gagnier, Pierre-Yves, Alain R. M. Blieck, and Gabriela Rodrigo S. 1986. ‘First Ordovician Vertebrate from South America’. *Geobios* 19 (5): 629–34. https://doi.org/10.1016/S0016-6995(86)80058-4.

Gai, Zhikun, Philip C. J. Donoghue, Min Zhu, Philippe Janvier, and Marco Stampanoni. 2011. ‘Fossil Jawless Fish from China Foreshadows Early Jawed Vertebrate Anatomy’. *Nature* 476 (7360): 324–27. https://doi.org/10.1038/nature10276.

Gai, Zhikun, Shan Xian-Ren, Zhixin Sun, et al. 2020. *A Redescription of the Silurian Sinogaleaspis Shankouensis (Galeaspida, Stem-Gnathostomata) from Jiangxi, China*. 58 (April). https://doi.org/10.19615/j.cnki.1000-3118.191105.

Gans, C., and R. G. Northcutt. 1983. ‘Neural Crest and the Origin of Vertebrates: A New Head’. *Science (New York, N.Y.)* 220 (4594): 268–73. https://doi.org/10.1126/science.220.4594.268.

Gardiner, B. G., and B. G. Gardiner. 1984. ‘The Relationships of the Palaeoniscid Fishes, a Review Based on New Specimens of Mimia and Moythomasia from the Upper Devonian of Western Australia’. *Bulletin of the British Museum (Natural History) Geology* 37: 173--428.

Garman, S. 1888. ‘Lateral Canal System of the Selachia and Holocephala’. *Bulletin of The Museum of Comparative Zoology* 17: 57–120.

Gelman, S., A. Ayali, T. Kiemel, E. Sanovich, and A. H. Cohen. 2008. ‘Metamorphosis-Related Changes in the Lateral Line System of Lampreys, Petromyzon Marinus’. *Journal of Comparative Physiology. A, Neuroethology, Sensory, Neural, and Behavioral Physiology* 194 (11): 945–56. https://doi.org/10.1007/s00359-008-0367-6.

Ghysen, Alain, and Christine Dambly-Chaudière. 2004. ‘Development of the Zebrafish Lateral Line’. *Current Opinion in Neurobiology* 14 (1): 67–73. https://doi.org/10.1016/j.conb.2004.01.012.

Gibbs, Melissa A., and R. Glenn Northcutt. 2004. ‘Development of the Lateral Line System in the Shovelnose Sturgeon’. *Brain, Behavior and Evolution* 64 (2): 70–84. https://doi.org/10.1159/000079117.

Giles, Sam, Martin Rücklin, and Philip C.J. Donoghue. 2013. 'Histology of "Placoderm" Dermal Skeletons: Implications for the Nature of the Ancestral Gnathostome'. *Journal of Morphology* 274 (6): 627–44. https://doi.org/10.1002/jmor.20119.

Gillis, J. Andrew, Els C. Alsema, and Katharine E. Criswell. 2017. 'Trunk Neural Crest Origin of Dermal Denticles in a Cartilaginous Fish'. *Proceedings of the National Academy of Sciences* 114 (50): 13200–13205. https://doi.org/10.1073/pnas.1713827114.

Gillis, J. Andrew, Scott Bennett, Katharine E. Criswell, et al. 2022. 'Big Insight from the Little Skate: *Leucoraja Erinacea* as a Developmental Model System'. In *Current Topics in Developmental Biology*, edited by Bob Goldstein and Mansi Srivastava, vol. 147. Emerging Model Systems in Developmental Biology. Academic Press. https://doi.org/10.1016/bs.ctdb.2021.12.016.

Gillis, J. Andrew, Melinda S. Modrell, R. Glenn Northcutt, Kenneth C. Catania, Carl A. Luer, and Clare V. H. Baker. 2012. 'Electrosensory Ampullary Organs Are Derived from Lateral Line Placodes in Cartilaginous Fishes'. *Development* 139 (17): 3142–46. https://doi.org/10.1242/dev.084046.

Goodyear, Richard J., P. Kevin Legan, Jeffrey R. Christiansen, et al. 2010. 'Identification of the Hair Cell Soma-1 Antigen, HCS-1, as Otoferlin'. *Journal of the Association for Research in Otolaryngology* 11 (4): 573–86. https://doi.org/10.1007/s10162-010-0231-6.

Gordon, AD. 1986. 'Consensus Supertrees: The Synthesis of Rooted Trees Containing Overlapping Sets of Labeled Leaves'. *Journal of Classification* 3 (2): 335–48. https://doi.org/10.1007/BF01894195.

Graham-Smith, Francis, and Francis Rex Parrington. 1997. 'On Some Variations in the Latero-Sensory Lines of the Placoderm Fish Bothriolepis'. *Philosophical Transactions of the Royal Society of London. B, Biological Sciences* 282 (986): 1–39. https://doi.org/10.1098/rstb.1978.0008.

Graham-Smith W. and Parrington Francis Rex. 1978. 'On the Lateral Lines and Dermal Bones in the Parietal Region of Some Crossopterygian and Dipnoan Fishes'. *Philosophical Transactions of the Royal Society of London. B, Biological Sciences* 282 (986): 41–105. https://doi.org/10.1098/rstb.1978.0009.

Grant, Kelly A., David W. Raible, and Tatjana Piotrowski. 2005. 'Regulation of Latent Sensory Hair Cell Precursors by Glia in the Zebrafish Lateral Line'. *Neuron* 45 (1): 69–80. https://doi.org/10.1016/j.neuron.2004.12.020.

Gregory, J. E., A. Iggo, A. K. McIntyre, and U. Proske. 1987. 'Electroreceptors in the Platypus'. *Nature* 326 (6111): 386–87. https://doi.org/10.1038/326386a0.

Gross, Joshua B., and Amanda K. Powers. 2023. 'Reinterpreting the Work of Charles Breder: Sensory Neuromasts and Orbital Skeleton Variation in Eyeless *Astyanax* Cavefish'. *Developmental Biology* 493 (January): 13–16. https://doi.org/10.1016/j.ydbio.2022.11.004.

Haas, Petra, and Darren Gilmour. 2006. 'Chemokine Signaling Mediates Self-Organizing Tissue Migration in the Zebrafish Lateral Line'. *Developmental Cell* 10 (5): 673–80. https://doi.org/10.1016/j.devcel.2006.02.019.

Hall, Brian K. 1998. 'Germ Layers and the Germ-Layer Theory Revisited'. In *Evolutionary Biology*, edited by Max K. Hecht, Ross J. Macintyre, and Michael T. Clegg. Springer US. https://doi.org/10.1007/978-1-4899-1751-5_5.

Hamburger, Viktor. 1961. 'Experimental Analysis of the Dual Origin of the Trigeminal Ganglion in the Chick Embryo'. *Journal of Experimental Zoology* 148 (2): 91–123. https://doi.org/10.1002/jez.1401480202.

Hamm, Alyssa R., and Joshua B. Gross. 2025. ‘Integration of the Sensory and Skeletal Systems: A Classical Perspective on Neuromast-Bone Interactions’. *Developmental Biology* 524 (August): 48–54. https://doi.org/10.1016/j.ydbio.2025.04.012.

Hanke, Gavin F., and Mark V. H. Wilson. 2006. ‘Anatomy of the Early Devonian Acanthodian Brochoadmones Milesi Based on Nearly Complete Body Fossils, with Comments on the Evolution and Development of Paired Fins’. *Journal of Vertebrate Paleontology* 26 (3): 526–37. https://doi.org/10.1671/0272-4634(2006)26[526:AOTEDA]2.0.CO;2.

Harper, David A. T., Emma U. Hammarlund, and Christian M. Ø. Rasmussen. 2014. ‘End Ordovician Extinctions: A Coincidence of Causes’. *Gondwana Research* 25 (4): 1294–307. https://doi.org/10.1016/j.gr.2012.12.021.

Harrison, Ross Granville. 1903. ‘Experimentelle Untersuchungen Über die Entwicklung der Sinnesorgane der Seitenlinie bei den Ampkibien’. *Archiv für mikroskopische Anatomie* 63 (1): 35–149. https://doi.org/10.1007/BF02978174.

Harvey, R., J. H. S. Blaxter, and R. D. Hoyt. 1992. ‘Development of Superficial and Lateral Line Neuromasts in Larvae and Juveniles of Plaice (*Pleuronectes Platessa*) and Sole (*Solea Solea*)’. *Journal of the Marine Biological Association of the United Kingdom* 72 (3): 651–68. https://doi.org/10.1017/S0025315400059427.

Heimberg, Alysha M., Richard Cowper-Sal·lari, Marie Sémon, Philip C. J. Donoghue, and Kevin J. Peterson. 2010. ‘microRNAs Reveal the Interrelationships of Hagfish, Lampreys, and Gnathostomes and the Nature of the Ancestral Vertebrate’. *Proceedings of the National Academy of Sciences* 107 (45): 19379–83. https://doi.org/10.1073/pnas.1010350107.

Hernández, Pedro P., Francisco A. Olivari, Andrés F. Sarrazin, Pablo C. Sandoval, and Miguel L. Allende. 2007. ‘Regeneration in Zebrafish Lateral Line Neuromasts: Expression of the Neural Progenitor Cell Marker Sox2 and Proliferation-Dependent and-Independent Mechanisms of Hair Cell Renewal’. *Developmental Neurobiology* 67 (5): 637–54. https://doi.org/10.1002/dneu.20386.

Herzog, Hendrik, Birgit Klein, and Alexander Ziegler. 2017. ‘Form and Function of the Teleost Lateral Line Revealed Using Three-Dimensional Imaging and Computational Fluid Dynamics’. *Journal of the Royal Society Interface* 14 (130): 20160898. https://doi.org/10.1098/rsif.2016.0898.

Hetherington, Thomas E., and Marvalee H. Wake. 1979. ‘The Lateral Line System in larvalIchthyophis (Amphibia: Gymnophiona)’. *Zoomorphologie* 93 (3): 209–25. https://doi.org/10.1007/BF00994000.

Higgs, D. M., and C. A. Radford. 2013. ‘The Contribution of the Lateral Line to “Hearing” in Fish’. *Journal of Experimental Biology* 216 (8): 1484–90. https://doi.org/10.1242/jeb.078816.

Hilton, Eric J., Lance Grande, and William E. Bemis. 2011. ‘Skeletal Anatomy of the Shortnose Sturgeon, Acipenser Brevirostrum Lesueur, 1818, and the Systematics of Sturgeons (Acipenseriformes, Acipenseridae)’. *Fieldiana Life and Earth Sciences* 2011 (3): 1–168. https://doi.org/10.3158/2158-5520-3.1.1.

Hilton, Eric J., and Eric J. Hilton. 2002. *Osteology of the Extant North American Fishes of the Genus Hiodon Lesueur, 1818 (Teleostei: Osteoglossomorpha: Hiodontiformes)*. Field Museum of Natural History. https://doi.org/10.5962/bhl.title.2666.

Holmes, R. 1997. ‘The Carboniferous Amphibian Proterogyrinus Scheelei Romer, and the Early Evolution of Tetrapods’. *Philosophical Transactions of the Royal Society of London. B, Biological Sciences* 306 (1130): 431–524. https://doi.org/10.1098/rstb.1984.0103.

Holmes, Robert B., Robert L. Carroll, and Robert R. Reisz. 1998. 'The First Articulated Skeleton of Dendrerpeton Acadianum (Temnospondyli, Dendrerpetontidae) from the Lower Pennsylvanian Locality of Joggins, Nova Scotia, and a Review of Its Relationships'. *Journal of Vertebrate Paleontology* 18 (1): 64–79. https://doi.org/10.1080/02724634.1998.10011034.

Holmgren, Nils. 1940. 'STUDIES ON THE HEAD IN FISHES. | EBSCOhost'. January 1. https://openurl.ebsco.com/contentitem/gcd:13283218?sid=ebsco:plink:crawler&id=ebsco:gcd:13283218.

Holmgren, Nils. 1942. *General Morphology of the Lateral Sensory Line System of the Head in Fish*. Vol. 20. Kungl. Svenska Vetenskapsakademiens Handlingar 3. Almqvist and Wiksell. https://cir.nii.ac.jp/crid/1130000795203675776.

Holmgren, Nils. 1943. 'Studies on the Head of Fishes'. *Acta Zoologica* 24 (1–3): 1–188. https://doi.org/10.1111/j.1463-6395.1943.tb00014.x.

Holmgren, Nils, and Torsten Pehrson. 1949. 'SOME REMARKS ON THE ONTOGENETICAL DEVELOPMENT OF THE SENSORY LINES ON THE CHEEK IN FISHES AND AMPHIBIANS'. *Acta Zoologica* 30 (1-2): 249–314. https://doi.org/10.1111/j.1463-6395.1949.tb00508.x.

Howard, Lauren E., William M. Holmes, Sara Ferrando, et al. 2013. 'Functional Nasal Morphology of Chimaerid Fishes'. *Journal of Morphology* 274 (9): 987–1009. https://doi.org/10.1002/jmor.20156.

Iwasaki, Miki, Hayato Yokoi, Tohru Suzuki, Koichi Kawakami, and Hironori Wada. 2020. 'Development of the Anterior Lateral Line System through Local Tissue-Tissue Interactions in the Zebrafish Head'. *Developmental Dynamics: An Official Publication of the American Association of Anatomists* 249 (12): 1440–54. https://doi.org/10.1002/dvdy.225.

Janvier, Philippe. 1974. 'The Sensory Line System and Its Innervation in the Osteostraci (Agnatha, Cephalaspidomorphi)'. *Zoologica Scripta* 3 (2): 91–99. https://doi.org/10.1111/j.1463-6409.1974.tb00807.x.

Janvier, Philippe. 1996. *Early Vertebrates*. Oxford University Press. https://doi.org/10.1093/oso/9780198540472.001.0001.

Janvier, Philippe (19- ; paléontologue) Auteur du texte. 1985. *Les Céphalaspides Du Spitsberg : Anatomie, Phylogénie et Systématique Des Ostéostracés Siluro-Dévoniens : Révision Des Ostéostracés de La Formation de Wood Bay (Dévonien Inférieur Du Spitsberg / Par Philippe Janvier,...* https://gallica.bnf.fr/ark:/12148/bpt6k33345411.

Jarman, Andrew P., Yves Grau, Lily Y. Jan, and Yuh Nung Jan. 1993. 'Atonal Is a Proneural Gene That Directs Chordotonal Organ Formation in the Drosophila Peripheral Nervous System'. *Cell* 73 (7): 1307–21. https://doi.org/10.1016/0092-8674(93)90358-W.

Jarvik, E. 1980. *Basic Structure and Evolution of Vertebrates*. Basic Structure and Evolution of Vertebrates, v. 1. Academic Press. https://books.google.com/books?id=UMwKAQAAIAAJ.

Johnson, Sydney Evans. 1917. 'Structure and Development of the Sense Organs of the Lateral Canal System of Selachians (Mustelus Canis and Squalus Acanthias)'. *Journal of Comparative Neurology* 28 (1): 1–74. https://doi.org/10.1002/cne.900280102.

Kague, Erika, Michael Gallagher, Sally Burke, Michael Parsons, Tamara Franz-Odendaal, and Shannon Fisher. 2012. 'Skeletogenic Fate of Zebrafish Cranial and Trunk Neural Crest'. *PLoS ONE* 7 (11): 1–13. https://doi.org/10.1371/journal.pone.0047394.

Kaufmann, Anna, Michaela Mickoleit, Michael Weber, and Jan Huisken. 2012. 'Multilayer Mounting Enables Long-Term Imaging of Zebrafish Development in a Light Sheet Microscope'. *Development* 139 (17): 3242–47. https://doi.org/10.1242/dev.082586.

Keating, Joseph N., and Philip C. J. Donoghue. 2016. 'Histology and Affinity of Anaspids, and the Early Evolution of the Vertebrate Dermal Skeleton'. *Proceedings. Biological Sciences* 283 (1826): 20152917. https://doi.org/10.1098/rspb.2015.2917.

Kimmel, Charles B., William W. Ballard, Seth R. Kimmel, Bonnie Ullmann, and Thomas F. Schilling. 1995. 'Stages of Embryonic Development of the Zebrafish'. *Developmental Dynamics* 203 (3): 253–310. https://doi.org/10.1002/aja.1002030302.

King, Benedict, Tuo Qiao, Michael S. Y. Lee, Min Zhu, and John A. Long. 2017. 'Bayesian Morphological Clock Methods Resurrect Placoderm Monophyly and Reveal Rapid Early Evolution in Jawed Vertebrates'. *Systematic Biology* 66 (4): 499–516. https://doi.org/10.1093/sysbio/syw107.

Kligman, Ben T., Bryan M. Gee, Adam D. Marsh, et al. 2023. 'Triassic Stem Caecilian Supports Dissorophoid Origin of Living Amphibians'. *Nature* 614 (7946): 102–7. https://doi.org/10.1038/s41586-022-05646-5.

Klug, Christian, Björn Kröger, Wolfgang Kiessling, et al. 2010. 'The Devonian Nekton Revolution'. *Lethaia* 43 (4): 465–77. https://doi.org/10.1111/j.1502-3931.2009.00206.x.

Koontz, Alison, Hugo A. Urrutia, and Marianne E. Bronner. 2023. 'Making a Head: Neural Crest and Ectodermal Placodes in Cranial Sensory Development'. *Seminars in Cell & Developmental Biology*, Special Issue: Neural Crest Formation by Tatjana Sauka-Spengler / Special Issue: Metabolism in time and space by Jason M. Tennessen and Elizabeth J. Rideout, vol. 138 (March): 15–27. https://doi.org/10.1016/j.semcdb.2022.06.009.

Kubota, Shimpei I., Kei Takahashi, Jun Nishida, et al. 2017. 'Whole-Body Profiling of Cancer Metastasis with Single-Cell Resolution'. *Cell Reports* 20 (1): 236–50. https://doi.org/10.1016/j.celrep.2017.06.010.

Kucenas, Sarah, Norio Takada, Hae-Chul Park, Elvin Woodruff, Kendal Broadie, and Bruce Appel. 2008. 'CNS-Derived Glia Ensheath Peripheral Nerves and Mediate Motor Root Development'. *Nature Neuroscience* 11 (2): 143–51. https://doi.org/10.1038/nn2025.

Kulczycki, J. 1960. 'Porolepis (Crossopterygii) from the Lower Devonian of the Holy Cross Mountains'. *Acta Palaeontologica Polonica* 05 (1). http://agro.icm.edu.pl/agro/element/bwmeta1.element.agro-14868027-504a-4362-8e09-953b83d7c0b5.

Kuraku, Shigehiro, Daisuke Hoshiyama, Kazutaka Katoh, Hiroshi Suga, and Takashi Miyata. 1999. 'Monophyly of Lampreys and Hagfishes Supported by Nuclear DNA–Coded Genes'. *Journal of Molecular Evolution* 49 (6): 729–35. https://doi.org/10.1007/PL00006595.

Kuratani, Shigeru. 2005. 'Cephalic Neural Crest Cells and the Evolution of Craniofacial Structures in Vertebrates: Morphological and Embryological Significance of the Premandibular–Mandibular Boundary'. *Zoology* 108 (1): 13–25. https://doi.org/10.1016/j.zool.2004.12.001.

Landacre, F. L. 1910. 'The Origin of the Cranial Ganglia in Ameiurus'. *Journal of Comparative Neurology and Psychology* 20 (4): 309–412. https://doi.org/10.1002/cne.920200404.

Landacre, Francis Leroy, and A. C. Conger. 1913. *The Origin of the Lateral Line Primordia in Lepidosteus Osseus*.

Lebedev, Oleg A., Zerina Johanson, Alexander N. Kuznetsov, Alekey Tsessarsky, Kate Trinajstic, and Farkhad B. Isakhodzayev. 2022. 'Feeding in the Devonian Antiarch Placoderm Fishes: A Study Based upon Morphofunctional Analysis of Jaws'. *Journal of Paleontology* 96 (6): 1413–30. https://doi.org/10.1017/jpa.2022.54.

Ledent, Valérie. 2002. 'Postembryonic Development of the Posterior Lateral Line in Zebrafish'. *Development* 129 (3): 597–604. https://doi.org/10.1242/dev.129.3.597.

Leitch, Duncan B., and Kenneth C. Catania. 2012. 'Structure, Innervation and Response Properties of Integumentary Sensory Organs in Crocodilians'. *The Journal of Experimental Biology* 215 (23): 4217–30. https://doi.org/10.1242/jeb.076836.

Lekander, Bertil. 1949. 'The Sensory Line System and the Canal Bones in the Head of Some Ostariophysi'. *Acta Zoologica* 30 (1–2): 1–131. https://doi.org/10.1111/j.1463-6395.1949.tb00503.x.

Li, Qiang, You-an Zhu, Jing Lu, et al. 2021. 'A New Silurian Fish Close to the Common Ancestor of Modern Gnathostomes'. *Current Biology* 31 (16): 3613-3620.e2. https://doi.org/10.1016/j.cub.2021.05.053.

Liao, James C. 2006. 'The Role of the Lateral Line and Vision on Body Kinematics and Hydrodynamic Preference of Rainbow Trout in Turbulent Flow'. *Journal of Experimental Biology* 209 (20): 4077–90. https://doi.org/10.1242/jeb.02487.

Lombard, R Eric, and Bolt John R. 1995. 'A New Primitive Tetrapod, Whatcheeria Deltae, from the Lower Carboniferous of Iowa'. *Palaeontology* 38: 471–94.

López-Schier, Hernán, and A. J. Hudspeth. 2005. 'Supernumerary Neuromasts in the Posterior Lateral Line of Zebrafish Lacking Peripheral Glia'. *Proceedings of the National Academy of Sciences of the United States of America* 102 (5): 1496–501. https://doi.org/10.1073/pnas.0409361102.

Lu, Jing, Sam Giles, Matt Friedman, Jan L. den Blaauwen, and Min Zhu. 2016. 'The Oldest Actinopterygian Highlights the Cryptic Early History of the Hyperdiverse Ray-Finned Fishes'. *Current Biology* 26 (12): 1602–8. https://doi.org/10.1016/j.cub.2016.04.045.

Lu, Jing, Min Zhu, John A. Long, et al. 2012. 'The Earliest Known Stem-Tetrapod from the Lower Devonian of China'. *Nature Communications* 3 (1): 1160. https://doi.org/10.1038/ncomms2170.

Lubitz, D. K. J. Ekström von. 1981. 'Ultrastructure of the Lateral-Line Sense Organs of the Ratfish, Chimaera Monstrosa'. *Cell and Tissue Research* 215 (3): 651–65. https://doi.org/10.1007/BF00233539.

Lund, Richard. 1985. 'The Morphology of Falcatus Falcatus (St. John and Worthen), a Mississippian Stethacanthid Chondrichthyan from the Bear Gulch Limestone of Montana'. *Journal of Vertebrate Paleontology* 5 (1): 1–19. https://doi.org/10.1080/02724634.1985.10011842.

Lush, Mark E, and Tatjana Piotrowski. 2014. 'ErbB Expressing Schwann Cells Control Lateral Line Progenitor Cells via Non-Cell-Autonomous Regulation of Wnt/β-Catenin'. *eLife* 3 (March): e01832. https://doi.org/10.7554/eLife.01832.

Lyons, David A., Hans-Martin Pogoda, Matthew G. Voas, et al. 2005. 'Erbb3 and Erbb2 Are Essential for Schwann Cell Migration and Myelination in Zebrafish'. *Current Biology* 15 (6): 513–24. https://doi.org/10.1016/j.cub.2005.02.030.

MacIver, Malcolm A., Lars Schmitz, Ugurcan Mugan, Todd D. Murphey, and Curtis D. Mobley. 2017. 'Massive Increase in Visual Range Preceded the Origin of Terrestrial Vertebrates'. *Proceedings of the National Academy of Sciences* 114 (12): E2375–84. https://doi.org/10.1073/pnas.1615563114.

Mandal, Amrita, Hiu-Tung C. Wong, Katherine Pinter, et al. 2021. 'Retrograde Mitochondrial Transport Is Essential for Organelle Distribution and Health in Zebrafish Neurons'. Research Articles. *Journal of Neuroscience* 41 (7): 1371–92. https://doi.org/10.1523/JNEUROSCI.1316-20.2020.

Marinelli, Wilhelm, and Anneliese Strenger. 1954. *Vergleichende Anatomie und Morphologie der Wirbeltiere: Lampetra fluviatilis (L.) / Mit 65 Abb. nach Originalzeichn. von M. Wimmer*. Deuticke.

Maro, Géraldine S., Matthieu Vermeren, Octavian Voiculescu, et al. 2004. 'Neural Crest Boundary Cap Cells Constitute a Source of Neuronal and Glial Cells of the PNS'. *Nature Neuroscience* 7 (9): 930–38. https://doi.org/10.1038/nn1299.

Maruska, Karen P. 2001. 'Morphology of the Mechanosensory Lateral Line System in Elasmobranch Fishes: Ecological and Behavioral Considerations'. *Environmental Biology of Fishes* 60 (1): 47–75. https://doi.org/10.1023/A:1007647924559.

Masselink, Wouter, and Elly M. Tanaka. 2023. 'Ethyl Cinnamate-Based Tissue Clearing Strategies'. *Methods in Molecular Biology (Clifton, N.J.)* 2562: 123–33. https://doi.org/10.1007/978-1-0716-2659-7_7.

Maxwell, Erin E., Nadia B. Fröbisch, and Audrey C. Heppleston. 2008. 'Variability and Conservation in Late Chondrichthyan Development: Ontogeny of the Winter Skate (Leucoraja Ocellata)'. *The Anatomical Record* 291 (9): 1079–87. https://doi.org/10.1002/ar.20719.

McCarroll, Matthew N., and Alex V. Nechiporuk. 2013. 'Fgf3 and Fgf10a Work in Concert to Promote Maturation of the Epibranchial Placodes in Zebrafish'. *PLoS ONE* 8 (12): e85087. https://doi.org/10.1371/journal.pone.0085087.

Meinke, Deborah K. 1984. 'A Review of Cosmine: Its Structure, Development, and Relationship to Other Forms of the Dermal Skeleton in Osteichthyans'. *Journal of Vertebrate Paleontology* 4 (3): 457–70. JSTOR.

Milner, A. R., and S. E. K. Sequeira. 1993. 'The Temnospondyl Amphibians from the Viséan of East Kirkton, West Lothian, Scotland'. *Earth and Environmental Science Transactions of The Royal Society of Edinburgh* 84 (3–4): 331–61. https://doi.org/10.1017/S0263593300006155.

Miyashita, Tetsuto, Michael I. Coates, Robert Farrar, et al. 2019. 'Hagfish from the Cretaceous Tethys Sea and a Reconciliation of the Morphological–Molecular Conflict in Early Vertebrate Phylogeny'. *Proceedings of the National Academy of Sciences* 116 (6): 2146–51. https://doi.org/10.1073/pnas.1814794116.

Miyashita, Tetsuto, Philippe Janvier, Kristen Tietjen, et al. 2025. 'Novel Assembly of a Head–Trunk Interface in the Sister Group of Jawed Vertebrates'. *Nature*, August 6, 1–6. https://doi.org/10.1038/s41586-025-09329-9.

Modrell, Melinda S., William E. Bemis, R. Glenn Northcutt, Marcus C. Davis, and Clare V. H. Baker. 2011. 'Electrosensory Ampullary Organs Are Derived from Lateral Line Placodes in Bony Fishes'. *Nature Communications* 2 (October): 496. https://doi.org/10.1038/ncomms1502.

Mogdans, Joachim. 2019. ‘Sensory Ecology of the Fish Lateral-Line System: Morphological and Physiological Adaptations for the Perception of Hydrodynamic Stimuli’. *Journal of Fish Biology* 95 (1): 53–72. https://doi.org/10.1111/jfb.13966.

Moodie, Roy L. 1908. ‘The Lateral Line System in Extinct Amphibia’. *Journal of Morphology* 19 (2): 511–40. https://doi.org/10.1002/jmor.1050190206.

Morsch, Marco, Rowan A. W. Radford, Emily K. Don, et al. 2017. ‘Triggering Cell Stress and Death Using Conventional UV Laser Confocal Microscopy’. *Journal of Visualized Experiments : JoVE*, no. 120 (February): 54983. https://doi.org/10.3791/54983.

Moy-Thomas, J. A. 1941. ‘Development of the Frontal Bones of the Rainbow Trout’. *Nature* 147 (3735): 681. https://doi.org/10.1038/147681a0.

Moy-Thomas, J. A. 1971. *Palaeozoic Fishes*. Springer US. https://doi.org/10.1007/978-1-4684-6465-8.

Münz, Heinrich. 1979. ‘Morphology and Innervation of the Lateral Line System inSarotherodon Niloticus (L.) (Cichlidae, Teleostei)’. *Zoomorphologie* 93 (1): 73–86. https://doi.org/10.1007/BF02568676.

Nagayoshi, Saori, Eriko Hayashi, Gembu Abe, et al. 2008. ‘Insertional Mutagenesis by the Tol2 Transposon-Mediated Enhancer Trap Approach Generated Mutations in Two Developmental Genes: Tcf7and Synembryn-Like’. *Development* 135 (1): 159–69. https://doi.org/10.1242/dev.009050.

Nakae, Masanori, Shinji Asai, and Kunio Sasaki. 2006. ‘The Lateral Line System and Its Innervation in Champsodon Snyderi (Champsodontidae): Distribution of Approximately 1000 Neuromasts’. *Ichthyological Research* 53 (3): 209–15. https://doi.org/10.1007/s10228-006-0335-5.

Nakae, Masanori, Mari Kuroki, Mao Sato, and Kunio Sasaki. 2021. ‘The Lateral Line System and Its Innervation in the Japanese Eel Anguilla Japonica (Teleostei: Elopomorpha: Anguillidae)’. *Journal of Morphology* 282 (6): 863–73. https://doi.org/10.1002/jmor.21353.

Nakae, Masanori, and Kunio Sasaki. 2010. ‘Lateral Line System and Its Innervation in Tetraodontiformes with Outgroup Comparisons: Descriptions and Phylogenetic Implications’. *Journal of Morphology* 271 (5): 559–79. https://doi.org/10.1002/jmor.10817.

Naylor, Gavin J. P., J. N. (Janine Nicole) Caira, K. (Kirsten) Jensen, K. a. M. Rosana, William T. (William Toby) White, and P. R. Last. 2012. *A DNA Sequence-Based Approach to the Identification of Shark and Ray Species and Its Implications for Global Elasmobranch Diversity and Parasitology. (Bulletin of the American Museum of Natural History, No. 367)*. June 21. http://hdl.handle.net/2246/6183.

Neave, D. A. 1986. ‘The Development of the Lateral Line System in Plaice *(Pleuronectes Platessa)* and Turbot *(Scophthalmus Maximus)*’. *Journal of the Marine Biological Association of the United Kingdom* 66 (3): 683–93. https://doi.org/10.1017/S0025315400042284.

Neelathi, Uma M., Damian Dalle Nogare, and Ajay B. Chitnis. 2018. ‘Cxcl12a Induces Snail1b Expression to Initiate Collective Migration and Sequential Fgf-Dependent Neuromast Formation in the Zebrafish Posterior Lateral Line Primordium’. *Development* 145 (14): dev162453. https://doi.org/10.1242/dev.162453.

Nikaido, Masataka, Joaquin Navajas Acedo, Kohei Hatta, and Tatjana Piotrowski. 2017. ‘Retinoic Acid Is Required and Fgf, Wnt, and Bmp Signaling Inhibit Posterior Lateral Line Placode Induction in Zebrafish’. *Developmental Biology* 431 (2): 215–25. https://doi.org/10.1016/j.ydbio.2017.09.017.

Nogare, Damian Dalle, Masataka Nikaido, Katherine Somers, Jeffery Head, Tatjana Piotrowski, and Ajay B. Chitnis. 2017. 'In Toto Imaging of the Migrating Zebrafish Lateral Line Primordium at Single Cell Resolution'. *Developmental Biology* 422 (1): 14–23. https://doi.org/10.1016/j.ydbio.2016.12.015.

Northcutt, R. G., K. C. Catania, and B. B. Criley. 1994. 'Development of Lateral Line Organs in the Axolotl'. *The Journal of Comparative Neurology* 340 (4): 480–514. https://doi.org/10.1002/cne.903400404.

Northcutt, R. G., P. H. Holmes, and J. S. Albert. 2000. 'Distribution and Innervation of Lateral Line Organs in the Channel Catfish'. *The Journal of Comparative Neurology* 421 (4): 570–92.

Northcutt, R. Glenn. 1989. 'The Phylogenetic Distribution and Innervation of Craniate Mechanoreceptive Lateral Lines'. In *The Mechanosensory Lateral Line*, edited by Sheryl Coombs, Peter Görner, and Heinrich Münz. Springer New York.

Northcutt, R. Glenn. 1997. 'Evolution of Gnathostome Lateral Line Ontogenies'. *Brain, Behavior and Evolution* 50 (1): 25–37. https://doi.org/10.1159/000113319.

Northcutt, R. Glenn, and Carl Gans. 1983. 'The Genesis of Neural Crest and Epidermal Placodes: A Reinterpretation of Vertebrate Origins'. *The Quarterly Review of Biology* 58 (1): 1–28. https://doi.org/10.1086/413055.

Olson, Hannah M., and Alex V. Nechiporuk. 2018. 'Using Zebrafish to Study Collective Cell Migration in Development and Disease'. *Frontiers in Cell and Developmental Biology* 6 (August). https://doi.org/10.3389/fcell.2018.00083.

Owen, Richard. 1859. 'On the orders of fossil and recent Reptilia and their distribution in time.' *Report of the British Asociation for the Advancement of Science* 1859: 153-166.

Pardo, Jason D., Matt Szostakiwskyj, Per E. Ahlberg, and Jason S. Anderson. 2017. 'Hidden Morphological Diversity among Early Tetrapods'. *Nature* 546 (7660): 642–45. https://doi.org/10.1038/nature22966.

Parichy, David M., Michael R. Elizondo, Margaret G. Mills, Tiffany N. Gordon, and Raymond E. Engeszer. 2009. 'Normal Table of Postembryonic Zebrafish Development: Staging by Externally Visible Anatomy of the Living Fish'. *Developmental Dynamics* 238 (12): 2975–3015. https://doi.org/10.1002/dvdy.22113.

Parker, Hugo J., Marianne E. Bronner, and Robb Krumlauf. 2014. 'A Hox Regulatory Network of Hindbrain Segmentation Is Conserved to the Base of Vertebrates'. *Nature* 514 (7523): 490–93. https://doi.org/10.1038/nature13723.

Parrington, F. R. 2009. 'A Theory of the Relations of Lateral Lines to Dermal Bones.' *Proceedings of the Zoological Society of London* 119 (1): 65–78. https://doi.org/10.1111/j.1096-3642.1949.tb00868.x.

Parsons, Michael J., Harshan Pisharath, Shamila Yusuff, et al. 2009. 'Notch-Responsive Cells Initiate the Secondary Transition in Larval Zebrafish Pancreas'. *Mechanisms of Development* 126 (10): 898–912. https://doi.org/10.1016/j.mod.2009.07.002.

Patten, William. 1902. 'On the Structure and Classification of the Trematapidæ'. *The American Naturalist* 36 (425): 379–93. https://doi.org/10.1086/278139.

Pehrson, Torsten. 1922. 'Some Points in the Cranial Development of TELeostomian Fishes'. *Acta Zoologica* 3 (1): 1–63. https://doi.org/10.1111/j.1463-6395.1922.tb01016.x.

Pehrson, Torsten. 1949. 'The Ontogeny of the Lateral Line System in the Head of Dipnoans'. *Acta Zoologica* 30 (1–2): 153–82. https://doi.org/10.1111/j.1463-6395.1949.tb00505.x.

Peloggia, Julia, Daniela Münch, Paloma Meneses-Giles, et al. 2021. 'Adaptive Cell Invasion Maintains Lateral Line Organ Homeostasis in Response to Environmental Changes'. *Developmental Cell* 56 (9): 1296-1312.e7. https://doi.org/10.1016/j.devcel.2021.03.027.

Pende, Marko, Karim Vadiwala, Hannah Schmidbaur, et al. 2020. 'A Versatile Depigmentation, Clearing, and Labeling Method for Exploring Nervous System Diversity'. *Science Advances* 6 (22): eaba0365. https://doi.org/10.1126/sciadv.aba0365.

Perez-Rojas, Sebastian Enrique, and Adriana Jerez. 2022. 'Comparative Integumentary Morphology in Four Species of Pipa (Anura: Pipidae) from Colombia'. *Papéis Avulsos de Zoologia* 62 (February): e202262008–e202262008. https://doi.org/10.11606/1807-0205/2022.62.008.

Piotrowski, Tatjana, and Clare V.H. Baker. 2014. 'The Development of Lateral Line Placodes: Taking a Broader View'. *Developmental Biology* 389 (1): 68–81. https://doi.org/10.1016/j.ydbio.2014.02.016.

Pisano, Gina C., Samantha M. Mason, Nyembezi Dhliwayo, Robert V. Intine, and Michael P. Sarras,. 2014. 'An Assay for Lateral Line Regeneration in Adult Zebrafish'. *Journal of Visualized Experiments : JoVE*, no. 86 (April): 51343. https://doi.org/10.3791/51343.

Powers, Amanda K., Tyler E. Boggs, and Joshua B. Gross. 2018. 'Canal Neuromast Position Prefigures Developmental Patterning of the Suborbital Bone Series in *Astyanax* Cave- and Surface-Dwelling Fish'. *Developmental Biology*, Cavefish Development, vol. 441 (2): 252–61. https://doi.org/10.1016/j.ydbio.2018.04.001.

Pradel, Alan, Ivan. J Sansom, Pierre-Yves Gagnier, Ricardo Cespedes, and Philippe Janvier. 2006. 'The Tail of the Ordovician Fish Sacabambaspis'. *Biology Letters* 3 (1): 73–76. https://doi.org/10.1098/rsbl.2006.0557.

Prince, Victoria E., Cecilia B. Moens, Charles B. Kimmel, and Robert K. Ho. 1998. 'Zebrafish Hox Genes: Expression in the Hindbrain Region of Wild-Type and Mutants of the Segmentation Gene, Valentino'. *Development* 125 (3): 393–406. https://doi.org/10.1242/dev.125.3.393.

Pujol-Martí, Jesús, Andrea Zecca, Jean-Pierre Baudoin, et al. 2012. 'Neuronal Birth Order Identifies a Dimorphic Sensorineural Map'. Articles. *Journal of Neuroscience* 32 (9): 2976–87. https://doi.org/10.1523/JNEUROSCI.5157-11.2012.

Quinzio, Silvia, and Marissa Fabrezi. 2014. 'The Lateral Line System in Anuran Tadpoles: Neuromast Morphology, Arrangement, and Innervation'. *The Anatomical Record* 297 (8): 1508–22. https://doi.org/10.1002/ar.22952.

Raible, David W., and Gregory J. Kruse. 2000. 'Organization of the Lateral Line System in Embryonic Zebrafish'. *The Journal of Comparative Neurology* 421 (2): 189–98. https://doi.org/10.1002/(SICI)1096-9861(20000529)421:2<189::AID-CNE5>3.0.CO;2-K.

Randle, Emma, Joseph N. Keating, and Robert S. Sansom. 2022. 'A Phylogeny for Heterostraci (Stem-Gnathostomes)'. Preprint, bioRxiv, August 13. https://doi.org/10.1101/2022.08.11.503478.

Reisz, Robert R., David C. Evans, Eric M. Roberts, Hans-Dieter Sues, and Adam M. Yates. 2012. 'Oldest Known Dinosaurian Nesting Site and Reproductive Biology of the Early Jurassic Sauropodomorph Massospondylus'. *Proceedings of the National Academy of Sciences* 109 (7): 2428–33. https://doi.org/10.1073/pnas.1109385109.

Rigon, Francesca, Thomas Stach, Federico Caicci, Fabio Gasparini, Paolo Burighel, and Lucia Manni. 2013. 'Evolutionary Diversification of Secondary Mechanoreceptor Cells in Tunicata'. *BMC Evolutionary Biology* 13 (1): 112. https://doi.org/10.1186/1471-2148-13-112.

Rind, F. Claire, Stefan Wernitznig, Peter Pölt, et al. 2016. 'Two Identified Looming Detectors in the Locust: Ubiquitous Lateral Connections among Their Inputs Contribute to Selective Responses to Looming Objects'. *Scientific Reports* 6 (October): 35525. https://doi.org/10.1038/srep35525.

Ritchie, Alexander. 1967. 'Ateleaspis Tessellata Traquair, a Non-Cornuate Cephalaspid from the Upper Silurian of Scotland'. *Journal of the Linnean Society of London, Zoology* 47 (311): 69–81. https://doi.org/10.1111/j.1096-3642.1967.tb01396.x.

Ritchie, Alexander, and Joyce Gilbert-Tomlinson. 1977. 'First Ordovician Vertebrates from the Southern Hemisphere'. *Alcheringa: An Australasian Journal of Palaeontology* 1 (4): 351–68. https://doi.org/10.1080/03115517708527770.

Rizzato, Pedro P., Anna Pospisilova, Eric J. Hilton, and Flávio A. Bockmann. 2020. 'Ontogeny and Homology of Cranial Bones Associated with Lateral-Line Canals of the Senegal Bichir, Polypterus Senegalus (Actinopterygii: Cladistii: Polypteriformes), with a Discussion on the Formation of Lateral-Line Canal Bones in Fishes'. *Journal of Anatomy* 237 (3): 439–67. https://doi.org/10.1111/joa.13202.

Rocha, M., N. Singh, K. Ahsan, A. Beiriger, and V.E. Prince. 2020. 'Neural Crest Development: Insights from the Zebrafish'. *Developmental Dynamics* 249 (1). https://doi.org/10.1002/dvdy.122.

Rocha, Manuel, Anastasia Beiriger, Elaine E. Kushkowski, et al. 2020. 'From Head to Tail: Regionalization of the Neural Crest'. *Development* 147 (20): dev193888. https://doi.org/10.1242/dev.193888.

Rosenberg, Allison F., Jesse Isaacman-Beck, Clara Franzini-Armstrong, and Michael Granato. 2014. 'Schwann Cells and Deleted in Colorectal Carcinoma Direct Regenerating Motor Axons Towards Their Original Path'. Articles. *Journal of Neuroscience* 34 (44): 14668–81. https://doi.org/10.1523/JNEUROSCI.2007-14.2014.

Roth, Gerhard, Ursula Dicke, and Kiisa Nishikawa. 1992. 'How Do Ontogeny, Morphology, and Physiology of Sensory Systems Constrain and Direct the Evolution of Amphibians?' *The American Naturalist* 139 (March): S105–24. https://doi.org/10.1086/285307.

Ruta, Marcello, and Michael I. Coates. 2007. 'Dates, Nodes and Character Conflict: Addressing the Lissamphibian Origin Problem'. *Journal of Systematic Palaeontology* 5 (1): 69–122. https://doi.org/10.1017/S1477201906002008.

Sahly, I., Peter Andermann, and C. Petit. 1999. 'The Zebrafish Eya1 Gene and Its Expression Pattern during Embryogenesis'. *Development Genes and Evolution* 209 (7): 399–410. https://doi.org/10.1007/s004270050270.

Sallan, Lauren Cole, and Michael I. Coates. 2010. 'End-Devonian Extinction and a Bottleneck in the Early Evolution of Modern Jawed Vertebrates'. *Proceedings of the National Academy of Sciences* 107 (22): 10131–35. https://doi.org/10.1073/pnas.0914000107.

Sansom, I. J., M. P. Smith, H. A. Armstrong, and M. M. Smith. 1992. 'Presence of the Earliest Vertebrate Hard Tissue in Conodonts'. *Science (New York, N.Y.)* 256 (5061): 1308–11. https://doi.org/10.1126/science.1598573.

Sansom, Ivan J., M. Paul Smith, Moya M. Smith, and Peter Turner. 1997. ‘Astraspis - The Anatomy and Histology of an Ordovician Fish’. *Palaeontology* 40 (3): 625–43.

Sansom, Robert S. 2009. ‘Phylogeny, Classification and Character Polarity of the Osteostraci (Vertebrata)’. *Journal of Systematic Palaeontology* 7 (1): 95–115. https://doi.org/10.1017/S1477201908002551.

Sapède, Dora, Nicolas Gompel, Christine Dambly-Chaudière, and Alain Ghysen. 2002. ‘Cell Migration in the Postembryonic Development of the Fish Lateral Line’. *Development* 129 (3): 605–15. https://doi.org/10.1242/dev.129.3.605.

Sarrazin, Andres F., Viviana A. Nuñez, Dora Sapède, Valériane Tassin, Christine Dambly-Chaudière, and Alain Ghysen. 2010. ‘Origin and Early Development of the Posterior Lateral Line System of Zebrafish’. Articles. *Journal of Neuroscience* 30 (24): 8234–44. https://doi.org/10.1523/JNEUROSCI.5137-09.2010.

Schindelin, Johannes, Ignacio Arganda-Carreras, Erwin Frise, et al. 2012. ‘Fiji: An Open-Source Platform for Biological-Image Analysis’. *Nature Methods* 9 (7): 676–82. https://doi.org/10.1038/nmeth.2019.

Schlosser, Gerhard. 2006. ‘Induction and Specification of Cranial Placodes’. *Developmental Biology* 294 (2): 303–51. https://doi.org/10.1016/j.ydbio.2006.03.009.

Schoch, Rainer R. 2013. ‘The Evolution of Major Temnospondyl Clades: An Inclusive Phylogenetic Analysis’. *Journal of Systematic Palaeontology* 11 (6): 673–705. https://doi.org/10.1080/14772019.2012.699006.

Schoch, Rainer R. 2019. ‘Osteology of the Temnospondyl Trematosaurus Brauni Burmeister, 1849 from the Middle Buntsandstein of Bernburg, Germany’. *Palaeodiversity* 12 (1): 41–63. https://doi.org/10.18476/pale.v12.a4.

Schoch, Rainer R. 2022. ‘Phylogeny of the Amphibamiform Temnospondyls: The Relationship of Taxa Known by Adults, Larvae and Neotenes’. *Journal of Systematic Palaeontology* 20 (1): 1–30. https://doi.org/10.1080/14772019.2022.2113831.

Schoch, Rainer R., and Florian Witzmann. 2024. ‘The Evolution of Larvae in Temnospondyls and the Stepwise Origin of Amphibian Metamorphosis’. *Biological Reviews* 99 (5): 1613–37. https://doi.org/10.1111/brv.13084.

Schuster, Kevin, Christine Dambly-Chaudière, and Alain Ghysen. 2010. ‘Glial Cell Line-Derived Neurotrophic Factor Defines the Path of Developing and Regenerating Axons in the Lateral Line System of Zebrafish’. *Proceedings of the National Academy of Sciences* 107 (45): 19531–36. https://doi.org/10.1073/pnas.1002171107.

Scott, Elliott, Duncan E. Edgley, Alan Smith, et al. 2023. ‘Lateral Line Morphology, Sensory Perception and Collective Behaviour in African Cichlid Fish’. *Royal Society Open Science* 10 (1): 221478. https://doi.org/10.1098/rsos.221478.

Servais, Thomas, and David A.T. Harper. 2018. ‘The Great Ordovician Biodiversification Event (GOBE): Definition, Concept and Duration’. *Lethaia* 51 (2): 151–64. https://doi.org/10.1111/let.12259.

Sifuentes-Romero, Itzel, Estephany Ferrufino, and Johanna E. Kowalko. 2023. ‘Application of CRISPR-Cas9 for Functional Analysis in A. Mexicanus’. In *Emerging Model Organisms*, edited by Wei Wang, Nicolas Rohner, and Yongfu Wang. Springer US. https://doi.org/10.1007/978-1-0716-2875-1_14.

Smith, StevenC., MichaelJ. Lannoo, and JohnB. Armstrong. 1990. ‘Development of the Mechanoreceptive Lateral-Line System in the Axolotl: Placode Specification, Guidance of Migration, and the Origin of Neuromast Polarity’. *Anatomy and Embryology* 182 (2). https://doi.org/10.1007/BF00174016.

Song, J. K., and R. G. Northcutt. 1991. ‘Morphology, Distribution and Innervation of the Lateral-Line Receptors of the Florida Gar, Lepisosteus Platyrhincus’. *Brain, Behavior and Evolution* 37 (1): 10–37. https://doi.org/10.1159/000114343.

Stensio, Erik A. 1947. ‘The Sensory Lines and Dermal Bones of the Cheek in Fishes and Amphibians’. *K Sevenska Vetensk Akad Handl* 24: 1–195.

Stensiö, Erik Andersson, Erik Andersson Stensiö, and British Museum (Natural History). 1932. *The Cephalaspids of Great Britain*. Printed by order of the Trustees of the British Museum. https://doi.org/10.5962/bhl.title.118830.

Steventon, Ben, Roberto Mayor, and Andrea Streit. 2014. ‘Neural Crest and Placode Interaction during the Development of the Cranial Sensory System’. *Developmental Biology* 389 (1): 28–38. https://doi.org/10.1016/j.ydbio.2014.01.021.

Stone, L. S. 1928. ‘Experiments on the Transplantation of Placodes of the Cranial Ganglia in the Amphibian Embryo. III. Preauditory and Postauditory Placodal Materials Interchanged’. *Journal of Comparative Neurology* 47 (1): 117–54. https://doi.org/10.1002/cne.900470107.

Stundl, Jan, Megan L. Martik, Donglei Chen, et al. 2023. ‘Ancient Vertebrate Dermal Armor Evolved from Trunk Neural Crest’. *Proceedings of the National Academy of Sciences* 120 (30): e2221120120. https://doi.org/10.1073/pnas.2221120120.

Tarby, Melissa L., and Jacqueline F. Webb. 2003. ‘Development of the Supraorbital and Mandibular Lateral Line Canals in the Cichlid, Archocentrus Nigrofasciatus’. *Journal of Morphology* 255 (1): 44–57. https://doi.org/10.1002/jmor.10045.

Theveneau, Eric, Benjamin Steventon, Elena Scarpa, et al. 2013. ‘Chase-and-Run between Adjacent Cell Populations Promotes Directional Collective Migration’. *Nature Cell Biology* 15 (7): 763–72. https://doi.org/10.1038/ncb2772.

Thomas, Eric D., Ivan A. Cruz, Dale W. Hailey, and David W. Raible. 2015. ‘There and Back Again: Development and Regeneration of the Zebrafish Lateral Line System’. *Wiley Interdisciplinary Reviews. Developmental Biology* 4 (1): 1–16. https://doi.org/10.1002/wdev.160.

Thomson, Keith Stewart. 1975. *On the Biology of Cosmine*. Peabody Museum of Natural History, Yale University.

Trinajstic, Kate, and Kate Roelofs. 2019. ‘Placoderm Morphology’. In *Encyclopedia of Animal Cognition and Behavior*. Springer, Cham. https://doi.org/10.1007/978-3-319-47829-6_1212-1.

Venkataraman, Vishruth, Marco Lopez, Victoria E. Prince, and Michael I. Coates. 2025. ‘Re-Make, Re-Model: Evolution and Development of Vertebrate Cranial Lateral Lines’. *Biological Reviews of the Cambridge Philosophical Society*, ahead of print, June 7. https://doi.org/10.1111/brv.70045.

Venkataraman, Vishruth, Noel H. McGrory, Theresa J. Christiansen, Joaquin Navajas Acedo, Michael I. Coates, and Victoria E. Prince. 2025. ‘Development of the Zebrafish Anterior Lateral Line System Is Influenced by Underlying Cranial Neural Crest’. *Developmental Biology* 525 (September): 102–21. https://doi.org/10.1016/j.ydbio.2025.05.025.

Villalobos-Segura, Eduardo, Giuseppe Marramà, Giorgio Carnevale, et al. 2022. 'The Phylogeny of Rays and Skates (Chondrichthyes: Elasmobranchii) Based on Morphological Characters Revisited'. *Diversity* 14 (6): 456. https://doi.org/10.3390/d14060456.

Voronina, Elena P., Valentina G. Sideleva, and Dianne R. Hughes. 2021. 'Lateral Line System of Flatfishes (Pleuronectiformes): Diversity and Taxonomic Distribution of Its Characters'. *Acta Zoologica* 102 (1): 1–25. https://doi.org/10.1111/azo.12311.

Wada, Hironori, Christine Dambly-Chaudière, Koichi Kawakami, and Alain Ghysen. 2013. 'Innervation Is Required for Sense Organ Development in the Lateral Line System of Adult Zebrafish'. *Proceedings of the National Academy of Sciences of the United States of America* 110 (14): 5659–64. https://doi.org/10.1073/pnas.1214004110.

Wada, Hironori, Alain Ghysen, Chie Satou, et al. 2010. 'Dermal Morphogenesis Controls Lateral Line Patterning during Postembryonic Development of Teleost Fish'. *Developmental Biology* 340 (2): 583–94. https://doi.org/10.1016/j.ydbio.2010.02.017.

Wada, Hironori, Satoshi Hamaguchi, and Mitsuru Sakaizumi. 2008. 'Development of Diverse Lateral Line Patterns on the Teleost Caudal Fin'. *Developmental Dynamics* 237 (10): 2889–902. https://doi.org/10.1002/dvdy.21710.

Wada, Hironori, Miki Iwasaki, and Koichi Kawakami. 2014. 'Development of the Lateral Line Canal System through a Bone Remodeling Process in Zebrafish'. *Developmental Biology* 392 (1): 1–14. https://doi.org/10.1016/j.ydbio.2014.05.004.

Wake, Marvalee H. 1992. 'Reproduction in Caecilians'. In *Reproductive Biology of South American Vertebrates*. Springer, New York, NY. https://doi.org/10.1007/978-1-4612-2866-0_8.

Watson, D. M. S. 1937. 'The Acanthodian Fishes'. *Philosophical Transactions of the Royal Society of London. Series B, Biological Sciences* 228 (549): 49–146.

Webb, J. F., and R. G. Northcutt. 1997. 'Morphology and Distribution of Pit Organs and Canal Neuromasts in Non-Teleost Bony Fishes'. *Brain, Behavior and Evolution* 50 (3): 139–51. https://doi.org/10.1159/000113328.

Webb, Jacqueline F. 1989. 'Gross Morphology and Evolution of the Mechanoreceptive Lateral-Line System in Teleost Fishes'. *Brain, Behavior and Evolution* 33 (1): 34–53. https://doi.org/10.1159/000115896.

Webb, Jacqueline F. 2014. 'Lateral Line Morphology and Development and Implications for the Ontogeny of Flow Sensing in Fishes'. In *Flow Sensing in Air and Water: Behavioral, Neural and Engineering Principles of Operation*, edited by Horst Bleckmann, Joachim Mogdans, and Sheryl L. Coombs. Springer. https://doi.org/10.1007/978-3-642-41446-6_10.

Webb, Jacqueline F., John C. Montgomery, and Joachim Mogdans. 2008. 'Bioacoustics and the Lateral Line System of Fishes'. In *Fish Bioacoustics: With 81 Illustrations*, edited by Jacqueline F. Webb, Richard R. Fay, and Arthur N. Popper. Springer. https://doi.org/10.1007/978-0-387-73029-5_5.

Webb, Jacqueline F., and Jonathan E. Shirey. 2003. 'Postembryonic Development of the Cranial Lateral Line Canals and Neuromasts in Zebrafish'. *Developmental Dynamics* 228 (3): 370–85. https://doi.org/10.1002/dvdy.10385.

Westoll, T. S. 1937. 'On the Cheek-Bones in Teleostome Fishes'. *Journal of Anatomy* 71 (Pt 3): 362–82.

Westoll, T. Stanley. 1936a. ‘On the Structures of the Dermal Ethmoid Shield of Osteolepis’. *Geological Magazine* 73 (4): 157–71. https://doi.org/10.1017/S0016756800097296.

Westoll, T. Stanley. 1936b. ‘On the Structures of the Dermal Ethmoid Shield of Osteolepis’. *Geological Magazine* 73 (4): 157–71. https://doi.org/10.1017/S0016756800097296.

Westoll, T. Stanley. 1941. ‘Latero-Sensory Canals and Dermal Bones’. *Nature* 148 (3745): 168–168. https://doi.org/10.1038/148168a0.

Whalen, Christopher D., and Derek E. G. Briggs. 2018. ‘The Palaeozoic Colonization of the Water Column and the Rise of Global Nekton’. *Proceedings of the Royal Society B: Biological Sciences*, ahead of print, July 25. world. https://doi.org/10.1098/rspb.2018.0883.

White, David T., and Jeff S. Mumm. 2013. ‘The Nitroreductase System of Inducible Targeted Ablation Facilitates Cell-Specific Regenerative Studies in Zebrafish’. *Methods*, Zebrafish Methods, vol. 62 (3): 232–40. https://doi.org/10.1016/j.ymeth.2013.03.017.

Williams, J. A, and N Holder. 2000. ‘Cell Turnover in Neuromasts of Zebrafish Larvae’. *Hearing Research* 143 (1): 171–81. https://doi.org/10.1016/S0378-5955(00)00039-3.

Wilson, M V, and T Märss. 2009. ‘Thelodont Phylogeny Revisited, with Inclusion of Key Scale-Based Taxa’. *Estonian Journal of Earth Sciences* 58 (4): 297. https://doi.org/10.3176/earth.2009.4.08.

Wilson, Mark V. H., and Michael W. Caldwell. 1993. ‘New Silurian and Devonian Fork-Tailed “thelodonts” Are Jawless Vertebrates with Stomachs and Deep Bodies’. *Nature* 361 (6411): 442–44. https://doi.org/10.1038/361442a0.

Wilson, Mark V. H., and Michael W. Caldwell. 1998. ‘The Furcacaudiformes: A New Order of Jawless Vertebrates with Thelodont Scales, Based on Articulated Silurian and Devonian Fossils from Northern Canada’. *Journal of Vertebrate Paleontology* 18 (1): 10–29. https://doi.org/10.1080/02724634.1998.10011031.

Winklbauer, Rudolf, and Eter Hausen. 1983. ‘Development of the Lateral Line System in Xenopus Laevis : I. Normal Development and Cell Movement in the Supraorbital System’. *Development* 76 (1): 265–81. https://doi.org/10.1242/dev.76.1.265.

Witzmann, Florian. 2005. ‘Cranial Morphology and Ontogeny of the Permo-Carboniferous Temnospondyl Archegosaurus Decheni Goldfuss, 1847 from the Saar–Nahe Basin, Germany’. *Earth and Environmental Science Transactions of The Royal Society of Edinburgh* 96 (2): 131–62. https://doi.org/10.1017/S0263593300001279.

Wueringer, B.E., S.C. Peverell, J. Seymour, Jr. Squire L., and S.P. Collin. 2011. ‘Sensory Systems in Sawfishes. 2. The Lateral Line’. *Brain Behavior and Evolution* 78 (2): 150–61. https://doi.org/10.1159/000329518.

Yang, CHEN, LI Qiang, ZHOU Zheng-Da, et al. n.d. ‘A New Genus of Galeaspids (Jawless Stem-Gnathostomata) from the Early Silurian Chongqing Lagerstätte, China’. *Vertebrata PalAsiatica* 62 (4).

Yoshizawa, Masato, Ernest Hixon, and William R. Jeffery. 2018. ‘Neural Crest Transplantation Reveals Key Roles in the Evolution of Cavefish Development’. *Integrative and Comparative Biology* 58 (3): 411–20. https://doi.org/10.1093/icb/icy006.

Yuan, Tian, Joshua R. York, and David W. McCauley. 2020. ‘Neural Crest and Placode Roles in Formation and Patterning of Cranial Sensory Ganglia in Lamprey’. *Genesis* 58 (5): e23356. https://doi.org/10.1002/dvg.23356.

Zhu, Min, and Per E. Ahlberg. 2004. ‘The Origin of the Internal Nostril of Tetrapods’. *Nature* 432 (7013): 7013. https://doi.org/10.1038/nature02843.

Zhu, Min, Per E. Ahlberg, Zhaohui Pan, et al. 2016. ‘A Silurian Maxillate Placoderm Illuminates Jaw Evolution’. *Science (New York, N.Y.)* 354 (6310): 334–36. https://doi.org/10.1126/science.aah3764.

Zhu, Min, and Zhikun Gai. 2007. ‘Phylogenetic Relationships of Galeaspids (Agnatha)’. *Frontiers of Biology in China* 2 (2): 151–69. https://doi.org/10.1007/s11515-007-0022-6.

Zhu, Min, Xiaobo Yu, Per Erik Ahlberg, et al. 2013. ‘A Silurian Placoderm with Osteichthyan-like Marginal Jaw Bones’. *Nature* 502 (7470): 188–93. https://doi.org/10.1038/nature12617.

Zhu, You-an, Sam Giles, Gavin C. Young, et al. 2021. ‘Endocast and Bony Labyrinth of a Devonian “Placoderm” Challenges Stem Gnathostome Phylogeny’. *Current Biology* 31 (5): 1112-1118.e4. https://doi.org/10.1016/j.cub.2020.12.046.

Zhu, You-an, Qiang Li, Jing Lu, et al. 2022. ‘The Oldest Complete Jawed Vertebrates from the Early Silurian of China’. *Nature* 609 (7929): 954–58. https://doi.org/10.1038/s41586-022-05136-8.